

FINITE DIFFERENCE ANALYSIS OF
CURVED LATTICE SPACE STRUCTURES

A thesis presented for the degree of
Doctor of Philosophy in Civil Engineering
at the University of Canterbury
Christchurch, New Zealand

by

PETER NORMAN DAVENPORT

June 1977

ABSTRACT

An analytic technique, the finite difference calculus, is presented as a method that can be used, subject to certain restrictions, to produce mathematical models for the response of curved lattice space structures when subject to load. The restrictions are that the structure is linear elastic and has a regular lattice layout on a shallow curved surface.

The method produces partial difference equations, which together with their boundary conditions may be solved analytically to give a formulae for the unknown joint deformations. Having this solution, the structural analyst need only evaluate the formulae for the values of the parameters that describe a particular structure.

Solutions are given for three types of structures which all lie on a shallow second order surface, i.e. cylinders and elliptic or hyperbolic paraboloids. Single layer structures with pin jointed rods or rigid jointed beams and a double layered structure with pin jointed members are analysed. In all cases the structures are supported by gables on all four sides of a rectangular boundary.

For these structures the solution for the displacements takes the form of a double trigonometric series with a finite number of terms. Numerical results obtained with a digital computer are compared with those from other methods, principally the direct stiffness method. The finite difference calculus method proved to be accurate and more economic to use.

The effect of varying structural and geometrical parameters is discussed and of particular interest is the interaction between the rises of the curved surface in the two directions. A critical geometry for the hyperbolic paraboloid which has a rise and sag of equal magnitude is found. At this critical shape, the response of the structure shows an undesirable feature that load is carried by bending action rather than by membrane action.

ACKNOWLEDGEMENTS

The research was conducted in the Department of Civil Engineering, University of Canterbury, with Departmental Head Professor H.J. Hopkins.

I acknowledge the assistance received during the course of the project and extend my thanks to:

Dr. J.C. Scrivener, my supervisor, for his continual encouragement, guidance, helpful criticism and patience throughout the study.

Dr. A.J. Carr, who gave advice on the numerical work and read parts of the draft.

The University Grants Committee, for financial assistance by way of a Postgraduate Scholarship.

Christine McConnell for her patient typing of a difficult manuscript and Barry Simpson for assistance with preparation of the diagrams.

Finally, I wish to thank Barbara Crawford for her indispensable encouragement, particularly in the final stages of the project.

TABLE OF CONTENTS

	Page
ABSTRACT	i
ACKNOWLEDGEMENTS	ii
TABLE OF CONTENTS	iii
LIST OF FIGURES	viii
LIST OF TABLES	xi
LIST OF SYMBOLS	xii
CHAPTER 1 - INTRODUCTION	1
1.1 Problem Statement	1
1.2 Chapter Details	3
CHAPTER 2 - FINITE DIFFERENCE CALCULUS METHOD	5
2.1 Introduction	5
2.2 Review of Finite Difference Calculus	5
2.3 Review of Application of Finite Difference Calculus to Structural Mechanics	7
2.4 Characteristics of Suitable Structures	12
2.5 Outline of General Method	13
2.5.1 Member Relations	13
2.5.2 Shift Operators	16
2.5.3 Equilibrium of Typical Joint	17
2.5.4 Boundary Conditions	18
2.5.5 Solution Form	18
2.5.6 Displacements	20
2.5.7 Member Actions	20

	Page
2.5.8 Joint Residuals and Reactions	20
CHAPTER 3 - ALTERNATIVE ANALYSIS METHODS	21
3.1 Introduction	21
3.2 Direct Stiffness Method	21
3.3 Analogous Continuum Method	25
3.4 Physical Model Method	27
CHAPTER 4 - ANALYSIS OF A SINGLE LAYER PIN JOINTED STRUCTURE	29
4.1 Description of the Structure	29
4.2 Derivation of Governing Equations	32
4.3 Boundary Conditions	40
4.4 Solution of Governing Equations	43
4.5 Displacements	47
4.6 Member Actions	47
4.7 Joint Residuals	47
CHAPTER 5 - ANALYSIS OF A SINGLE LAYER RIGID JOINTED STRUCTURE	48
5.1 Description of the Structure	48
5.2 Derivation of Governing Equations	48
5.3 Boundary Conditions	52
5.4 Solution of Governing Equation	55
5.5 Displacement	57
5.6 Member Actions	57
5.7 Joint Residuals	57
CHAPTER 6 - ANALYSIS OF A DOUBLE LAYER PIN JOINTED STRUCTURE	58
6.1 Description of the Structure	58
6.2 Derivation of Governing Equations	58

	Page
6.3 Boundary Conditions	67
6.4 Solution of Governing Equation	69
6.5 Displacements	71
6.6 Member Actions	71
6.7 Joint Residuals	71
CHAPTER 7 - NUMERICAL TECHNIQUES	72
7.1 Introduction	72
7.2 General Outline of Numerical Procedures	72
7.3 Special Numerical Techniques	74
7.3.1 Trigonometric Functions	76
7.3.2 Analytic Evaluation of Fourier Coefficients	77
7.4 Computer Program	80
7.5 Numerical Verification of the Analysis	80
7.5.1 Choice of Test Structures	82
7.5.2 Choice of Quantities to be compared	87
7.6 Comparison of Results	89
7.6.1 Displacements and Actions	89
7.6.2 Computer Resources	101
7.7 Conclusions about Verification	109
CHAPTER 8 - SENSITIVITY ANALYSIS	111
8.1 General Behaviour of the Structure	111
8.2 Choice of Parameter Values	114
8.3 Choice of a Measure of the Response	115

	Page
8.4 Results of Analyses	119
8.4.1 Results for Single Layer Structure	119
8.4.2 Results for Double Layer Structure	125
8.5 Summary	125
CHAPTER 9 - NON LINEAR BEHAVIOUR	131
9.1 Introduction	131
9.2 Treatment of Non Linear Behaviour	132
9.3 Numerical Examples	133
9.4 Conclusions Regarding Non Linear Behaviour	141
CHAPTER 10 - SUMMARY AND CONCLUSIONS	144
REFERENCES	147
APPENDIX A - ACTION OF FINITE DIFFERENCE OPERATIONS ON TRIGONOMETRIC FUNCTIONS	A-1
APPENDIX B - EXPANSION OF LOAD FUNCTIONS IN TRIGONOMETRIC SERIES	B-1
B.1 General Functions	B-1
B.2 Special Functions	B-2
B.2.1 Unit Point Load	B-2
B.2.2 Unit Uniformly Distributed Load	B-4
APPENDIX C - MATRICIES K_{ij} FOR MEMBERS	C-1
C.1 Rod Member	C-1
C.2 Beam Member	C-2
APPENDIX D - GOVERNING PARTIAL DIFFERENCE EQUATIONS	D-1
D.1 Single Layer Pin Jointed Lattice	D-1
D.2 Single Layer Rigid Jointed Lattice	D-1

	Page
D.3 Double Layer Pin Jointed Lattice	D-4
APPENDIX E - FORCE BOUNDARY CONDITIONS	E-1
E.1 Single Layer Pin Jointed Lattice	E-1
E.2 Single Layer Rigid Jointed Lattice	E-2
E.3 Double Layer Pin Jointed Lattice	E-6
APPENDIX F - MATRIX EQUATIONS FOR DISPLACEMENT	
COEFFICIENTS	F-1
F.1 Single Layer Pin Jointed Lattice	F-1
F.2 Single Layer Rigid Jointed Lattice	F-2
F.3 Double Layer Pin Jointed Lattice	F-4
APPENDIX G - DETAILS AND LISTING OF COMPUTER PROGRAM	G-1
APPENDIX H - ANALOGOUS CONTINUUM METHOD	H-1
H.1 Continuum Analogy for a Single Layer Lattice	H-1
H.2 Continuum Analogy for Double Layer Lattice	H-10
H.3 Analysis of the Continuum Shell	H-13

LIST OF FIGURES

<u>FIGURE</u>	<u>DESCRIPTION</u>	<u>PAGE</u>
2.1	Beam Member Axes, Displacements and Actions	14
4.1	Structure Shapes	30
4.2	Member Layout	31
4.3	Bar Member Axes, Displacements and Actions	32
4.4	Orientation of α, β, γ Axes	34
4.5	Definition of Angles ψ and ϕ	36
4.6	Boundary Joints	41
5.1	Beam Member Axes, Displacements and Actions	49
6.1	Double Layer Structure Layout	59
6.2	Bar Member Axes, Displacements and Actions	60
6.3	Double Layer Structure Joints	63
6.4	Lower Layer Boundary Joints	68
7.1	Flowchart for Computer Program	81
7.2	Lines for Comparison - Single Layer Structure	88
7.3	Lines for Comparison - Double Layer Structure	88
7.4	Results for Single Layer Structure No 1 ($H_x=0.0$, $H_y=0.0$)	90
7.5	Results for Single Layer Structure No 2 ($H_x=+1.0$, $H_y=+1.0$)	92
7.6	Results for Single Layer Structure No 3 ($H_x=0.0$, $H_y=+1.0$)	95
7.7	Results for Single Layer Structure No.4 ($H_x=-1.0$, $H_y=+1.0$)	97
7.8	Results for Single Layer Structure No. 5 ($H_x=-2.0$, $H_y=+1.0$)	99

<u>FIGURE</u>	<u>DESCRIPTION</u>	<u>PAGE</u>
7.9	Result for Double Layer Structure No.6 (Hx=0.0, Hy=0.0)	102
7.10	Results for Double Layer Structure No 7 (Hx=+1.0, Hy=+1.0)	103
7.11	Results for Double Layer Structure No 8 (Hx=0.0, Hy=+1.0)	104
7.12	Results for Double Layer Structure No 9 (Hx=-1.0, Hy=+1.0)	105
7.13	Results for Double Layer Structure No 10 (Hx=-2.0, Hy=+1.0)	106
8.1	Single Layer Rigid Jointed Structure Response Quantities	118
8.2	Double Layer Pin Jointed Structure Response Quantities	118
8.3	Results for Single Layer Structures - Base Case	120
8.4	Results for Single Layer Structures - Vary Hy	121
8.5	Results for Single Layer Structures - Vary N and Lx	122
8.6	Results for Single Layer Structures - Vary Ix etc	123
8.7	Results for Double Layer Structure - Base Case	126
8.8	Results for Double Layer Structure - Vary Hy	127
8.9	Results for Double Layer Structures - Vary N and Lx	128
8.10	Results for Double Layer Structures - Vary D	129
9.1	Centre Deflection/Load Characteristics of Structure No 1 (Hx=0.0, Hy=0.0)	136

<u>FIGURE</u>	<u>DESCRIPTION</u>	<u>PAGE</u>
9.2	Centre Deflection/Load Characteristic of Structure No 2 ($H_x=+1.0$, $H_y=+1.0$)	137
9.3	Centre Deflection/Load Characteristics of Structure No 3 ($H_y=0.0$, $H_y=+1.0$)	138
9.4	Centre Deflection/Load Characteristics of Structure No 4 ($H_x=-1.0$, $H_y=+1.0$)	139
9.5	Centre Deflection/Load Characteristics of Structure No 5 ($H_x=-2.0$, $H_y=+1.0$)	140
9.6	Regions of Large Displacements	143
H.1	Lattice Layout	H-2
H.2	Lattice Member Actions and Displacements	H-2
H.3	Continuum Actions and Displacements	H-4
H.4	Member Crossing x face and y face	H-4
H.5	Repeating Lattice module	H-6
H.6	Deformation under strain ϵ_x	H-6
H.7	Double Layer Structure Layout	H-11
H.8	Continuum Shell	H-14

LIST OF TABLES

<u>TABLE</u>	<u>DESCRIPTION</u>	<u>PAGE</u>
4.1	Member Orientations and Properties	39
6.1	Double Layer Member Orientation and Properties	66
7.1	Operations, Computing Work and Storage Requirements for Finite Difference Method	75
7.2	Details of Test Structures for Single Layer Rigid Jointed Structure Analyses	83
7.3	Details of Test Structures for Double Layer Pin Jointed Structure Analyses	86
7.4	Computer Times and Storage Requirements for Single Layer Rigid Jointed Structure	107
7.5	Computer Times and Storage Requirements for Double Layer Pin Jointed Structure	107
8.1	Parameter Values for Single Layer Structures	116
8.2	Parameter Values for Double Layer Structures	117
A.1	Result of Operators on Trigonometric Functions	A-3
B.1	General Load Function Coefficients	B-3
B.2	Unit Point Load Function Coefficients	B-5
B.3	Unit Uniform Load Function Coefficients	B-6
H.1	Members crossing x and y faces	H-5

LIST OF SYMBOLS

(Note: Symbols or uses of symbols occurring in one section only are generally not listed.)

A	Member area
$a_{ij}, b_{ij}, \dots, f_{ij}$	Displacement fourier coefficients
D	Double layer structure separation distance
E	Member elastic modulus
E^*	Continuum shell elastic modulus
E_α^g, E_β^h	Finite difference shift operators
G	Member shear modulus
g, h	Change in α, β coordinate
H_X, H_Y	Rise of structure in X, Y direction
h^*	Continuum shell thickness
I_X, I_Y, I_Z	Member moments of inertia about x,y,z axes
$K_{11}, K_{12}, K_{21}, K_{22}$	Member stiffness submatrices in structure coordinate system
$[K(E_\alpha, E_\beta)]$	Matrix in governing partial difference equation
$k_{11}, k_{12}, k_{21}, k_{22}$	Member stiffness submatrices in element coordinate system
L	Member length
L_X, L_Y	Length of structure in X, Y direction
m_X, m_Y, m_Z	Member end moments about x,y,z axes
$m_\alpha, m_\beta, m_\gamma$	Member end moments about α, β, γ axes
N, M	Number of joints in structure in X, Y directions
$\{P_x\}$	Vector of member end actions in element coordinate system
$\{P_\alpha\}$	Vector of member end actions in structure coordinate system
$\{\bar{P}_\alpha\}$	Vector of member end actions at lower layer joints in structure coordinate system
$p_{ij}, q_{ij}, \dots, u_{ij}$	Load fourier coefficients
p_X, p_Y, p_Z	Member end actions in x,y,z directions
$p_\alpha, p_\beta, p_\gamma$	Member end actions in α, β, γ directions

$\overline{p}_\alpha, \overline{p}_\beta, \overline{p}_\gamma$	Member end actions at lower layer joints in α, β, γ directions
S	Member axial stiffness EA/L
$[T], [T^T]$	Transformation matrix for x, y, z to α, β, γ coordinates and its transpose
$[v]$	General matrix
v_{11}, v_{12} etc.	General matrix elements
$\{w_\alpha\}$	Vector of joint loads in structure coordinate system
$\{\overline{w}_\alpha\}$	Vector of joint loads at lower layer joints in structure coordinate system
$w_\alpha, w_\beta, w_\gamma$	Joint loads in α, β, γ directions
$\overline{w}_\alpha, \overline{w}_\beta, \overline{w}_\gamma$	Joint loads at lower layer joints in α, β, γ directions
X, Y, Z	Global coordinate system
x, y, z	Element coordinate system
α, β, γ	Structure coordinate system
$\{\Delta_x\}$	Vector of joint deformations in element coordinate system
$\{\Delta_\alpha\}$	Vector of joint deformations in structure coordinate system
$\{\overline{\Delta}_\alpha\}$	Vector of joint deformations at lower layer joints in structure coordinate system
$\delta_x, \delta_y, \delta_z$	Joint displacements in x, y, z directions
$\delta_\alpha, \delta_\beta, \delta_\gamma$	Joint displacements in α, β, γ directions
$\overline{\delta}_\alpha, \overline{\delta}_\beta, \overline{\delta}_\gamma$	Joint displacements at lower layer joints in α, β, γ directions
θ	Angle in transformation
$\theta_x, \theta_y, \theta_z$	Joint rotations about x, y, z axes
$\theta_\alpha, \theta_\beta, \theta_\gamma$	Joint rotations about α, β, γ axes
ν	Continuum shell Poissons ratio
π	= 3.14159... conventional use
σ	Angle in transformation
ϕ	Angle in transformation
ψ	Angle in transformation

CHAPTER ONE

INTRODUCTION

Lattice space structures are characterised by having many similar members (beams or rods) connected at joints that lie in or near a regular surface. An essential feature of these structures is that the structural action is three dimensional, and that they cannot be considered and analysed as assemblages of independent planar sub structures.

Such lattice space structures have become increasingly popular as a structural form over recent years. A use for such structures, particularly the doubly curved types considered in this thesis, is for roofing large column free areas such as may be required for sports arenas, warehouses, aircraft hangars, to name a few. There are many other applications for different types of lattice space structures and examples can be found in the literature [16, 45, 81, 94].

One requirement for large structures is that they are efficient in the use of materials. Another requirement is that they be aesthetically pleasing. Lattice space structures can meet both of these requirements and particularly so for large spans when conventional truss structures become heavy and may be unsightly. The inherent efficiency of the three dimensional action of space structures leads to economy of materials and the repetition of members aids the mass production of components and the subsequent assembly process. Recent conferences [16, 45, 81, 94] contain excellent background material on the use, design and construction of space lattice and other related structures.

1.1 PROBLEM STATEMENT

The analysis, and thus the design, of lattice space structures is not without its problems. A lot of the difficulties stem from the large size and complexity of the structures. Numerical techniques of

analysis have usually been based on conventional approaches such as the direct stiffness or finite element method. However, these methods tend to be expensive because the structure size, as characterised by the number of joints and members, is so great. Other methods involve spreading out the lattice properties to obtain an equivalent continuum and the solution of the resulting differential equations is by an analytic or numerical procedure. The testing of small scale models is yet another method that has been used.

These methods are examined in chapter 3 and as pointed out there, they are in some ways unsatisfactory. The problems usually take the form of expenses (of computer time or manpower) or excessive approximation. The present work is directed towards the application of a technique, the finite difference calculus, that gives adequate accuracy without being prohibitively expensive.

The finite difference method is described in chapter 2 and briefly, involves writing operator equations for the unknown quantities, displacements in this case. These operator equations are solved analytically for a functional solution for the unknown. The functions can be evaluated at any location the numerical solution is required.

It must be emphasised that the finite difference technique used here is not the same as that commonly used in numerical work as an approximate method of solving continuum problems. However it is not new and is the branch of mathematics that is naturally applicable, without approximation, to discrete structures. As outlined in chapter 2, it has been applied in the past to several structural types with some success.

1.2 CHAPTER DETAILS

The general method used is outlined in chapter 2 and applications to three classes of structures are made in chapters 4, 5 and 6. These three classes of structure are all doubly curved, in the form of second order surfaces, and bounded by rectangles. Pin jointed and rigid jointed single layer structures and pin jointed double layer structures are considered and the appropriate discrete mathematical model is formulated in each case. A solution which satisfies the equations and the boundary conditions is given in the form of a finite double trigonometric series.

Chapter 3 outlines other analysis methods that are generally available for these types of structures. Some indication of the capabilities and limitations of each method is given. This is done so that the results of the numerical procedures presented in chapter 7 can be viewed together with results from other methods. Also presented in chapter 7 is a computer program that is used to evaluate the solution. It is shown that this is viable both in terms of accuracy and cost.

After proving that the program works, it is used to obtain the response of the structures to changes of geometry and structural properties. The results of these numerical experiments are presented in chapter 8. Finally in chapter 9, the extension to account for non linear behaviour of the structure is considered.

The present work is intended to present and apply a technique (the finite difference calculus) to the problem of structural analysis and give some results for a small group of structures which are restricted in form and layout. It is not intended that this thesis is an exhaustive treatment of lattice space structures in general. There are many problems associated with such structures. These include the choice of geometry, member layout, joint design and structure buckling, to name a few which are not treated. The results which are given are

available directly to the structural analyst but it is envisaged that the method can be extended to other classes of structure with more general characteristics. The objective is to show that the method is applicable to curved lattice space structures.

CHAPTER TWO

FINITE DIFFERENCE CALCULUS METHOD2.1 INTRODUCTION

The use of the analytic method of finite differences in treating physical problems is not new. Prior to about 1900, there was a scientific hypothesis that "nature does not make jumps". On this hypothesis, continuity is the only permissible medium for constructing mathematical models of the physical universe. All changes were assumed to be continuous and "natural laws" were expressible as equations between rates of change. Thus it was thought that differential equations were the proper mathematics of the physical sciences. About 1900 with the advent of quanta in radiation theory and of genetics in biology, it was seen that not all natural phenomena are conveniently described in terms of continuity. It was about this time that the use of finite differences increased and applications were made in various fields of study.

The next section gives the background of the development of the mathematics of finite differences and section 2.3 outlines the development of finite difference methods applied to structural mechanics.

2.2 REVIEW OF FINITE DIFFERENCE CALCULUS

Although, as explained previously, the general use of finite differences started about 1900, there were some theoretical results available much earlier than this. The beginnings of the calculus of finite differences are traceable to the early 1700's with Stirling [80] and Bernoulli [6] and later in the 1750's with Euler [31]. These early developments were principally to facilitate numerical calculation by interpolation formulae in the areas of astronomy, table construction and mechanical quadrature. Later there were applications in combinational analysis and probability theory, especially by Laplace [53]. Boole [9]

in 1860 summarises most of the work that had been done before that time and, although much of the theory has since been updated and extended, this text does contain many results which are still relevant.

At that stage, the calculus of finite differences had developed into three inter-related branches: the difference calculus, the summation calculus and the theory of difference equations. The first two are concerned mainly with numerical methods of interpolation and approximate integration using finite differences. The last topic of difference equations is mainly of an analytic nature and is the branch used in this thesis. Boole, in his text, treats all three of these branches of the calculus.

The modern theory of difference equations starts with Poincaré [65] in 1885 with his treatment of the general linear difference equation with variable coefficients. Birkhoff [7] gave a treatment in 1911 and after this there appeared many texts on the calculus of finite differences. The notable ones are by Nörlund [62], Steffensen [79], Milne-Thompson [59], Fort [35] and Jordan [51]. All of these treat the three branches of the finite difference calculus and span the period from the early 1900's to 1950.

In the 1950's with the development of the digital computer, there was an increase in the use of finite differences in numerical methods. Many texts appeared on this aspect of finite differences but they are not of much use to the analytic theory.

More recently, some texts on the analytic theory of finite difference equations have been published. These include Levey and Lessman [54], Brand [10], Saaty [74] and Miller [58]. All of these treat finite difference equations in their own right without concentrating on the numerical procedures. While most available texts treat only linear equations, Saaty [74] treats simple non-linear equations.

2.3 REVIEW OF APPLICATION OF FINITE DIFFERENCE CALCULUS TO STRUCTURAL MECHANICS

The first major application of the finite difference calculus to structural mechanics was in 1927 with the publication of the text by Bleich and Melan [8]. This work, in German, although extensive and thorough was very general and did not emphasise the savings in computational effort that could be obtained with certain classes of structures. Possibly because the method did not apparently offer any advantage over other better known methods, no significant development followed for a considerable period.

In 1940, Von Karman and Biot [85] presented a short treatment of the uses of finite differences in engineering. They considered stresses in a continuous beam on equidistant supports, the stability of a latticed truss and other examples of electrical and mechanical systems. In a similar manner, Pipes [64] in 1946 gave some examples of engineering systems analysed by finite difference techniques.

The static analysis of a beam grillage was treated by Holman [43] and also by Ellington and McCallion [29], both in 1957. These marked a revised interest in the use of finite difference methods. In 1959, Ellington and McCallion extended their treatment to include the dynamic analysis of a beam grillage [30].

The developments of Dean and his associates over the period from 1959 to the present (1977) include much which is relevant to the treatment here. In 1959, Dean and Tauber [17] derived the finite difference models for regular parallel chord Vierendeel and triangulated trusses and gave closed form solutions to these equations. They argued for further use of finite difference techniques. In 1960 they published a paper [83] containing the mathematical background for solutions of finite difference equations.

A paper by Dean [18] in 1960, extended the use of finite difference techniques to three dimensional structures by reducing the problem to an equivalent one dimensional model for which a solution was presented. Appendices to this paper presented the solutions for difference equations with symmetric quartic operators in one variable.

There was a further significant extension in 1963, when Dean and Ugarte [19], presented the analysis of regular net-like structures. This involved formulating a mathematical model for the vertical deflexion of the regularly spaced joints of the cables of the net. The model was an equation for a single dependent variable (the vertical deflexion of the joint) of two independent variables (the coordinates which describe the location of the joint in the structure). The two components of the horizontal deflexion were neglected in this analysis. A solution was proposed in the form of a double trigonometric series and both uniform and general load cases were considered. A similar method was used by Dean [20] to analyse a beam composed of regularly interconnected lamellas. A grid constructed in a similar manner was also analysed.

In a dissertation in 1965, Ugarte [84] considered the analysis of latticed structural shells using finite difference calculus methods. She used a stress function approach to obtain a solution for the equilibrium equations of a statically determinate lattice structure. Various shapes of structure were considered including a shell of revolution under symmetric loading, a right conoid and a hyperbolic paraboloid. The force deformation relations were also considered and a finite series type solution was presented for the deformations of a cylindrical latticed shell. The treatment considered only members with axial loads and pin-jointed ends.

Dean [21] also in 1965, presented the static analysis of several lattice shells which were internally statically determinate. He proposed a stress function type solution to the equilibrium equations for a hyperbolic paraboloid and an elliptic paraboloid. For these structures to be statically determinate, it was possible to consider only one degree of freedom for each joint and thus only vertical loads. The member layout differs somewhat from that treated in this thesis, so the two cannot be compared directly.

The dissertation by Mithaiwala [60] in 1968, presented the analysis of cylindrical ribbed and latticed shells. In this he presented a micro analysis where he started with the basic elements and obtained a governing equation. The solution was then obtained by a method of summation over the whole structure. Also presented was a macro approach where the total structure was considered as the starting point. Any unknown interactions at nodal points were determined by considering compatibility of deformations at the nodes. These two approaches are broadly equivalent to the stiffness and flexibility methods of structural analysis. Mithaiwala used these two methods to demonstrate the advantages of each. His solution in both cases was in the form of a finite double trigonometric series for the displacements.

The application of finite differences to two dimensional frames by Dean and Ugarte [22] is of considerable relevance to this thesis, even though it did not consider a space structure as such. The techniques used there for the formulation and solution of the system of governing partial difference equations are very similar to the techniques used in this thesis. Given as an appendix to the paper is a treatment of the use of finite series solutions for difference equations and an outline of the requirements for the form of the equations and for the boundary conditions so that a series solution is viable.

The use of finite difference techniques to a non-linear structure was demonstrated by Avent [2] in 1969. The vertical displacements and the forces in a two-way network of prestressed cables, under static out-of-plane loading were determined by solving a set of finite difference equations numerically by a walk-through method so that equilibrium was satisfied at each joint in turn. Non-linear behaviour was considered along with various shaped boundaries. Even though a numerical solution was developed, the use of finite difference techniques resulted in less effort being required than would have been the case if a more conventional analysis method had been used.

Dean and Gang Rao [24] used the macro approach to analyse structures which consist of an assemblage of discrete and continuous components. The resulting models involved summation equations and summation-integral equations. The important aspect of this approach is the ability to analyse structures where discrete and continuous components interact.

Other papers of interest given in the bibliography [3, 23, 26, 36, 77] treated various shapes and types of structure. Many of the presentations noted above are summarised in the paper by Dean and Avent [27] which outlines the state of the art up to the Second International Conference on Space Structures [81] held in 1975.

Another researcher who used finite difference techniques was Wah with publications from 1963 to 1970. He considered in the main, uniform grillages [86, 87, 88, 89] subject to static and dynamic loads as well as stability problems. The solutions generally took the form of finite trigonometric series. In another paper [90], Wah presented the stability analysis of a stiffened plate under in-plane compression. Along with some other material, the results in the papers above are presented in a text by Wah and Calcote [91] published in 1970. This text represents one of the few attempts to collect such material and present it in a form suitable for general use and teaching.

Renton also made use of the finite difference calculus in the analysis of grillages, space grids and trusses [67, 68, 69, 70, 71, 72]. Renton's techniques generally involved formulating the mathematical model of the physical system as difference equations. These were then either solved directly in terms of elementary functions or transformed, by using a Taylor series expansion, to an approximate differential equation. This latter equation would then be solved. In effect this was forming an analogy between the discrete system and a continuous one. While this technique does introduce approximations into the model, it demonstrates one means of using the finite difference calculus in formulating the analysis of a structure.

Other researchers include Gutkowski [40, 41] who analysed a cylindrical space lattice, Suzuki, Kitarmaru and Yamada [82] with the analysis of a double layer flat grid, Hussey, Tarzi and Theron [44] also with the analysis of a double layer flat grid, and Grigorian [38, 39] who gave the vibration analysis of multi-thread networks and of flat gridworks of Vierendeel trusses.

Sherman et al presented a bibliography [75] as at 1972 and a state-of-the-art report [76] as at 1976 on the broad topic of lattice structures generally. While it considered many facets other than the structural analysis, the bibliography [75] gives many references on this topic and in particular on the use of finite difference techniques in the analysis procedure. The use of finite differences was treated in some detail in the report [76] and it is certainly a good starting point to obtain an introduction to the subject as well as references to further material.

2.4 CHARACTERISTICS OF SUITABLE STRUCTURES

The type of structure that is suitable for analysis by the analytic techniques of finite differences is characterised by a regular layout of discrete components such that the structure may be sub-divided into a number of identical modules. Within each module, the number, the geometric layout and mechanical properties of the joints and members are the same as in any other module. The internal complexity of the module determines, to some extent, the complexity of the analysis process.

Chapter 4 treats a single layer structure with a module containing one joint and six members each capable of resisting axial forces only, while chapter 5 extends this treatment to account for members which can resist bending. Chapter 6 considers a double layer structure with a more complex module which contains two joints and fifteen pin jointed members.

If the structure cannot be sub-divided into identical modules, it may still be possible to formulate the analysis problem by using the finite difference techniques, but in general for such cases it is not possible to find an analytic solution. In these cases the major advantage of the method is lost and other methods (e.g. direct stiffness) may prove easier to use.

The main treatment in this thesis considers linear elastic behaviour of the members and of the total structure. One implication of this is that the member stress levels due to any loading are such that member strains and displacements are small. This is to ensure that the member behaves linearly elastically and that no member buckling or other non-linear behaviour can occur. Another implication is that the total structure deformations are small so that structure buckling does not occur.

Extension of the method to non-linear behaviour, both material and geometric will be considered in chapter 9.

2.5 OUTLINE OF GENERAL METHOD

The remainder of this chapter contains an outline of the general method of using the finite difference calculus to analyse regular structures. The purpose of this outline is to show how the analysis is developed without delving into the fine detail that is necessary for the analysis of particular structures. Chapters 4, 5 and 6 contain the detailed application of the method to three classes of structures.

2.5.1 Member Relations

Consider a component element which may be any structural element say a bar, a beam or a shell segment. For this element load-deformation relations in the local or element coordinate system (e.g. x, y, z) can be determined from slope deflexion equations or by finite element methods. These are the same as the element stiffness relations as used in the direct stiffness method and can be written as

$$\begin{Bmatrix} \{P_x\}_1 \\ \{P_x\}_2 \end{Bmatrix} = \begin{bmatrix} k_{11} & k_{12} \\ k_{21} & k_{22} \end{bmatrix} \begin{Bmatrix} \{\Delta_x\}_1 \\ \{\Delta_x\}_2 \end{Bmatrix} \quad \dots (2-1)$$

where $\{P_x\}_1$, $\{P_x\}_2$ are vectors of the member end actions at ends 1 and 2 of the member, and $\{\Delta_x\}_1$, $\{\Delta_x\}_2$ are the vectors of the end displacements. These are shown in figure 2.1. The size of the vector depends on the complexity of the element. For a bar member the vectors $\{P_x\}_1$ etc. have three members and for a beam member they have six members. The matrices $[k_{11}]$, $[k_{12}]$, $[k_{21}]$ and $[k_{22}]$ contain the stiffness properties of the element and as noted above can be obtained from the slope deflexion equations.

These relations are in a coordinate system that is related to the individual member and as the members may have differing orientations, the

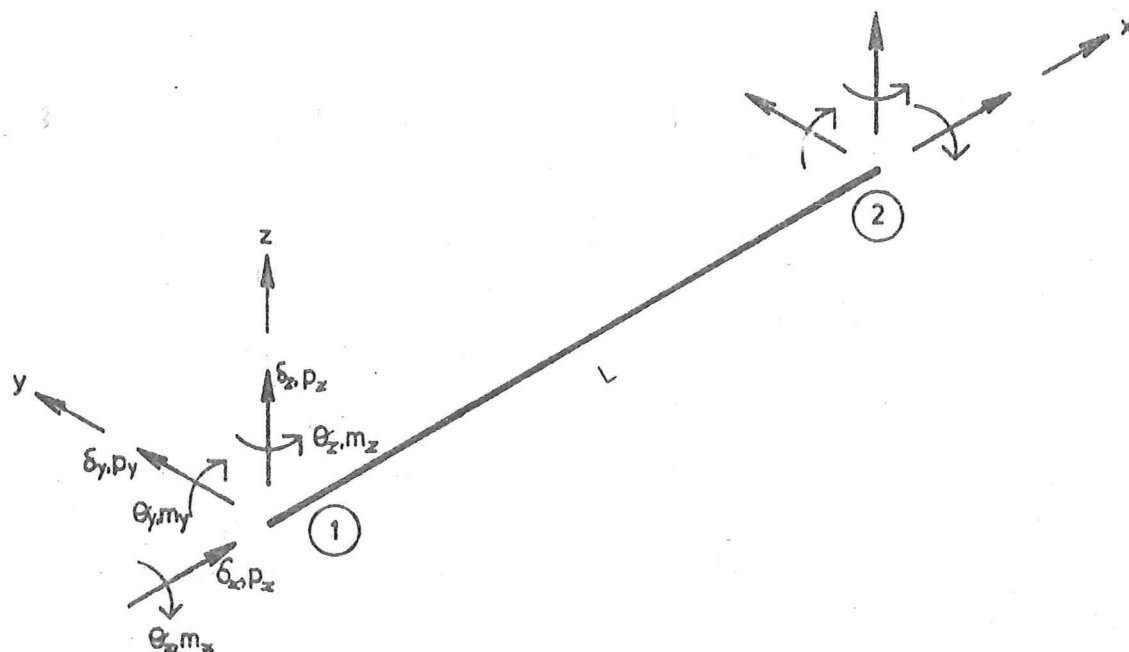


Fig. 2.1 BEAM MEMBER AXES, DISPLACEMENTS AND ACTIONS.

coordinate system may be different for each member. In order to form equilibrium equations at a joint where several members meet, the member end actions and displacements are transformed into a more convenient coordinate system that is related to the structure. This structure coordinate system (α, β, γ) need not be a cartesian one and in general a curvilinear one may be more convenient. For such a case, the transformations between the element and structure coordinate systems will differ at the two ends of the member. These transformations can be written as

$$\begin{aligned} \{P_{\alpha}\}_i &= [T_i] \{P_x\}_i \\ \{\Delta_{\alpha}\}_i &= [T_i] \{\Delta_x\}_i \end{aligned} \quad \dots (2-2a)$$

where $i = 1$ or 2 denotes the appropriate end of the member. The vectors $\{P_{\alpha}\}_i$ and $\{\Delta_{\alpha}\}_i$ are the actions and displacements in the structure coordinate system and the vectors $\{P_x\}_i$ and $\{\Delta_x\}_i$ are actions and displacements in the member coordinate system. The transformation matrices

$[T_i]$ are composed of direction cosines and for an orthogonal transformation as considered here, the inverse of $[T_i]$ is also the transpose of $[T_i]$.

Thus

$$\begin{aligned} \{P_x\}_i &= [T_i^{-1}] \{P_\alpha\}_i = [T_i^T] \{P_\alpha\}_i \\ \{\Delta_x\}_i &= [T_i^{-1}] \{\Delta_\alpha\}_i = [T_i^T] \{\Delta_\alpha\}_i \end{aligned} \quad \dots(2-2b)$$

Carrying out these transformations, firstly of the end displacements gives

$$\begin{Bmatrix} \{P_x\}_1 \\ \{P_x\}_2 \end{Bmatrix} = \begin{bmatrix} k_{11}T_1^T & k_{12}T_2^T \\ k_{21}T_1^T & k_{22}T_2^T \end{bmatrix} \begin{Bmatrix} \{\Delta_\alpha\}_1 \\ \{\Delta_\alpha\}_2 \end{Bmatrix} \quad \dots(2-3)$$

This relates the member end actions in the member coordinate system to the member end displacements in the structure coordinate system and it will be used in section 2.5.7 to determine the member actions.

Secondly, transforming the end actions gives

$$\begin{Bmatrix} \{P_\alpha\}_1 \\ \{P_\alpha\}_2 \end{Bmatrix} = \begin{bmatrix} T_1k_{11}T_1^T & T_1k_{12}T_2^T \\ T_2k_{21}T_1^T & T_2k_{22}T_2^T \end{bmatrix} \begin{Bmatrix} \{\Delta_\alpha\}_1 \\ \{\Delta_\alpha\}_2 \end{Bmatrix} \quad \dots(2-4)$$

which can be abbreviated to

$$\begin{Bmatrix} \{P_\alpha\}_1 \\ \{P_\alpha\}_2 \end{Bmatrix} = \begin{bmatrix} K_{11} & K_{12} \\ K_{21} & K_{22} \end{bmatrix} \begin{Bmatrix} \{\Delta_\alpha\}_1 \\ \{\Delta_\alpha\}_2 \end{Bmatrix} \quad \dots(2-5)$$

where

$$[K_{ij}] = [T_i] [k_{ij}] [T_j^T] \quad \dots(2-6)$$

for $i = 1, 2$ and $j = 1, 2$

Relation 2-5 gives the member end actions in terms of the end displacements where all quantities are in the structure coordinate system. As it is only necessary to consider the end actions at one end of the member when writing equilibrium equations, it is convenient to partition relation 2-5 to give the end actions at end 1 as

$$\{P_\alpha\}_1 = [K_{11}] \{\Delta_\alpha\}_1 + [K_{12}] \{\Delta_\alpha\}_2 \quad \dots(2-7)$$

2.5.2 Shift Operators

The joint displacement vector is different for each joint and can be considered as a function of the joint coordinates. Thus if end 1 of the member considered in section 2.5.1 has coordinates (α, β) then end 2 has coordinates $(\alpha + g, \beta + h)$, where g and h depend on the member length and orientation with respect to the α and β axes. The member end displacements can then be written as

$$\{\Delta_{\alpha}\}_1 = \{\Delta_{\alpha}(\alpha, \beta)\} \quad \dots(2-8)$$

$$\{\Delta_{\alpha}\}_2 = \{\Delta_{\alpha}(\alpha + g, \beta + h)\} \quad \dots(2-9)$$

It is convenient to introduce here the finite difference shift operator defined by the relation

$$E_k^j f(k) = f(k + j)$$

where $f(k)$ is a function of the variable k and E_k^j is the finite difference shift operator of order j on variable k . It is seen that the effect of the shift operator on a function is to give the value of the function at a displaced value of the argument.

Using this concept, the end displacement at end 2 of the member can be expressed as

$$\begin{aligned} \{\Delta_{\alpha}\}_2 &= \{\Delta_{\alpha}(\alpha + g, \beta + h)\} \\ &= E_{\alpha}^g E_{\beta}^h \{\Delta_{\alpha}(\alpha, \beta)\} \end{aligned} \quad \dots(2-10)$$

where E_{α}^g and E_{β}^h are the finite difference shift operators of orders g and h in the α and β directions respectively. Substituting these into the previous relation 2-7 for the member end action gives

$$\begin{aligned} \{P_{\alpha}(\alpha, \beta)\} &= [K_{11}] \{\Delta_{\alpha}(\alpha, \beta)\} + [K_{12}] \{\Delta_{\alpha}(\alpha + g, \beta + h)\} \\ &= [K_{11}] \{\Delta_{\alpha}(\alpha, \beta)\} + [K_{12}] E_{\alpha}^g E_{\beta}^h \{\Delta_{\alpha}(\alpha, \beta)\} \\ &= \left[[K_{11}] + [K_{12}] E_{\alpha}^g E_{\beta}^h \right] \{\Delta_{\alpha}(\alpha, \beta)\} \end{aligned} \quad \dots(2-11)$$

The vector $\{P_{\alpha}(\alpha, \beta)\}$ contains the member end actions at end 1 which is at coordinates (α, β) and is also considered a function of the coordinates.

2.5.3 Equilibrium of Typical Joint

As several members meet at the typical joint at coordinates (α, β) , the sum of the effects of all such members must be obtained to get the total joint reaction, which for equilibrium must balance the applied joint load. The member end actions as given in the relation 2-11 for a single member are summed over all members meeting at the joint to give

$$\begin{aligned} \{W_{\alpha}(\alpha, \beta)\} &= \sum_{i=1}^n \{P_{\alpha}(\alpha, \beta)\}_i \\ &= \left[\sum_{i=1}^n \left([K_{11}]_i + [K_{12}]_i E_{\alpha}^{g_i} E_{\beta}^{h_i} \right) \right] \{\Delta_{\alpha}(\alpha, \beta)\} \quad \dots(2-12) \end{aligned}$$

where subscript i designates the member, from 1 to n , and $\{W_{\alpha}(\alpha, \beta)\}$ is the vector of applied joint loads. The equation 2-12 can be abbreviated to

$$\{W_{\alpha}(\alpha, \beta)\} = [K(E_{\alpha}, E_{\beta})] \{\Delta_{\alpha}(\alpha, \beta)\} \quad \dots(2-13)$$

$$\text{where } [K(E_{\alpha}, E_{\beta})] = \left[\sum_{i=1}^n \left([K_{11}]_i + [K_{12}]_i E_{\alpha}^{g_i} E_{\beta}^{h_i} \right) \right] \quad \dots(2-14)$$

This is for the case where the typical module as described in section 2.4 contains only one joint. Where the typical module contains more than one joint, the basic procedure is similar except that the final assembly of $[K(E_{\alpha}, E_{\beta})]$ is more complex and consists of sub-matrices giving the equilibrium relations at each joint in the module. An example of a structure with two joints in the typical module is treated in chapter 6.

The relation 2-13 is a system of linear partial difference equations for the vector of unknown displacement functions $\{\Delta_{\alpha}(\alpha, \beta)\}$, given the member properties (contained in the matrices $[K_{11}]_i$ and $[K_{12}]_i$), the member orientations (contained in g_i and h_i) and the vector of applied joint loads $\{W_{\alpha}(\alpha, \beta)\}$.

The elements of $[K(E_{\alpha}, E_{\beta})]$ involve the finite difference shift operators E_{α} and E_{β} and may also involve the coordinates of the joint i.e. α and β . When the joint coordinates are involved, it means the

structure is not regular and that the geometry and/or member properties vary with the coordinates. For such cases the solution to equation 2-13 is very difficult and may be analytically intractable.

For the more special cases of a regular structure, the elements of matrix $[K(E_\alpha, E_\beta)]$ while still involving the shift operators E_α and E_β do not involve the coordinates α and β . Such cases are treated in this thesis and for them, equation 2-13 is a system of linear partial difference equations with constant coefficients.

2.5.4 Boundary Conditions

The boundary conditions on a structure are of two types. Firstly there are conditions on the boundary displacements and secondly there are conditions on the boundary force reactions. These can be illustrated by a diaphragm type support to a lattice structure. For such a diaphragm, the displacement in the plane of the diaphragm must be zero and the displacements normal to the diaphragm are unrestricted. Where rotational deformations are possible, further conditions are required. The force conditions for a diaphragm are that the forces in the plane of the diaphragm are unrestricted and the forces normal to the diaphragm must be zero. Where moments are possible, there are further conditions on them.

Because the forces at a joint, due to the members meeting there, can be related to the displacements at that joint and at adjacent joints (those at the far ends of the members considered), it is possible to formulate the force boundary conditions as conditions on the displacements. For the finite difference model of a lattice structure, the force boundary conditions will involve the shift operators acting on the displacement functions.

2.5.5 Solution Form

The form of the solution used is a series of the eigenfunctions of the homogeneous equations together with the boundary conditions. For

a finite difference equation on a finite interval, the number of distinct eigenfunctions is also finite and these eigenfunctions are mutually orthogonal over that interval. Because there are only a finite number of eigenfunctions, the series solution contains a finite number of terms and thus there is no concern about convergence of the series as is necessary with the infinite series of eigenfunctions of a differential equation.

The non-homogeneous or loading terms (vector $\{W\}$ in equation 2-13) must also be expanded into a series of the eigenfunctions. This does not impose any restriction on the form of the loading as an arbitrarily general discrete function over the finite interval considered can be expanded into such a series by numerical methods. In some special cases, it is possible to obtain analytic expressions for the series coefficients and this reduces the numerical calculations.

The assumed series form for the displacements and the series expansion for the loading terms are substituted into the equations and, because of the orthogonality of the eigenfunction, term for term matching results in equations for the displacement series coefficients. These equations, one for each series term, are solved analytically if possible or numerically otherwise.

From the description above it will be seen that the requirements for a series of orthogonal functions (the eigenfunctions) limits the method to those cases where the appropriate eigenfunctions of the difference equation and the boundary conditions can be found. For a specific type of structure viz. one on a shallow second order surface and bounded by a rectangle with diaphragm type supports, the appropriate eigenfunctions are combinations of trigonometric sine and cosine functions. This is the shape of the structures considered in detail in chapters 4, 5 and 6 of this thesis.

2.5.6 Displacements

Once all the displacement series coefficients have been determined they can be used in the evaluation of the series to give the displacements of the joints. This evaluation would generally be done numerically and only at one joint at a time. The computational effort involved is the same for each joint, and thus, if only one or a few joint displacements are required, then only these should be evaluated with the series.

In passing it will be noted that the direct stiffness method of analysis requires all displacements to be evaluated whether they are required or not. By this selective evaluation of the displacement series, the finite difference method offers some saving in computational effort.

2.5.7 Member Actions

Having evaluated the displacements at the two ends of a member, they can be used in expression 2-3 to determine the member end actions. This expression gives the member actions in the member local coordinate system.

2.5.8 Joint Residuals and Reactions

The resultant action at a joint due to all the members meeting there can be determined numerically after the joint displacements are known. Expression 2-7 or 2-11 is used to determine the member actions in the surface coordinate system for each member. The sum from all members meeting at a joint should balance the applied joint load at the internal joints. Any difference between them is an indication of computational error.

For boundary joints, the residual joint force from the members meeting there is balanced by the reaction of the boundary.

CHAPTER THREE

ALTERNATIVE ANALYSIS METHODS3.1 INTRODUCTION

The methods which are presently available to analyse a lattice space structure can generally be classified as belonging to one of four approaches. One of these is the finite difference method discussed in chapter 2. The others are the direct stiffness method, the analogous continuum method and the physical model method. The bibliographies [75,76] are the source of many references on analysis methods.

In order to compare the performance of the finite difference method with the performance of the other methods, a brief description of them is given in this chapter. Indications of the uses and restrictions are given for each method. In chapter 7 there is presented the results of analysis, by the finite difference method, the direct stiffness method and the analogous continuum method, of several space frames. These analyses are used to compare the performance of the methods.

3.2 DIRECT STIFFNESS METHOD

The direct stiffness method of analysis is the most common numerical method of structural analysis in use at present. It is one of a group of methods that involve solving systems of linear algebraic equations and, in most cases, proves the easiest to apply. The method is capable of handling structures with almost any layout of members and joints. It is also possible to consider a wide variety of boundary conditions. There are many more mathematical methods, e.g. flexibility coefficients, slope deflexion, moment distribution and others, but these are for special applications or are variations of the direct stiffness approach.

The direct stiffness method for a linear structure is described in many papers and texts on structural analysis, e.g. [48, 73]. In applying any mathematical method to a physical problem it is necessary to make certain assumptions and simplifications. Those made in using the direct stiffness method for a framed structure are that the properties of the section are assumed to be concentrated on their centrelines and that these line members are assumed to be connected together at the joints or nodes. Thus the structure is idealised to a system of lines and points representing the structure members and joints respectively. The member material is assumed to be linearly elastic and also the member deformation and the structure deflexions are assumed to be small. This is necessary so that the resulting system of simultaneous equations is linear. The possible extension to non linear behaviour will be considered later in this section.

The analysis procedure starts with the member and forms, numerically, the stiffness matrix relating the joint forces and the joint deformations. For frame members the joints are at the two ends of the member. The size of the stiffness matrix depends on the member deformations that are considered significant. For members that can resist only axial loads, the linear displacements of the two ends are relevant and as there are three of these at each of the two ends, the stiffness matrix has six rows and six columns. When the member can resist transverse bending, torsion and shear as well as axial loads, the relevant displacements are three linear displacements and three rotations at each end. The member stiffness matrix then has 12 rows and 12 columns.

When all the member stiffness matrices have been formed they can be assembled into the total structure stiffness matrix. The assembly is performed according to the connectivity of the members and involves summing, at each joint, the effects of all members that meet there.

The total structure stiffness matrix relates the joint forces on the total structure to the joint displacements, and this matrix is square of size 3 (for pin joints) or 6 (for rigid joints) times the number of joints less any boundary constraints.

The system of equations involving the structure stiffness matrix and the applied joint loading is solved for the joint displacements. Once these joint displacements are known, the member end actions can be determined from the member stiffness matrices and any boundary reactions can be computed from the total structure stiffness matrix or from the member end actions.

When a structure undergoes large displacements or the material does not have a linear stress strain relationship, then the resulting equations are non linear. For such cases it is possible to use an incremental method where the structure is linearized and subjected to a series of small load increments. In this way, the response of the structure can be found. For some types of problems it is possible to use an iterative approach for non linear behaviour.

In making use of the direct stiffness method, the structural analyst is faced with certain assumptions, requirements and problems and he should be aware of them.

The method idealizes the frame as a set of line members that meet at points. For the types of structures that are considered in this thesis, this is a good representation. Other types of structure, particularly ones with short, deep members, would not be as accurately represented by lines and points.

The volume of numerical work in using the method, makes the use of a digital computer necessary. There are available many standard computer programs, e.g. [12, 32, 55] to perform the required computa-

tions. In general, these programs try to simplify and ease the burden of data preparation that is needed. Even so, the amount of data is generally large as it is necessary to specify, either explicitly or implicitly, the coordinates of every joint, the connectivity and properties of every member and the applied loading on every joint. The task of preparing and subsequently checking this data is generally very time-consuming. This process of checking for erroneous data is particularly important, as a complete re-analysis is necessary if mistakes in the data are made. If the analyst requires a change of layout, boundary conditions or loading, a re-analysis is also required.

It was noted earlier that a digital computer is required because of the volume of numerical work. One aspect of this is that the computation time and the storage requirement needed to analyse a given structure may be prohibitive unless efficient methods are devised. The greatest need is during the process of solving the system of equations and much work has been devoted to this [46, 61, 78]. For a given computer there is a limit to the size of the structure that can be analysed using fast, or primary, storage. It is possible to analyse larger structures by using slower secondary storage, i.e. magnetic discs and tapes, but this involves increased computation time. The trade-off between computer time and storage is characteristic of this type of problem.

A further aspect of the large volume of calculations is a danger of inaccuracy in the computing process of truncation of products and sums. This can cause the results of the analysis to be erroneous and before the analysis is performed, it is difficult to assess if and when this may happen. Indeed, even after the computer results are known, it is not always possible to know if significant error has occurred.

3.3 ANALOGOUS CONTINUUM METHOD

The analogous continuum method makes use of the postulate that a discrete lattice structure can be approximated by a continuum. The method has been used by many investigators for various types of structures, e.g. [5, 14, 70] and in particular for lattice space structures, e.g. [15, 33, 57, 71, 92, 93].

Several assumptions and approximations need to be made to use this method of analysis. The usual ones are that the deformations of the members and structure are small and that the material of the lattice members and of the continuum is linearly elastic. These are so that the behaviour of the structure is linear.

There are two basic approaches in determining the analogous continuum. In the first, the approximating continuum is a shell-like structure with mechanical properties determined from the properties of the discrete lattice. For this approach the deformations of the shell and the lattice are assumed to be the same at the node points, and the stress resultants in the shell are assumed to be statically equivalent to the member actions in the lattice. These assumptions give continuum strain/member deformation and continuum stress/member action relationships which can be combined with the member deformation/member action relationship, from the lattice member properties, to yield the continuum stress/strain relationship. This stress/strain, or constitutive, relationship can then be used in a classical shell theory to produce a differential equation describing the behaviour of the shell and hence describing the approximate behaviour of the lattice.

The second approach involves formulating the structural problem in the lattice by a finite difference technique to produce finite difference equations for the unknowns, e.g. displacements. These unknowns which only have any significance at the discrete nodes in the

lattice, are now approximated by continuous functions and the finite difference equations are approximated by differential equations - the reverse of the more common procedure. There results a differential equation which approximately describes the behaviour of the lattice.

The two approaches result in a governing differential equation which, together with mathematical statement of the boundary conditions, may be solved for the continuum displacements when the structure load is given. Knowing the continuum displacements and hence by analogy, the lattice frame displacements, it is possible to determine the member actions and so complete the solution.

In practice, the solution of the differential equation may be very difficult or even analytically intractable. For some very restrictive cases, the equations may be the same as those for a homogeneous, isotropic shell. In such cases, any known solutions, e.g. [34, 37, 47] can be used. More general layouts of the lattice may result in the equations being similar to those for a non-homogeneous and anisotropic shell for which there are no available general analytic solutions. Where there is no analytic solution for the shell and in the most general case where the equations do not have an analogous shell, the analyst must resort to the use of a numerical solution of the differential equations. The use of such a numerical solution can be as time-consuming as the original lattice problem but because of the approximations made, the solution may be less accurate.

In using the method, the accuracy attained depends on many factors. Some of the factors that lead to greater accuracy include a "fine" lattice spacing when compared with the overall size of the structure and a "smooth" loading function. The geometry also has a large effect on the accuracy and shapes where the member actions are principally axial forces and bending stresses are low, lead generally

to better results.

The amount of computation involved in using the method is dependent on the technique used to solve the differential equations. It can vary from very little (e.g. use of a slide rule) to a great amount requiring a digital computer. For certain shapes and layouts where the effort is small to moderate and the accuracy reasonable, the method is excellent as a design tool. By using it, the designer can obtain stress and deformation distributions under the given loading. This may be sufficient as a final design or a more powerful analysis may be required.

3.4 PHYSICAL MODEL METHOD

This method of analysis involves constructing a physical model, such as a small-scale replica, which mimics the characteristics of the full sized structure. In the past, the method has been used for many types of structures [11, 13, 42] including lattice space frames [4, 56, 63].

There are some problems with the use of such models as it is very difficult to construct a model that will represent all the characteristics of the structure with sufficient accuracy. It is sometimes possible to model some of the characteristics adequately but not all of them. This gives rise to errors in the model analysis.

The most common type of model is the small-scale replica. For lattice space structures, such models tend to be intricate with many members and joints and thus the construction of such models needs meticulous care. Instrumentation also causes problems for small models because the size of the instruments may have an appreciable effect on the model structure and hence on the results.

The effect of such problems is to make the use of physical models both time-consuming and expensive. Their use is generally restricted to research projects and analysis checks on unusual structures. They would not generally be suitable as initial design tools.

CHAPTER FOUR

ANALYSIS OF A SINGLE LAYER PIN JOINTED STRUCTURE4.1 DESCRIPTION OF THE STRUCTURE

The structure treated in detail in this chapter is one with the joints lying in a single layer defined by the shallow second order surface (fig. 4.1).

$$Z = 4 \left[H_X \left(\frac{X}{L_X} \right) \left(1 - \frac{X}{L_X} \right) + H_Y \left(\frac{Y}{L_Y} \right) \left(1 - \frac{Y}{L_Y} \right) \right] \quad \dots(4-1)$$

and bounded by diaphragm type supports on a rectangular boundary at $X = 0$, $X = L_X$, $Y = 0$ and $Y = L_Y$. H_X and H_Y are the rises of the surface in the X and Y directions respectively.

For various values of the parameters H_X and H_Y , this surface is the shape of an elliptic paraboloid (fig. 4.1a), hyperbolic paraboloid (fig. 4.1b), translational paraboloid (fig. 4.1c and 4.1d) or a flat surface.

A small portion of the structure is shown in figure 4.2a to indicate the layout of the joints and members in the surface. The typical module contains one joint which has six members framing into it. The orientation and layout of these members is shown in figure 4.2b. It will be seen that the members form triangles on the surface of the structure. For the structure to be regular, both the triangles and the joint layout must be uniform which is only possible on a flat or singly curved surface. However, an approximately regular layout can be obtained on a shallow doubly curved surface.

In this chapter members are restricted to those with pin jointed ends. The members are only subject to axial loads. Linear behaviour of the structure is assumed.

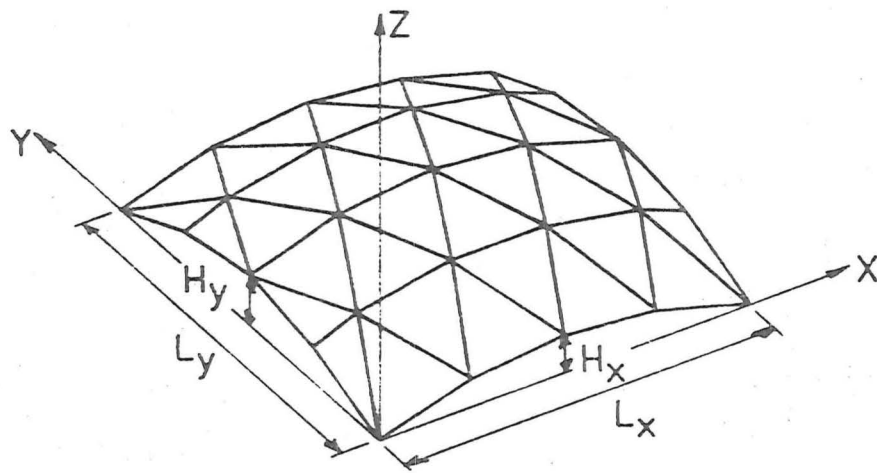


Fig. 4-1a ELLIPTIC PARABOLOID

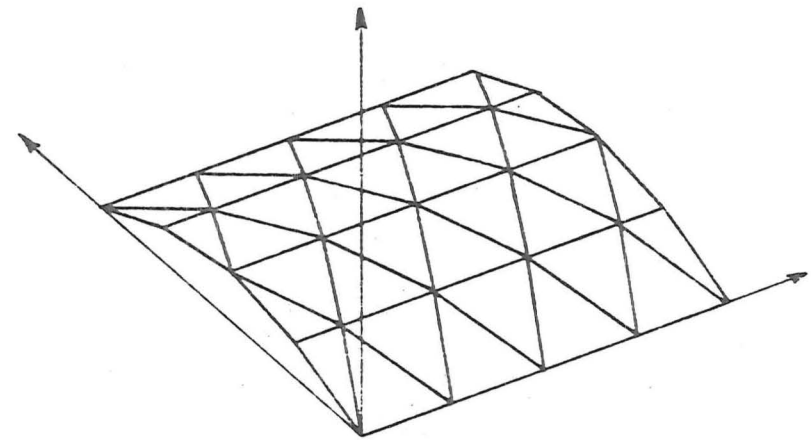


Fig. 4-1c TRANSLATIONAL PARABOLOID

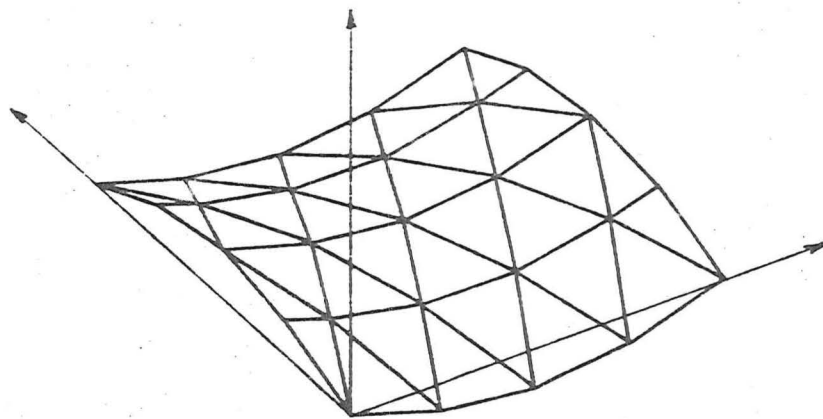


Fig. 4-1b HYPERBOLIC PARABOLOID

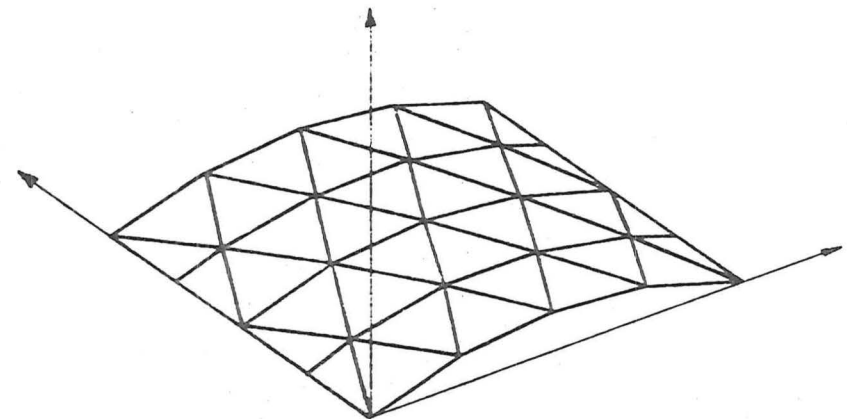


Fig. 4-1d TRANSLATIONAL PARABOLOID

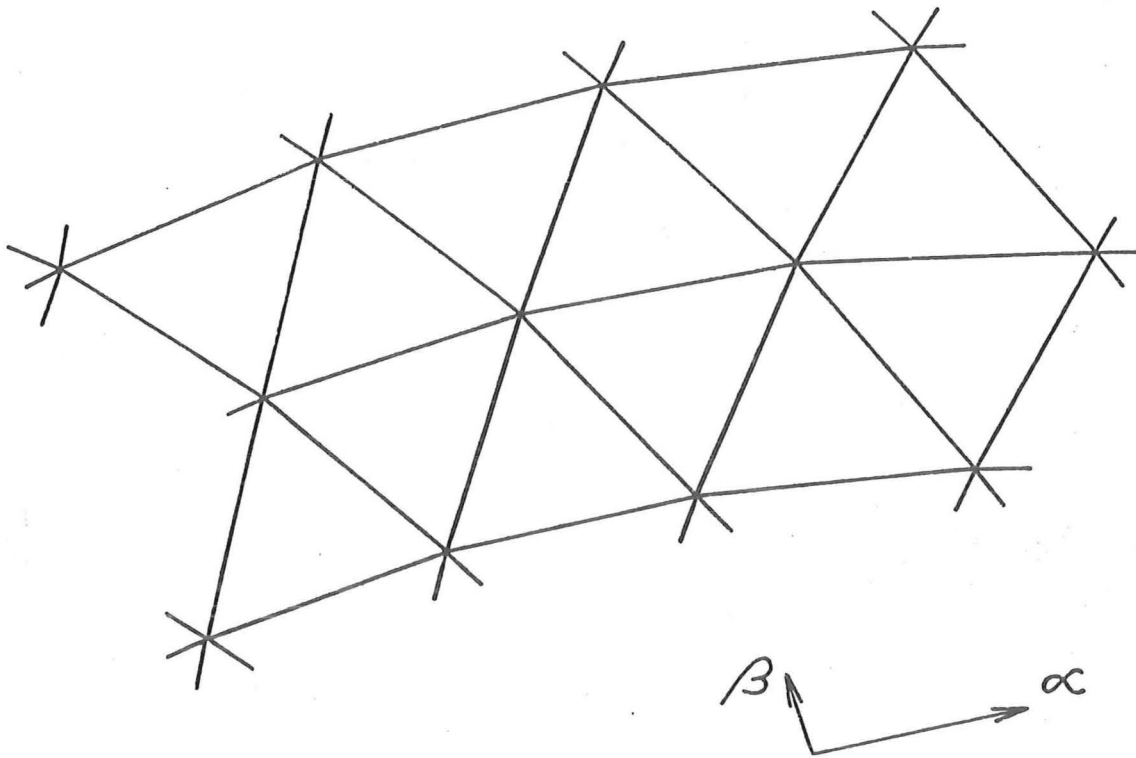


Fig. 4-2a. PORTION OF SINGLE LAYER STRUCTURE.

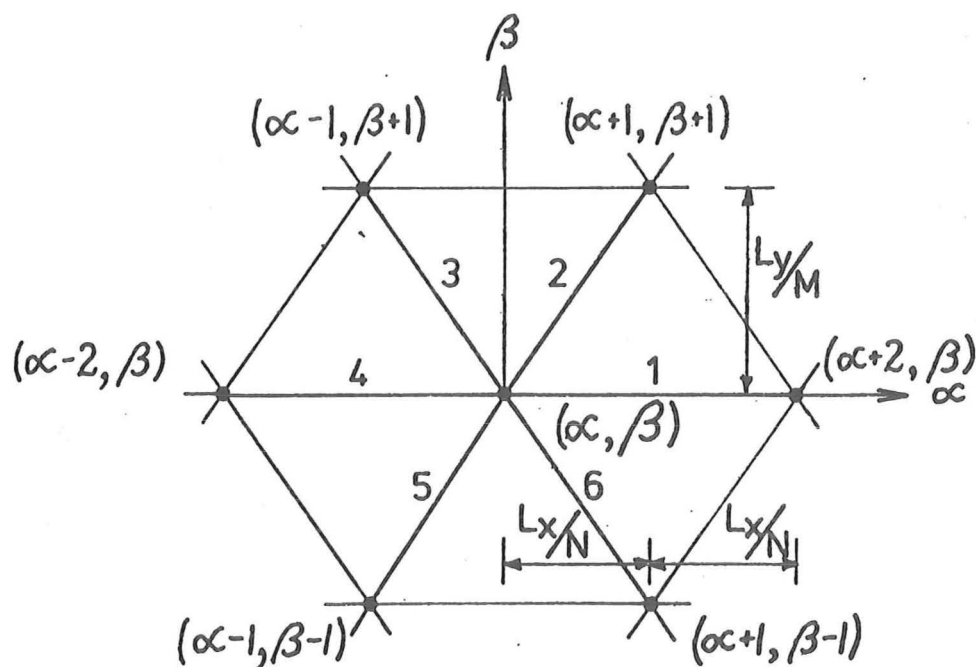


Fig. 4-2b. TYPICAL JOINT.

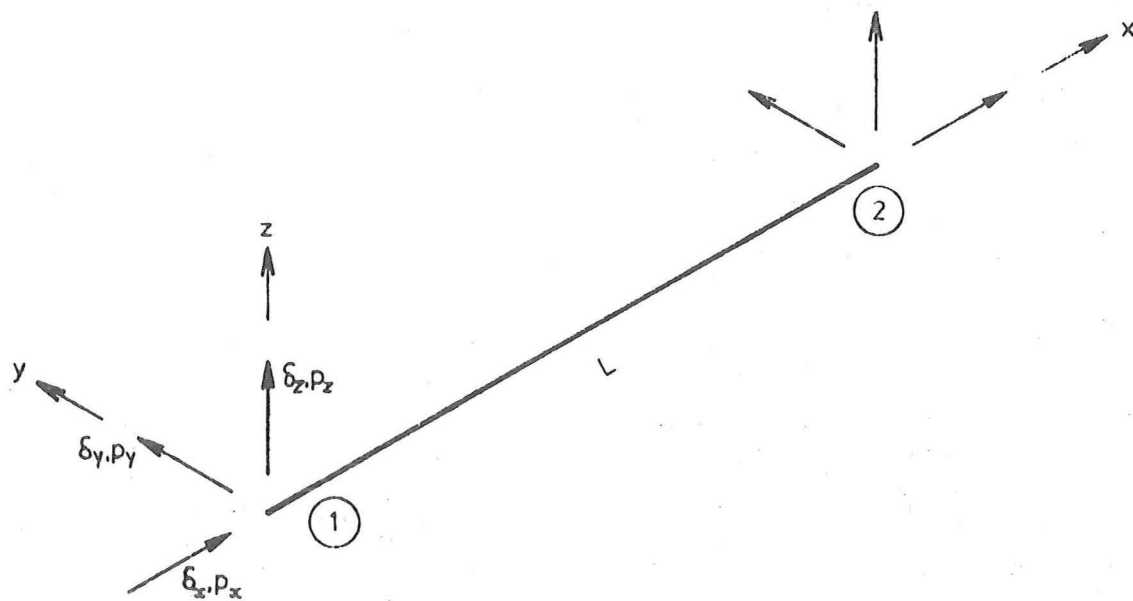


Fig. 4.3 BAR MEMBER AXES, DISPLACEMENTS AND ACTIONS.

4.2 DERIVATION OF GOVERNING EQUATIONS

Following the general outline as given in chapter 2, the derivation of the mathematical model of the structure starts with the element properties. The basic element, a bar, with its local coordinate system is shown in figure 4.3. Also shown are the three linear displacements and the three corresponding forces in the x , y , z directions for each end of the member. Positive displacements and forces are in the positive directions of the member axes.

The load deformation relations for the bar element can be written in this member coordinate system as

$$\begin{Bmatrix} \{P_x\}_1 \\ \{P_x\}_2 \end{Bmatrix} = \begin{bmatrix} k_{11} & k_{12} \\ k_{21} & k_{22} \end{bmatrix} \begin{Bmatrix} \{\Delta_x\}_1 \\ \{\Delta_x\}_2 \end{Bmatrix} \quad \dots (4-2)$$

where

$$\{P_x\}_i = \begin{Bmatrix} p_x \\ p_y \\ p_z \end{Bmatrix}_i ; \quad \{\Delta_x\}_i = \begin{Bmatrix} \delta_x \\ \delta_y \\ \delta_z \end{Bmatrix}_i \quad \text{for } i = 1 \text{ and } 2$$

$$\text{and} \quad [k_{11}] = [k_{22}] = -[k_{12}] = -[k_{21}] = \begin{bmatrix} \frac{EA}{L} & \cdot & \cdot \\ \cdot & \cdot & \cdot \\ \cdot & \cdot & \cdot \end{bmatrix}$$

δ_x , δ_y and δ_z are the displacements of the end of the member in the x, y and z directions, p_x , p_y and p_z are the corresponding forces and the subscripts 1 and 2 indicate the two ends of the member. E, A and L are the member elastic modulus, cross-sectional area and length respectively.

To write equilibrium equations at a joint, the member end forces of all members meeting there should be in a common coordinate system. Thus it is necessary to change the relations 4-2 from the local element coordinate system to the common coordinate system at the joint. A convenient coordinate system is one related to the curved surface and is denoted by the axes α , β and γ . The γ axis is normal to the surface at a joint and the α and β axes are in the tangent plane at the joint. The α and β axes are oriented so that the projections of the α and β axes on the X, Y plane are parallel to the X and Y axes respectively. This is shown in figure 4.4. For a shallow curved surface the α , β , γ axes form an orthogonal curvilinear coordinate system. The γ coordinate is zero in the surface and thus a pair of values (α, β) is sufficient to describe the location of a joint. It is convenient to scale the coordinates so that every joint has integral values of α and β . This results in having $\alpha = 0$ at the edge $X = 0$ and $\alpha = N$ (an integer) at the edge $X = L_X$. The value of N is the number of joint locations in the X direction. In a similar manner $\beta = 0$ at the edge $Y = 0$ and $\beta = M$ (an integer) at the edge $Y = L_Y$, with the value of M being the number of joint locations in the Y direction.

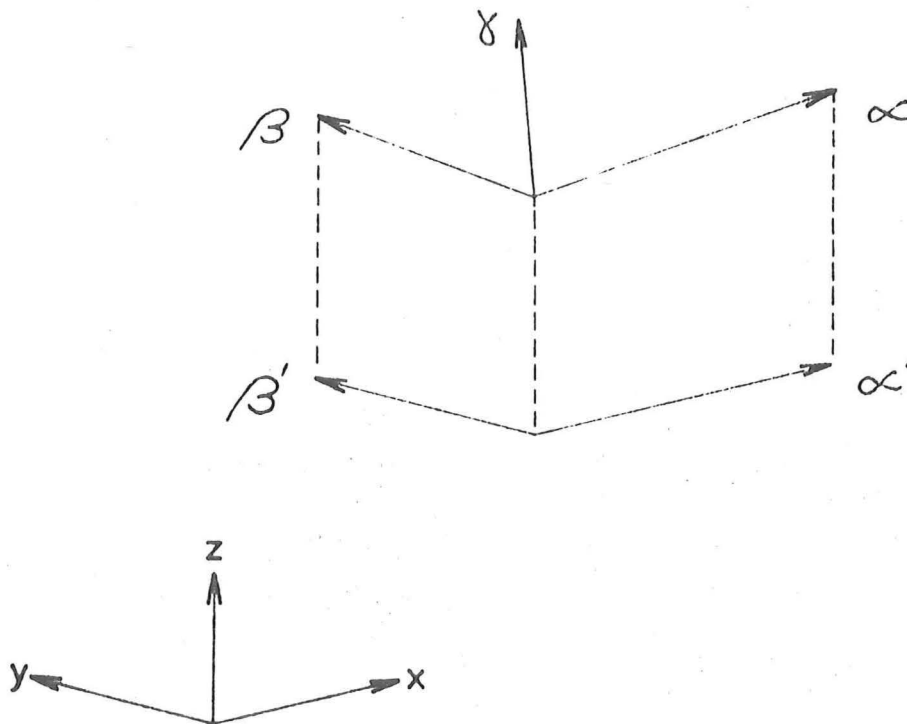


Fig. 4.4 ORIENTATION OF α, β, γ AXES.

The α, β, γ coordinate system is a curvilinear one and so the transformation of quantities from the element x, y, z to the structure α, β, γ coordinate system will, in general, be different at the two ends of the member. However the form of the transformation is the same, and for the forces $\{P_x\}$ it is

$$\{P_\alpha\}_i = [T_i] \{P_x\}_i \quad \dots(4-3)$$

where $\{P_x\}_i$ is as defined in equation 4-2, $\{P_\alpha\}_i$ is the vector of forces at end i in the α, β, γ coordinate system and is defined by

$$\{P_\alpha\}_i = \begin{Bmatrix} P_\alpha \\ P_\beta \\ P_\gamma \end{Bmatrix}_i$$

and $[T_i]$ is the transformation matrix and is defined by

$$[T_i] = \begin{bmatrix} + \cos \psi_i \cos \phi_i & + \sin \psi_i & - \cos \psi_i \sin \phi_i \\ - \sin \psi_i \cos \phi_i & + \cos \psi_i & + \sin \psi_i \sin \phi_i \\ + \sin \phi_i & 0 & + \cos \phi_i \end{bmatrix} \quad \dots (4-4)$$

The values of ϕ and ψ at the two ends are, in general, different. They are the rotation angles about the y and z axes respectively and are determined from the curvature of the surface and the orientation of the member in the surface. The value of ψ is the angle, in the α, β plane, that is turned through in going from the projection of the x axis of the member on the α, β plane to the α axis. This is shown in figure 4.5a.

For the structure considered here, the values of ψ_1 and ψ_2 are the same and are determined from

$$\tan \psi = (L_Y/M)/(L_X/N) \quad \dots (4-5)$$

The value of ϕ is the angle in the plane containing the member and the γ axis that is turned through in going from the α, β plane to the x axis of the member. It is determined from the radius of curvature of the surface in the direction of the member and the member length. The surface radius of curvature (R) in the direction of the member is given by

$$\frac{1}{R} = \frac{8H_X}{L_X^2} \cos^2 \psi + \frac{8H_Y}{L_Y^2} \sin^2 \psi$$

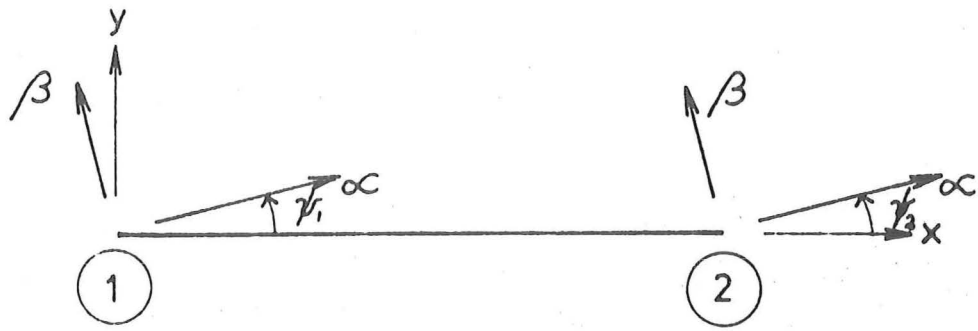
The values of ϕ are then given by (see figure 4.5b)

$$\sin \phi_1 = - L/2R \quad \dots (4-6a)$$

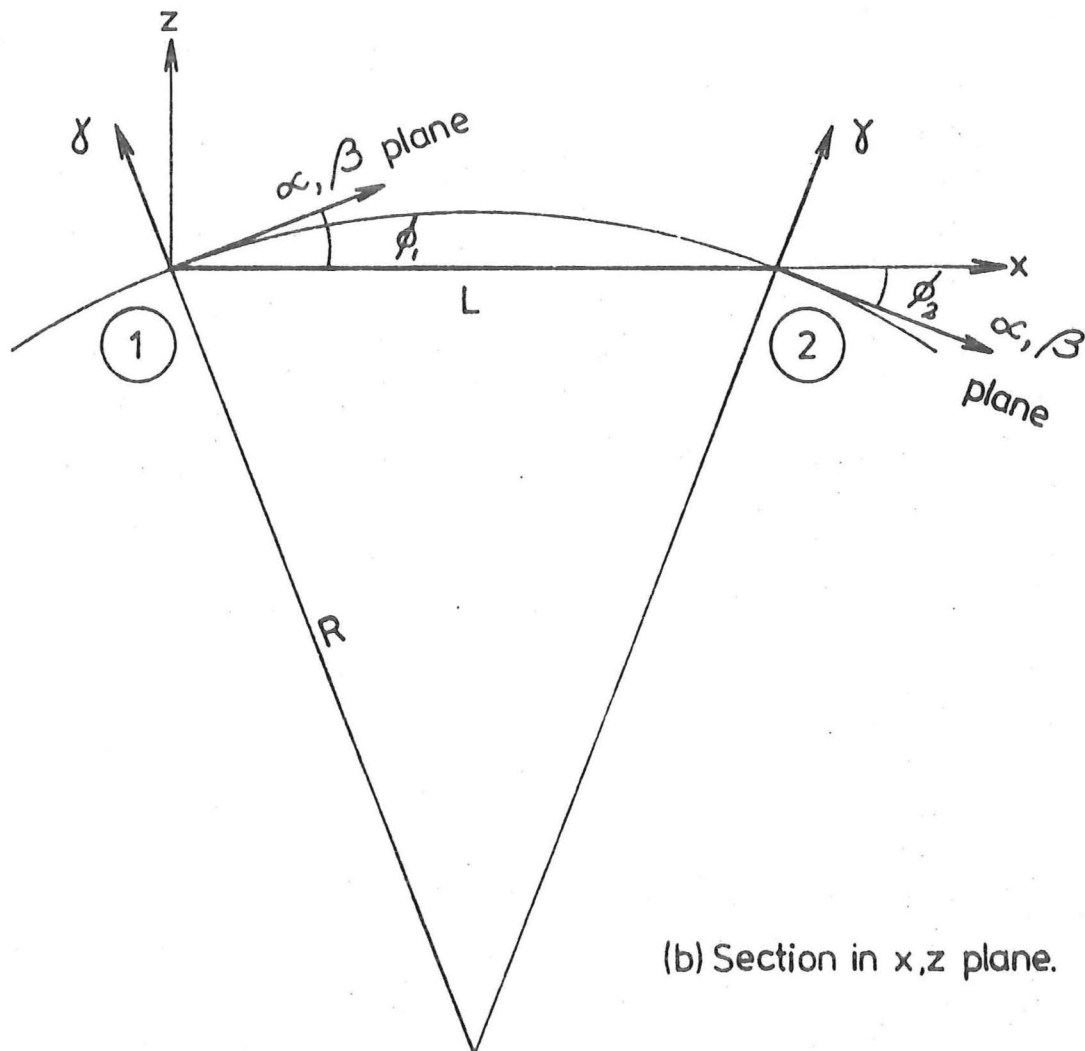
$$\text{and} \quad \sin \phi_2 = + L/2R \quad \dots (4-6b)$$

where L is the member length. ϕ_1 and ϕ_2 have the same magnitude but have opposite signs.

The inverse transformation from the α, β, γ to the x, y, z coordinate system is obtained by inverting the matrix $[T_i]$. Because the transformation is orthogonal, the inverse matrix is also the transposed matrix and hence can be written directly as



(a) Section in x,y plane.



(b) Section in x,z plane.

Fig. 4.5 DEFINITION OF ANGLES γ AND ϕ .

$$[T_i^{-1}] = [T_i^T] = \begin{bmatrix} + \cos \psi_i \cos \phi_i & - \sin \psi_i \cos \phi_i & + \sin \phi_i \\ + \sin \psi_i & + \cos \psi_i & 0 \\ - \cos \psi_i \sin \phi_i & + \sin \psi_i \sin \phi_i & + \cos \phi_i \end{bmatrix}$$

The inverse transformation for the forces can then be written as

$$\{P_x\}_i = [T_i^T] \{P_\alpha\}_i \quad \dots(4-7)$$

For the end displacements $\{\Delta_\alpha\}_i$ and $\{\Delta_x\}_i$, the transformations are identical to those for the end forces $\{P_\alpha\}_i$ and $\{P_x\}_i$.

These transformations can now be used in the load deformation relations. First transforming the end displacements gives

$$\begin{Bmatrix} \{P_x\}_1 \\ \{P_x\}_2 \end{Bmatrix} = \begin{bmatrix} k_{11}T_1^T & k_{12}T_2^T \\ k_{21}T_1^T & k_{22}T_2^T \end{bmatrix} \begin{Bmatrix} \{\Delta_\alpha\}_1 \\ \{\Delta_\alpha\}_2 \end{Bmatrix} \quad \dots(4-8)$$

This relation, which gives the member end actions in the member coordinate system in terms of the end displacements in the surface coordinate system, will be used later to obtain the member end actions.

Following this, the end actions are transformed to give

$$\begin{Bmatrix} \{P_\alpha\}_1 \\ \{P_\alpha\}_2 \end{Bmatrix} = \begin{bmatrix} T_1 k_{11} T_1^T & T_1 k_{12} T_2^T \\ T_2 k_{21} T_1^T & T_2 k_{22} T_2^T \end{bmatrix} \begin{Bmatrix} \{\Delta_\alpha\}_1 \\ \{\Delta_\alpha\}_2 \end{Bmatrix} \quad \dots(4-9)$$

which can be written in the abbreviated form

$$\begin{Bmatrix} \{P_\alpha\}_1 \\ \{P_\alpha\}_2 \end{Bmatrix} = \begin{bmatrix} K_{11} & K_{12} \\ K_{21} & K_{22} \end{bmatrix} \begin{Bmatrix} \{\Delta_\alpha\}_1 \\ \{\Delta_\alpha\}_2 \end{Bmatrix} \quad \dots(4-10)$$

where

$$[K_{ij}] = [T_i] [k_{ij}] [T_j^T] \quad \dots(4-11)$$

$$\text{for } i = 1, 2 \quad \text{and} \quad j = 1, 2$$

Details of matrices $[K_{ij}]$ are given in appendix C. Relation 4-10 can be partitioned to give only the forces at end 1 in terms of the displacements at both end 1 and end 2. This results in

$$\{P_\alpha\}_1 = [K_{11}] \{\Delta_\alpha\}_1 + [K_{12}] \{\Delta_\alpha\}_2 \quad \dots(4-12)$$

The end forces and end displacements can be considered as functions of the joint coordinates. If end 1 of the member is at coordinates (α, β) and end 2 is at coordinates $(\alpha + g, \beta + h)$ and making use of the finite difference shift operators E_{α}^g and E_{β}^h as described in section 2.5.2 then relation 4-12 can be written as

$$\{P_{\alpha}(\alpha, \beta)\} = \left[[K_{11}] + [K_{12}] E_{\alpha}^g E_{\beta}^h \right] \{\Delta_{\alpha}(\alpha, \beta)\} \quad \dots(4-13)$$

Relation 4-13 applies only to a single member. At a joint, equilibrium requires the sum of the member actions from all members meeting there to balance the applied load on the joint. This summation over the six members meeting at a typical joint gives

$$\{W_{\alpha}(\alpha, \beta)\} = \left[\sum_{i=1}^6 \left([K_{11}]_i + [K_{12}]_i E_{\alpha}^{g_i} E_{\beta}^{h_i} \right) \right] \{\Delta_{\alpha}(\alpha, \beta)\} \quad \dots(4-14)$$

where subscript i denotes the member number, from 1 to 6, as shown in figure 4.2b. Vector $\{W_{\alpha}(\alpha, \beta)\}$ is the applied joint loads and has three components. These are the loads in the α , β and γ directions.

The matrices $[K_{11}]_i$ and $[K_{12}]_i$ and the parameters g_i and h_i in expression 4-14 are derived from the properties and orientations of the members. For the structure considered here with the layout shown in figure 4.2b, the values of the relevant variables are given in table 4.1. Due to symmetry about both the α and β axes, ϕ , ψ and (EA/L) take on only two independent values. One value applies to members 1 and 4 and the other value applies to members 2, 3, 5 and 6. The values of g and h are determined from the change in the α and β coordinate in going from the typical joint to the other end of the member. The values are integers because each joint has its (α, β) coordinates as integers.

Substituting the values given in table 4.1 into the relation 4-14 yields the governing partial difference equation for the structure.

$$\begin{Bmatrix} w_{\alpha}(\alpha, \beta) \\ w_{\beta}(\alpha, \beta) \\ w_{\gamma}(\alpha, \beta) \end{Bmatrix} = \begin{bmatrix} v_{11} & v_{12} & v_{13} \\ v_{21} & v_{22} & v_{23} \\ v_{31} & v_{32} & v_{33} \end{bmatrix} \begin{Bmatrix} \delta_{\alpha}(\alpha, \beta) \\ \delta_{\beta}(\alpha, \beta) \\ \delta_{\gamma}(\alpha, \beta) \end{Bmatrix} \quad \dots(4-15)$$

TABLE 4.1 Single Layer Structure Member Orientations and Properties

Member No	End 1		End 2		Member	g_i	h_i
i	ϕ	ψ	ϕ	ψ	Property Type		
1	$-\sigma_1$	0	σ_1	0	1	+2	0
2	$-\sigma_2$	$-\theta$	σ_2	$-\theta$	2	+1	+1
3	$-\sigma_2$	$-\pi + \theta$	σ_2	$-\pi + \theta$	2	-1	+1
4	$-\sigma_1$	$-\pi$	σ_1	$-\pi$	1	-2	0
5	$-\sigma_2$	$-\pi - \theta$	σ_2	$-\pi - \theta$	2	-1	-1
6	$-\sigma_2$	$-2\pi + \theta$	σ_2	$-2\pi + \theta$	2	+1	-1

where

$$\theta = \tan^{-1} \left\{ \frac{L_Y}{M} / \frac{L_X}{N} \right\}$$

$$\sigma_1 = \frac{8H_X}{NL_X}$$

$$\sigma_2 = \frac{4H_X}{NL_X} \cos \theta + \frac{4H_Y}{ML_Y} \sin \theta$$

where

$$\begin{aligned}
 v_{11} &= S_1 \cos^2 \sigma_1 [2 - (E_{\alpha}^{+2} + E_{\alpha}^{-2})] \\
 &\quad + S_2 \cos^2 \theta \cos^2 \sigma_2 [4 - (E_{\alpha}^{+1} + E_{\alpha}^{-1}) (E_{\beta}^{+1} + E_{\beta}^{-1})] \\
 v_{12} = v_{21} &= S_2 \cos \theta \sin \theta \cos^2 \sigma_2 [- (E_{\alpha}^{+1} - E_{\alpha}^{-1}) (E_{\beta}^{+1} - E_{\beta}^{-1})] \\
 v_{13} = -v_{31} &= S_1 \cos \sigma_1 \sin \sigma_1 [- (E_{\alpha}^{+2} - E_{\alpha}^{-2})] \\
 &\quad + S_2 \cos \theta \cos \sigma_2 \sin \sigma_2 [- (E_{\alpha}^{+1} - E_{\alpha}^{-1}) (E_{\beta}^{+1} + E_{\beta}^{-1})] \\
 v_{22} &= S_2 \sin^2 \theta \cos^2 \sigma_2 [4 - (E_{\alpha}^{+1} + E_{\alpha}^{-1}) (E_{\beta}^{+1} + E_{\beta}^{-1})] \\
 v_{23} = -v_{32} &= S_2 \sin \theta \cos \sigma_1 \sin \sigma_1 [- (E_{\alpha}^{+1} + E_{\alpha}^{-1}) (E_{\beta}^{+1} - E_{\beta}^{-1})] \\
 v_{33} &= S_1 \sin^2 \sigma_1 [2 + (E_{\alpha}^{+2} + E_{\alpha}^{-2})] + S_2 \sin^2 \sigma_2 [4 + (E_{\alpha}^{+1} + E_{\alpha}^{-1}) (E_{\beta}^{+1} + E_{\beta}^{-1})]
 \end{aligned}$$

and $S_i = (EA/L)_i$ where i denotes the property type 1 or 2.

4.3 BOUNDARY CONDITIONS

The structure has diaphragm supports on all edges and this must be expressed as a set of mathematical conditions on the solution. A diaphragm is assumed to be infinitely rigid in its own plane and infinitely flexible normal to its plane. This requires that no deformations occur in that plane and no reactions occur normal to that plane. These can be expressed mathematically as, firstly, for the in-plane conditions

$$\delta_{\alpha}(\alpha, \beta) = 0 \text{ at } \beta = 0 \text{ and } \beta = M \quad \dots (4-16a)$$

$$\delta_{\beta}(\alpha, \beta) = 0 \text{ at } \alpha = 0 \text{ and } \alpha = N \quad \dots (4-16b)$$

$$\begin{aligned}
 \delta_{\gamma}(\alpha, \beta) &= 0 \text{ at } \alpha = 0 \text{ and } \alpha = N \\
 &\text{and } \beta = 0 \text{ and } \beta = M
 \end{aligned} \quad \dots (4-16c)$$

and secondly, for the out-of-plane conditions (see fig. 4.6)

$$(p_{\alpha})_1 + (p_{\alpha})_2 + (p_{\alpha})_6 = 0 \text{ at } \alpha = 0 \quad \dots (4-17a)$$

$$(p_{\alpha})_3 + (p_{\alpha})_4 + (p_{\alpha})_5 = 0 \text{ at } \alpha = N \quad \dots (4-17b)$$

$$(p_{\beta})_2 + (p_{\beta})_3 = 0 \text{ at } \beta = 0 \quad \dots (4-17c)$$

$$(p_{\beta})_5 + (p_{\beta})_6 = 0 \text{ at } \beta = M \quad \dots (4-17d)$$

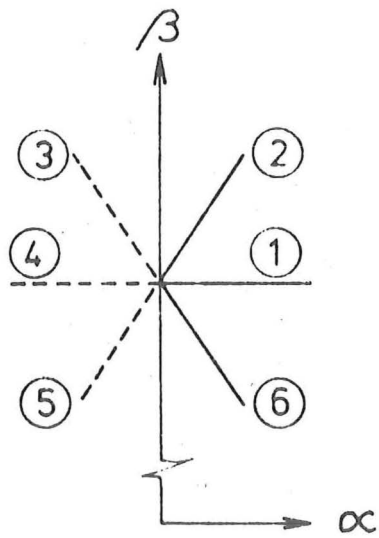
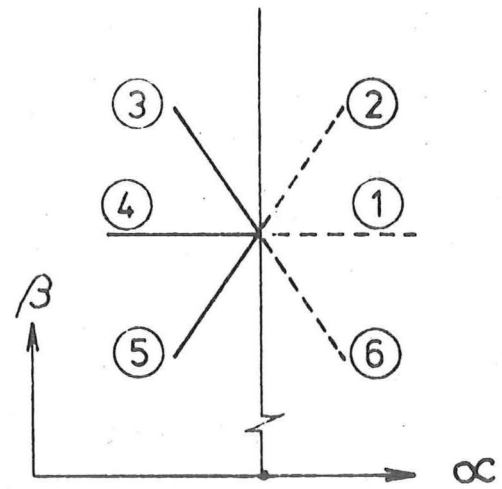
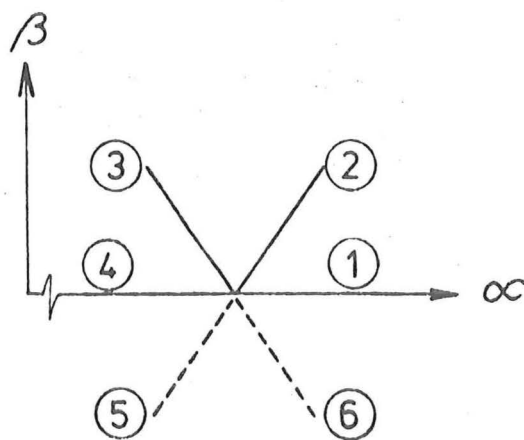
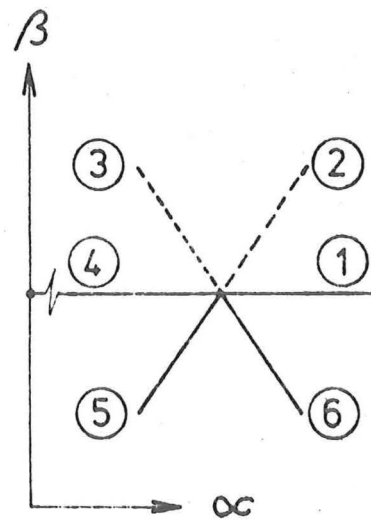
(a) $\alpha = 0$ edge(b) $\alpha = N$ edge(c) $\beta = 0$ edge(d) $\beta = M$ edge

Fig.4.6 BOUNDARY JOINTS.

These latter conditions on the forces can be simplified by the following procedure. Consider the structure extended to the left and right at the $\alpha = 0$ and $\alpha = N$ edges respectively. The extended members are shown dashed in figures 4.6a and 4.6b. The full equilibrium equation 4-14 then holds for this extended structure. Taking the α direction component, with the applied load as zero, gives

$$(p_{\alpha})_1 + (p_{\alpha})_2 + (p_{\alpha})_3 + (p_{\alpha})_4 + (p_{\alpha})_5 + (p_{\alpha})_6 = 0$$

which can be re-arranged as

$$[(p_{\alpha})_1 + (p_{\alpha})_2 + (p_{\alpha})_6] + [(p_{\alpha})_3 + (p_{\alpha})_4 + (p_{\alpha})_5] = 0 \quad \dots(4-18)$$

where the first group contains the effect of members to the right of the diaphragm and the second group those to the left. The force boundary condition at $\alpha = 0$ requires that the first group is zero and hence the second group is also zero. At $\alpha = N$ the force boundary condition requires the second group is zero and thus also the first. Because of this the boundary conditions at both $\alpha = 0$ and $\alpha = N$ can be combined into the single condition

$$[(p_{\alpha})_1 + (p_{\alpha})_2 + (p_{\alpha})_6] - [(p_{\alpha})_3 + (p_{\alpha})_4 + (p_{\alpha})_5] = 0 \quad \dots(4-19)$$

This is a form which makes later manipulation easier when it is expressed as a condition on the displacements.

The α component of each member as given by expression 4-12 and table 4.1 can now be substituted in expression 4-19, which after simplification gives for the force boundary condition, the requirement that

$$\begin{aligned} & [S_1 \cos^2 \sigma_1 (E_{\alpha}^{+2} - E_{\alpha}^{-2}) + S_2 \cos^2 \theta \cos^2 \sigma_2 (E_{\alpha}^{+1} - E_{\alpha}^{-1}) (E_{\beta}^{+1} + E_{\beta}^{-1})] \delta_{\alpha}(\alpha, \beta) \\ & + [S_2 \cos \theta \sin \theta \cos^2 \sigma_2 (E_{\alpha}^{+1} + E_{\alpha}^{-1}) (E_{\beta}^{+1} - E_{\beta}^{-1})] \delta_{\beta}(\alpha, \beta) \\ & + [2S_1 \cos \sigma_1 \sin \sigma_1 + S_1 \cos \sigma_1 \sin \sigma_1 (E_{\alpha}^{+2} + E_{\alpha}^{-2}) \\ & + 4S_2 \cos \theta \cos \sigma_2 \sin \sigma_2 + S_2 \cos \theta \cos \sigma_2 \sin \sigma_2 (E_{\alpha}^{+1} + E_{\alpha}^{-1}) (E_{\beta}^{+1} + E_{\beta}^{-1})] \delta_{\gamma}(\alpha, \beta) \\ & = 0 \quad \dots(4-20a) \end{aligned}$$

at $\alpha = 0$ and $\alpha = N$

In a similar manner the conditions 4-17c and 4-17d can be combined by extending the structure in the β direction as shown in figures 4.6c and d. The resulting condition on the displacements is then

$$\begin{aligned}
 & \left[S_2 \cos \theta \sin \theta \cos^2 \sigma_2 (E_{\alpha}^{+1} - E_{\alpha}^{-1}) (E_{\beta}^{+1} + E_{\beta}^{-1}) \right] \delta_{\alpha}(\alpha, \beta) \\
 & + \left[S_2 \sin^2 \theta \cos^2 \sigma_2 (E_{\alpha}^{+1} + E_{\alpha}^{-1}) (E_{\beta}^{+1} - E_{\beta}^{-1}) \right] \delta_{\beta}(\alpha, \beta) \\
 & + \left[4S_2 \sin \theta \cos \sigma_2 \sin \sigma_2 + S_2 \sin \theta \cos \sigma_2 \sin \sigma_2 (E_{\alpha}^{+1} + E_{\alpha}^{-1}) (E_{\beta}^{+1} + E_{\beta}^{-1}) \right] \delta_{\gamma}(\alpha, \beta) \\
 & = 0 \quad \dots (4-20b)
 \end{aligned}$$

at $\beta = 0$ and $\beta = M$

The boundary conditions of diaphragm supports on all four edges that is just considered, is not the only one that can be treated. In the case of a fully restrained boundary joint, equation 4-19 still holds, except that the two terms in brackets are equal to p_{α} , say, rather than zero. Then equation 4-18 with the right hand side equal to $2p_{\alpha}$ would be satisfied. This equation is the α component of the governing partial difference equation which would then apply at the restrained joint with a load of $2p_{\alpha}$ applied there.

The value to give to the joint load $2p_{\alpha}$ is chosen so that the displacements of the boundary joints are zero as required when the structure is subject to its load and to the restraining forces on the boundary joints. This is achieved by carrying out a two stage analysis procedure and involves setting up and solving a system of linear equations with the number of unknowns being the number of constrained joints.

Numerical results were obtained for several structures with fully restrained joints by this process without any difficulty. They are not reported here, however.

4.4 SOLUTION OF GOVERNING EQUATIONS

The procedure used to find the solution to the governing equations is to assume the functions for the displacements as finite double

trigonometric series with unknown fourier coefficients such that the assumed series satisfies the boundary conditions. The double series, when substituted into the governing equations, should also yield the same form as the series used to represent the corresponding loading term. Matching like terms of the corresponding series yields algebraic equations for the unknown coefficients of the double series.

A suitable form for the displacement solution is

$$\begin{Bmatrix} \delta_{\alpha}(\alpha, \beta) \\ \delta_{\beta}(\alpha, \beta) \\ \delta_{\gamma}(\alpha, \beta) \end{Bmatrix} = \sum_{i=0}^N \sum_{j=0}^M \begin{Bmatrix} a_{ij} \cos \frac{i\pi\alpha}{N} \sin \frac{j\pi\beta}{M} \\ b_{ij} \sin \frac{i\pi\alpha}{N} \cos \frac{j\pi\beta}{M} \\ c_{ij} \sin \frac{i\pi\alpha}{N} \sin \frac{j\pi\beta}{M} \end{Bmatrix} \quad \dots(4-21)$$

It must be shown that this expression satisfies the governing equations and the boundary conditions. It is obvious that the displacement conditions in equation 4-16 are satisfied. To prove that the assumed solution satisfies the governing equation 4-15 and the force boundary condition equations 4-20, it is necessary to determine the effect of the finite difference operations on the assumed solution.

Consider $\delta_{\alpha}(\alpha, \beta)$ as given above and the operation E_{α}^{+g} acting on it, thus

$$\begin{aligned} E_{\alpha}^{+g} \delta_{\alpha}(\alpha, \beta) &= E_{\alpha}^{+g} \sum_{i=0}^N \sum_{j=0}^M (a_{ij} \cos \frac{i\pi\alpha}{N} \sin \frac{j\pi\beta}{M}) \\ &= \sum_{i=0}^N \sum_{j=0}^M (a_{ij} \cos \frac{i\pi(\alpha+g)}{N} \sin \frac{j\pi\beta}{M}) \\ &= \sum_{i=0}^N \sum_{j=0}^M (a_{ij} \{ \cos \frac{i\pi\alpha}{N} \cos \frac{i\pi g}{N} - \sin \frac{i\pi\alpha}{N} \sin \frac{i\pi g}{N} \} \sin \frac{j\pi\beta}{M}) \end{aligned}$$

The operator E_{α}^{+g} always appears paired with the operator E_{α}^{-g} . The effect of E_{α}^{-g} on $\delta_{\alpha}(\alpha, \beta)$ is given by

$$E_{\alpha}^{-g} \delta_{\alpha}(\alpha, \beta) = \sum_{i=0}^N \sum_{j=0}^M (a_{ij} \{ \cos \frac{i\pi\alpha}{N} \cos \frac{i\pi g}{N} + \sin \frac{i\pi\alpha}{N} \sin \frac{i\pi g}{N} \} \sin \frac{j\pi\beta}{M})$$

These two operators appear in the pairs $E_{\alpha}^{+g} + E_{\alpha}^{-g}$ and $E_{\alpha}^{+g} - E_{\alpha}^{-g}$ which

operating on $\delta_\alpha(\alpha, \beta)$ give

$$(E_\alpha^{+g} + E_\alpha^{-g}) \delta_\alpha(\alpha, \beta) = \sum_{i=0}^N \sum_{j=0}^M (a_{ij} \{2 \cos \frac{i\pi g}{N}\} \cos \frac{i\pi \alpha}{N} \sin \frac{j\pi \beta}{M})$$

$$(E_\alpha^{+g} - E_\alpha^{-g}) \delta_\alpha(\alpha, \beta) = \sum_{i=0}^N \sum_{j=0}^M (a_{ij} \{-2 \sin \frac{i\pi g}{N}\} \sin \frac{i\pi \alpha}{N} \sin \frac{j\pi \beta}{M})$$

In a similar manner the effects of these two combinations and of the two combinations $E_\beta^{+h} + E_\beta^{-h}$ and $E_\beta^{+h} - E_\beta^{-h}$ on the functions for $\delta_\alpha(\alpha, \beta)$, $\delta_\beta(\alpha, \beta)$ and $\delta_\gamma(\alpha, \beta)$ can be determined. A complete list is given in Appendix A.

With these operator effects known, it is now possible to show the force boundary conditions 4-20 are satisfied. To do this, the displacement functions can be substituted into the boundary condition equations and the effect of the operators carried out. As this involves a considerable amount of algebraic manipulation it would be better to use a more compact method such as that used by Mithaiwala [60]. From Appendix A it will be seen that a symmetric difference operator $L(\$)$, such as $E_\alpha^{+g} + E_\alpha^{-g}$, when applied to a sine or cosine function yields the same trigonometric function while an anti-symmetric difference operator $L(a/\$)$, such as $E_\alpha^{+g} - E_\alpha^{-g}$, applied to a trigonometric sine or cosine function yields the opposite function, that is, cosine and sine respectively. Using this, equation 4-20a can be written in the more concise form

$$L(a/\$)_\alpha L(\$)_\beta \delta_\alpha(\alpha, \beta) + L(\$)_\alpha L(a/\$)_\beta \delta_\beta(\alpha, \beta) + L(\$)_\alpha L(\$)_\beta \delta_\gamma(\alpha, \beta) = 0 \quad \dots (4-22)$$

where $L(\$)_\alpha$, $L(a/\$)_\alpha$, $L(\$)_\beta$ and $L(a/\$)_\beta$ are the symmetric and anti-symmetric operators in the α and β directions respectively. When the functions for $\delta_\alpha(\alpha, \beta)$, $\delta_\beta(\alpha, \beta)$ and $\delta_\gamma(\alpha, \beta)$ are substituted into this equation it gives

$$\sum_{i=0}^N \sum_{j=0}^M \left[B_{ij} \sin \frac{i\pi \alpha}{N} \sin \frac{j\pi \beta}{M} \right] \text{ at } \begin{matrix} \alpha=0 \\ \alpha=N \end{matrix} = 0$$

where B_{ij} is some non-zero expression obtained from the operator results of equation 4-22. It is thus shown that the boundary condition 4-20a is satisfied. In a similar manner it can be shown that the boundary condition 4-20b is also satisfied by the displacement functions 4-21.

The loading function $\{w_\alpha(\alpha, \beta)\}$ must also be expressed as the finite double trigonometric series

$$\begin{Bmatrix} w_\alpha(\alpha, \beta) \\ w_\beta(\alpha, \beta) \\ w_\gamma(\alpha, \beta) \end{Bmatrix} = \sum_{i=0}^N \sum_{j=0}^M \begin{Bmatrix} p_{ij} \cos \frac{i\pi\alpha}{N} \sin \frac{j\pi\beta}{M} \\ q_{ij} \sin \frac{i\pi\alpha}{N} \cos \frac{j\pi\beta}{M} \\ r_{ij} \sin \frac{i\pi\alpha}{N} \sin \frac{j\pi\beta}{M} \end{Bmatrix} \quad \dots (4-23)$$

where the fourier coefficients p_{ij} , q_{ij} and r_{ij} must be determined from the known loading functions. The procedure to obtain them for a general function and some special functions is given in appendix B.

The assumed series solution for the displacements can now be substituted into the governing equations together with the series for the loading. The effect of the operators is performed and like terms are equated to give equations for the unknown fourier coefficients a_{ij} , b_{ij} and c_{ij} in terms of the coefficients p_{ij} , q_{ij} and r_{ij} . These equations are

$$\begin{bmatrix} v_{11} & v_{12} & v_{13} \\ v_{21} & v_{22} & v_{23} \\ v_{31} & v_{32} & v_{33} \end{bmatrix}_{ij} \begin{Bmatrix} a_{ij} \\ b_{ij} \\ c_{ij} \end{Bmatrix} = \begin{Bmatrix} p_{ij} \\ q_{ij} \\ r_{ij} \end{Bmatrix} \quad \dots (4-24)$$

for $i = 0, 1, \dots, N$ and $j = 0, 1, \dots, M$

where

$$v_{11} = 2S_1 \cos^2 \sigma_1 (1 - \cos \frac{i\pi 2}{N}) + 4S_2 \cos^2 \theta \cos^2 \sigma_2 (1 - \cos \frac{i\pi}{N} \cos \frac{j\pi}{M})$$

$$v_{12} = v_{21} = 4S_2 \cos \theta \sin \theta \cos^2 \sigma_2 (\sin \frac{i\pi}{N} \sin \frac{j\pi}{M})$$

$$v_{13} = v_{31} = -2S_1 \cos \sigma_1 \sin \sigma_1 (\sin \frac{i\pi 2}{N}) - 4S_2 \cos \theta \cos \sigma_2 \sin \sigma_2 (\sin \frac{i\pi}{N} \cos \frac{j\pi}{M})$$

$$v_{22} = 4S_2 \sin^2 \theta \cos^2 \sigma_2 (1 - \cos \frac{i\pi}{N} \cos \frac{j\pi}{M})$$

$$v_{23} = v_{32} = -4S_2 \sin \theta \cos \sigma_2 \sin \sigma_2 (\cos \frac{i\pi}{N} \sin \frac{j\pi}{M})$$

$$v_{33} = 2S_1 \sin^2 \sigma_1 (1 + \cos \frac{i\pi 2}{N}) + 4S_2 \sin^2 \sigma_2 (1 + \cos \frac{i\pi}{N} \cos \frac{j\pi}{M})$$

This is a set of three simultaneous linear algebraic equations in the three unknowns a_{ij} , b_{ij} and c_{ij} . There are $(N+1)(M+1)$ such sets to cover all pairs of values of i and j .

4.5 DISPLACEMENTS

Once the displacement series coefficients a_{ij} , b_{ij} and c_{ij} have been determined (from expression 4-24) for all the values of the subscripts i from 0 to N and j from 0 to M , they can be used in expression 4-21 to give the displacements $\delta_\alpha(\alpha, \beta)$, $\delta_\beta(\alpha, \beta)$ and $\delta_\gamma(\alpha, \beta)$. These series would be evaluated numerically in the majority of cases. It is conceivable that in certain cases the series can be evaluated analytically but such cases would be rare and need not be considered here.

4.6 MEMBER ACTIONS

When the displacements at the two ends of a member are known, the member end actions can be obtained using expression 4-8. This method of determining the member actions is the same as that used in the direct stiffness method of analysis.

4.7 JOINT RESIDUALS

The accuracy of the numerical work can be checked by determining the resultant actions at a joint, due to all members meeting there. At an internal joint, the resultant actions should balance the applied load. Any discrepancy is an indication of errors or inaccurate calculations.

At the edge or boundary joints, the residual actions are the reactions supplied by the boundary supports.

CHAPTER FIVE

ANALYSIS OF A SINGLE LAYER RIGID JOINTED STRUCTURE5.1 DESCRIPTION OF THE STRUCTURE

The structure dealt with in this chapter is an extension of the one treated in chapter 4. The surface shape and the layout of joints and members are the same (see figures 4.1 and 4.2). The difference is that, for this chapter, members which can resist bending, shear and torsion as well as axial loads are considered. The joints are assumed to be capable of transmitting these extra actions from member to member and so are rigid joints.

5.2 DERIVATION OF GOVERNING EQUATIONS

The derivation given here follows the general outline as given in chapter 2 and also the specific application given in chapter 4. The steps taken and the results produced are in some places identical to those in chapter 4. At such places, the detailed derivation has been omitted from this chapter, as including it would be unnecessary duplication. However, to assist the reader and to avoid excessive cross referencing, the results have been quoted when needed. In general the detailed equations are more complicated than in chapter 4 because more joint displacement modes and member actions are considered.

The basic element is a beam in space shown in figure 5.1. Also shown is the local x, y, z coordinate system, the end joint displacements and the end actions. The end joint displacements are the three linear displacements (δ_x , δ_y and δ_z) and the three rotations (θ_x , θ_y and θ_z). The end actions are the three forces (p_x , p_y and p_z) and the three moments (m_x , m_y and m_z). Positive displacements and forces are in the positive directions of the member axes and positive rotations and moments are in positive direction of rotations in a right handed coordinate system.

For the beam element in this member coordinate system, the load deformation relations can be written as

$$\begin{Bmatrix} \{P_x\}_1 \\ \{P_x\}_2 \end{Bmatrix} = \begin{bmatrix} k_{11} & k_{12} \\ k_{21} & k_{22} \end{bmatrix} \begin{Bmatrix} \{\Delta_x\}_1 \\ \{\Delta_x\}_2 \end{Bmatrix} \quad \dots (5-1)$$

where

$$\{P_x\}_i = \begin{Bmatrix} p_x \\ p_y \\ p_z \\ m_x \\ m_y \\ m_z \end{Bmatrix}_i ; \{\Delta_x\}_i = \begin{Bmatrix} \delta_x \\ \delta_y \\ \delta_z \\ \theta_x \\ \theta_y \\ \theta_z \end{Bmatrix}_i$$

for $i = 1$ and 2 ,

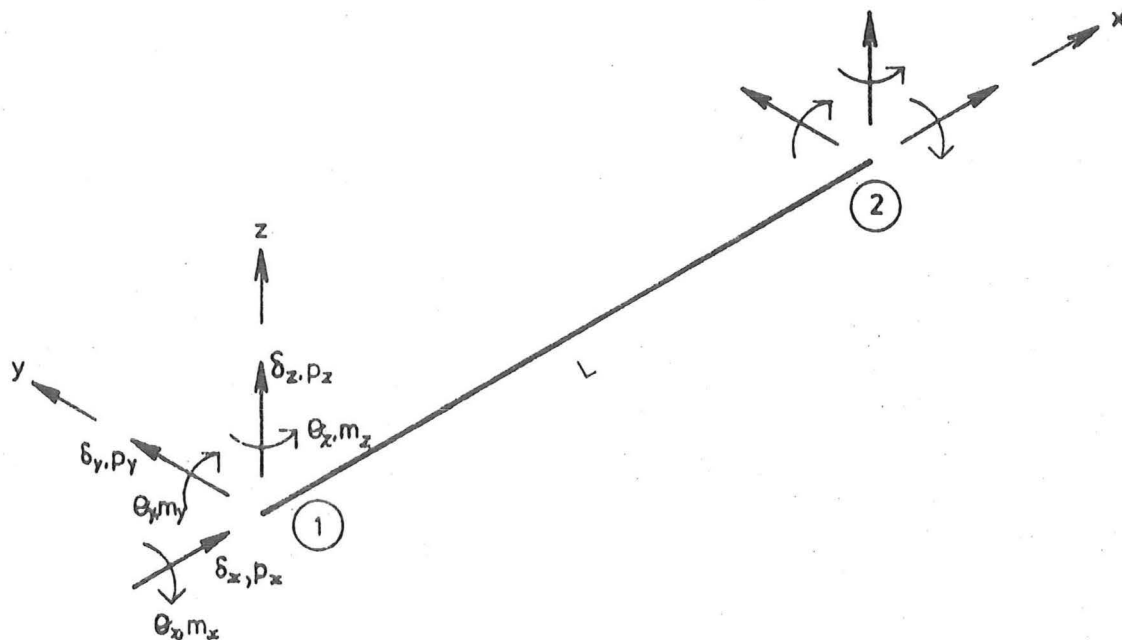


Fig. 5-1 BEAM MEMBER AXES, DISPLACEMENTS AND ACTIONS.

$$\begin{aligned}
[k_{11}] &= \begin{bmatrix} \frac{EA}{L} & \cdot & \cdot & \cdot & \cdot & \cdot \\ \cdot & \frac{12EI}{L^3}z & \cdot & \cdot & \cdot & \frac{6EI}{L^2}z \\ \cdot & \cdot & \frac{12EI}{L^3}y & \cdot & \frac{-6EI}{L^2}y & \cdot \\ \cdot & \cdot & \cdot & \frac{GI}{L}x & \cdot & \cdot \\ \cdot & \cdot & \frac{-6EI}{L^2}y & \cdot & \frac{4EI}{L}y & \cdot \\ \cdot & \frac{6EI}{L^2}z & \cdot & \cdot & \cdot & \frac{4EI}{L}z \end{bmatrix} \\
[k_{12}] = [k_{21}^T] &= \begin{bmatrix} -\frac{EA}{L} & \cdot & \cdot & \cdot & \cdot & \cdot \\ \cdot & \frac{-12EI}{L^3}z & \cdot & \cdot & \cdot & \frac{6EI}{L^2}z \\ \cdot & \cdot & \frac{-12EI}{L^3}y & \cdot & \frac{-6EI}{L^2}y & \cdot \\ \cdot & \cdot & \cdot & \frac{-GI}{L}x & \cdot & \cdot \\ \cdot & \cdot & \frac{6EI}{L^2}y & \cdot & \frac{2EI}{L}y & \cdot \\ \cdot & \frac{-6EI}{L^2}z & \cdot & \cdot & \cdot & \frac{2EI}{L}z \end{bmatrix} \\
[k_{22}] &= \begin{bmatrix} \frac{EA}{L} & \cdot & \cdot & \cdot & \cdot & \cdot \\ \cdot & \frac{12EI}{L^3}z & \cdot & \cdot & \cdot & \frac{-6EI}{L^2}z \\ \cdot & \cdot & \frac{12EI}{L^3}y & \cdot & \frac{6EI}{L^2}y & \cdot \\ \cdot & \cdot & \cdot & \frac{GI}{L}x & \cdot & \cdot \\ \cdot & \cdot & \frac{6EI}{L^2}y & \cdot & \frac{4EI}{L}y & \cdot \\ \cdot & \frac{-6EI}{L^2}z & \cdot & \cdot & \cdot & \frac{4EI}{L}z \end{bmatrix}
\end{aligned}$$

E and G are the elastic and shear modulus of the member material. A, I_x , I_y and I_z are cross sectional area and the second moments of area about the x, y and z axes respectively. L is the member length.

In transforming to a coordinating system related to the structure, the rotations and moments transform in an identical manner to the linear displacements and forces as detailed in chapter 4. Thus the transformation for the end actions can be written

$$\{P_{\alpha}\}_i = [T_i] \{P_x\}_i \quad \dots(5-2a)$$

$$\text{and} \quad \{P_x\}_i = [T_i^T] \{P_{\alpha}\}_i \quad \dots(5-2b)$$

$$\text{where} \quad [T_i] = \begin{bmatrix} +\cos\psi_i \cos\phi_i & +\sin\psi_i & -\cos\psi_i \sin\phi_i & | & \\ -\sin\psi_i \cos\phi_i & +\cos\psi_i & +\sin\psi_i \sin\phi_i & | & 0 \\ +\sin\phi_i & 0 & +\cos\phi_i & | & \\ \hline & 0 & & | & \text{as} \\ & & & | & \text{quadrant} \\ & & & | & 1 \end{bmatrix}$$

and $\{P_{\alpha}\}_i$ is the vector of member end actions in the α, β, γ coordinate system. The angles ϕ_i and ψ_i are defined in section 4.2 following equation 4-4.

Identical transformations hold for the end displacements $\{\Delta_{\alpha}\}$ and $\{\Delta_x\}$ as given for the end actions $\{P_{\alpha}\}$ and $\{P_x\}$ above.

Following the procedure used in chapter 4, these transformations can be used in the load deformation relations. The matrix steps are the same and equations 4-8 to 4-14 are applicable. The size of the matrices is greater by a factor of 2 as now rotational deformations and moments are considered. Details of the matrices $[K_{ij}]$ as defined in relation 4-11 are given in appendix C. The resulting governing difference equation

$$\{W_{\alpha}(\alpha, \beta)\} = \left[\sum_{i=1}^6 ([K_{11}]_i + [K_{12}]_i \begin{matrix} g_i & h_i \\ E_{\alpha} & E_{\beta} \end{matrix}) \right] \{\Delta_{\alpha}(\alpha, \beta)\} \quad \dots(5-3)$$

is the same as equation 4-14.

Vector $\{W_{\alpha}(\alpha, \beta)\}$, the applied joint loads, has six components. They are the three loads in the α, β and γ directions and the three moments about these axes.

The matrices $[K_{11}]_i$ and $[K_{12}]_i$ and the parameters g_i and h_i in expression 5-3 are derived from the properties and orientations of the members. For the structure considered, the values of the relevant variables are the same as for those of chapter 4 and are given in table 4.1.

Substituting the values given into the matrix equation 5-3 yields the governing partial difference equation for the single layer rigid jointed lattice

$$\begin{bmatrix} v_{11} & v_{12} & v_{13} & \cdot & \cdot & v_{16} \\ v_{21} & v_{22} & & & & \\ v_{31} & & \cdot & & & \\ \cdot & & & \text{etc} & & \\ \cdot & & & & \cdot & \\ v_{61} & & & & & v_{66} \end{bmatrix} \begin{Bmatrix} \delta_{\alpha} \\ \delta_{\beta} \\ \delta_{\gamma} \\ \theta_{\alpha} \\ \theta_{\beta} \\ \theta_{\gamma} \end{Bmatrix} = \begin{Bmatrix} w_{\alpha} \\ w_{\beta} \\ w_{\gamma} \\ m_{\alpha} \\ m_{\beta} \\ m_{\gamma} \end{Bmatrix}$$

where two typical terms of the matrix are

$$\begin{aligned} v_{11} = & \left(\frac{EA}{L}\right)_1 \cos^2 \sigma_1 \{2 - (E_{\alpha}^{+2} + E_{\alpha}^{-2})\} + \left(\frac{12EI}{L^3} Y\right)_1 \sin^2 \sigma_1 \{2 + (E_{\alpha}^{+2} + E_{\alpha}^{-2})\} \\ & + \left(\frac{EA}{L}\right)_2 \cos^2 \theta \cos^2 \sigma_2 \{4 - (E_{\alpha}^{+1} + E_{\alpha}^{-1})(E_{\beta}^{+1} + E_{\beta}^{-1})\} \\ & + \left(\frac{12EI}{L^3} Y\right)_2 \cos^2 \theta \sin^2 \sigma_2 \{4 + (E_{\alpha}^{+1} + E_{\alpha}^{-1})(E_{\beta}^{+1} + E_{\beta}^{-1})\} \\ & + \left(\frac{12EI}{L^3} Z\right)_2 \sin^2 \theta \{4 - (E_{\alpha}^{+1} + E_{\alpha}^{-1})(E_{\beta}^{+1} + E_{\beta}^{-1})\} \\ \text{and } v_{14} = & \left(\frac{6EI}{L^2} Y\right)_2 \cos \theta \sin \theta \sin \sigma_2 \{+(E_{\alpha}^{+1} - E_{\alpha}^{-1})(E_{\beta}^{+1} - E_{\beta}^{-1})\} \\ & + \left(\frac{6EI}{L^2} Z\right)_2 \cos \theta \sin \theta \sin \sigma_2 \{+(E_{\alpha}^{+1} - E_{\alpha}^{-1})(E_{\beta}^{+1} - E_{\beta}^{-1})\} \end{aligned}$$

As can be seen, the terms are rather bulky and thus are not all presented here but are given in full in appendix D.

5.3 BOUNDARY CONDITIONS

Although the diaphragm supports of this structure are the same as those of chapter 4, additional conditions on the rotations and moments are needed.

The in-plane conditions are

$$\delta_{\alpha}(\alpha, \beta) = 0 \quad \text{at } \beta = 0 \text{ and } \beta = M \quad \dots(5-4a)$$

$$\delta_{\beta}(\alpha, \beta) = 0 \quad \text{at } \alpha = 0 \text{ and } \alpha = N \quad \dots(5-4b)$$

$$\delta_{\gamma}(\alpha, \beta) = 0 \quad \begin{array}{l} \text{at } \alpha = 0 \text{ and } \alpha = N \\ \text{and } \beta = 0 \text{ and } \beta = M \end{array} \quad \dots(5-4c)$$

$$\theta_{\alpha}(\alpha, \beta) = 0 \quad \text{at } \alpha = 0 \text{ and } \alpha = N \quad \dots(5-4d)$$

$$\theta_{\beta}(\alpha, \beta) = 0 \quad \text{at } \beta = 0 \text{ and } \beta = M \quad \dots(5-4e)$$

and the out-of-plane conditions are (see figure 4.6)

$$(p_{\alpha})_1 + (p_{\alpha})_2 + (p_{\alpha})_6 = 0 \quad \text{at } \alpha = 0 \quad \dots(5-5a)$$

$$(p_{\alpha})_3 + (p_{\alpha})_4 + (p_{\alpha})_5 = 0 \quad \text{at } \alpha = N \quad \dots(5-5b)$$

$$\frac{1}{2}(p_{\beta})_1 + (p_{\beta})_2 + (p_{\beta})_3 + \frac{1}{2}(p_{\beta})_4 = 0 \quad \text{at } \beta = 0 \quad \dots(5-5c)$$

$$\frac{1}{2}(p_{\beta})_1 + \frac{1}{2}(p_{\beta})_4 + (p_{\beta})_5 + (p_{\beta})_6 = 0 \quad \text{at } \beta = M \quad \dots(5-5d)$$

$$(m_{\beta})_1 + (m_{\beta})_2 + (m_{\beta})_6 = 0 \quad \text{at } \alpha = 0 \quad \dots(5-5e)$$

$$(m_{\beta})_3 + (m_{\beta})_4 + (m_{\beta})_5 = 0 \quad \text{at } \alpha = N \quad \dots(5-5f)$$

$$\frac{1}{2}(m_{\alpha})_1 + (m_{\alpha})_2 + (m_{\alpha})_3 + \frac{1}{2}(m_{\alpha})_4 = 0 \quad \text{at } \beta = 0 \quad \dots(5-5g)$$

$$\frac{1}{2}(m_{\alpha})_1 + \frac{1}{2}(m_{\alpha})_4 + (m_{\alpha})_5 + (m_{\alpha})_6 = 0 \quad \text{at } \beta = M \quad \dots(5-5h)$$

$$(m_Y)_1 + (m_Y)_2 + (m_Y)_6 = 0 \quad \text{at } \alpha = 0 \quad \dots(5-5i)$$

$$(m_Y)_3 + (m_Y)_4 + (m_Y)_5 = 0 \quad \text{at } \alpha = N \quad \dots(5-5j)$$

$$\frac{1}{2}(m_Y)_1 + (m_Y)_2 + (m_Y)_3 + \frac{1}{2}(m_Y)_4 = 0 \quad \text{at } \beta = 0 \quad \dots(5-5k)$$

$$\frac{1}{2}(m_Y)_1 + \frac{1}{2}(m_Y)_4 + (m_Y)_5 + (m_Y)_6 = 0 \quad \text{at } \beta = M \quad \dots(5-5l)$$

Again following the procedure outlined in section 4.3 the latter conditions on the forces and on the moments can be simplified. Expressions 5-5a and 5-5b combine to become

$$[(p_{\alpha})_1 + (p_{\alpha})_2 + (p_{\alpha})_6] - [(p_{\alpha})_3 + (p_{\alpha})_4 + (p_{\alpha})_5] = 0 \quad \dots(5-6)$$

at $\alpha = 0$ and $\alpha = N$

The α direction force component for each member, as given by expression 4-12 and table 4.1, can be substituted into expression 5-6 to lead to the condition on the displacements of

$$\left[\left\{ \left(\frac{EA}{L} \right)_1 \cos^2 \sigma_1 - \left(\frac{12EI}{L^3} Y \right)_1 \sin^2 \sigma_1 \right\} \{- (E_{\alpha}^{+2} - E_{\alpha}^{-2}) \} \right. \\ \left. + \left\{ \left(\frac{EA}{L} \right)_2 \cos^2 \theta \cos^2 \sigma_2 - \left(\frac{12EI}{L^3} Y \right)_2 \cos^2 \theta \sin^2 \sigma_2 + \left(\frac{12EI}{L^3} Z \right)_2 \sin^2 \theta \right\} \right]$$

$$\begin{aligned}
& \{-(E_{\alpha}^{+1}-E_{\alpha}^{-1})(E_{\beta}^{+1}+E_{\beta}^{-1})\} \delta_{\alpha} \\
& + \left[\left\{ \left(\frac{EA}{L} \right)_2 \cos\theta \sin\theta \cos^2\sigma_2 - \left(\frac{12EI}{L^3} Y \right)_2 \cos\theta \sin\theta \sin^2\sigma_2 - \left(\frac{12EI}{L^3} Z \right)_2 \cos\theta \sin\theta \right\} \right. \\
& \quad \left. \{-(E_{\alpha}^{+1}+E_{\alpha}^{-1})(E_{\beta}^{+1}-E_{\beta}^{-1})\} \right] \delta_{\beta} \\
& + \left[\left\{ \left(\frac{EA}{L} \right)_1 \cos\sigma_1 \sin\sigma_1 - \left(\frac{12EI}{L^3} Y \right)_1 \cos\sigma_1 \sin\sigma_1 \right\} \{-2\} \right. \\
& \quad \left. + \left\{ \left(\frac{EA}{L} \right)_1 \cos\sigma_1 \sin\sigma_1 + \left(\frac{12EI}{L^3} Y \right)_1 \cos\sigma_1 \sin\sigma_1 \right\} \{-(E_{\alpha}^{+2}+E_{\alpha}^{-2})\} \right. \\
& \quad \left. + \left\{ \left(\frac{EA}{L} \right)_2 \cos\theta \cos\sigma_2 \sin\sigma_2 - \left(\frac{12EI}{L^3} Y \right)_2 \cos\theta \cos\sigma_2 \sin\sigma_2 \right\} \{-4\} \right. \\
& \quad \left. + \left\{ \left(\frac{EA}{L} \right)_2 \cos\theta \cos\sigma_2 \sin\sigma_2 + \left(\frac{12EI}{L^3} Y \right)_2 \cos\theta \cos\sigma_2 \sin\sigma_2 \right\} \right. \\
& \quad \left. \{-(E_{\alpha}^{+1}+E_{\alpha}^{-1})(E_{\beta}^{+1}+E_{\beta}^{-1})\} \right] \delta_{\gamma} \\
& + \left[\left\{ \left(\frac{6EI}{L^2} Y \right)_2 \cos\theta \sin\theta \sin\sigma_2 + \left(\frac{6EI}{L^2} Z \right)_2 \cos\theta \sin\theta \sin\sigma_2 \right\} \right. \\
& \quad \left. \{+(E_{\alpha}^{+1}+E_{\alpha}^{-1})(E_{\beta}^{+1}-E_{\beta}^{-1})\} \right] \theta_{\alpha} \\
& + \left[\left\{ \left(\frac{6EI}{L^2} Y \right)_1 \sin\sigma_1 \right\} \{-(E_{\alpha}^{+2}-E_{\alpha}^{-2})\} \right. \\
& \quad \left. + \left\{ \left(\frac{6EI}{L^2} Y \right)_2 \cos^2\theta \sin\sigma_2 - \left(\frac{6EI}{L^2} Z \right)_2 \sin^2\theta \sin\sigma_2 \right\} \right. \\
& \quad \left. \{-(E_{\alpha}^{+1}-E_{\alpha}^{-1})(E_{\beta}^{+1}+E_{\beta}^{-1})\} \right] \theta_{\beta} \\
& + \left[\left\{ \left(\frac{6EI}{L^2} Z \right)_2 \sin\theta \cos\sigma_2 \right\} \{-(E_{\alpha}^{+1}-E_{\alpha}^{-1})(E_{\beta}^{+1}-E_{\beta}^{-1})\} \right] \theta_{\gamma} \\
& = 0 \quad \text{at } \alpha = 0 \text{ and } \alpha = N
\end{aligned}$$

In a like manner the other out-of-plane requirements 5-5c to 5-5l can be combined in pairs and simplified to produce conditions on the displacements. The detailed conditions are quite bulky and are thus given in full in appendix E.

5.4 SOLUTION OF GOVERNING EQUATION

For this structure involving 6 displacements at each joint, it is proposed that a suitable form for the displacement function is

$$\begin{Bmatrix} \delta_{\alpha}(\alpha, \beta) \\ \delta_{\beta}(\alpha, \beta) \\ \delta_{\gamma}(\alpha, \beta) \\ \theta_{\alpha}(\alpha, \beta) \\ \theta_{\beta}(\alpha, \beta) \\ \theta_{\gamma}(\alpha, \beta) \end{Bmatrix} = \sum_{i=0}^N \sum_{j=0}^M \begin{Bmatrix} a_{ij} \cos \frac{i\pi\alpha}{N} \sin \frac{j\pi\beta}{M} \\ b_{ij} \sin \frac{i\pi\alpha}{N} \cos \frac{j\pi\beta}{M} \\ c_{ij} \sin \frac{i\pi\alpha}{N} \sin \frac{j\pi\beta}{M} \\ d_{ij} \sin \frac{i\pi\alpha}{N} \cos \frac{j\pi\beta}{M} \\ e_{ij} \cos \frac{i\pi\alpha}{N} \sin \frac{j\pi\beta}{M} \\ f_{ij} \cos \frac{i\pi\alpha}{N} \cos \frac{j\pi\beta}{M} \end{Bmatrix} \quad \dots(5-7)$$

The form of the solution for the displacements δ_{α} , δ_{β} and δ_{γ} is the same as used in chapter 4. The rotations θ_{α} , θ_{β} and θ_{γ} also take on a finite series of trigonometric functions.

The solution fits the displacement conditions 5-4 as can be seen by inspection, and thus it is only necessary to show that it also fits the governing equation 5-3 and the force conditions in Appendix E obtained from the modification of expressions 5-5.

Both the governing equations and the boundary conditions involve the finite difference operators. Complete lists of all the operators and functions encountered are given in appendix A.

The force boundary conditions given in appendix E can be written in more concise forms using the notion of symmetric and anti-symmetric difference operations as introduced in section 4.4. In this manner it can be shown that all force boundary conditions are satisfied.

The load function $\{W_{\alpha}(\alpha, \beta)\}$ must also be expanded into a finite double series of the same form that is used for the displacements, viz.

$$\begin{Bmatrix} w_{\alpha}(\alpha, \beta) \\ w_{\beta}(\alpha, \beta) \\ w_{\gamma}(\alpha, \beta) \\ m_{\alpha}(\alpha, \beta) \\ m_{\beta}(\alpha, \beta) \\ m_{\gamma}(\alpha, \beta) \end{Bmatrix} = \sum_{i=0}^N \sum_{j=0}^M \begin{Bmatrix} p_{ij} \cos \frac{i\pi\alpha}{N} \sin \frac{j\pi\beta}{M} \\ q_{ij} \sin \frac{i\pi\alpha}{N} \cos \frac{j\pi\beta}{M} \\ r_{ij} \sin \frac{i\pi\alpha}{N} \sin \frac{j\pi\beta}{M} \\ s_{ij} \sin \frac{i\pi\alpha}{N} \cos \frac{j\pi\beta}{M} \\ t_{ij} \cos \frac{i\pi\alpha}{N} \sin \frac{j\pi\beta}{M} \\ u_{ij} \cos \frac{i\pi\alpha}{N} \cos \frac{j\pi\beta}{M} \end{Bmatrix} \quad \dots(5-8)$$

where the fourier coefficients p_{ij} , q_{ij} , ..., u_{ij} are determined from the known loading functions. The method to determine these is given in appendix B.

The assumed displacement form can be substituted into the governing equations together with the series for the loading. The effects of the operators are carried out and like terms are equated to give equations for the unknown coefficients a_{ij} , b_{ij} , ..., f_{ij} in terms of the known loading coefficients p_{ij} , q_{ij} , ..., u_{ij} . This results in $(N + 1) \times (M + 1)$ sets of six equations in six unknowns - one set for each value of i and j . The equations can be written in the abbreviated form

$$[V]_{ij} \begin{Bmatrix} a_{ij} \\ b_{ij} \\ \vdots \\ f_{ij} \end{Bmatrix} = \begin{Bmatrix} p_{ij} \\ q_{ij} \\ \vdots \\ u_{ij} \end{Bmatrix} \quad \dots(5-9)$$

where matrix $[V]_{ij}$ is a six by six matrix with each element dependent on the value of i and j . Typical elements are

$$\begin{aligned} v_{11} = & +2\left(\frac{EA}{L}\right)_1 \cos^2 \sigma_1 \left\{1 - \cos \frac{i\pi 2}{N}\right\} + 4\left(\frac{EA}{L}\right)_2 \cos^2 \theta \cos^2 \sigma_2 \left\{1 - \cos \frac{i\pi}{N} \cos \frac{j\pi}{M}\right\} \\ & + 24\left(\frac{EI}{L^3}\right)_1 \sin^2 \sigma_1 \left\{1 + \cos \frac{i\pi 2}{N}\right\} + 48\left(\frac{EI}{L^3}\right)_2 \cos^2 \theta \sin^2 \sigma_2 \left\{1 + \cos \frac{i\pi}{N} \cos \frac{j\pi}{M}\right\} \\ & + 48\left(\frac{EI}{L^3}\right)_2 \sin^2 \theta \left\{1 - \cos \frac{i\pi}{N} \cos \frac{j\pi}{M}\right\} \end{aligned}$$

$$v_{14} = -24 \left(\frac{EI}{L^3} \right) {}_2 \cos \theta \sin \theta \sin \sigma_2 \left\{ \sin \frac{i\pi}{N} \sin \frac{j\pi}{M} \right\} \\ - 24 \left(\frac{EI}{L^3} \right) {}_2 \cos \theta \sin \theta \sin \sigma_2 \left\{ \sin \frac{i\pi}{N} \sin \frac{j\pi}{M} \right\}$$

Detailed expressions for each element are given in appendix F.

5.5 DISPLACEMENTS

When the displacement series coefficients a_{ij} , b_{ij} , ..., f_{ij} have been determined for all values of i and j , they can be used in expression 5-7 for the displacements $\delta_\alpha(\alpha, \beta)$, $\delta_\beta(\alpha, \beta)$, ..., $\theta_\gamma(\alpha, \beta)$. These series would be evaluated numerically and involve the summation of a finite series of trigonometric functions for the displacement of each joint.

5.6 MEMBER ACTIONS

The displacements at the two ends of a member are used in expression 4-8 to give the end actions. For this type of member, there are an axial force, two transverse shear forces, two transverse bending moments and a torsional moment to be determined.

5.7 JOINT RESIDUALS

The numerical accuracy of the calculations can be checked by computing the resultant forces due to the member actions of all members meeting at a joint. For an internal joint, these residual forces should balance the applied joint loads. Any difference indicates an error or inaccurate calculations.

For an edge joint, the resulting forces are balanced by the reactions supplied by the boundary supports.

CHAPTER SIX

ANALYSIS OF A DOUBLE LAYER PIN JOINTED STRUCTURE6.1 DESCRIPTION OF THE STRUCTURE

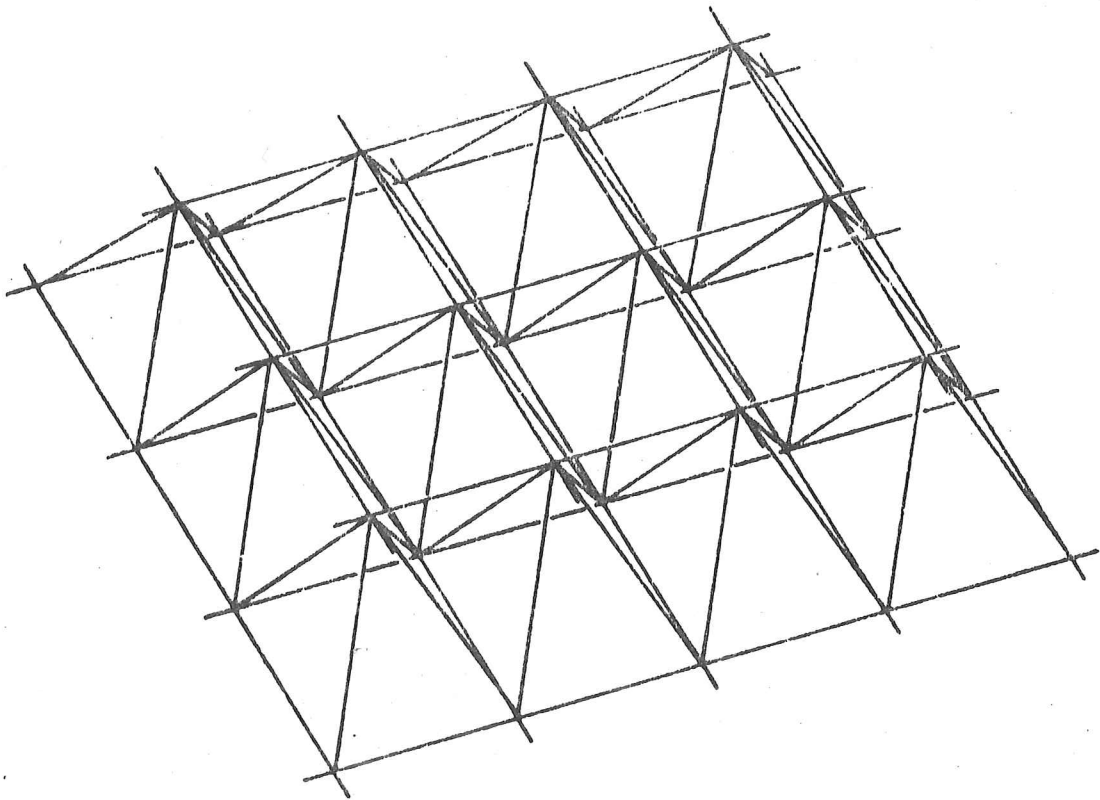
The structure considered in this chapter has the lattice joints lying in two distinct layers with a constant spacing (D) between these two layers. The middle surface, halfway between the two layers, lies on a shallow doubly curved surface whose equation is the same as equation 4-1 which represented the surface of the single layer structure of chapters 4 and 5. The boundaries are also the same. For various values of the surface parameters, the surface takes on the shapes described in chapter 4 (see fig. 4.1).

The layout of joints and members is different from that used in chapter 4. A small portion of the structure is shown in figure 6.1a to indicate the layout. Both the upper and lower layers contain an arrangement of members lying wholly within the appropriate layer, with the two layers being connected by web type members. The typical module is shown in figure 6.1b and, unlike the structures treated in chapters 4 and 5, here the typical module contains two distinct joints. This involves an extension to the procedure used before, and the present chapter is included to demonstrate the technique.

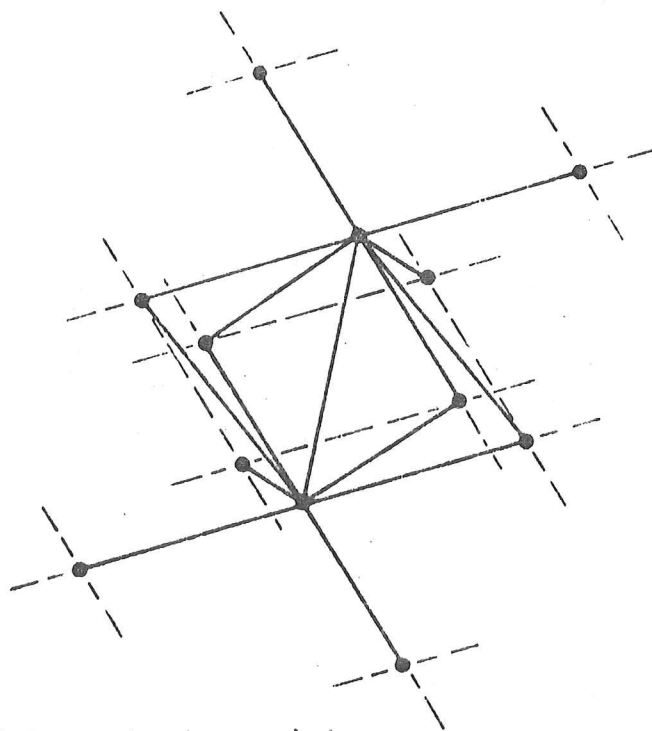
The members have pin jointed ends and are subjected only to axial loads. Linear behaviour of the component members and of the complete structure is considered.

6.2 DERIVATION OF GOVERNING EQUATIONS

The derivation of the governing equations follows the general outline given in chapter 2, with the extension to a module which contains more than one joint. The basic element used for all members is a pin ended bar as shown in figure 6.2. Also shown are the displacements, actions and



(a) Portion of structure



(b) Typical module

Fig. 6.1 DOUBLE LAYER STRUCTURE LAYOUT.

local x, y, z coordinate system axes. The element is the same as that used in chapter 4 and the load deformation relations are the same as given there (see equation 4-2).

The transformation between the local and curvilinear coordinate systems is also the same as used in chapter 4 and is given in equation 4-4. The values of the angles ϕ and ψ , however, are determined in a different manner. The resulting load deformation relation in the curvilinear α, β, γ coordinate system is

$$\begin{Bmatrix} \{P_\alpha\}_1 \\ \{P_\alpha\}_2 \end{Bmatrix} = \begin{bmatrix} K_{11} & K_{12} \\ K_{21} & K_{22} \end{bmatrix} \begin{Bmatrix} \{\Delta_\alpha\}_1 \\ \{\Delta_\alpha\}_2 \end{Bmatrix} \quad \dots(6-1)$$

$$\text{where } [K_{ij}] = [T_i][k_{ij}][T_j^T] \quad \dots(6-2)$$

for $i = 1, 2$ and $j = 1, 2$

Details of the matrices $[K_{ij}]$ for this rod member are given in appendix C.

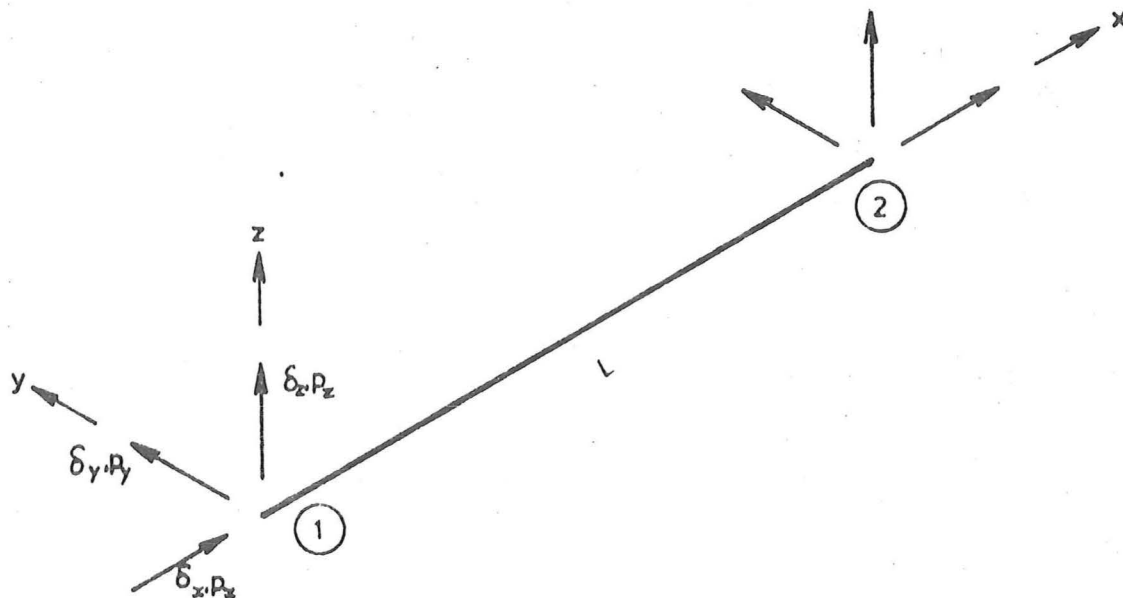


Fig.6.2 BAR MEMBER AXES, DISPLACEMENTS AND ACTIONS.

For equilibrium at a joint, the actions at end 1 of the member are needed. Relation 6-1 is partitioned to give these as

$$\{P_{\alpha}\}_1 = [K_{11}]\{\Delta_{\alpha}\}_1 + [K_{12}]\{\Delta_{\alpha}\}_2 \quad \dots(6-3)$$

Up to this point, the procedure is the same as that followed in chapters 4 and 5. It is here that consideration must be made that the typical module of the structure shown in figure 6.1b contains two types of joint, characterised by the layer of the structure, upper or lower, in which it lies. The displacements of the joints are functions of the (discrete) coordinates (α, β) describing the location of the joint and thus the member end displacements are represented by an upper layer joint displacement function $\{\Delta_{\alpha}(\alpha, \beta)\}$ or by a lower layer joint displacement function $\{\bar{\Delta}_{\alpha}(\alpha, \beta)\}$.

For a member wholly in the upper layer, the joint displacements can be expressed as

$$\begin{aligned} \{\Delta_{\alpha}\}_1 &= \{\Delta_{\alpha}(\alpha, \beta)\} \\ \{\Delta_{\alpha}\}_2 &= \{\Delta_{\alpha}(\alpha+g, \beta+h)\} \\ &= E_{\alpha}^g E_{\beta}^h \{\Delta_{\alpha}(\alpha, \beta)\} \end{aligned} \quad \dots(6-4)$$

where $E_{\alpha}^g, E_{\beta}^h$ are the shift operators described in section 3.6.2 and g, h depend on the member length and orientation. When these displacements are substituted into expression 6-3, the end actions at end 1 (the joint at coordinates (α, β)) are given by

$$\{P_{\alpha}(\alpha, \beta)\} = [K_{11}]\{\Delta_{\alpha}(\alpha, \beta)\} + [K_{12}]E_{\alpha}^g E_{\beta}^h \{\Delta_{\alpha}(\alpha, \beta)\} \quad \dots(6-5)$$

For a member wholly in the lower layer, both joints are lower layer joints and the end displacements are

$$\begin{aligned} \{\Delta_{\alpha}\}_1 &= \{\bar{\Delta}_{\alpha}(\alpha, \beta)\} \\ \{\Delta_{\alpha}\}_2 &= E_{\alpha}^g E_{\beta}^h \{\bar{\Delta}_{\alpha}(\alpha, \beta)\} \end{aligned} \quad \dots(6-6)$$

and the member actions are

$$\{\bar{P}_\alpha(\alpha, \beta)\} = [K_{11}]\{\bar{\Delta}_\alpha(\alpha, \beta)\} + [K_{12}]E_\alpha^g E_\beta^h \{\bar{\Delta}_\alpha(\alpha, \beta)\} \quad \dots(6-7)$$

For a member that links the upper and lower layers, two situations can arise. One is that the joint at end 1 is in the upper layer and thus end 2 is in the lower layer. For this case the displacements are

$$\begin{aligned} \{\Delta_\alpha\}_1 &= \{\Delta_\alpha(\alpha, \beta)\} \\ \{\Delta_\alpha\}_2 &= E_\alpha^g E_\beta^h \{\bar{\Delta}_\alpha(\alpha, \beta)\} \end{aligned} \quad \dots(6-8)$$

and the end actions are

$$\{P_\alpha(\alpha, \beta)\} = [K_{11}]\{\Delta_\alpha(\alpha, \beta)\} + [K_{12}]E_\alpha^g E_\beta^h \{\bar{\Delta}_\alpha(\alpha, \beta)\} \quad \dots(6-9)$$

The other situation is for end 1 to be in the lower layer and end 2 to be in the upper layer. The displacements are then given by

$$\begin{aligned} \{\Delta_\alpha\}_1 &= \{\bar{\Delta}_\alpha(\alpha, \beta)\} \\ \{\Delta_\alpha\}_2 &= E_\alpha^g E_\beta^h \{\Delta_\alpha(\alpha, \beta)\} \end{aligned} \quad \dots(6-10)$$

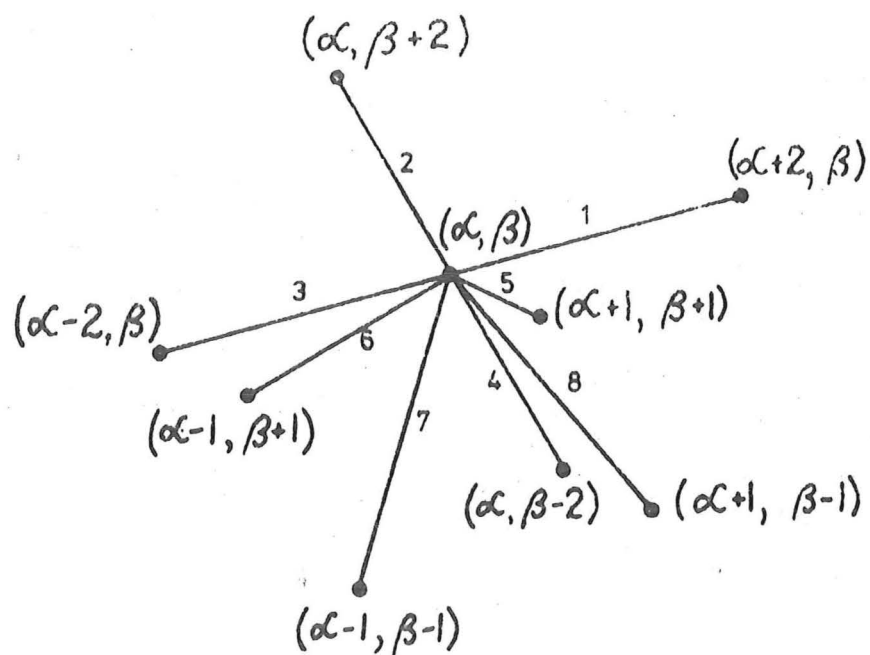
The end action then becomes

$$\{\bar{P}_\alpha(\alpha, \beta)\} = [K_{11}]\{\bar{\Delta}_\alpha(\alpha, \beta)\} + [K_{12}]E_\alpha^g E_\beta^h \{\Delta_\alpha(\alpha, \beta)\} \quad \dots(6-11)$$

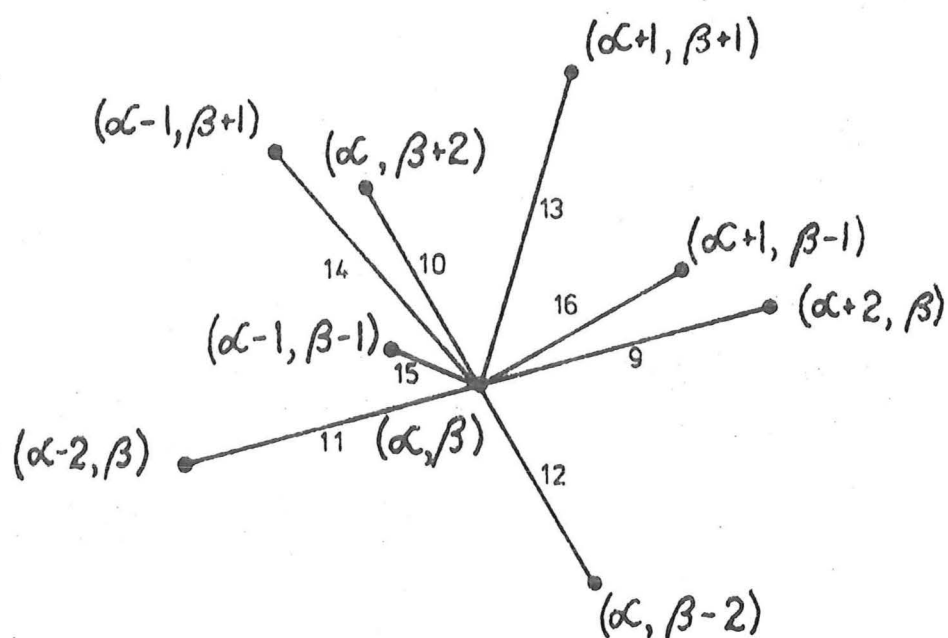
These four cases are all that are possible for this structure.

Now that the member end actions are known for each type of member, it is possible to form equilibrium equations at the two typical joints. One joint will be considered at a time to assist the explanation of how they are formed.

Consider first the typical joint in the upper layer as shown in figure 6.3a. There are 8 members meeting there and of these, 4 lie completely in the upper layer and 4 link the upper and lower layers. The applied load vector $\{W_\alpha(\alpha, \beta)\}$ is balanced by the sum of the end actions of these members. With the numbering of the members shown in figure 6.3a, the equilibrium equation becomes



(a) Upper layer joint



(b) Lower layer joint

Fig. 6.3 DOUBLE LAYER STRUCTURE JOINTS

$$\begin{aligned}
\{W_\alpha(\alpha, \beta)\} &= \sum_{i=1}^8 \{P_\alpha(\alpha, \beta)\}_i \\
&= \sum_{i=1,2,3,4} \left([K_{11}]_i + [K_{12}]_i E_\alpha^{g_i} E_\beta^{h_i} \right) \{\Delta_\alpha(\alpha, \beta)\} \\
&\quad + \sum_{i=5,6,7,8} \left([K_{11}]_i \{\Delta_\alpha(\alpha, \beta)\} + [K_{12}]_i E_\alpha^{g_i} E_\beta^{h_i} \{\bar{\Delta}_\alpha(\alpha, \beta)\} \right) \\
&= \left[\sum_{i=1}^8 [K_{11}]_i \right] \{\Delta_\alpha(\alpha, \beta)\} + \sum_{i=1,2,3,4} \left[[K_{12}]_i E_\alpha^{g_i} E_\beta^{h_i} \right] \{\Delta_\alpha(\alpha, \beta)\} \\
&\quad + \sum_{i=5,6,7,8} \left[[K_{12}]_i E_\alpha^{g_i} E_\beta^{h_i} \right] \{\bar{\Delta}_\alpha(\alpha, \beta)\} \quad \dots (6-12)
\end{aligned}$$

In a similar manner, at the lower layer joint, the load vector $\{\bar{W}_\alpha(\alpha, \beta)\}$ is equated with the sum of the member actions to give (see figure 6.3b)

$$\begin{aligned}
\{\bar{W}_\alpha(\alpha, \beta)\} &= \sum_{i=9}^{16} \{\bar{P}_\alpha(\alpha, \beta)\}_i \\
&= \sum_{i=13,14,15,16} \left[[K_{12}]_i E_\alpha^{g_i} E_\beta^{h_i} \right] \{\Delta_\alpha(\alpha, \beta)\} \\
&\quad + \left[\sum_{i=9}^{16} [K_{11}]_i \right] \{\Delta_\alpha(\alpha, \beta)\} + \sum_{i=9,10,11,12} \left[[K_{12}]_i E_\alpha^{g_i} E_\beta^{h_i} \right] \{\bar{\Delta}_\alpha(\alpha, \beta)\} \quad \dots (6-13)
\end{aligned}$$

These summations appear to involve 16 members. However only 15 of these are distinct, as web members 7 and 13 are the same. They are given a different number for the two situations so as to make end 1 of the member in the upper and lower layers respectively. The values of ψ and ϕ are adjusted to make this so.

These two equations 6-12 and 6-13 can be combined into the single system of equations

$$\begin{Bmatrix} W_\alpha(\alpha, \beta) \\ \bar{W}_\alpha(\alpha, \beta) \end{Bmatrix} = \begin{bmatrix} V_{11} & V_{12} \\ V_{21} & V_{22} \end{bmatrix} \begin{Bmatrix} \Delta_\alpha(\alpha, \beta) \\ \bar{\Delta}_\alpha(\alpha, \beta) \end{Bmatrix} \quad \dots (6-14)$$

where

$$\begin{aligned}
 [V_{11}] &= \left[\sum_{i=1}^8 ([K_{11}]_i) + \sum_{i=1,2,3,4} ([K_{12}]_i E_{\alpha}^{g_i} E_{\beta}^{h_i}) \right] \\
 [V_{12}] &= \left[\sum_{i=5,6,7,8} ([K_{12}]_i E_{\alpha}^{g_i} E_{\beta}^{h_i}) \right] \\
 [V_{21}] &= \left[\sum_{i=1,3,14,15,16} ([K_{12}]_i E_{\alpha}^{g_i} E_{\beta}^{h_i}) \right] \\
 [V_{22}] &= \left[\sum_{i=9}^{16} ([K_{11}]_i) + \sum_{i=1,3,14,15,16} ([K_{12}]_i E_{\alpha}^{g_i} E_{\beta}^{h_i}) \right]
 \end{aligned}$$

The matrices $[K_{11}]_i$ and $[K_{12}]_i$ and the parameters g_i and h_i in expression 6-14 are derived from the properties and orientations of the members. The values of the relevant variables are given in Table 6.1. These values are derived from the layout shown in figure 6.1. There is symmetry about both the α and β axes and thus the variable take on only a few values.

When these values are substituted into expression 6-14 the result is the governing partial difference equation for the deflections,

$$\begin{bmatrix}
 V_{11} & V_{12} & V_{13} & \cdot & \cdot & V_{16} \\
 V_{21} & V_{22} & & & & \\
 V_{31} & & \cdot & & & \\
 \cdot & & & \text{etc} & & \\
 \cdot & & & & \cdot & \\
 V_{61} & & & & & V_{66}
 \end{bmatrix}
 \begin{Bmatrix}
 \delta_{\alpha} \\
 \delta_{\beta} \\
 \delta_{\gamma} \\
 \bar{\delta}_{\alpha} \\
 \bar{\delta}_{\beta} \\
 \bar{\delta}_{\gamma}
 \end{Bmatrix}
 =
 \begin{Bmatrix}
 w_{\alpha} \\
 w_{\beta} \\
 w_{\gamma} \\
 \bar{w}_{\alpha} \\
 \bar{w}_{\beta} \\
 \bar{w}_{\gamma}
 \end{Bmatrix}$$

where two typical elements of the matrix are

$$V_{11} = S_{\alpha} \cos^2 \sigma_{\alpha} \{2 - (E_{\alpha}^{+2} + E_{\alpha}^{-2})\} + S_d \cos^2 \theta \cos^2 \phi \{4\}$$

$$V_{14} = S_d \cos^2 \theta \cos^2 \phi \{-(E_{\alpha}^{+1} + E_{\alpha}^{-1})(E_{\beta}^{+1} + E_{\beta}^{-1})\}$$

where $S = (EA/L)$ with an appropriate subscript of α, β or d indicating the direction the member lies in. The other terms of the matrix are given in full in appendix D.

TABLE 6.1 Double Layer Structure Member Orientations and Properties

Member No	End 1		End 2		$S_i = \left(\frac{EA}{L}\right)_i$	g_i	h_i
i	ϕ	ψ	ϕ	ψ			
1	$-\sigma_\alpha$	0	σ_α	0	S_α	+2	0
2	$-\sigma_\beta$	$\pi/2$	σ_β	$\pi/2$	S_β	0	+2
3	$-\sigma_\alpha$	π	σ_α	π	S_α	-2	0
4	$-\sigma_\beta$	$3\pi/2$	σ_β	$3\pi/2$	S_β	0	-2
5	$-\phi$	θ	$-\phi$	θ	S_d	+1	+1
6	$-\phi$	$\pi-\theta$	$-\phi$	$\pi-\theta$	S_d	-1	+1
7	$-\phi$	$\pi+\theta$	$-\phi$	$\pi+\theta$	S_d	-1	-1
8	$-\phi$	$2\pi-\theta$	$-\phi$	$2\pi-\theta$	S_d	+1	-1
9	$-\sigma_\alpha$	0	σ_α	0	\bar{S}_α	+2	0
10	$-\sigma_\beta$	$\pi/2$	σ_β	$\pi/2$	\bar{S}_β	0	+2
11	$-\sigma_\alpha$	π	σ_α	π	\bar{S}_α	-2	0
12	$-\sigma_\beta$	$3\pi/2$	σ_β	$3\pi/2$	\bar{S}_β	0	-2
13	ϕ	θ	ϕ	θ	S_d	+1	+1
14	ϕ	$\pi-\theta$	ϕ	$\pi-\theta$	S_d	-1	+1
15	ϕ	$\pi+\theta$	ϕ	$\pi+\theta$	S_d	-1	-1
16	ϕ	$2\pi-\theta$	ϕ	$2\pi-\theta$	S_d	+1	-1

where

$$\theta = \tan^{-1} \left\{ \frac{L_Y}{M} / \frac{L_X}{N} \right\}$$

$$\sigma_\alpha = \frac{8H_X}{NL_X}$$

$$\sigma_\beta = \frac{8H_Y}{ML_Y}$$

$$\phi = \tan^{-1} \left\{ D / \sqrt{\left(\frac{L_Y}{M}\right)^2 + \left(\frac{L_X}{N}\right)^2} \right\}$$

6.3 BOUNDARY CONDITIONS

The structure is bounded by diaphragm type supports on a rectangular boundary, and thus the boundary conditions are similar to those for the single layer structure with the extension to two layers. The conditions in the plane of the diaphragm are

$$\delta_{\alpha}(\alpha, \beta) = \bar{\delta}_{\alpha}(\alpha, \beta) = 0 \quad \text{at } \beta = 0 \text{ and } \beta = M \quad \dots(6-15a)$$

$$\delta_{\beta}(\alpha, \beta) = \bar{\delta}_{\beta}(\alpha, \beta) = 0 \quad \text{at } \alpha = 0 \text{ and } \alpha = N \quad \dots(6-15b)$$

$$\delta_{\gamma}(\alpha, \beta) = \bar{\delta}_{\gamma}(\alpha, \beta) = 0 \quad \text{at } \alpha = 0 \text{ and } \alpha = N \text{ and } \beta = 0 \text{ and } \beta = M \quad \dots(6-15c)$$

The out of plane conditions are (see figure 6.4)

$$(p_{\alpha})_1 + (p_{\alpha})_5 + (p_{\alpha})_8 = 0 \quad \text{at } \alpha = 0 \quad \dots(6-16a)$$

$$(p_{\alpha})_3 + (p_{\alpha})_6 + (p_{\alpha})_7 = 0 \quad \text{at } \alpha = N \quad \dots(6-16b)$$

$$(\bar{p}_{\alpha})_9 + (\bar{p}_{\alpha})_{13} + (\bar{p}_{\alpha})_{16} = 0 \quad \text{at } \alpha = 0 \quad \dots(6-16c)$$

$$(\bar{p}_{\alpha})_{11} + (\bar{p}_{\alpha})_{14} + (\bar{p}_{\alpha})_{15} = 0 \quad \text{at } \alpha = N \quad \dots(6-16d)$$

$$(p_{\beta})_2 + (p_{\beta})_5 + (p_{\beta})_6 = 0 \quad \text{at } \beta = 0 \quad \dots(6-16e)$$

$$(p_{\beta})_4 + (p_{\beta})_7 + (p_{\beta})_8 = 0 \quad \text{at } \beta = M \quad \dots(6-16f)$$

$$(\bar{p}_{\beta})_{10} + (\bar{p}_{\beta})_{13} + (\bar{p}_{\beta})_{14} = 0 \quad \text{at } \beta = 0 \quad \dots(6-16g)$$

$$(\bar{p}_{\beta})_{12} + (\bar{p}_{\beta})_{15} + (\bar{p}_{\beta})_{16} = 0 \quad \text{at } \beta = M \quad \dots(6-16h)$$

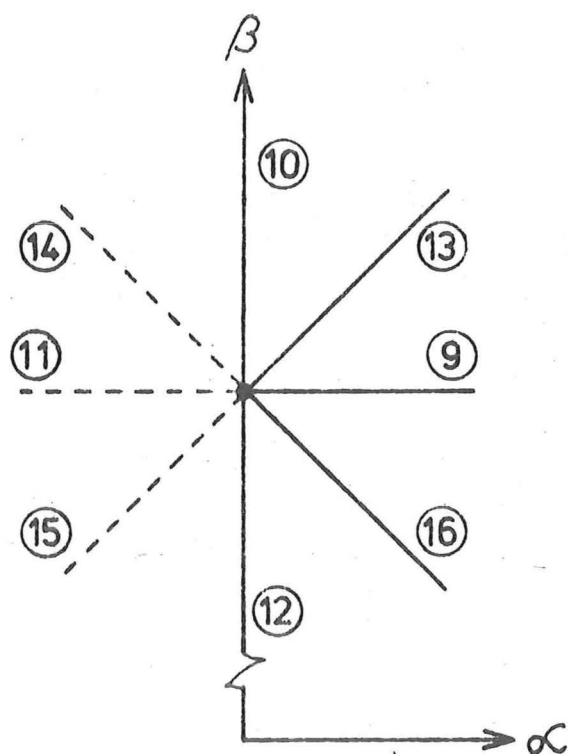
The procedure of logically extending the structure as outlined in section 4.3 can also be used here to combine and simplify the force boundary conditions. Expressions 6-16a and 6-16b combine to give

$$[(p_{\alpha})_1 + (p_{\alpha})_5 + (p_{\alpha})_8] - [(p_{\alpha})_3 + (p_{\alpha})_6 + (p_{\alpha})_7] = 0 \quad \dots(6-17)$$

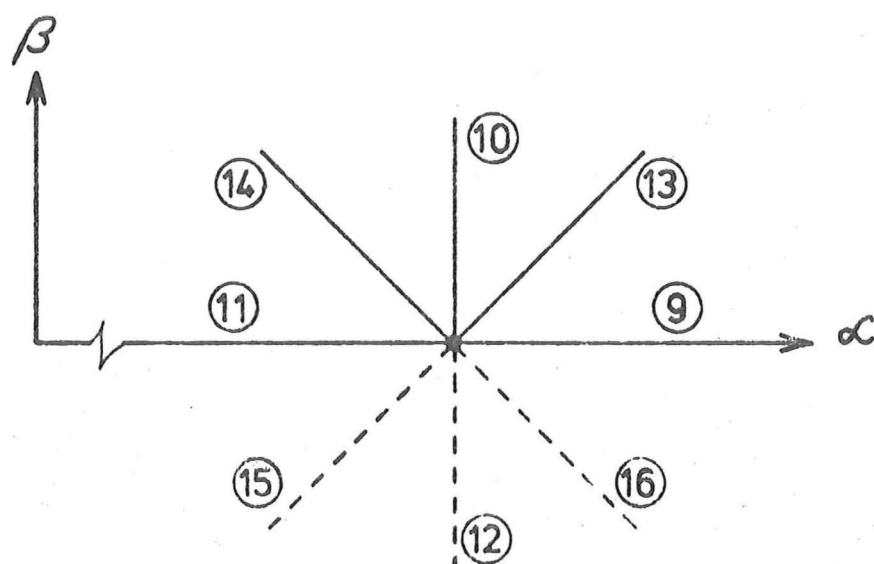
$$\text{at } \alpha = 0 \text{ and } \alpha = N$$

This can then be expressed in terms of the displacement functions and then becomes a condition on these of

$$\begin{aligned} & [s_{\alpha} \cos^2 \sigma_{\alpha} (E_{\alpha}^{+2} - E_{\alpha}^{-2})] \delta_{\alpha} \\ & + [0] \delta_{\beta} \\ & + [s_{\alpha} \cos \sigma_{\alpha} \sin \sigma_{\alpha} \{2 + (E_{\alpha}^{+2} + E_{\alpha}^{-2})\} + s_d \cos \theta \cos \phi \sin \phi \{4\}] \delta_{\gamma} \end{aligned}$$



(a) $\alpha = 0$ edge



(b) $\beta = 0$ edge

Fig. 6.4 LOWER LAYER BOUNDARY JOINTS

$$\begin{aligned}
& + [S_d \cos^2 \theta \cos^2 \phi (E_\alpha^{+1} - E_\alpha^{-1}) (E_\beta^{+1} + E_\beta^{-1})] \bar{\delta}_\alpha \\
& + [S_d \cos \theta \sin \theta \cos^2 \phi (E_\alpha^{+1} + E_\alpha^{-1}) (E_\beta^{+1} - E_\beta^{-1})] \bar{\delta}_\beta \\
& + [S_d \cos \theta \cos \phi \sin \phi \{-(E_\alpha^{+1} + E_\alpha^{-1}) (E_\beta^{+1} + E_\beta^{-1})\}] \bar{\delta}_\alpha = 0
\end{aligned}$$

at $\alpha = 0$ and $\alpha = N$

The other out of plane requirements can be treated in a similar manner and lead to the conditions on the displacements given in full in appendix E.

6.4 SOLUTION OF GOVERNING EQUATION

There are 6 unknown displacement functions for this structure, three for the upper layer and three for the lower layer. A suitable form for this is

$$\begin{Bmatrix} \delta_\alpha(\alpha, \beta) \\ \delta_\beta(\alpha, \beta) \\ \delta_\gamma(\alpha, \beta) \\ \bar{\delta}_\alpha(\alpha, \beta) \\ \bar{\delta}_\beta(\alpha, \beta) \\ \bar{\delta}_\alpha(\alpha, \beta) \end{Bmatrix} = \sum_{i=0}^N \sum_{j=0}^M \begin{Bmatrix} a_{ij} \cos \frac{i\pi\alpha}{N} \sin \frac{j\pi\beta}{M} \\ b_{ij} \sin \frac{i\pi\alpha}{N} \cos \frac{j\pi\beta}{M} \\ c_{ij} \sin \frac{i\pi\alpha}{N} \sin \frac{j\pi\beta}{M} \\ d_{ij} \cos \frac{i\pi\alpha}{N} \sin \frac{j\pi\beta}{M} \\ e_{ij} \sin \frac{i\pi\alpha}{N} \cos \frac{j\pi\beta}{M} \\ f_{ij} \sin \frac{i\pi\alpha}{N} \sin \frac{j\pi\beta}{M} \end{Bmatrix} \quad \dots(6-18)$$

It is necessary to show that this assumed solution fits the governing difference equations and the boundary conditions. By inspection it can be seen to fit the displacement boundary conditions 6-15 and by the technique of expressing the force boundary conditions 6-16 in terms of symmetric and anti symmetric operator expressions, as demonstrated in section 4-4, it is possible to show it also fits these conditions. The details of this are given in appendix E.

The load function $\{W_\alpha(\alpha, \beta)\}$ has to be expressed into a series similar to the displacement function, i.e.

$$\begin{Bmatrix} w_{\alpha}(\alpha, \beta) \\ w_{\beta}(\alpha, \beta) \\ w_{\gamma}(\alpha, \beta) \\ \bar{w}_{\alpha}(\alpha, \beta) \\ \bar{w}_{\beta}(\alpha, \beta) \\ \bar{w}_{\gamma}(\alpha, \beta) \end{Bmatrix} = \sum_{i=0}^N \sum_{j=0}^M \begin{Bmatrix} p_{ij} \cos \frac{i\pi\alpha}{N} \sin \frac{j\pi\beta}{M} \\ q_{ij} \sin \frac{i\pi\alpha}{N} \cos \frac{j\pi\beta}{M} \\ r_{ij} \sin \frac{i\pi\alpha}{N} \sin \frac{j\pi\beta}{M} \\ s_{ij} \cos \frac{i\pi\alpha}{N} \sin \frac{j\pi\beta}{M} \\ t_{ij} \sin \frac{i\pi\alpha}{N} \cos \frac{j\pi\beta}{M} \\ u_{ij} \sin \frac{i\pi\alpha}{N} \sin \frac{j\pi\beta}{M} \end{Bmatrix} \quad \dots(6-19)$$

The fourier coefficients p_{ij} , q_{ij} , ..., u_{ij} are determined from the known loading functions by the methods given in appendix B.

These fourier expansions for the displacements and the loads are now substituted into the governing equation 6-14 and the effects of the operators carried out. The orthogonality of the terms allows like members to be equated to give equations for the displacement coefficients a_{ij} , b_{ij} , ..., f_{ij} in terms of the loading coefficients p_{ij} , q_{ij} , ..., u_{ij} .

These equations are of the form

$$[V]_{ij} \begin{Bmatrix} a_{ij} \\ b_{ij} \\ \cdot \\ \cdot \\ \cdot \\ f_{ij} \end{Bmatrix} = \begin{Bmatrix} p_{ij} \\ q_{ij} \\ \cdot \\ \cdot \\ \cdot \\ u_{ij} \end{Bmatrix} \quad \dots(6-20)$$

for $i = 0, 1, \dots, N$ and $j = 0, 1, \dots, M$

where $[V]_{ij}$ is a 6×6 matrix with elements dependent on the values of i and j . Typical elements are

$$v_{11} = +2S_{\alpha} \cos^2 \sigma_{\alpha} \left\{ 1 - \cos \frac{i\pi 2}{N} \right\} + 4S_d \cos^2 \theta \cos^2 \phi$$

$$v_{14} = -4S_d \cos^2 \theta \cos^2 \phi \left\{ \cos \frac{i\pi}{N} \cos \frac{j\pi}{M} \right\}$$

Detailed expressions for all the elements of $[V]_{ij}$ are given in appendix F.

6.5 DISPLACEMENTS

Once the displacement coefficients a_{ij} , b_{ij} , ..., f_{ij} have been computed from expression 6-20, they can be used in expression 6-19 to give the displacements of the joints. The upper layer joint displacements are determined from the a_{ij} , b_{ij} and c_{ij} coefficients and the lower layer joint displacements from the d_{ij} , e_{ij} and f_{ij} coefficients. The series would generally be summed numerically using a digital computer.

6.6 MEMBER ACTIONS

The axial force in each member, the only action considered in this analysis, is determined from the displacements at the two ends of the member using expression 4-8 together with the appropriate values for the properties and orientations of the member.

6.7 JOINT RESIDUALS

The resulting forces due to the member actions of all members meeting at a joint can be computed. This serves as a check on the accuracy of the solution as, for internal joints, the resultant forces should balance the applied joint loads. At an edge joint, the resultant forces are balanced by the boundary reaction and thus effectively give the support reactions.

NUMERICAL TECHNIQUES7.1 INTRODUCTION

In chapters 4, 5 and 6 there were presented the mathematical models of three classes of lattice structures. For each of these three classes, a finite series solution was proposed and it was shown that the assumed form satisfied the equations and the boundary conditions. However, it was not indicated in those chapters how to make use of the series solutions and so one of the purposes of this chapter is to demonstrate the numerical procedures and special techniques that assist in using the solutions.

A further purpose is to describe the computer programs which were written to perform the numerical work and, by comparison with the results of the direct stiffness method and the analogous continuum method, to show when the proposed method is satisfactory and favourable in analysing the classes of structures treated.

7.2 GENERAL OUTLINE OF NUMERICAL PROCEDURES

The general form of the solutions for the three classes of structures considered in chapters 4, 5 and 6 are similar and thus the procedures to obtain numerical results are also similar for the three cases. Because of this it is only necessary to give the detail for one of them.

The numerical analysis starts with the description of the structure - the geometric and structural properties. From these, values for σ , ϕ and θ , the member length and material properties for each member can be determined for subsequent use.

The loading on the structure is then processed. This is given in the form of the load, with three (or six) components, on each joint, and, to be of use in this solution method, it must be expressed in the

form of a finite double trigonometric series. The procedure to do this is described in Appendix B and involves performing calculations of the form

$$p_{ij} = \frac{4}{NM} \sum_{\alpha=0}^N \sum_{\beta=0}^M w_{\alpha}(\alpha, \beta) \cos \frac{\alpha\pi i}{N} \sin \frac{\beta\pi j}{M}$$

for $i = 0, 1, \dots, N$ and $j = 0, 1, \dots, M$

to give the load series for each load component. These calculations involve a number of computations of the order $[(M+1)(N+1)]^2$ and storage requirements of $2(M+1)(N+1)$ locations.

The next step is to determine the displacement series coefficients from the load series coefficients and the properties of the lattice. This involves solving $(M+1)(N+1)$ sets of 3 (or 6) linear equations of the form

$$\begin{Bmatrix} p_{ij} \\ \cdot \\ \cdot \\ \cdot \end{Bmatrix} = \begin{bmatrix} \cdot \\ \cdot \\ \cdot \\ \cdot \end{bmatrix} v_{ij} \begin{Bmatrix} a_{ij} \\ \cdot \\ \cdot \\ \cdot \end{Bmatrix}$$

$$\text{for } i = 0, 1, \dots, N \text{ and } j = 0, 1, \dots, M$$

where p_{ij} , ... are the load series coefficients obtained above, a_{ij} , ... are the required displacement series coefficients and $[v_{ij}]$ is a 3 times 3 (or 6 times 6) matrix, the elements of which involve trigonometric functions of i and j . Thus the matrix $[v_{ij}]$ differs for each value of i and j and details of it are given in Appendix E. For this step, the volume of calculation work is in the order of $(N+1)(M+1)$ and the storage requirement is $2(N+1)(M+1)$.

The displacements are determined by summation of the finite series when the series coefficients are known. The requirement here is the evaluation of expressions of the form

$$\delta_{\alpha}(\alpha, \beta) = \sum_{i=0}^N \sum_{j=0}^M a_{ij} \cos \frac{i\pi\alpha}{N} \sin \frac{j\pi\beta}{M}$$

$$\text{for } \alpha = 0, 1, \dots, N \text{ and } \beta = 0, 1, \dots, M$$

This involves calculation work in the order of $[(N+1)(M+1)]^2$ and storage requirements of $2(N+1)(M+1)$.

The member actions can now be determined from the member stiffness matrices and the end displacements using relations of the form

$$\begin{Bmatrix} p \\ \cdot \\ \cdot \\ \cdot \end{Bmatrix}_1 = \begin{bmatrix} k_{11} \end{bmatrix} \begin{Bmatrix} \delta \\ \cdot \\ \cdot \\ \cdot \end{Bmatrix}_1 + \begin{bmatrix} k_{12} \end{bmatrix} \begin{Bmatrix} \delta \\ \cdot \\ \cdot \\ \cdot \end{Bmatrix}_2$$

This is performed for each member in the structure for which the stresses are required. If the member actions are required for all members, then the number of computations is of the order of $(N+1)(M+1)$.

In a similar manner, the reactions at each joint can be calculated from the displacements. This can be done as a check on the stability of the solution process and also to supply the reactions at the boundary of the structure.

The results, comprising the joint displacements, the member actions and the joint residuals can be output as a numerical print out, a graph plot or both.

A summary of the steps outlined above is given in table 7.1 together with the storage and computing requirements for each step.

7.3 SPECIAL NUMERICAL TECHNIQUES

From a preliminary study of the volume of computations, it became evident that the major amount of work is performed during the two steps, the fourier analysis of the loads and the evaluation of the displacement series. Both of these processes involve the summation of products of trigonometric functions.

Thus a detailed study of these areas with a view to reducing the volume of calculations will produce the most rewards in computing

TABLE 7.1 Operations, Computing Work and Storage Requirements for Finite Difference Analysis

Operation	Computing Work	Storage Requirements
1. Input geometric and structure data. Calculate preliminary data.	small	small
2. Input joint loads. Decompose into finite fourier series.	$(N+1)^2 (M+1)^2$	$2(N+1) (M+1)$
3. Determine displacement series coefficients from load series coefficients.	$(N+1) (M+1)$	$2(N+1) (M+1)$
4. Determine displacements from finite fourier series.	$(N+1)^2 (M+1)^2$	$2(N+1) (M+1)$
5. Determine member actions and boundary reactions.	$(N+1) (M+1)$	$(N+1) (M+1)$
6. Output results.	small	small

efficiency. It is towards this end that special techniques are used in these two segments of the calculations.

7.3.1 Trigonometric Functions

Most sections of the analysis involve the evaluation of trigonometric functions of the form

$$\cos \frac{k\pi\ell}{R} \quad \text{and} \quad \sin \frac{k\pi\ell}{R} \quad \begin{array}{l} \text{for } k = 0, 1, \dots, R \\ \text{and } \ell = 0, 1, \dots, R \end{array}$$

It was found that if these functions are evaluated using standard routines, then the computing time was quite large. As the functions are required at regular intervals of the argument, special properties of these functions can be used.

Consider the function $f(k) = e^{ki\theta}$ where $i = \sqrt{-1}$ and $e = 2.71828$, the base of the natural logarithms then $f(k+1) = e^{(k+1)i\theta}$

$$\begin{aligned} &= e^{ki\theta} \cdot e^{i\theta} \\ &= f(k) \cdot e^{i\theta} \end{aligned}$$

This is a one term recurrence relation for the function $f(k) = e^{ki\theta}$ given the value of $e^{i\theta}$ and the starting value $f(0) = e^0 = 1$. The function can be evaluated at the successive values of $k = 1, 2, 3, \dots$ in turn.

Making use of the identity,

$$\cos k\theta + i \sin k\theta = e^{ik\theta}$$

in the above formulation, gives

$$\begin{aligned} \cos(k+1)\theta + i \sin(k+1)\theta &= e^{(k+1)i\theta} \\ &= e^{ki\theta} \cdot e^{i\theta} \\ &= [\cos k\theta + i \sin k\theta][\cos\theta + i \sin\theta] \\ &= \{\cos k\theta \cos\theta - \sin k\theta \sin\theta\} \\ &\quad + i\{\cos k\theta \sin\theta + \sin k\theta \cos\theta\} \end{aligned}$$

Equating corresponding real and imaginary parts of this expression gives

$$\cos(k+1)\theta = \cos k\theta \cos \theta - \sin k\theta \sin \theta$$

$$\sin(k+1)\theta = \cos k\theta \sin \theta + \sin k\theta \cos \theta$$

These formulae provide a simple simultaneous recursive method of evaluating the successive values of the sine and cosine functions at uniform increments of the argument when given the starting values $\cos(0) = 1$ and $\sin(0) = 0$ and the increment θ or more specifically $\cos \theta$ and $\sin \theta$.

They may also be derived from the angle sum formulae of elementary trigonometry. However by using the method above, it can be seen that the technique is applicable to other functions, e.g. exponential and hyperbolic.

Tests were performed using the two approaches, direct evaluation versus recursion formulae, and these tests showed that on a Burroughs B6718 computer, the recursive formulae method took about one sixth of the computing time of the direct evaluation method. Accuracy did not appear to suffer due to the repeated summation process, with 7 digit accuracy after 750 increments.

7.3.2 Analytic Evaluation of Fourier Coefficients

The load on the structure must be decomposed into its fourier components in order to use the method advocated. This step accounts for just under one half of the total calculation work in the analysis and thus is one of the areas where improvements should be made if at all possible. For certain special load cases, the fourier coefficients can be determined analytically, rather than numerically, with a consequent saving in effort. Examples of such loadings include a point load and a uniformly distributed load. These two cases are discussed in detail here so as to demonstrate the techniques to be applied.

First consider the unit point function at location (ζ, η) defined by

$$\begin{aligned} f(\alpha, \beta) &= 1 \quad \text{at } \alpha = \zeta, \beta = \eta \\ &= 0 \quad \text{elsewhere} \end{aligned}$$

To expand $f(\alpha, \beta)$ into the finite series

$$f(\alpha, \beta) = \sum_{i=0}^N \sum_{j=0}^M a_{ij} \sin \frac{i\pi\alpha}{N} \sin \frac{j\pi\beta}{M}$$

involves determining the a_{ij} coefficients for $i = 0, 1, \dots, N$ and $j = 0, 1, \dots, M$. This has been shown for the general case in Appendix B and is

$$a_{ij} = \frac{4}{NM} \sum_{\alpha=0}^N \sum_{\beta=0}^M [f(\alpha, \beta) \sin \frac{i\pi\alpha}{N} \sin \frac{j\pi\beta}{M}]$$

When the values of $f(\alpha, \beta)$ given above are substituted into this expression, the only non zero value is at (ζ, η) and thus

$$\begin{aligned} a_{ij} &= \frac{4}{NM} \sin \frac{i\pi\zeta}{N} \sin \frac{j\pi\eta}{M} \\ &\text{for } i = 0, 1, \dots, N \text{ and } j = 0, 1, \dots, M \end{aligned}$$

The calculation work involved here is of the order $(N+1)(M+1)$ rather than $[(N+1)(M+1)]^2$ as for the general case.

Next consider a uniform unit load function over the entire structure as defined by

$$f(\alpha, \beta) = 1 \quad \text{for all } \alpha \text{ and } \beta$$

For the series expansion

$$f(\alpha, \beta) = \sum_{i=0}^N \sum_{j=0}^M a_{ij} \sin \frac{i\pi\alpha}{N} \sin \frac{j\pi\beta}{M}$$

the coefficients a_{ij} are given in the general case by

$$a_{ij} = \frac{4}{NM} \sum_{\alpha=0}^N \sum_{\beta=0}^M f(\alpha, \beta) \sin \frac{i\pi\alpha}{N} \sin \frac{j\pi\beta}{M}$$

and when the above form for $f(\alpha, \beta)$ is substituted, for the special case are given by

$$a_{ij} = \frac{4}{NM} \sum_{\alpha=0}^N \sum_{\beta=0}^M \sin \frac{i\pi\alpha}{N} \sin \frac{j\pi\beta}{M}$$

$$= \frac{4}{NM} \left[\sum_{\alpha=0}^N \sin \frac{i\pi\alpha}{N} \right] \left[\sum_{\beta=0}^M \sin \frac{j\pi\beta}{M} \right]$$

The summation

$$\sum_{\alpha=0}^N \sin \frac{i\pi\alpha}{N}$$

can be evaluated by using formulae 417 of reference [50] as then

$$\begin{aligned} \sum_{\alpha=0}^N \sin \frac{i\pi\alpha}{N} &= \sin \left[\frac{1}{2} (N+1) \frac{i\pi}{N} \right] \sin \left[\frac{N}{2} \frac{i\pi}{N} \right] \operatorname{cosec} \left[\frac{1}{2} \frac{i\pi}{N} \right] \\ &= \sin \frac{i\pi}{2} \sin \frac{i\pi}{2} \cot \frac{i\pi}{2N} + \sin \frac{i\pi}{2} \cos \frac{i\pi}{2} \end{aligned}$$

$$\begin{aligned} \text{Since } \sin \frac{i\pi}{2} &= 0 \text{ if } i \text{ is even} \\ &= +1 \text{ if } i = 4n+1 \\ &= -1 \text{ if } i = 4n-1 \end{aligned} \quad \begin{array}{l} \\ \\ n \text{ an integer} \end{array}$$

$$\begin{aligned} \text{and } \cos \frac{i\pi}{2} &= 0 \text{ if } i \text{ is odd} \\ &= +1 \text{ if } i = 4n \\ &= -1 \text{ if } i = 4n+2 \end{aligned} \quad \begin{array}{l} \\ \\ n \text{ an integer} \end{array}$$

$$\begin{aligned} \text{then } \sin \frac{i\pi}{2} \sin \frac{i\pi}{2} &= 0 \text{ if } i \text{ is even} \\ &= +1 \text{ if } i \text{ is odd} \end{aligned}$$

$$\text{and } \sin \frac{i\pi}{2} \cos \frac{i\pi}{2} = 0 \text{ for all } i.$$

And thus

$$\sum_{\alpha=0}^N \sin \frac{i\pi\alpha}{N} = \cot \frac{i\pi}{2N}$$

Finally the series coefficients are given by

$$a_{ij} = \frac{4}{NM} \cot \frac{i\pi}{2N} \cot \frac{j\pi}{2M}$$

Again the calculation work involved is only of the order of $(N+1)(M+1)$ for this case.

In a similar manner, the expressions for the coefficients for the series involving the other combinations of sine and cosine functions can

be determined. These are collected together and given for reference in Appendix B.

7.4 COMPUTER PROGRAM

The series solutions produced in chapters 4, 5 and 6 were evaluated by computer programs written in Fortran and executed on the Burroughs B6718 digital computer of the University of Canterbury Computer Centre.

These programs perform all the necessary computations to analyse the structures, starting with a description of the structure geometry and member properties. The output consists of the displacements at each joint, the member actions of each member and the residual forces at each joint. The load cases considered are the general load, the point load and uniform load. A flow chart of the process is given in figure 7.1. The same procedure is used for each of the structure types considered with the detailed calculations changed slightly for each. A listing of one of the programs - that for a single layer rigid jointed lattice - is given in Appendix G.

7.5 NUMERICAL VERIFICATION OF THE ANALYSIS

In order to verify that the method used in this thesis and the resulting computer programs are satisfactory, it is necessary to compare the analysis results with those from one or more other analysis methods. For this purpose a series of structures was chosen and analysed by the finite difference method, the direct stiffness method and the analogous continuum method.

The remainder of this section considers the choice of the test structures and the quantities to be compared. Section 7.6 contains the details of the comparisons and a discussion on them, along with a comparison of the computer resources that were used for the analyses. Finally

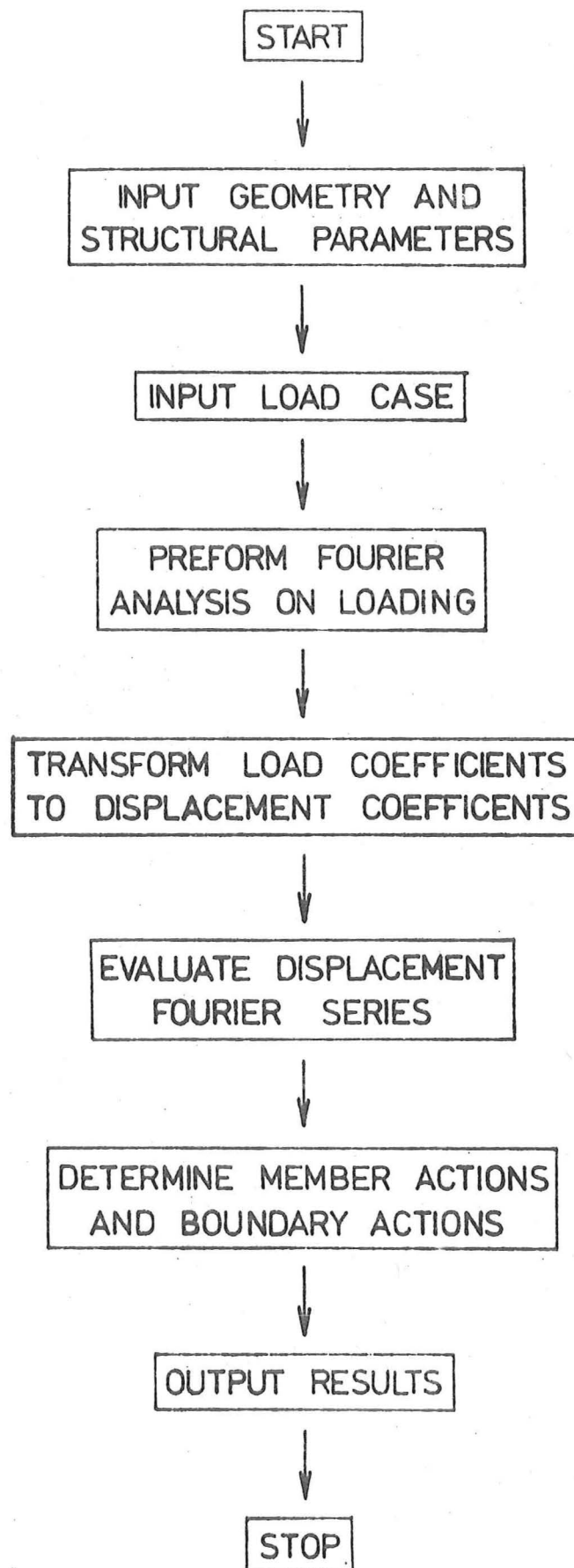


Fig.7.1 FLOWCHART FOR COMPUTER PROGRAM.

in section 7.7 there are some conclusions about the relative accuracy and cost of the methods.

7.5.1 Choice of Test Structures

Of the three classes of structures considered, the single layer pin jointed structure of chapter 4 can be considered as a special case of the single layer rigid jointed structure of chapter 5. The two are equivalent when the bending and torsional stiffnesses of the members are zero and numerical results that were obtained confirm this. For this reason there is no need to validate the analysis for the single layer pin jointed structure and it is only left to verify results for the single layer rigid jointed structure of chapter 5 and the double layer pin jointed structure of chapter 6.

The structures can be described by a series of parameters and because it is impractical to consider more than a few of these parameters and only a few values of those chosen, it is necessary to choose carefully so that they are representative. This will give the most confidence in determining the validity of the conclusions. For each of the structures considered, a preliminary study was carried out, from which it was determined that the most sensitive parameters are the rises (or sags) H_X and H_Y . Thus the value of each parameter except H_X and H_Y was allowed to remain the same for all of the test structures of that type, while the values of H_X and H_Y were varied to give a representative series of structures.

For the single layer rigid jointed structure, there were five sets of values chosen for the parameters H_X and H_Y . These, together with the values of all the other parameters are given in table 7.2.

Structure number 1, with H_X and H_Y both zero, is a flat beam grillage with no curvature and so all the load is resisted by bending of the members. There is no membrane type action and thus all axial

TABLE 7.2 Details of Test Structures for Single Layer Rigid Jointed Structure Analyses

Structure Geometry

$$L_X = 20.00 \text{ m}$$

$$N = 24$$

$$L_Y = 17.32 \text{ m}$$

$$M = 12$$

<u>Structure No</u>	<u>H_X</u>	<u>H_Y</u>
1	0.0 m	0.0 m
2	1.0 m	1.0 m
3	0.0 m	1.0 m
4	-1.0 m	1.0 m
5	-2.0 m	1.0 m

Member Properties

$$E = 211. \times 10^9 \text{ Pa}$$

$$I_X = 1.0 \times 10^{-6} \text{ m}^4$$

$$G = 79.2 \times 10^9 \text{ Pa}$$

$$I_Y = 0.5 \times 10^{-6} \text{ m}^4$$

for all
members

$$A = 1.0 \times 10^{-3} \text{ m}^2$$

$$I_Z = 0.5 \times 10^{-6} \text{ m}^4$$

Note: This is a steel tube 31.6 mm diam. by 5.0 mm wall thickness.

Loading

Uniform normal load of $2.0 \times 10^3 \text{ Pa}$ applied as a point load of $4.81 \times 10^3 \text{ N}$ at each joint.

forces are zero. This structure is included to test the bending only response when it is uncoupled from curvature effects.

Structures 2, 3, 4 and 5 all have $H_Y = +1.0$ while H_X varies from $+1.0$ to -2.0 and thus curvature effects are now important. Structure 2 with $H_X = +1.0$ is an elliptic paraboloid. This has positive gaussian curvature and the major load resistance is by axial forces in the bars while bending is minimal.

When H_X is zero (Structure number 3) a translational paraboloid is formed which has zero gaussian curvature. The load resistance is a mixture of bending and axial forces similar to that observed for a cylindrical shell.

Hyperbolic paraboloids, with negative gaussian curvature, are produced when H_X and H_Y have opposite signs. For the case with $H_Y = +1.0$, this is when H_X is negative. Structure 4 with $H_X = -1.0$ was analysed, and as will be discussed later, rather unsatisfactory comparisons were obtained and so a further structure, number 5, with $H_X = -2.0$ was included in the set.

A uniformly distributed load normal to the surface was applied as equivalent point loads on every joint. Cases of a single joint being loaded were computed and although the results are not presented here, good comparison was obtained between the finite difference and direct stiffness analyses.

The data given in table 7.2 is all that is needed to perform an analysis by the finite difference method and from this the data required for the direct stiffness analysis and the analogous continuum analysis must be generated. For the latter, a method similar to that due to Wright [92] was used to obtain the properties of the analogous shell. These properties are the same for all shells as they depend only on the

lattice member properties. Having determined the analogous shell properties, the shells were analysed by a method similar to that described by Ansah [1], programed for a computer. Details of the derivation of the shell properties and the analysis of the shell are given in Appendix H.

The direct stiffness analyses were carried out using a library program available in the Civil Engineering Department of the University of Canterbury. Because it was impossible to use coordinates other than rectangular cartesian ones, the structures analysed were not identical to those considered by the finite difference and analogous continuum methods which both use curvilinear coordinates aligned with the latticed surface. However for shallow shapes, the discrepancies between the structures are small, and thus of little consequence. The major difficulty arose with the boundary constraints at the edges of the lattice. The direct stiffness method used a gable type restraint which was vertical whereas the other two methods assumed that the gable was normal to the surface. The effects of this will be discussed along with the results.

Data for the direct stiffness analyses was prepared for all the test structures, for which the basic layout was the same with only the Z coordinate of the joints being different. There were 175 joints each of 6 degrees of freedom and 450 members in the structure. The joint numbering pattern was chosen to minimise the bandwidth of the stiffness matrix with a resulting value of 84.

For the double layer pin jointed test structures, the value of each of the parameters except H_X and H_Y was the same for all cases. The values they were given, along with the values given to H_X and H_Y are recorded in table 7.3. The values of H_X and H_Y for test structures 6 to 10 of this series are the same as used for structures 1 to 5 of the single layer series. The loading on each structure was a uniformly distributed load normal to the surface and applied as an equivalent point

TABLE 7.3 Details of Test Structures for Double Layer Pin Jointed Structure Analyses

Structure Geometry

$L_X = 20.00 \text{ m}$ $N = 24$
 $L_Y = 20.00 \text{ m}$ $M = 24$
 $D = 1.00 \text{ m}$

<u>Structure No</u>	<u>H_X</u>	<u>H_Y</u>
6	0.0 m	0.0 m
7	1.0 m	1.0 m
8	0.0 m	1.0 m
9	-1.0 m	1.0 m
10	-2.0 m	1.0 m

Member Properties

$EA = 211. \times 10^6 \text{ N}$ for all members.

Loading

Uniform normal load of $2.0 \times 10^3 \text{ Pa}$ on the upper layer applied as a point load of $5.56 \times 10^3 \text{ N}$ at each upper layer joint.

load on all of the upper layer joints.

The analogous continuum for these double layer structures was determined by a method similar to that used by Kollar [52] with the shell analysis being performed by the same method as used for the single layer structures. Details of the derivation and the analysis are given in Appendix H.

The double layer test structures were also analysed by the direct stiffness method as pin jointed space trusses using an available program. The same problem regarding coordinates which differ from the other methods also arose here. However it will be seen that it is not as important for this type of structure and caused little difficulty. For all structures there were 313 joints of 3 degrees of freedom each and 1152 members. The stiffness matrix had a bandwidth of 78.

7.5.2 Choice of Quantities to be Compared

As it is impractical to present all of the deformations and actions over the structure, representative results sufficient to show the adequacy of the analysis method are all that are presented. Maximum deformation and actions are of greatest interest to the analyst and preliminary studies indicated the regions where these occur.

It was found that the regions containing these maxima varied from structure to structure and as it was desired to quote the same quantities for all the test structures of each type, a series of lines in the structure were chosen which included most of the regions of interest.

For the single layer rigid jointed structure the quantities of interest are the normal displacement of the joints, the rotation of the member end, the axial force in a member and the bending moment in a member. These quantities are given along the lines shown in figure 7.2 and as can be seen these include a centreline and a diagonal line. In the case of

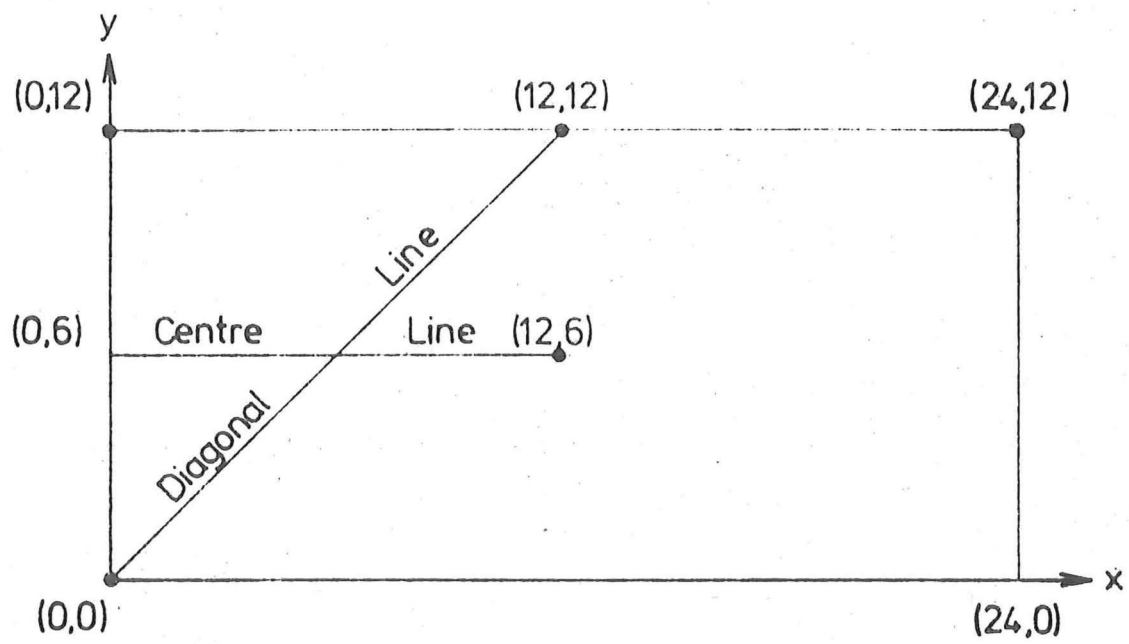


Fig.7.2 LINES FOR COMPARISON - SINGLE LAYER STRUCTURE.

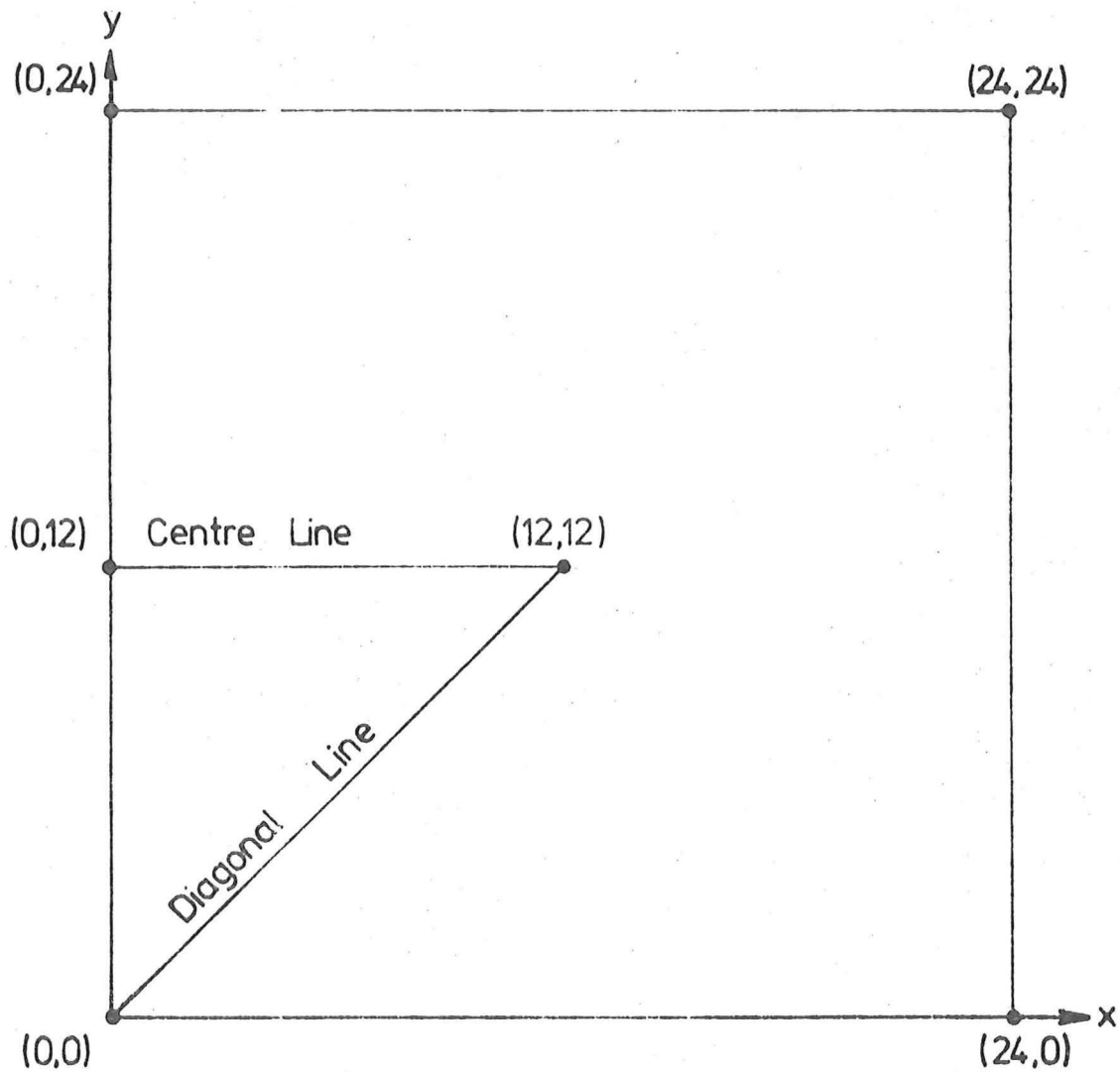


Fig.7.3 LINES FOR COMPARISON - DOUBLE LAYER STRUCTURE.

the analogous continuum results, only the deformations are presented as only these are obtained directly from the analysis method. Member actions are not determined explicitly by the method but must be gauged by the analyst and as this involves some judgement and hence the possibility of bias, it was not considered advantageous to do this here.

The quantities of interest for the double layer pin jointed structure are the normal displacement of the joints and the axial loads in the members. These quantities are given along the centreline and diagonal line shown in figure 7.3. As in the case of the single layer structure, from the analogous continuum analyses, only the deformations are presented.

7.6 COMPARISON OF RESULTS

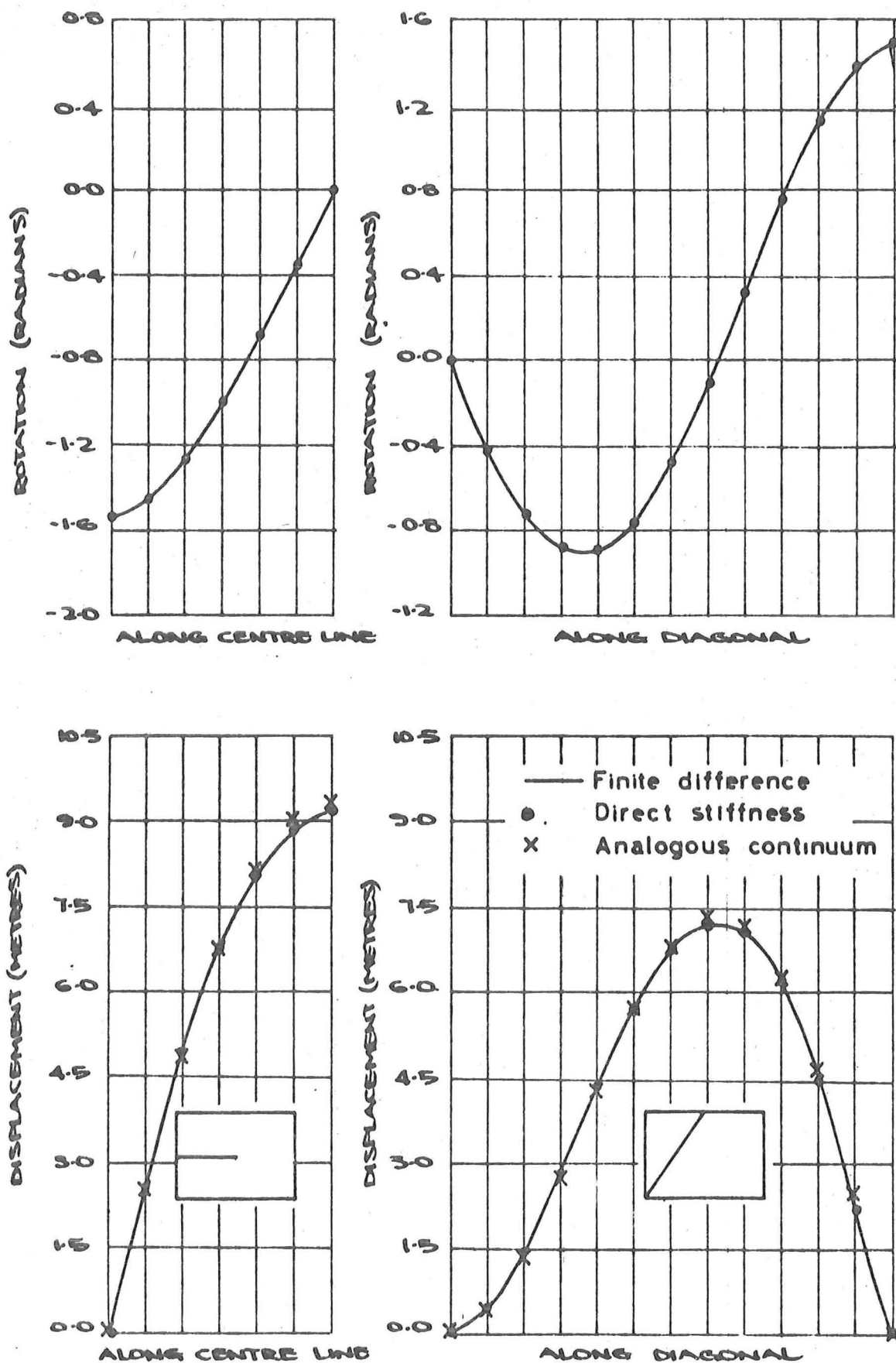
Displacements and actions are compared in section 7.6.1 while computer times and storage requirements are compared in section 7.6.2.

7.6.1 Displacements and Actions

The displacements and actions obtained are presented as graphs in figures 7.4 to 7.8 for the single layer structures and in figures 7.9 to 7.13 for the double layer structures.

For structure number 1 (H_X and H_Y both zero), the rotations and displacements are given in figure 7.4a while the bending moments and axial forces are given in figure 7.4b. It can be seen that the results of the various methods agree well with the discrepancies being a maximum of 4%. Such small discrepancies are hardly detectable on these plots. It should be noted that because the structure is flat, there are no axial forces in the members.

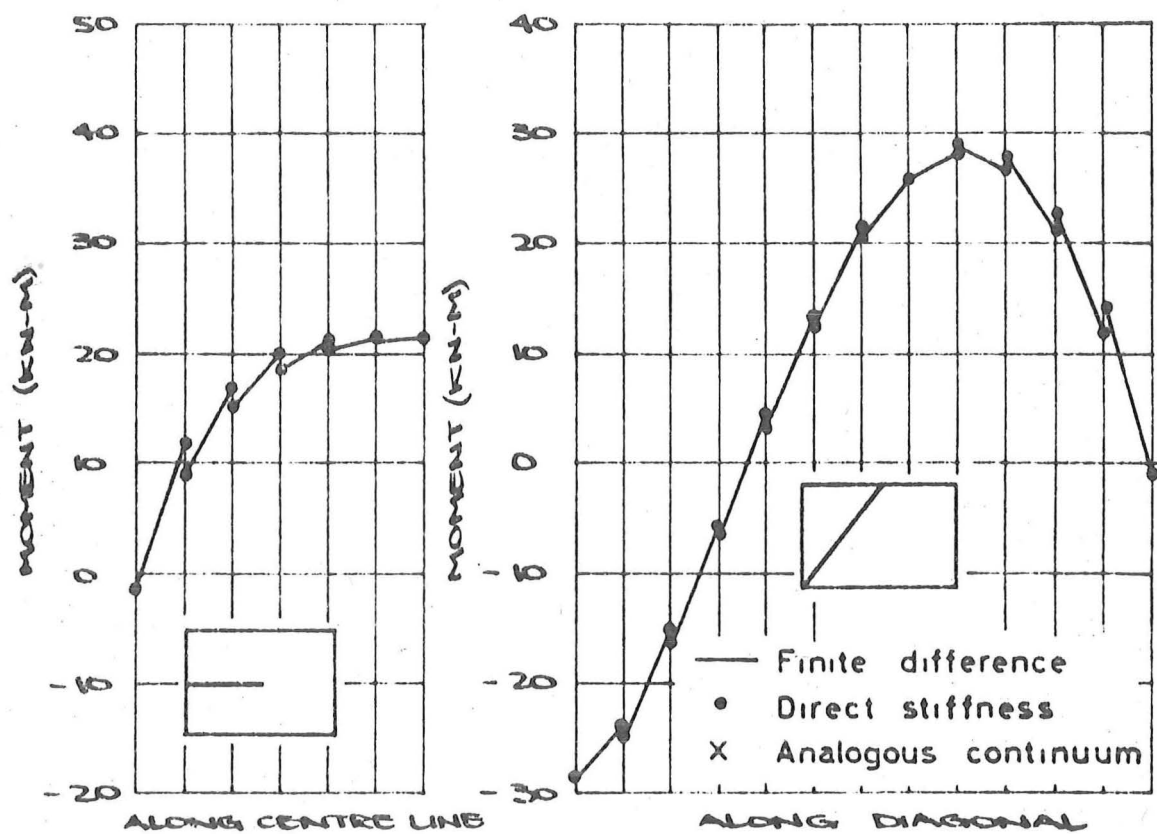
The results for structure 2, when $H_X = +1.0$ and $H_Y = +1.0$, are given in figures 7.5a and 7.5b from which it is evident that the methods are in close agreement. The largest differences occur in the normal



(a) Rotations and displacements

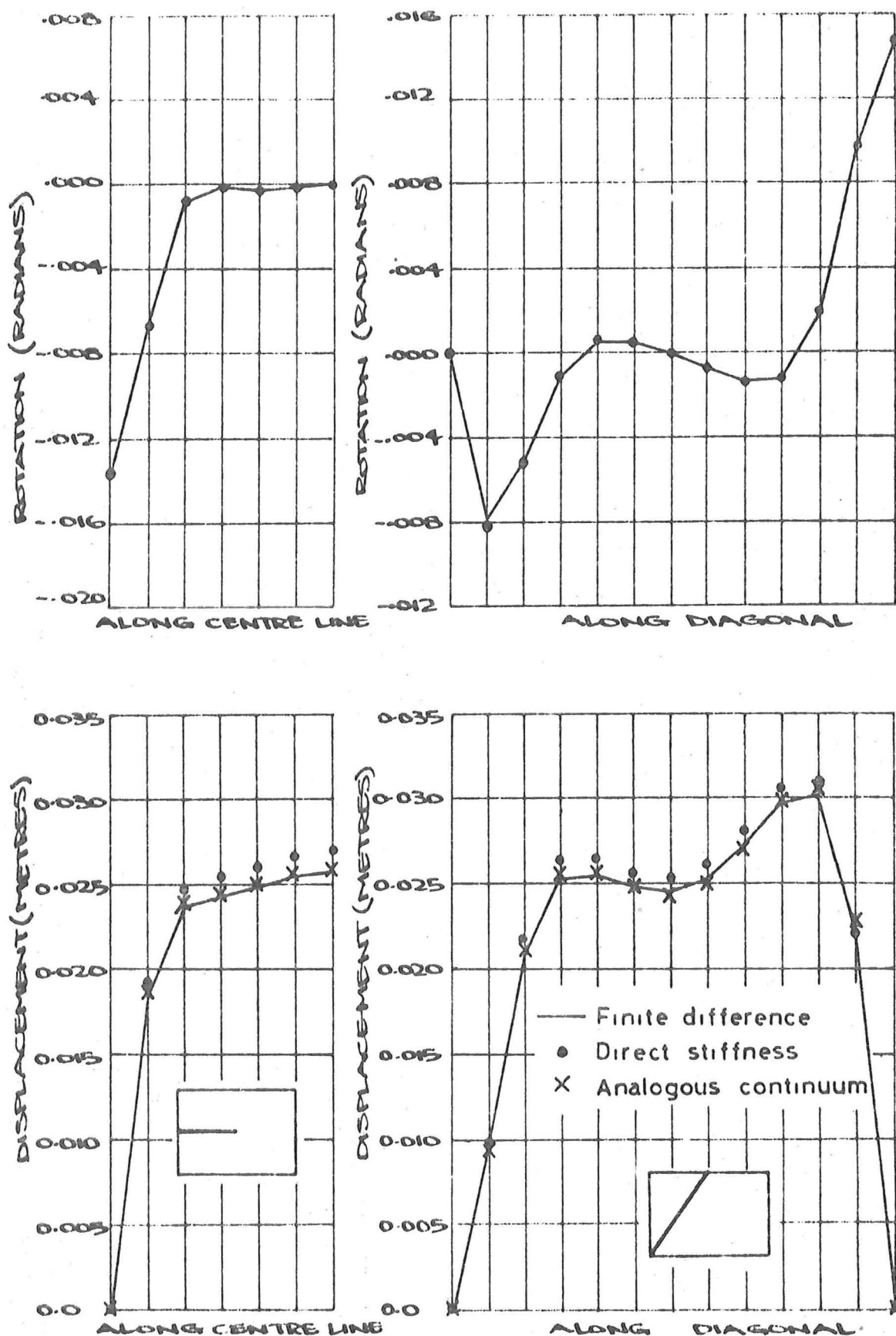
Fig. 74 RESULTS FOR SINGLE LAYER STRUCTURE

Nº1 ($H_x = 0.0$, $H_y = 0.0$)



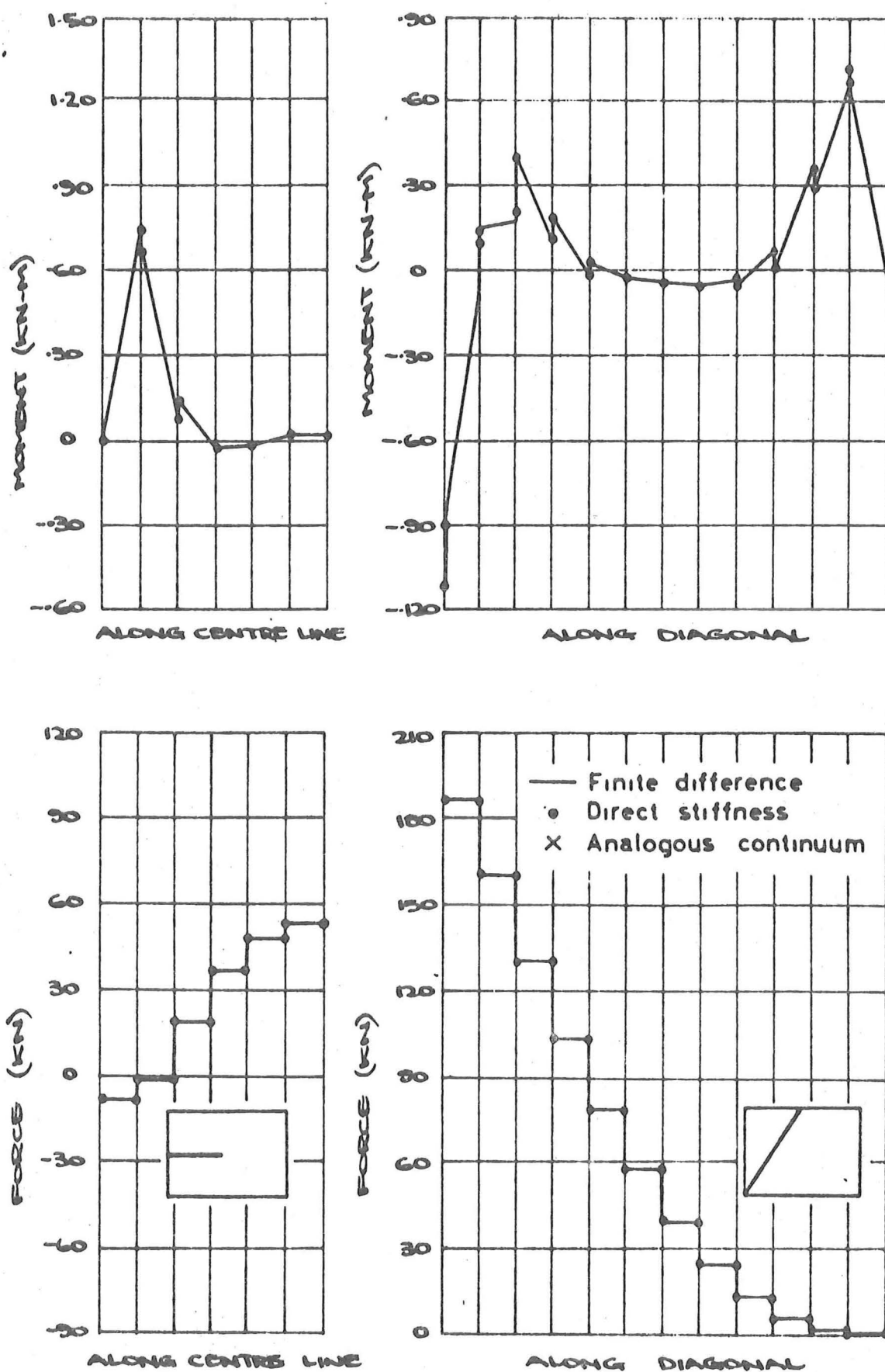
(b) Moments

Fig 7.4 (Continued)



(a) Rotations and displacements

Fig 7.5 RESULTS FOR SINGLE LAYER STRUCTURE
No. 2 ($H_x = +1.0$, $H_y = +1.0$)



(b) Moments and forces

Fig 7.5 (Continued)

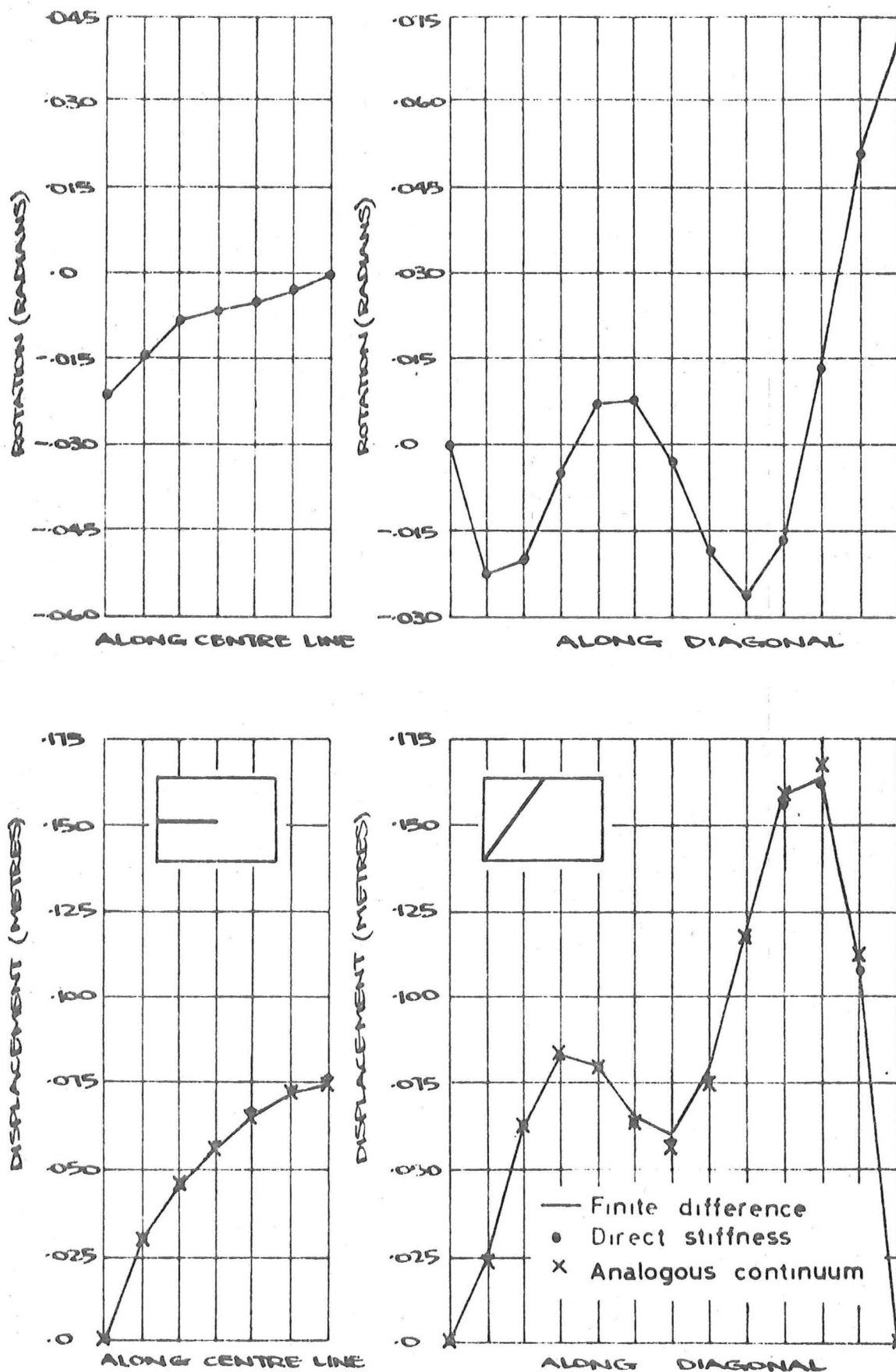
displacement with a maximum discrepancy of about 4%.

Figures 7.6a and 7.6b give the results for structure 3 with $H_X = 0.0$ and $H_Y = 1.0$. Again the displacements, rotations, bending moments and axial forces agree quite well.

Structure 4, with $H_X = 1.0 = -H_Y$, proved to be a "difficult" structure and several variations on it were analysed. The results shown in figures 7.7a and 7.7b indicate a large discrepancy between the methods. For this case it was suspected that the structure is very sensitive to the boundary conditions and as the direct stiffness results are based on having a vertical gable support whereas the finite difference results are based on a gable support which is normal to the surface, a modified structure with normal gable supports was also analysed by the direct stiffness method. This involved adding members with very large axial stiffness so that they prevented any movement normal to the surface. This is generally considered an undesirable practice but was the only option available with the computer program available. The results of this additional analyses are given on the graphs in figures 7.7a and 7.7b. It can be seen that this structure is very much stiffer than the previous one and so the sensitivity to the boundary conditions is confirmed. It is left until chapter 8 to explain the response of this particular structure where $H_X = -H_Y$.

Figures 7.8a and 7.8b give the results for structure 5 when $H_X = -2.0$ and $H_Y = +1.0$. This structure was included because of the discrepancies found for structure 4. The results for this structure show reasonable agreement amongst the methods with the largest differences being in the order of 6%.

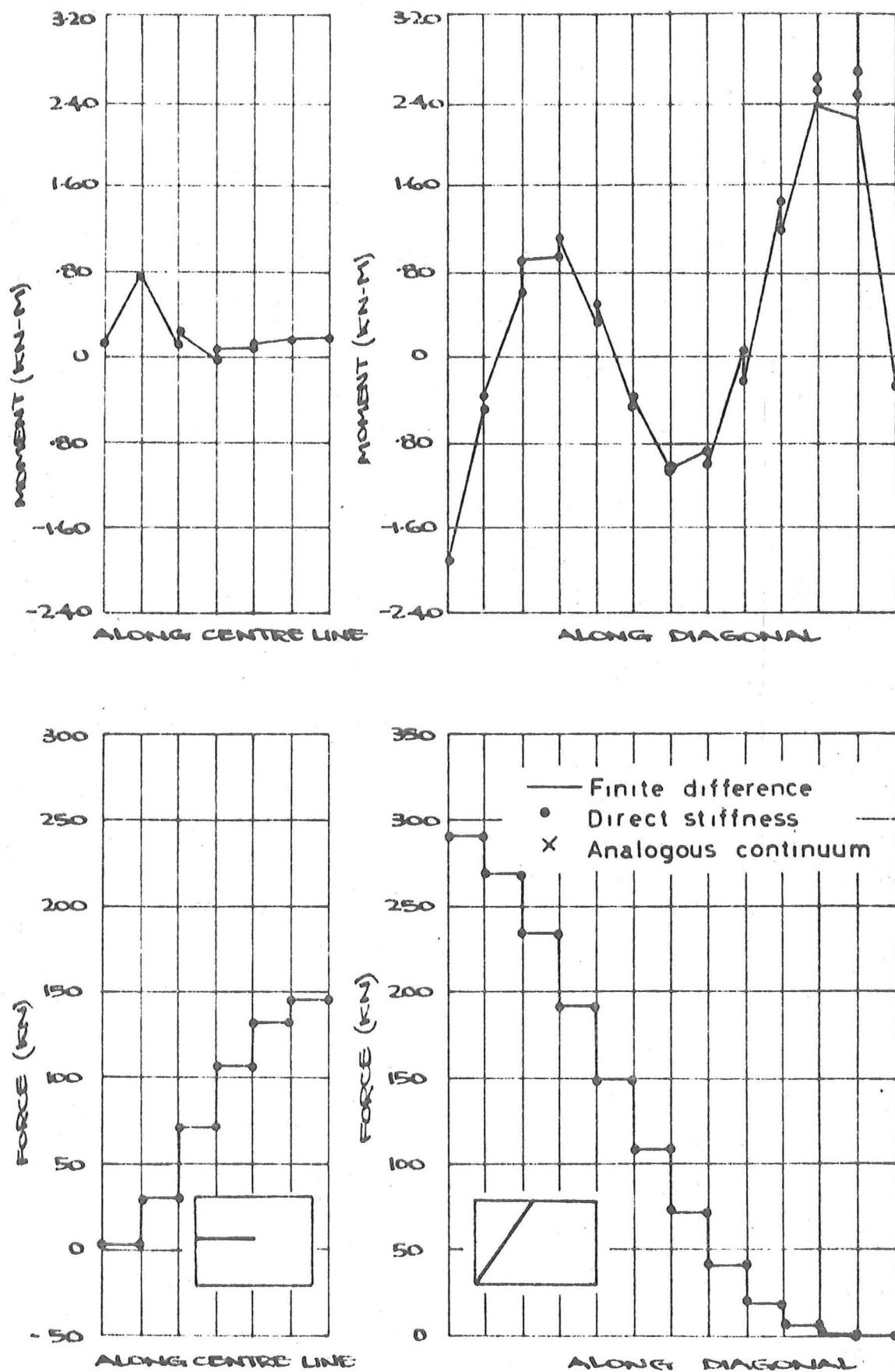
An overall view of the results presented, indicates that for the single layer structures the various methods agree except for the critical case where $H_X = -H_Y$.



(a) Rotations and displacements

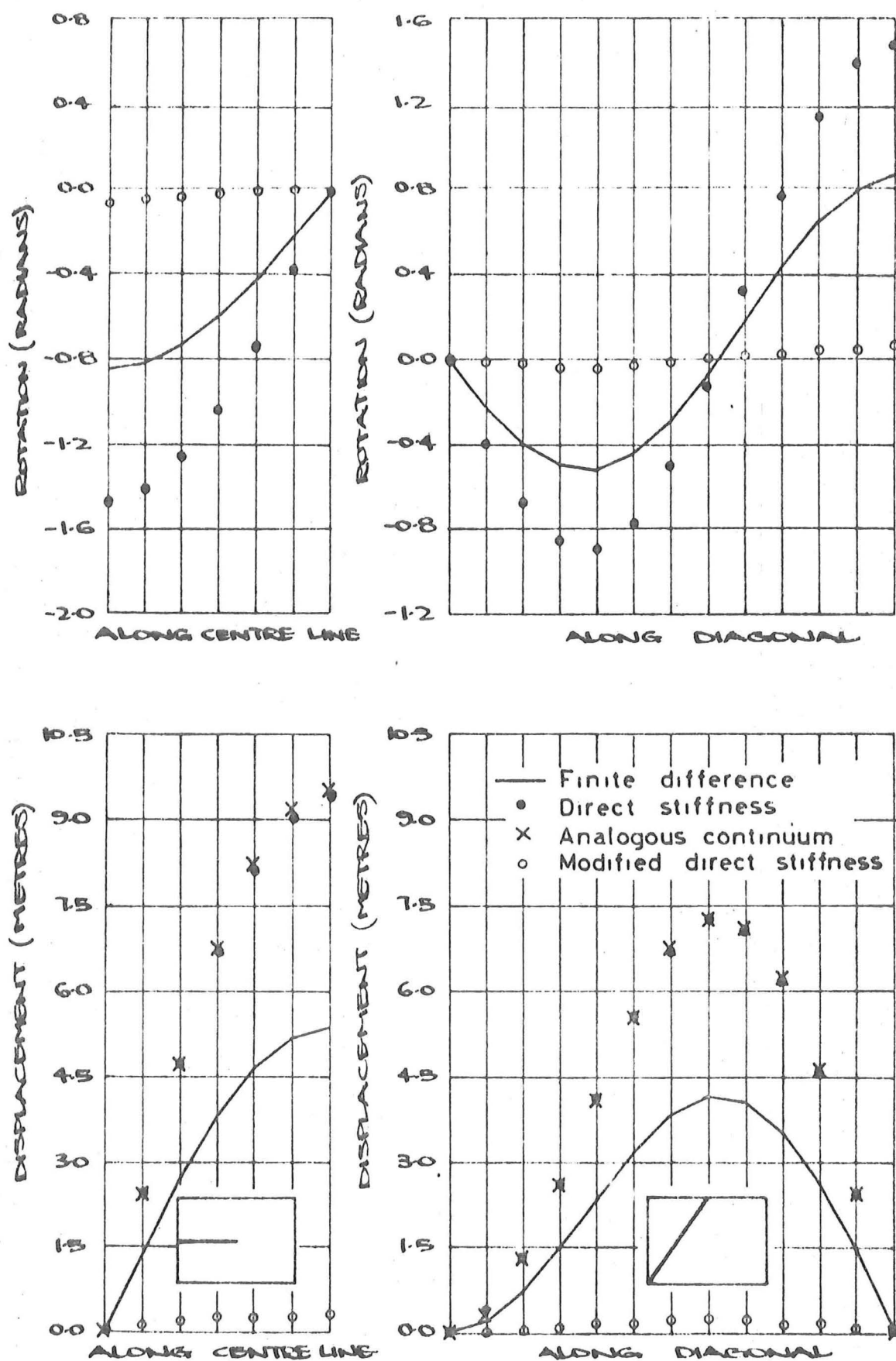
Fig 7.6 RESULTS FOR SINGLE LAYER STRUCTURE

No. 3 ($H_x = 0.0$, $H_y = 1.0$)



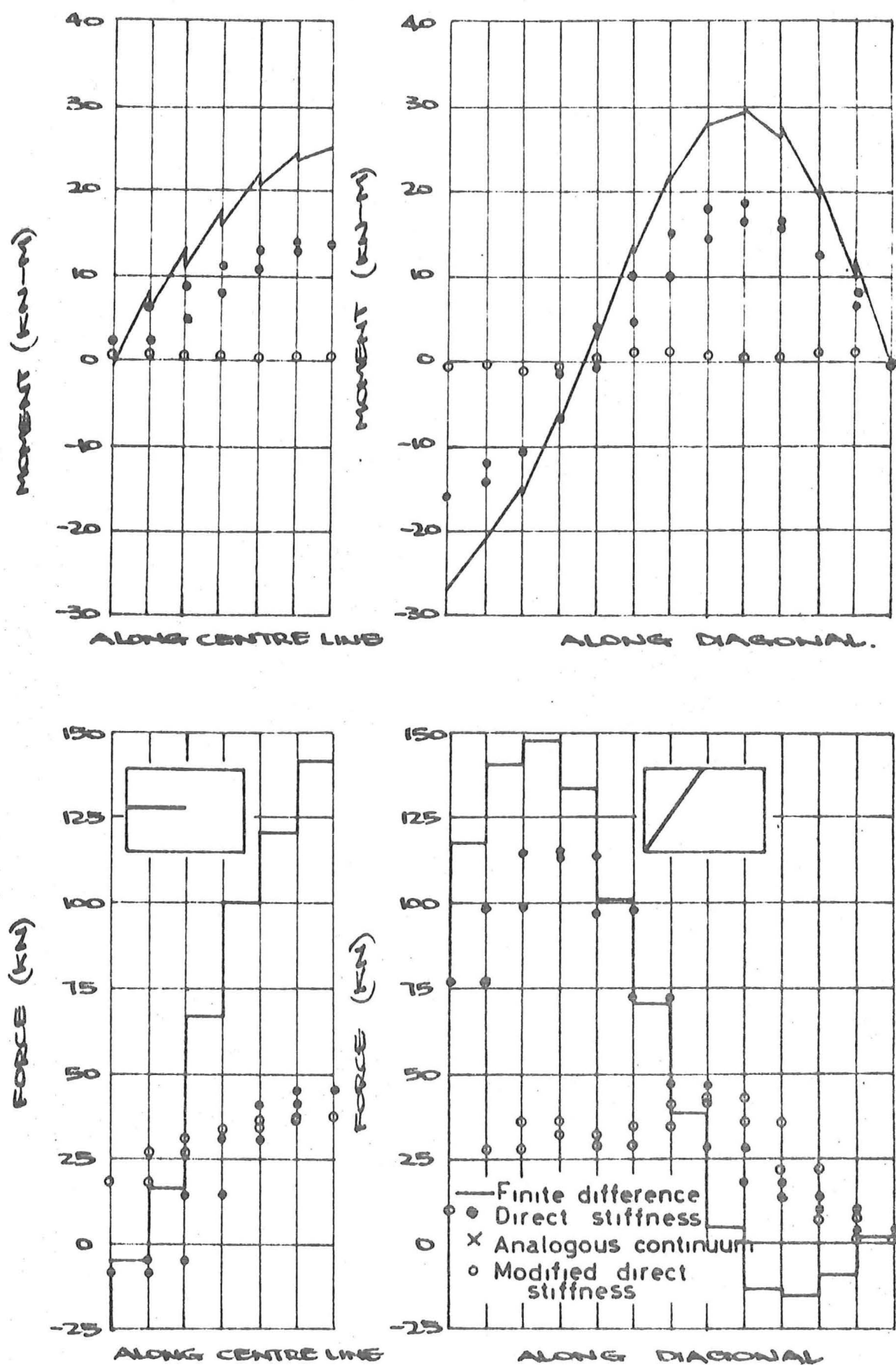
(b) Moments and forces

Fig 7-6 (Continued)



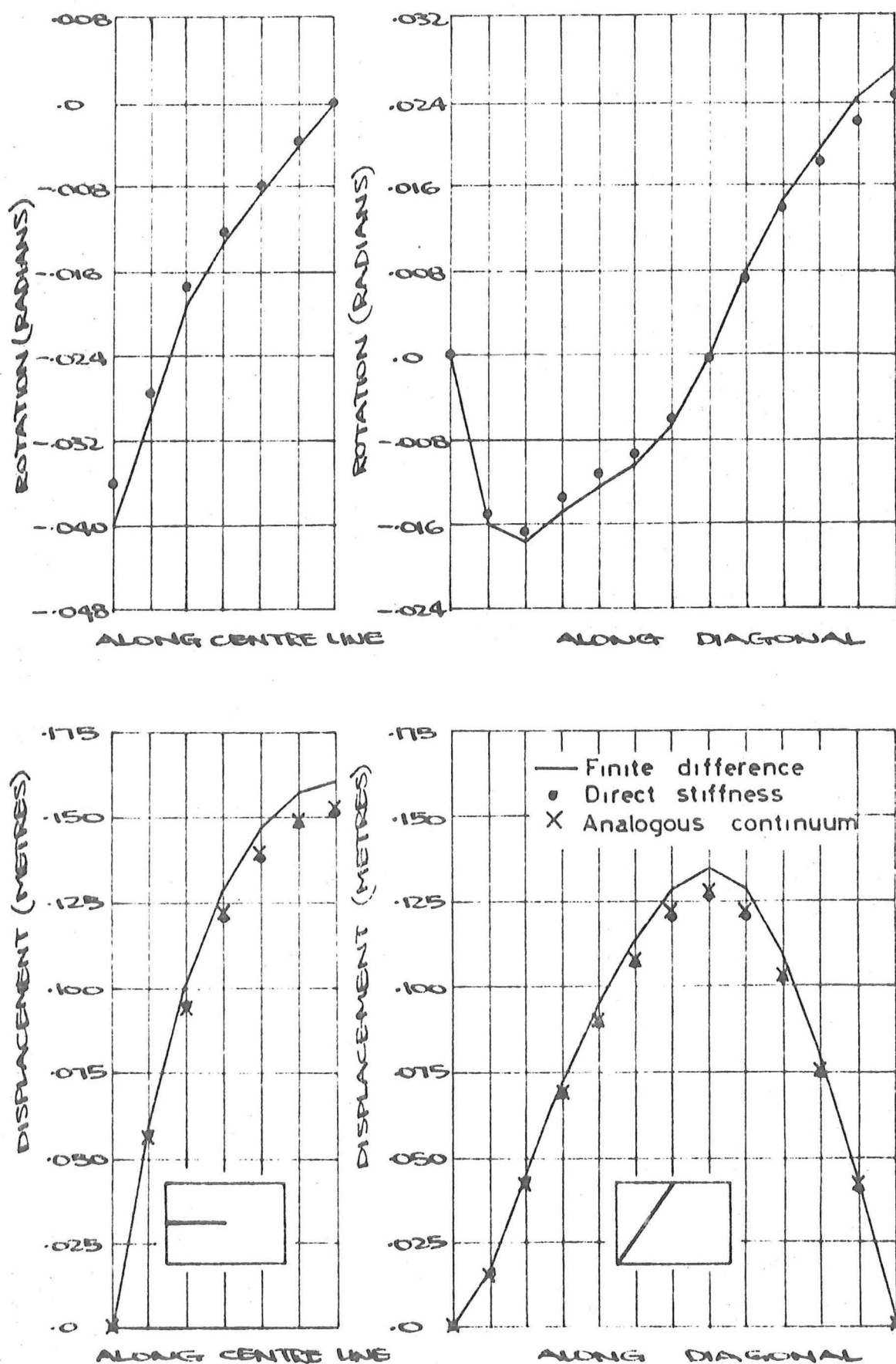
(a) Rotations and displacements

Fig 7.7 RESULTS FOR SINGLE LAYER STRUCTURE
N°4 ($H_x = -1.0$ $H_y = +1.0$)



(b) Moments and forces

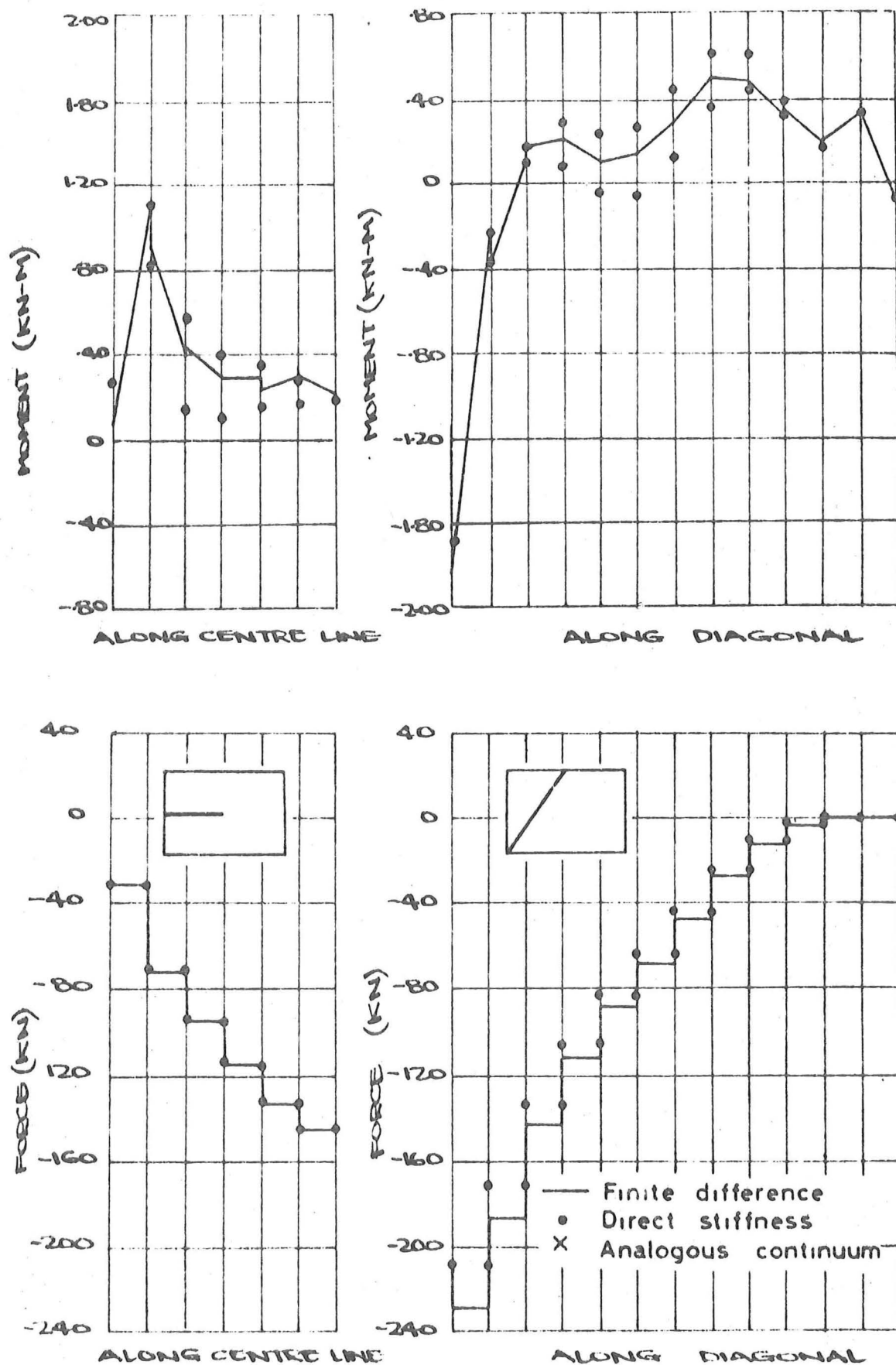
Fig 7.7 (Continued)



(a) Rotations and displacements

Fig 7.8 RESULTS FOR SINGLE LAYER STRUCTURE

Nº 5 ($H_x = -2.0$, $H_y = +1.0$)



(b) Moments and forces

Fig 7.8 (Continued)

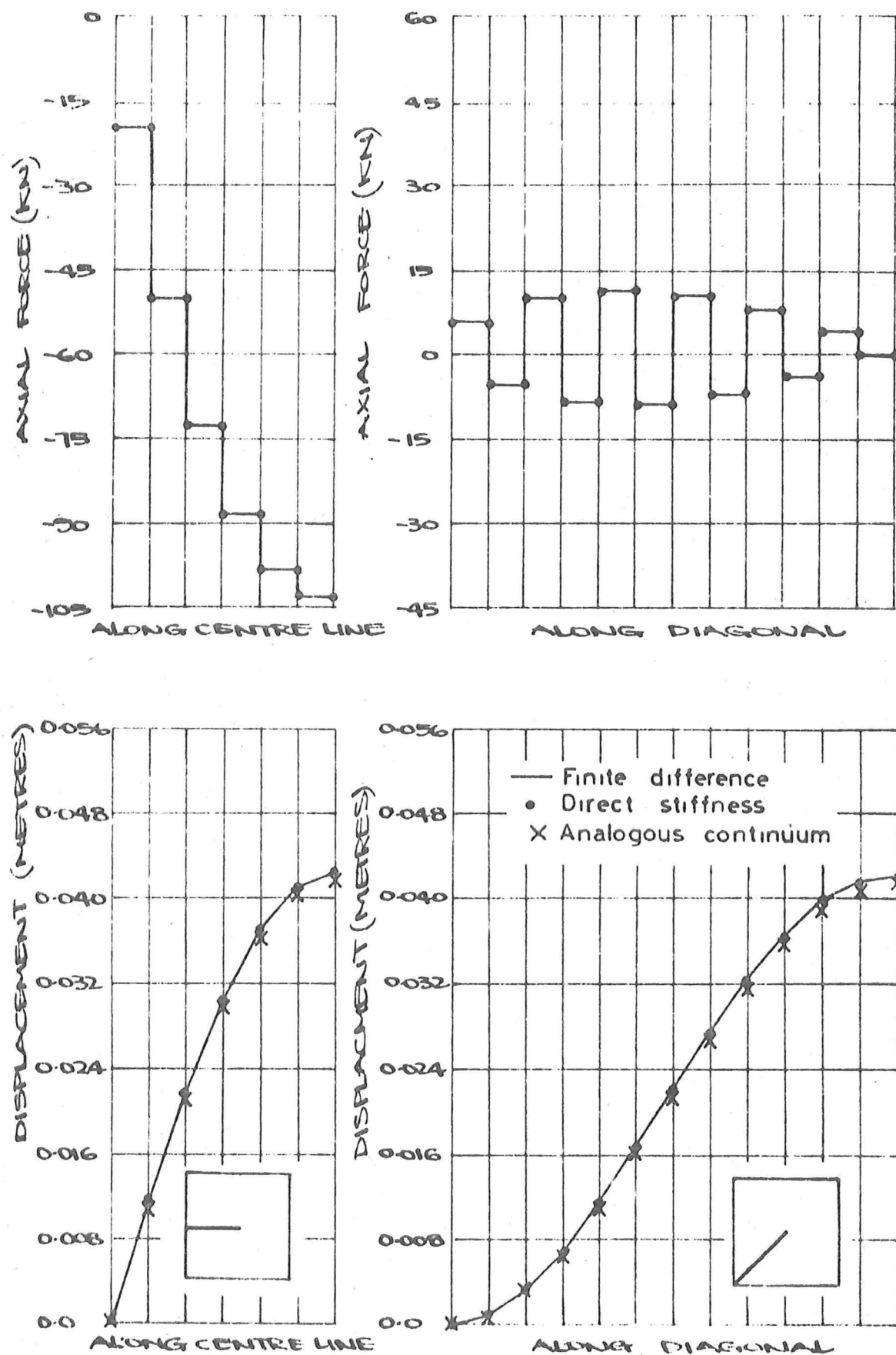
The results for the double layer structures are presented in figures 7.9 to 7.13 where for each case, the axial load and normal displacement are given along a centre line and a diagonal line. The displacements determined by the three methods agree well with the largest discrepancy being about 5%. The axial forces are generally consistent with the largest difference occurring for the elliptic paraboloid structure 7, where the forces in the diagonal web members differ by about 15%. The other structures show better agreement.

The problem which appeared with the single layer structure number 4 where $H_X = -H_Y = -1.0$ did not arise with the double layer type structure. The appropriate structure, number 9, gave good agreement between the methods (see figure 7.12). It is apparent that this structure is much stiffer than the single layer type and, as will be discussed in chapter 8, is not as sensitive to geometry and boundary constraints as was the single layer structure.

7.6.2 Computer Resources

To gauge the cost of the analyses, two measures are used. The first is the computing time to perform an analysis and the second is the computer memory requirements. These were measured for the finite difference and direct stiffness methods and a comparison of the resources was made.

For the single layer rigid jointed structure, the measured computer time and an estimate of the storage requirements for the test structures previously considered, are given in table 7.4. The computer times quoted are an average of the times required for each of the five analyses performed and include all processing and input-output operations. The storage requirements are estimates based on the known structure size and account only for the larger vectors and matrices that are required. There has been no allowance for the sundry variables or storage for the



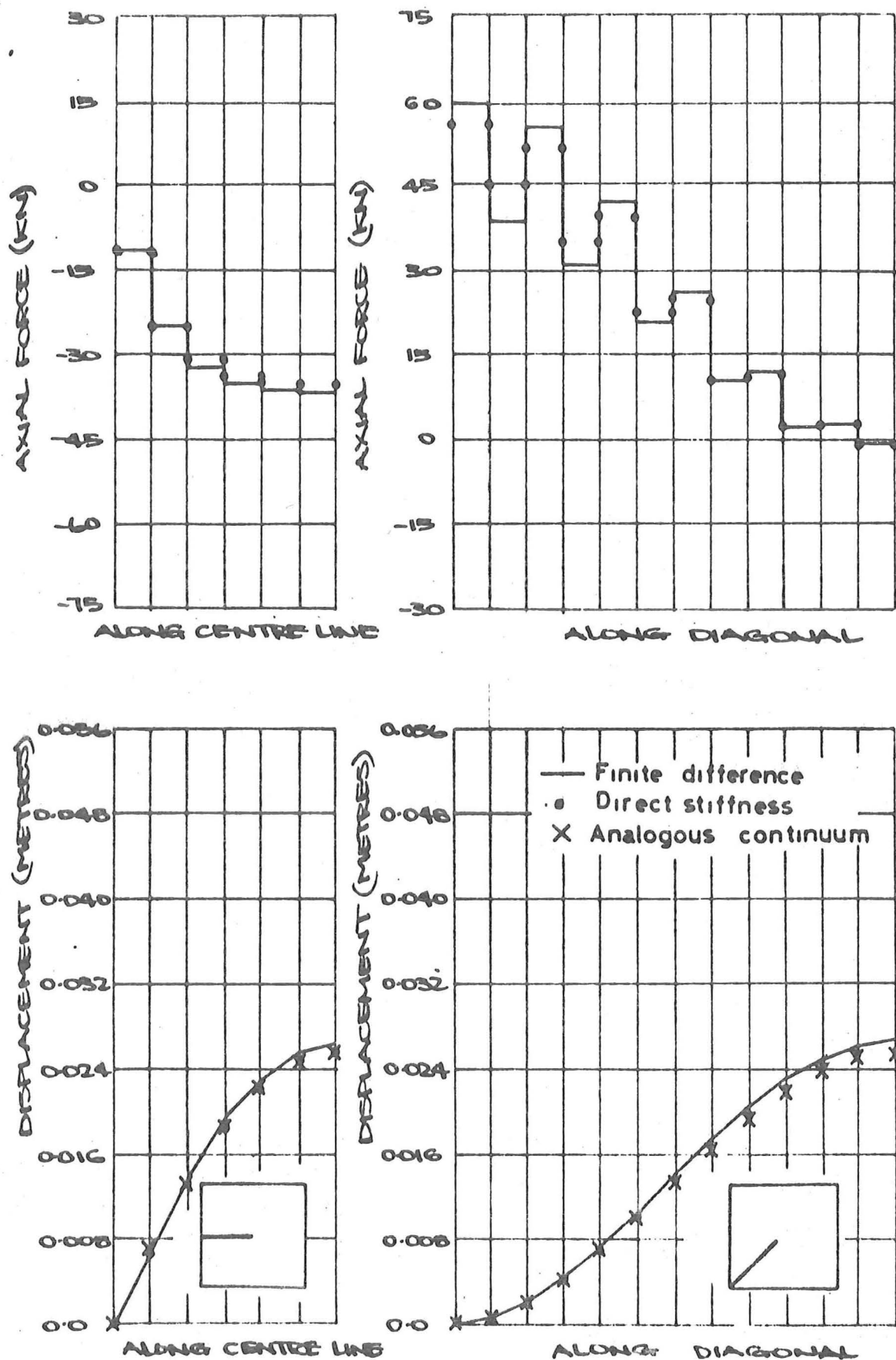


Fig 7.10 RESULTS FOR DOUBLE LAYER STRUCTURE
N°7 ($H_x = +1.0$, $H_y = +1.0$)

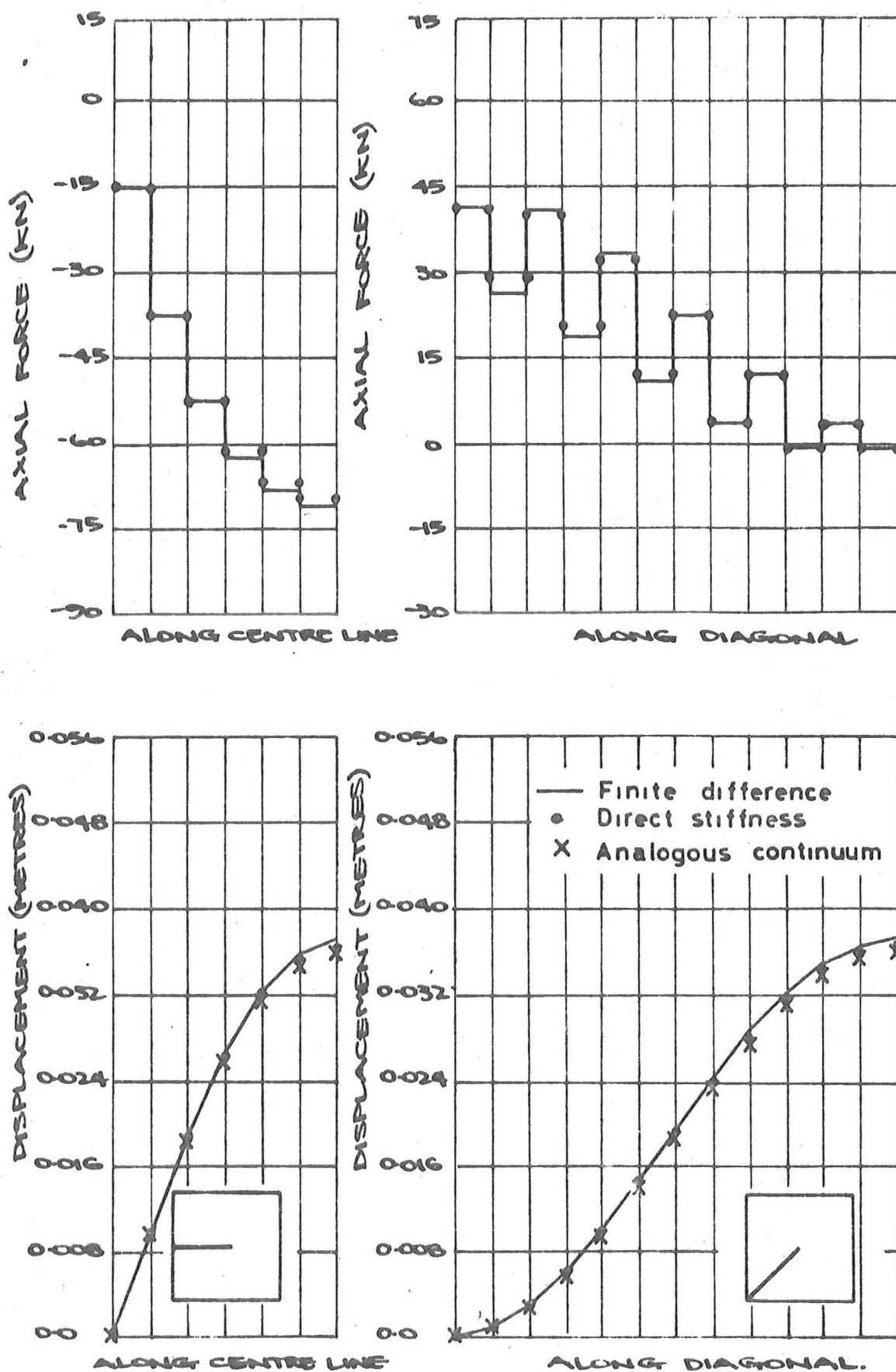


FIG 7.11 RESULTS FOR DOUBLE LAYER STRUCTURE
Nº 8 ($H_x = 0.0$, $H_y = +1.0$)

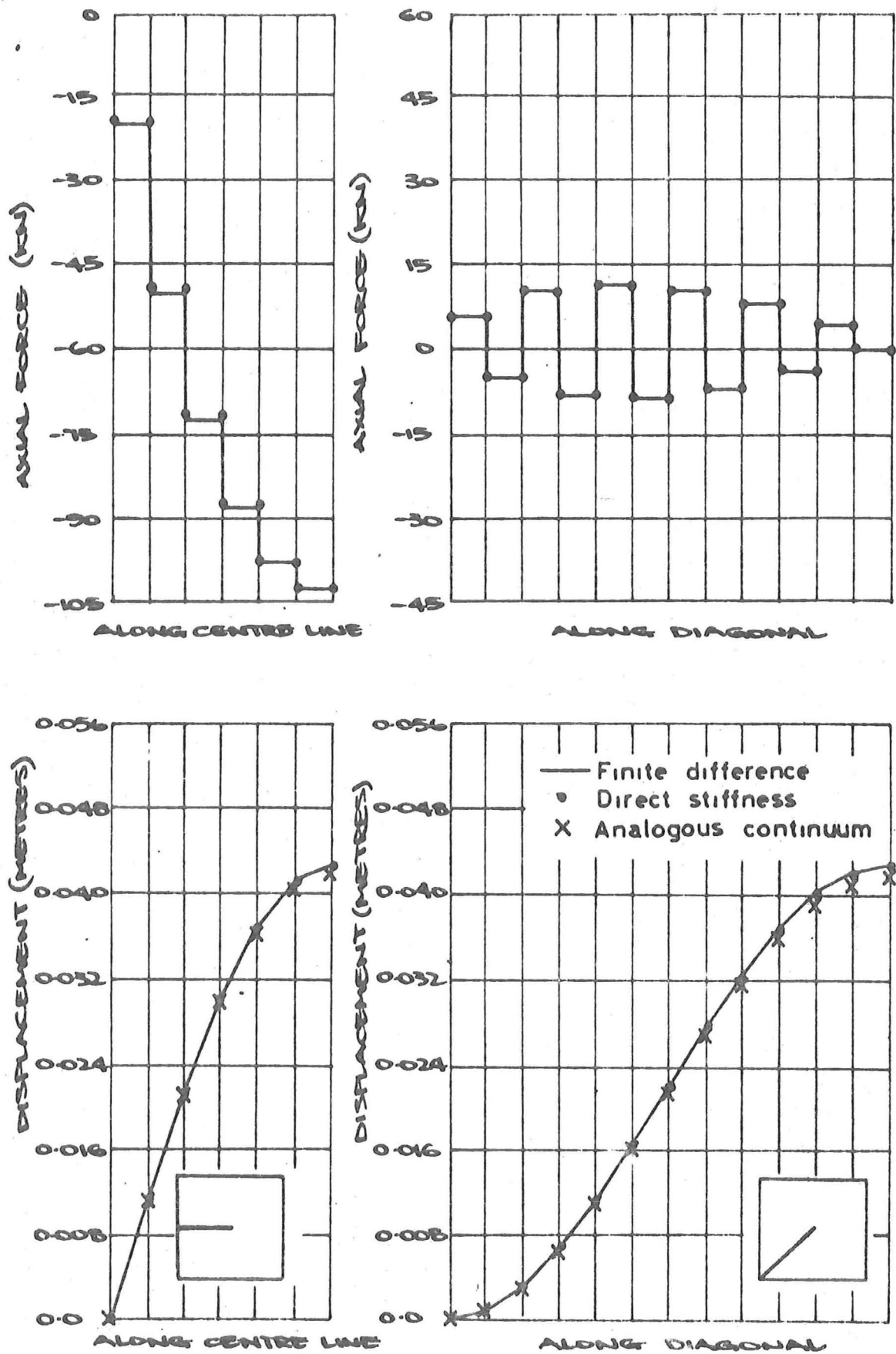


FIG 7.12 RESULTS FOR DOUBLE LAYER STRUCTURE
 N° 9 ($H_x = -1.0$, $H_y = +1.0$)

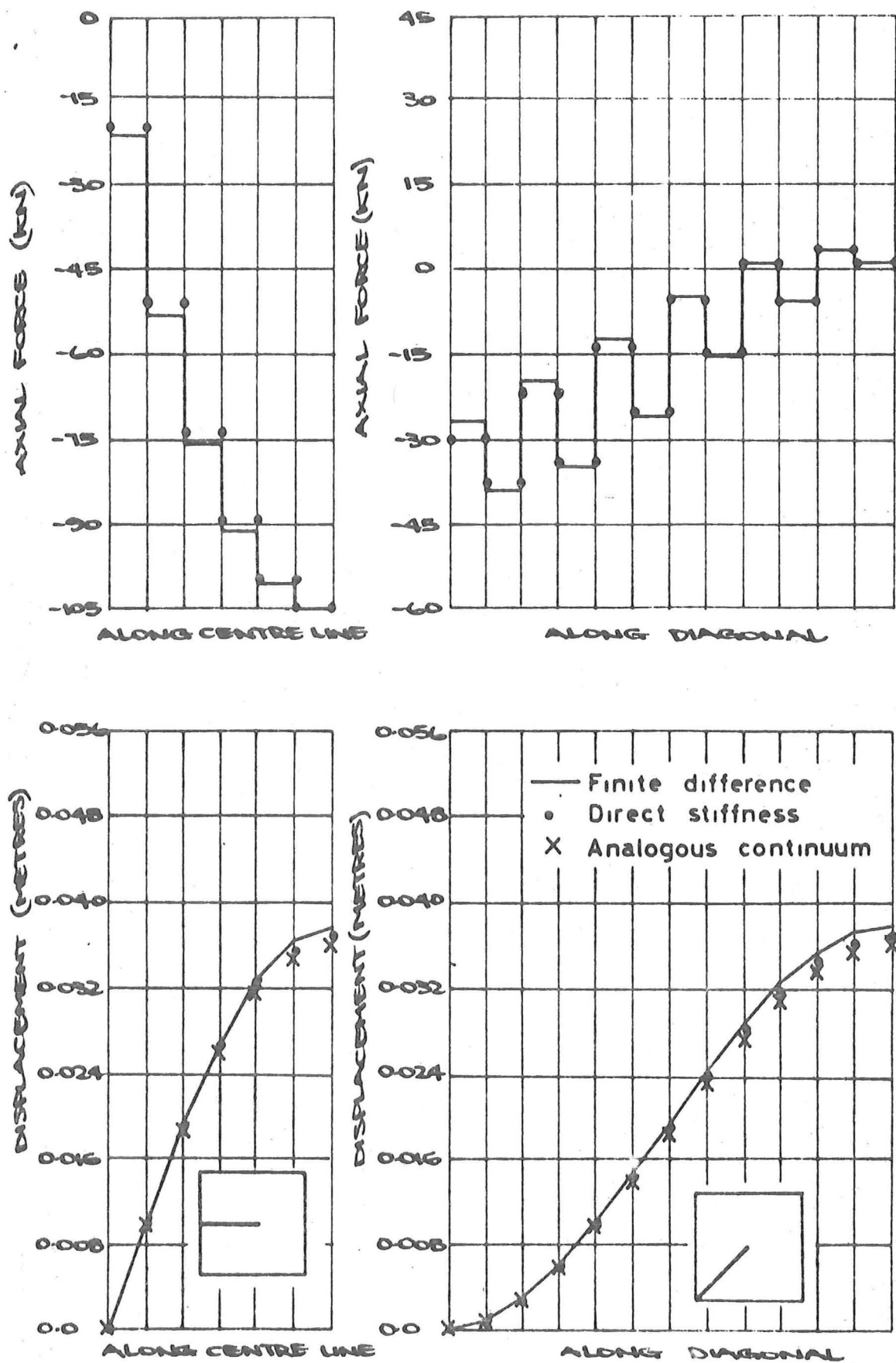


FIG 7.13 RESULTS FOR DOUBLE LAYER STRUCTURE

Nº 10 ($H_x = -2.0$, $H_y = +1.0$)

TABLE 7.4 Computer Times and Storage Requirements for Single Layer Rigid Jointed Structure

	Computer Time	Storage Requirement
Finite Difference method	39.5 sec	3900 words
Direct Stiffness method	738.1 sec	90300 words
ratio	$\frac{738.1}{39.5} = 18.7$	$\frac{90300}{3900} = 23.2$

TABLE 7.5 Computer Times and Storage Requirements for Double Layer Pin Jointed Structure

	Computer Time	Storage Requirement
Finite Difference method	58.1 sec	3750 words
Direct Stiffness method	551.2 sec	75120 words
ratio	$\frac{551.2}{58.1} = 9.5$	$\frac{75120}{3750} = 20.0$

NOTE

The times and storage requirements given in tables 7.4 and 7.5 above are for the complete analysis of the full structure. If the loading is symmetrical, only a quadrant would need to be analysed.

In that case the analysis times would be approximately 1/16 of the values given for both the finite difference and direct stiffness methods.

The storage requirements for the quadrant analysis would be $\frac{1}{4}$ the value given for the finite difference method and $\frac{1}{8}$ of the value given for the direct stiffness method.

program code and so the actual requirements will be slightly greater than those quoted. This extra requirement will be larger for the direct stiffness method which has more program code and also more sundry variables and minor matrices than has the finite difference method.

From the results quoted it will be seen that the direct stiffness method requires about 19 times the computer time and about 23 times the storage requirements of the finite difference method for this particular case. In order to estimate the computer time and storage requirements for any other sized structure, it is necessary to know how these quantities vary with the structure size. For the finite difference method, section 7.2 includes this data which is summarised in table 7.1. For large values of N and M , the computer time is proportional to the quantity $(N+1)^2 \times (M+1)^2$ and the storage times are proportional to $(N+1)(M+1)$. For the direct stiffness method a rough estimate of the computer time would be proportional to the product of the number of joints and the square of the bandwidth. The corresponding storage requirement would be proportional to the product of the number of joints and the bandwidth. The number of joints and the bandwidth can be taken as approximately proportional to the product $(N+1)(M+1)$ and $(M+1)$ respectively and hence for the direct stiffness method, an estimate of the computer time would be proportional to $(N+1)(M+1)^3$ and the storage requirements proportional to $(N+1)(M+1)^2$.

The conclusion is that for a given ratio of N to M , the relative computing time ratio of 19 for the two methods will remain about the same as the structure size varies whereas the storage requirement ratio of 23 will increase as the structure size increases. Both of these are in the favour of the finite difference method.

The requirements and comparisons for the double layer structures are given in table 7.5 where again the computer times are averages of the five analyses and the storage requirements are based on estimates neglect-

ting the program code and minor quantities. The results show that the direct stiffness method requires 10 times the computer time and 20 times the storage requirements of the finite difference method. As the structure size changes, these ratios will behave in a similar manner to those described for the single layer structure.

In both of these cases, the savings are seen to be very significantly in favour of the finite difference method.

7.7 CONCLUSIONS ABOUT VERIFICATION

The results presented in section 7.6 show that the finite difference method gives substantially the same results as the other methods as far as can be ascertained. At the critical shape when $H_X = -H_Y$ it is felt that no (linear) analysis method will give acceptable results as very small changes to the structure cause large changes in the response. This would cause some doubt that the mathematical models of the structure are in fact realistic representations of the real structure.

When compared with the direct stiffness method, the finite difference technique stands out as acceptable in regard to both computing times and storage requirements. Data preparation for the direct stiffness method is much greater than for the finite difference method. However it must be realised that the restrictions on the structure shape and layout are an essential part of the finite difference method and are necessary to produce these savings.

When compared to the analogous continuum method, the finite difference technique shows that it produces acceptable results for the cases studied. This is restricted to deformations as some judgement is needed on the part of the analyst to assess the member actions. This may lead to different results produced by different analysts. It is felt that this, together with the restriction to very simple cases, viz.

isotropic homogeneous shells with simple layouts and boundaries, may make the analogous continuum method inaccurate and time consuming for the analyst when used for the more general cases that the finite difference and direct stiffness methods can handle.

CHAPTER EIGHT

SENSITIVITY ANALYSIS

The finite difference method as described in chapter 2 and applied in chapters 4, 5 and 6 was shown in chapter 7 to be accurate and economic to use. Consequently it is a suitable method to study a series of structures with varying parameters. Trends in the response of the structures as the geometry and structural properties are changed can thus be obtained.

It is important to realise that the response of the structure to a change in one parameter is very dependent on the values of the other parameters and it is impossible to separate out the effect of a change in an individual parameter. However it is possible over a limited range of values - hopefully those found in practical structures - to assess the general trend when one parameter is varied. Keeping this limitation in mind, it is intended to comment on the changes in structural response when changes are made to several parameters, one at a time.

8.1 GENERAL BEHAVIOUR OF THE STRUCTURES

It is convenient to first consider in general terms how a doubly curved structure would respond to load. For this it is easier to use the concept of an analogous continuum shell because at the present time such structures are better understood than lattice type structures. This is used only to obtain a qualitative response and not a quantitative one. It will be seen that the regular lattice does indeed respond in a similar manner to a shell and that this qualitative model with numerical results supplied by the finite difference method does serve as a good indicator of what to expect.

The traditional explanation of the way a continuum shell sustains applied load is to consider two modes of resistance. These are membrane action and flexural action, with the combination of the two sustaining the total load. Membrane action involves in plane stresses and because the corresponding strains are much smaller than those associated with the bending stresses of flexural action, the strain energy involved is smaller. This results in membrane action generally being the more efficient way of resisting load and so the one to "encourage" by proper choice of geometry and structural properties if this is at all possible.

Loading normal to the shell surface is transmitted to membrane action in a complex manner but the process is often explained by an arch or cable type mechanism and relies on the curvature of the surface. Some membrane action also arises from differences of in plane shear stresses that are transmitted through the shell. Any load that cannot be taken by the arch or shear difference action is assumed to be taken by bending of the shell and thus resisted by flexural action.

This explanation is relatively easy to understand and it does give a realistic view of the processes taking place. However for the arch type mechanisms to work the appropriate support conditions must be present. This requires that the ends of the arch do not move relative to each other and if this is not fulfilled, then the arch mechanism breaks down and the load is taken by flexural action. In practice there is a range of conditions from full support to no support and thus a corresponding range of the proportion of the load resisted by membrane action to the load resisted by flexural action.

Other considerations apart from curvature and boundary conditions also affect this ratio of load carrying. Perhaps the next most important is the relative stiffness of the two modes of action. For the continuum

shell this is governed by the shell thickness. Flexural action is more prevalent in thicker shells.

Thus both geometry and structural properties affect the responses of the continuum shell. A shell with a given geometry such as the second order surface on a rectangular boundary can have a qualitative assessment of its response made from these ideas. For an elliptic paraboloid shaped shell with gable supports on all four sides the only fully restrained arches are the corner diagonal lines. All others are only partially restrained and thus only partly effective. Thus it would be expected that there would be some flexural action for all values of the rises and thickness but more so for lower rises and thicker shells.

Hyperbolic paraboloids on rectangular boundaries with gable supports also have the only fully restrained arches as the diagonal lines joining the corners. However for the particular case $H_X = -H_Y$, when the rises in the two directions are equal and opposite, the corner diagonal lines have no curvature. Thus there is no arch action at all in them and much, if not all, of the load is carried by bending. This results in deformations being relatively large, membrane actions being very low and bending actions being predominant.

The continuum shell model also explains the considerable effect of boundary conditions on the response of the structure with critical geometry $H_X = -H_Y$. When the gable support is vertical no reaction to the outward thrust of the arch is provided but when the gable support is normal to the surface in plane forces in the gable have a component in the horizontal direction and hence allow some membrane action to occur.

The effect of the gable is critical with the single layered lattices where the efficient structural resistance is as a membrane. With the double layered lattice bending action is the principal mode of

resistance and the actual angle of the gable is of little significance. This is reflected in the responses of the structures studied in chapter 7 where a pronounced effect is only seen for the single layer structure.

8.2 CHOICE OF PARAMETER VALUES

The continuum model presented in the last section may also be used to qualitatively assess the response of the structure as the parameters describing it are varied. For the type of shell studied the geometry parameters are the spans L_X, L_Y and the rises H_X, H_Y . The structural parameters are E^* , the elastic modulus, ν , the Poissons ratio and h^* , the thickness. For the lattice the geometry parameters above must be supplemented by the subdivision factors N, M while the parameters analogous to the material properties and thickness can be taken as combinations of the axial stiffness EA and the bending stiffness GI_X, EI_Y and EI_Z for the single layer structures and as combinations of the axial stiffness EA and layer separation D for the double layer structures.

These are the parameters which will be considered, but it is not necessary to consider them all, as ratios of some of them can be more relevant. This is true for the ratios of H_X to H_Y , of L_X to L_Y (with corresponding ratios of N to M) and of the stiffness factors. Thus it is considered satisfactory if only one of the quantities from each of these groupings is varied and the other retain a fixed value. In the case of the rises, the very marked sensitivity at the point $H_X = -H_Y$ as explained previously, dictates that several values of one of them be considered as the other varies.

Thus the scheme adopted for these numerical experiments was to choose fixed values for the parameters L_X, L_Y, N, M, H_Y and the structural properties E, A, I_X, I_Y and I_Z for the single layer structures and E, A and separation D for the double layer structures, along with

several values of the rise H_x . These constituted a series of base structures from which to vary one parameter at a time, the parameters being considered were the other rise H_y , the length L_x (together with an appropriate value of N) and the structural properties I_x , I_y and I_z for the single layer structures and the separation D for the double layer structures. For each type of structure there are then three parameters which are varied. The values chosen for the base structures and the values they are varied to are given in table 8.1 for the single layer structures and in table 8.2 for the double layer structures. It will be noted that the base structures include those studied in chapter 7 and numbered 2, 3, 4 and 5 in the case of the single layered ones and numbered 7, 8, 9 and 10 for the double layered case.

The loading applied to all these structures is a uniform normal load which is the same load as applied to obtain the results quoted in chapter 7.

8.3 CHOICE OF A MEASURE OF THE RESPONSE

Having chosen the structures that are to be studied, it is necessary to choose quantities to use as a measure of the response of the structure. Because a structural analyst is concerned with both deformations and stresses, each of these two types of quantity are chosen.

The single layer rigid jointed structure response is represented by the normal deflection of the centre joint, the axial load in the central longitudinal member, and the axial load and bending moment in the corner diagonal member. The location of these four quantities in the structure is shown in figure 8.1.

For the double layer pin jointed structure, the response is represented by the normal deflection of the centre joint, and the axial load in the central upper layer longitudinal and the corner diagonal

TABLE 8.1 Parameter Values for Single Layer Structures

Base Structures

$L_X = 20.00 \text{ m}$	$N = 24$	
$L_Y = 17.32 \text{ m}$	$M = 12$	$H_Y = 1.0 \text{ m}$
$H_X = 2.0, 1.5, 1.0, 0.5, 0.0, -0.5, -1.0, -1.5, -2.0 \text{ m}$ (9 cases)		
$E = 211. \times 10^9 \text{ Pa}$	$I_X = 1.0 \times 10^{-6} \text{ m}^4$	
$G = 79.2 \times 10^9 \text{ Pa}$	$I_Y = 0.5 \times 10^{-6} \text{ m}^4$	for all members
$A = 1.0 \times 10^{-3} \text{ m}^2$	$I_Z = 0.5 \times 10^{-6} \text{ m}^4$	

Vary H_Y

$H_Y = 0.0, 0.5, 1.0, 2.0, \text{ m}$ (4 cases)

All other variables as for base structures.

Vary L_X and N

L_X and N are varied jointly such that the ratio $\frac{L_X}{N}$ remains the same.

$L_X = 13.33, 20.00, 26.67, 40.00 \text{ m}$ (4 cases)

$N = 16, 24, 32, 48$

All other variables as for base structures.

Vary I_X , I_Y and I_Z

I_X , I_Y and I_Z are varied jointly such that

$I_Y = I_Z$ (bending) and $I_X = I_Y + I_Z$ (torsion)

$I_X = 1.0 \times 10^{-6}, 1.0 \times 10^{-5}, 1.0 \times 10^{-4} \text{ m}^4$

$I_Y = 0.5 \times 10^{-6}, 0.5 \times 10^{-5}, 0.5 \times 10^{-4} \text{ m}^4$ (3 cases)

$I_Z = 0.5 \times 10^{-6}, 0.5 \times 10^{-5}, 0.5 \times 10^{-4} \text{ m}^4$

All other variables as for base structures.

TABLE 8.2 Parameter Values for Double Layer Structures

Base Structures

$$L_x = 20.00 \text{ m} \quad N = 24$$
$$L_Y = 20.00 \text{ m} \qquad M = 24 \qquad H_Y = 1.0 \text{ m}$$
$$D = 1.0 \text{ m}$$
$$H_x = 2.0, 1.5, 1.0, 0.5, 0.0, -0.5, -1.0, -1.5, -2.0 \text{ m} \quad (9 \text{ cases})$$
$$EA = 211. \times 10^6 \text{ N for all members.}$$

Vary H_Y

$$H_V = 0.0, 1.0, 2.0 \text{ m} \quad (3 \text{ cases})$$

All other variables as for base structures.

Vary L_X and N

L_X and N are varied jointly such that the ratio $\frac{L_X}{N}$ remains the same.

$$L_x = 13.33, 20.00, 26.67, 40.00 \text{ m} \quad (4 \text{ cases})$$

N = 16, 24, 32, 48

All other variables as for base structures.

Vary D

$D = 0.5, 1.0, 2.0 \text{ m}$ (3 cases)

All other variables as for base structures.

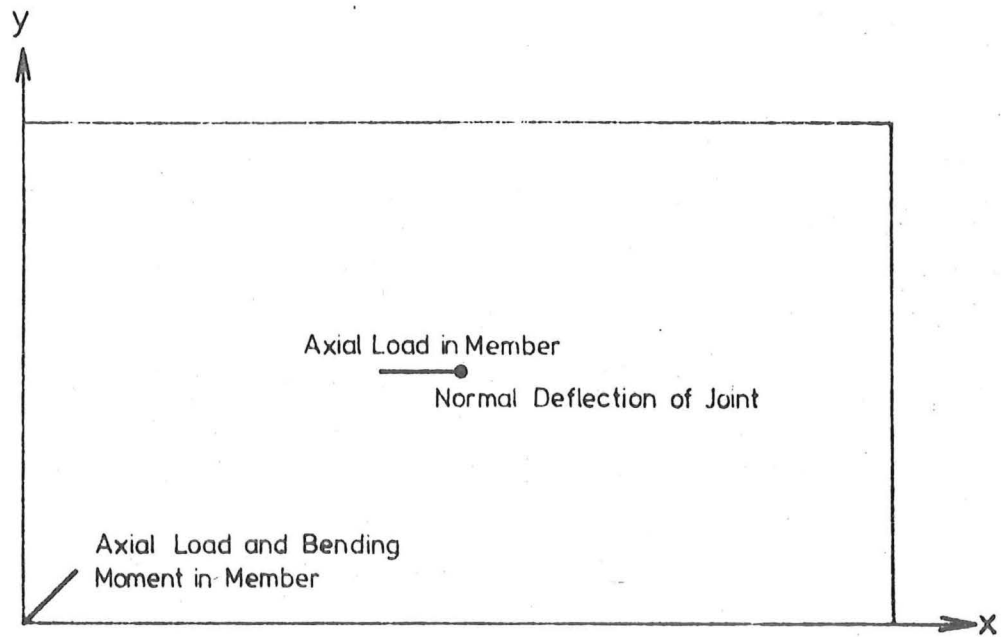


Fig.8.1 Single Layer Rigid Jointed Structure Response Quantities

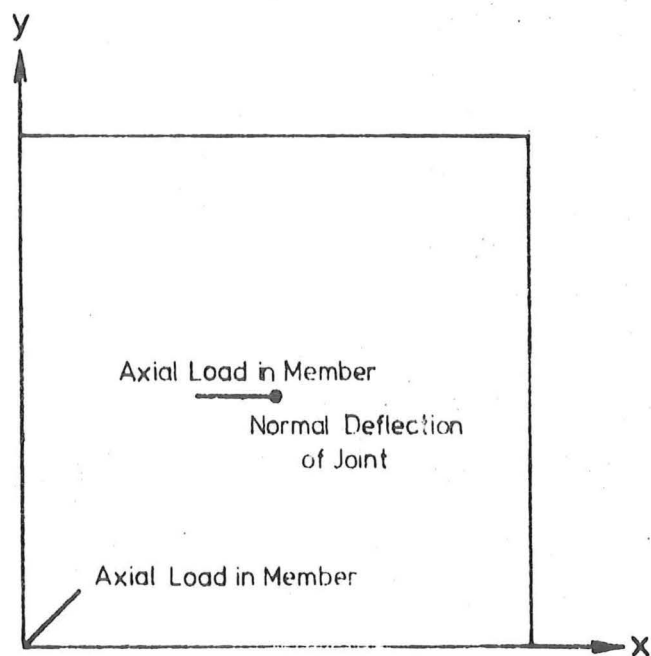


Fig.8.2 Double Layer Pin Jointed Structure Response Quantities

web members. Figure 8.2 shows the location of these three quantities in the structure.

8.4 RESULTS OF ANALYSIS

The results are presented in a graphical form. Figures 8.3 to 8.6 applying to the single layer structures and figures 8.7 to 8.10 applying to the double layer structures. Each of these will now be described in turn.

8.4.1 Results for Single Layer Structure

For the series of base structures, the results are given in figure 8.3 where the appropriate quantities are shown for the various values of the rise H_X . As predicted, for elliptic paraboloids where $H_X > 0$, the deformations and bending moments are small. Axial forces are moderate in size and membrane action appears to be the principal mode of resistance.

For hyperbolic paraboloids, with $H_X < 0$, the situation changes. Initially, as H_X varies from zero, the deformations and bending moments become larger. This however takes place only until the critical geometry where $H_X = -1.0 = -H_Y$, when these quantities reach a peak. The axial forces having reached a peak near this critical geometry, fall to be close to zero at the critical geometry. It is apparent that at the critical geometry the load is sustained almost entirely by bending action while membrane action is negligible.

When the magnitude of H_X is increased further the deformations and bending moments are reduced and the axial forces change sign. The membrane action is again becoming prominent but this time as "cables" rather than "arches" or vice versa.

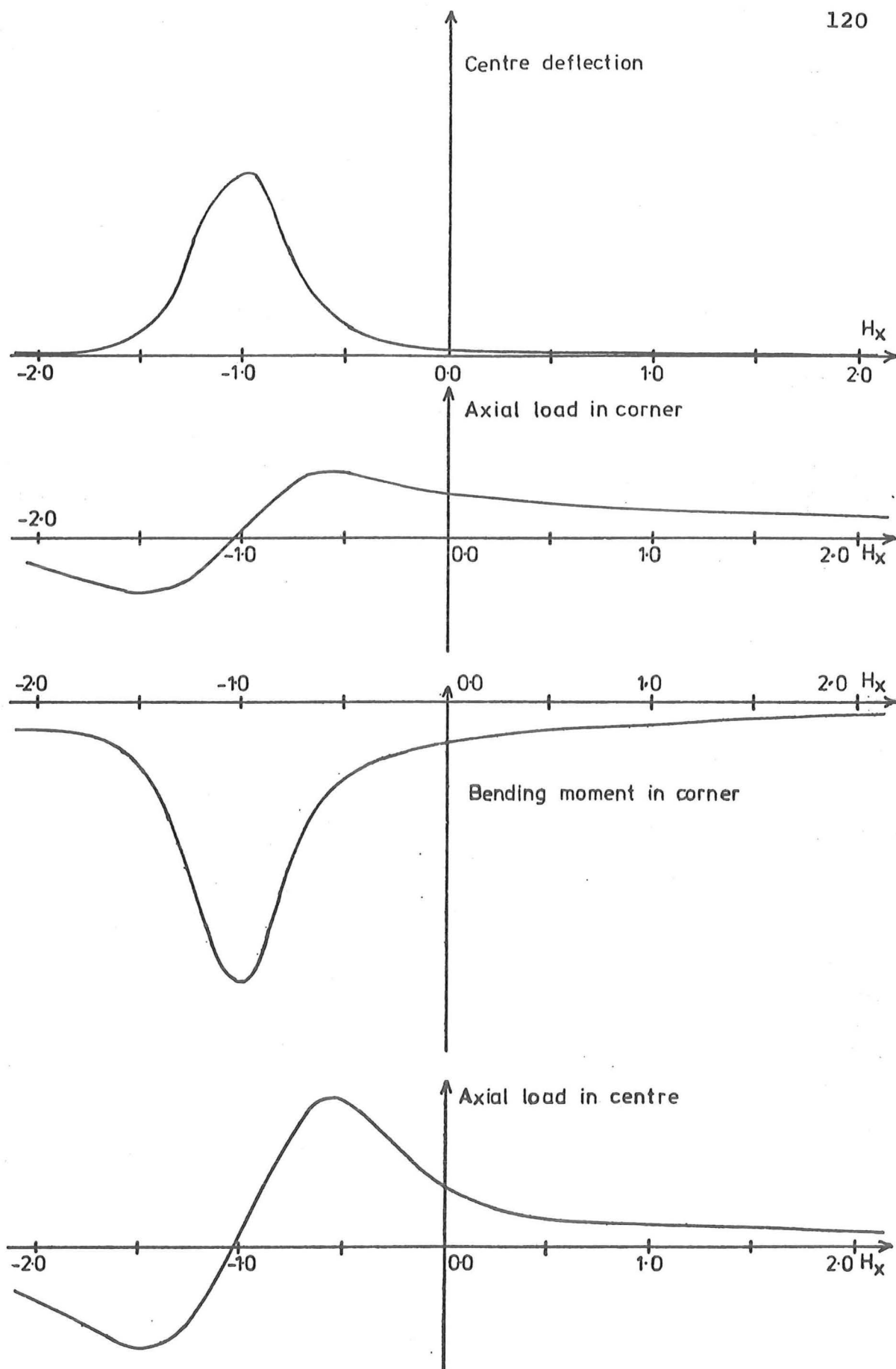


Fig. 83 RESULTS FOR SINGLE LAYER STRUCTURES -
BASE CASE

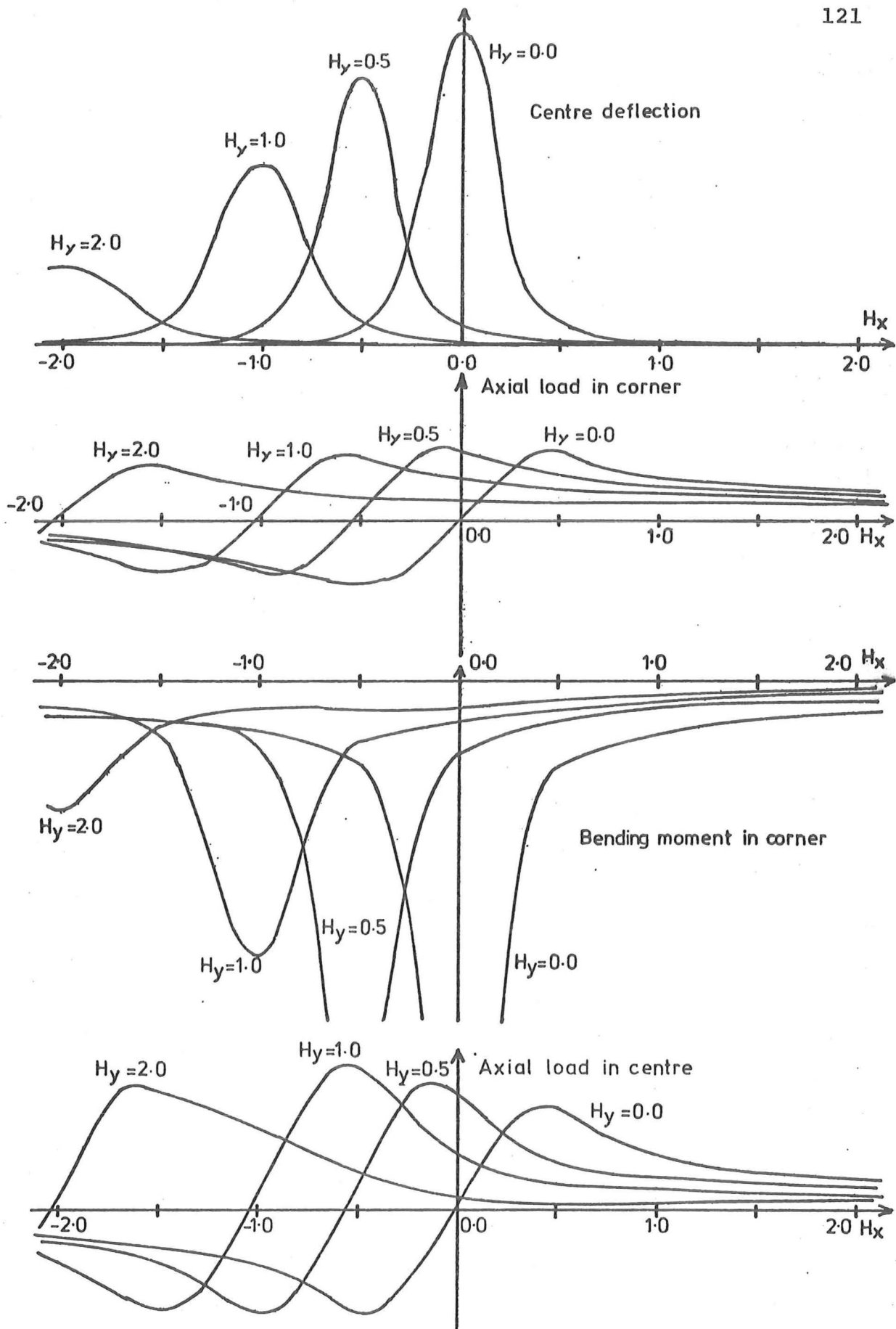


Fig. 8.4 RESULTS FOR SINGLE LAYER STRUCTURES -
VARY H_y

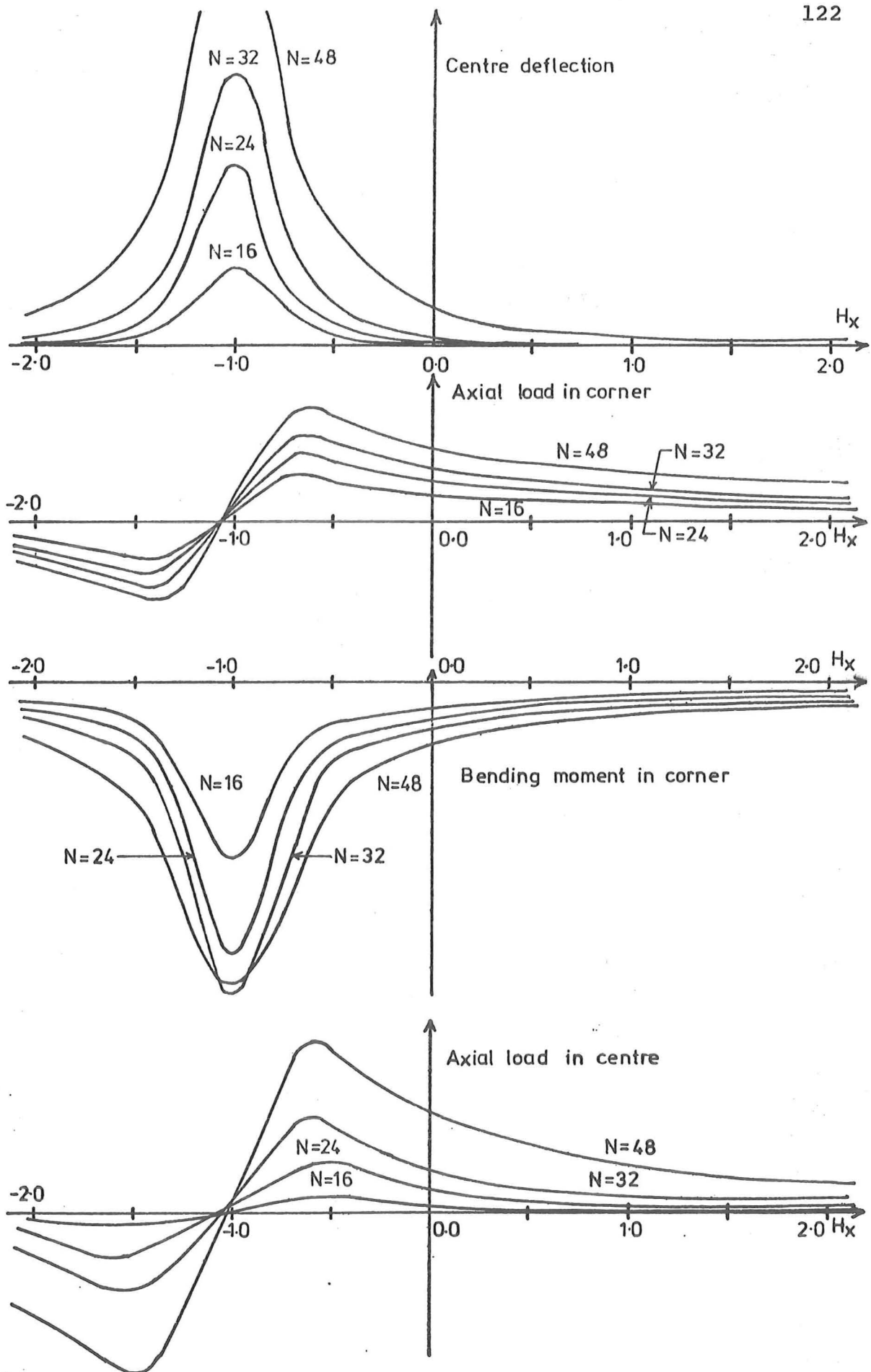


Fig. 8.5 RESULTS FOR SINGLE LAYER STRUCTURES -
VARY N AND L_x

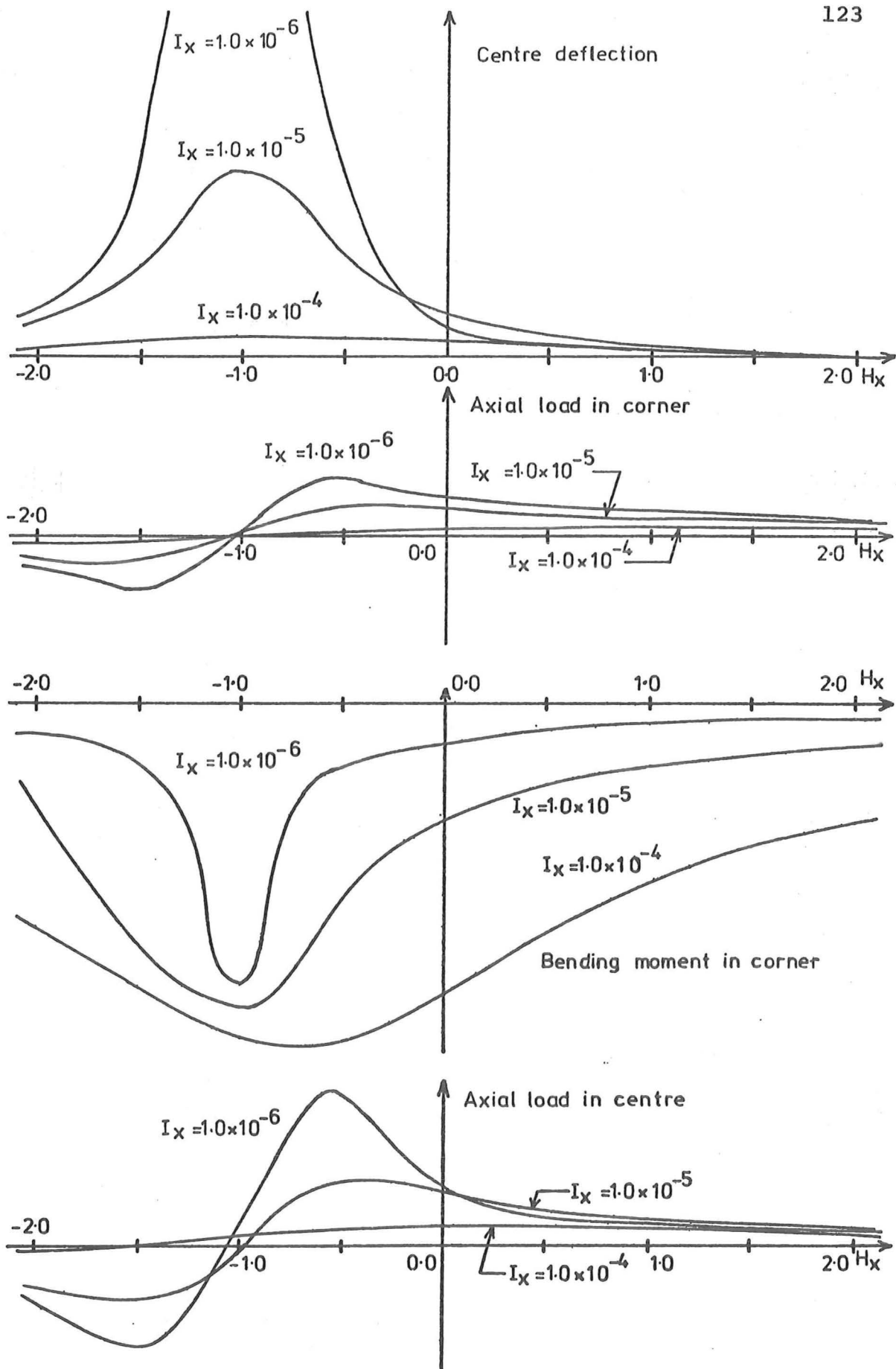


Fig. 8.6 RESULTS FOR SINGLE LAYER STRUCTURES -
VARY I_x etc.

The interesting feature about this graph is of course the behaviour when $H_X = -H_Y$, which is explained by the model put forward earlier. In order to verify that it also takes place for other values of the rise H_Y than the one presented in figure 8.3, several other values were used and the results are plotted as figure 8.4. The same trends as before are present for each of the families with a fixed value of H_Y , the peak of the deformation and bending moment curves being shifted to the point where $H_X = -H_Y$.

Another relevant trend shown in figure 8.4 is that, for a given value of H_X which is far enough from the critical geometry, both the bending moments and axial forces become smaller as H_Y increases. This is to be expected as with a more curved structure, two way action becomes more prevalent and the axial forces are more uniformly spread resulting in their being lower on the average. It must be remembered that the method presented here only applies to shallow curved surfaces and thus it may not be applicable if H_Y or H_X become too large.

Figure 8.5 shows the trend of results as the length L_X and subdivision N are varied from those of the base structure. The trend appears to be that the greater the span, the larger are all the quantities presented. The proportion is however not simply related to the change in span but is very dependent on the proximity to the critical point.

The results that are obtained when the member bending stiffnesses I_X , I_Y and I_Z are varied are presented in figure 8.6. At the critical point $H_X = -H_Y$ the effect on the deformations is quite significant, with a stiffer member giving smaller deformations. However when sufficiently far from this critical point, there is little effect on the deformation level. However the bending moments and axial forces are affected

for all values of the rise H_X . The bending moments are increased and axial forces decreased when the bending stiffness of the member is increased. This implies that more load is resisted by bending action as would be predicted for a "thicker" structure by the model proposed earlier.

8.4.2 Results for Double Layer Structure

The base structures for this type of structure, were analysed and the results are shown in figure 8.7. The trends seen here are the same as those for the single layer structure which are given in figure 8.3. However the peak at the point $H_X = -H_Y$ is certainly not as marked since this particular set of structures would correspond to a rather "thick" shell and bending action is quite significant.

For these structures, the axial force in the centre longitudinal member is in fact dependent on both the bending action and membrane action present in the corresponding shell and so must be interpreted in this light.

Figures 8.8 and 8.9 present the results when the rise H_Y and the length L_X respectively are varied. The trends shown here are similar trends to those exhibited by the single layer structure and so need no further comment here.

The results of varying the inter layer separation D are given in figure 8.10. This parameter is analogous to the thickness of a shell and the results correspond to such a conclusion. With a small distance between the layers, the structure shows larger deformations generally and a greater sensitivity as the rises approach the critical condition of $H_X = -H_Y$. A larger separation results in the opposite effect.

8.5 SUMMARY

From the numerical results presented in figures 8.3 to 8.10, it can be concluded that the qualitative model proposed in section 8.1 does

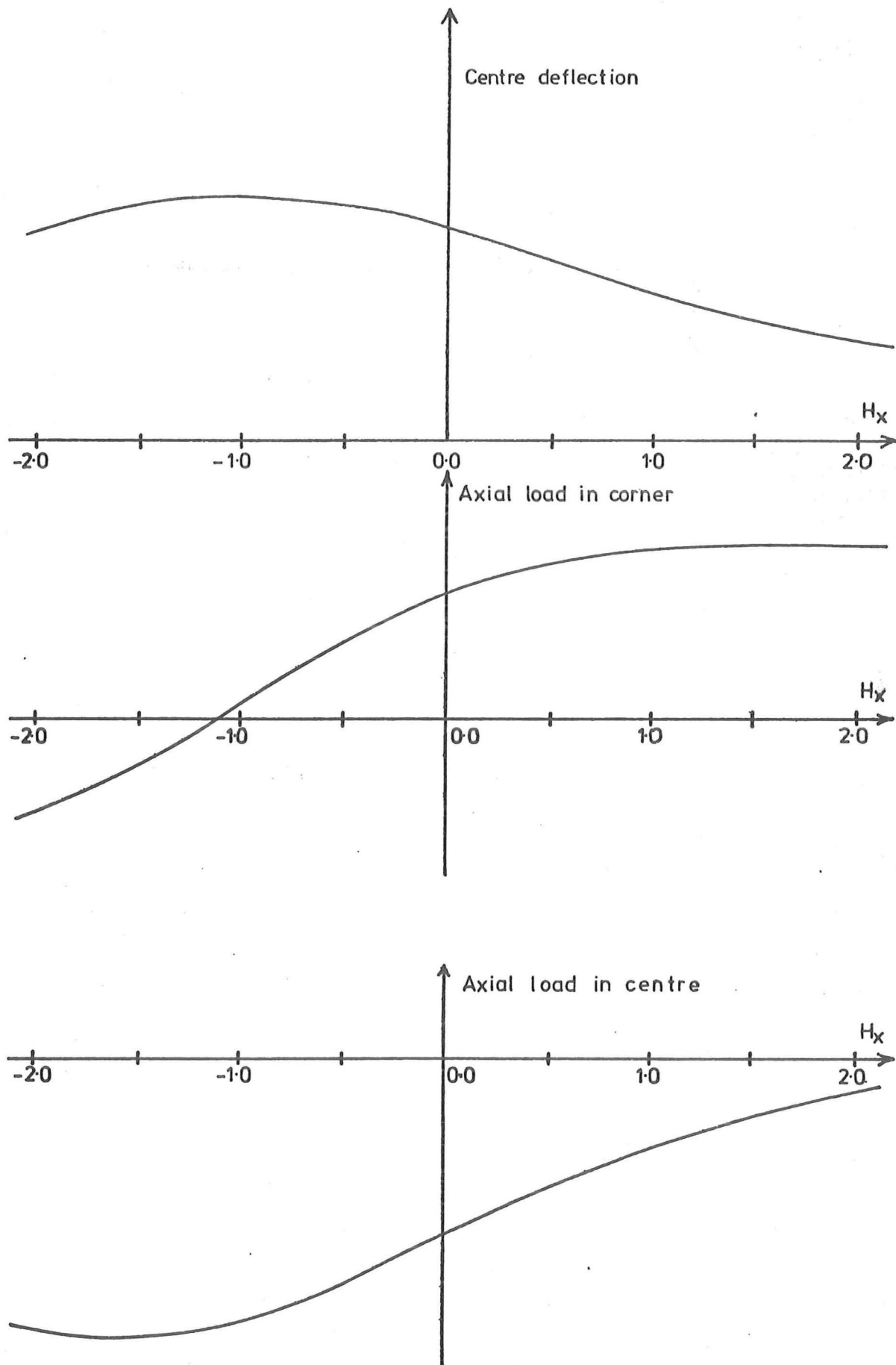


Fig. 8.7 RESULTS FOR DOUBLE LAYER STRUCTURES -
BASE CASE

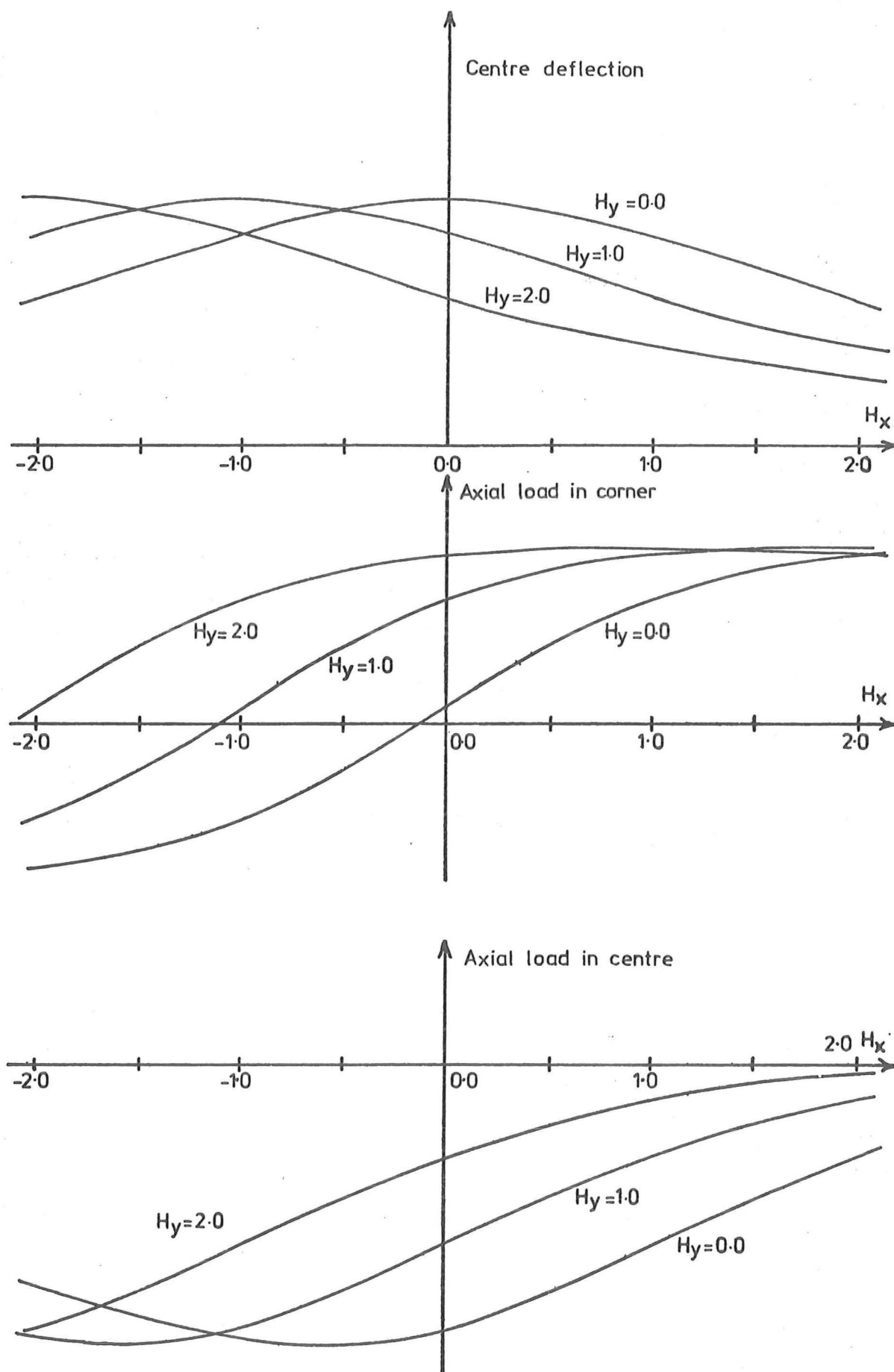


Fig. 8.8 RESULTS FOR DOUBLE LAYER STRUCTURES -
VARY H_y

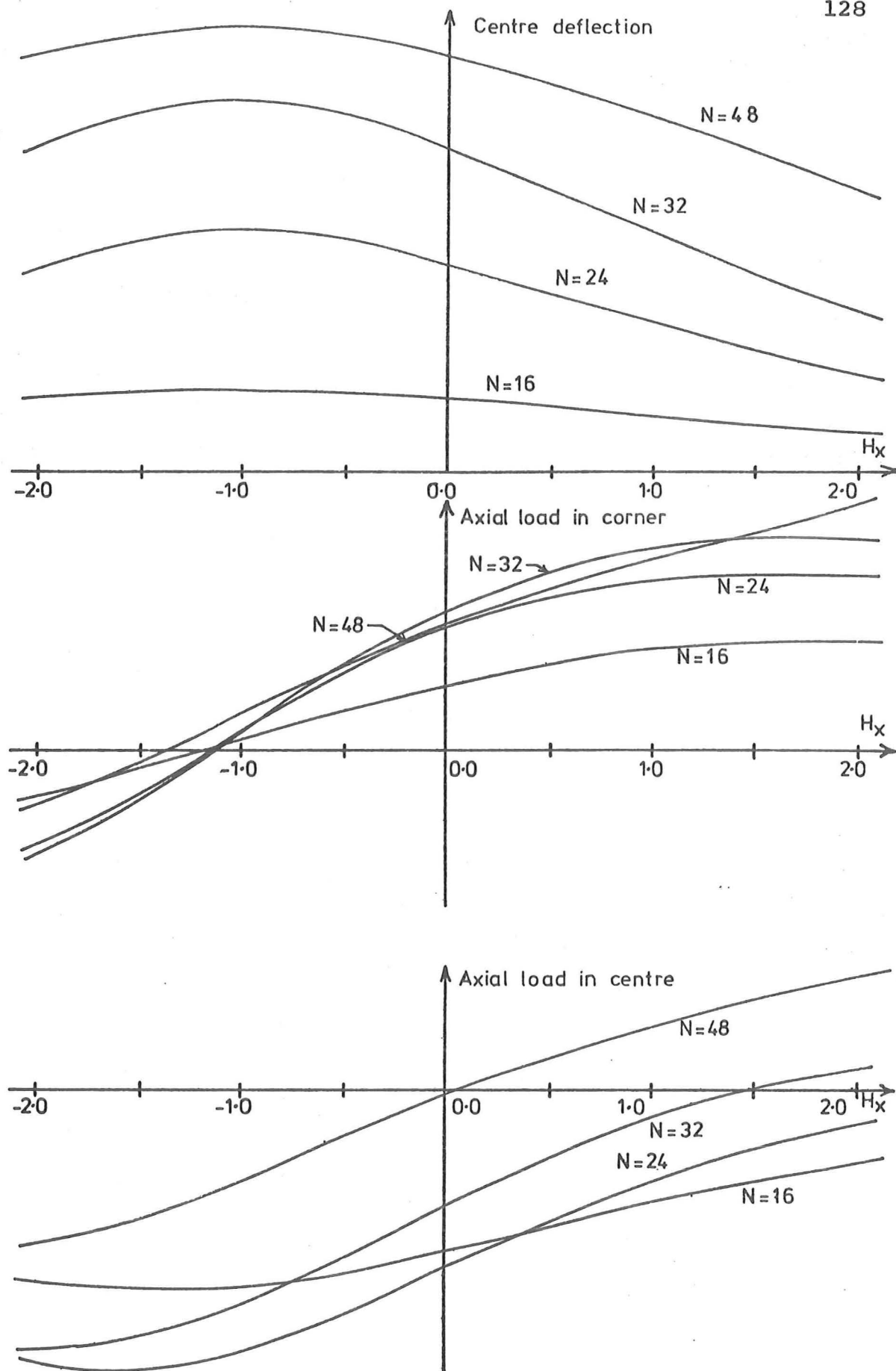


Fig. 8.9 RESULTS FOR DOUBLE LAYER STRUCTURES -
VARY N AND L_x

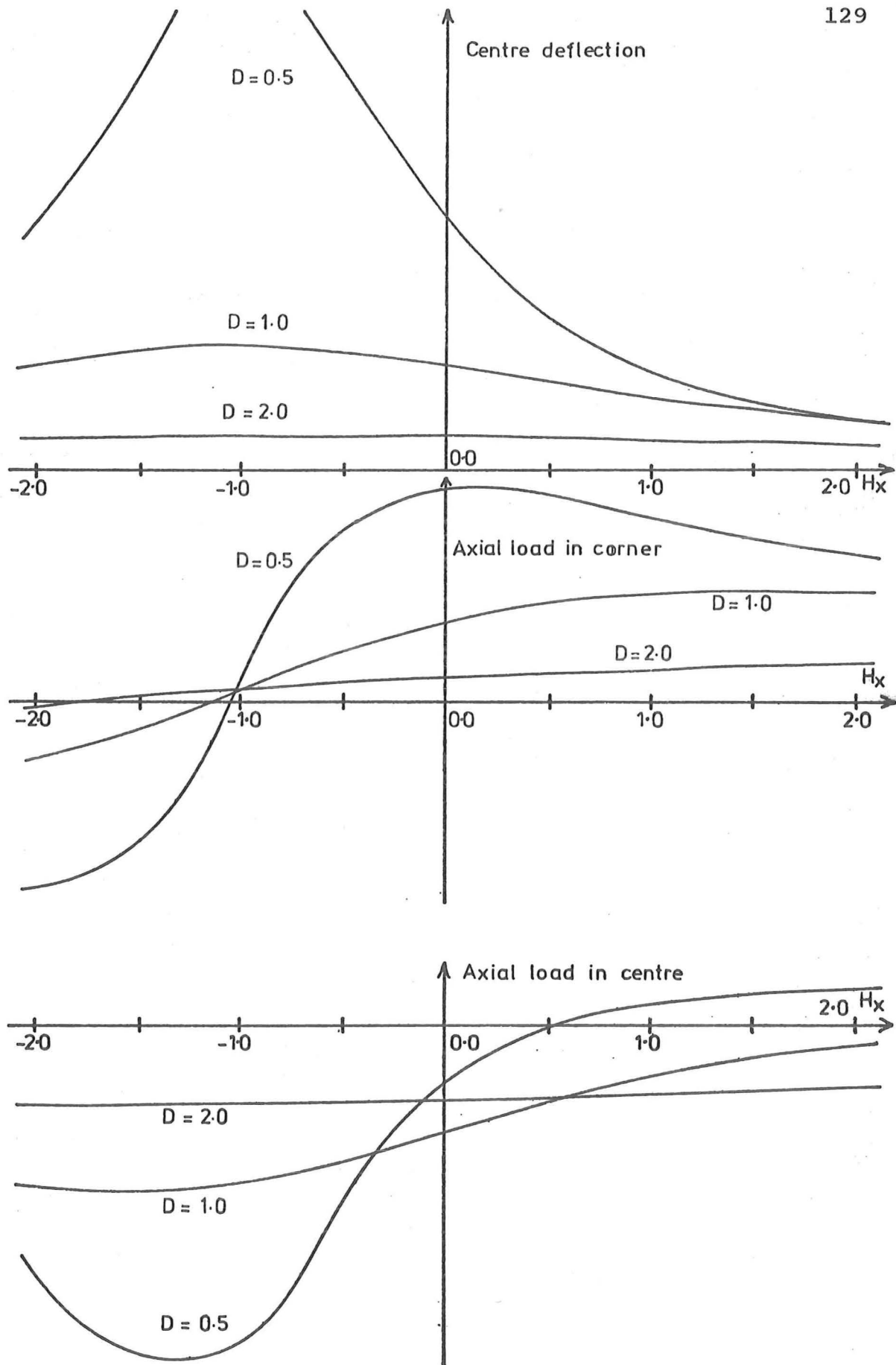


Fig. 8.10 RESULTS FOR DOUBLE LAYER STRUCTURES -
VARY D

in fact give a realistic indication of the response to be expected for both the single layer and the double layer type structures.

The base values for the parameters chosen for the single layer structures appear to correspond to a rather thin analogous shell while those chosen for the double layer structure lead to a thick analogous shell. This is based on the sensitivity that the structures show at the critical point $H_X = -H_Y$.

The prediction and explanation of the existence of this critical point is a strong argument in favour of the use of this qualitative model to determine the performance of curved lattices. The trends exhibited as the rises, the length and the thickness are varied do correspond with those that are predicted from the use of such a model.

Again it must be emphasised that the performance of a given structure cannot be assessed as the aggregate of the effect of each parameter considered separately but it is most important that the inter-dependence of all the parameters be considered. The results quoted here will hopefully indicate to the analyst the inter-relationships of the parameters.

CHAPTER NINE

NON LINEAR BEHAVIOUR9.1 INTRODUCTION

The analysis presented in chapter 2 and applied to the classes of structures in chapters 4, 5 and 6 was restricted to linear elastic behaviour. In this chapter, the types of non linear behaviour that are possible are presented and the importance and means of allowing for such behaviour is considered.

The types of non linear behaviour affecting the lattice space structures treated in this thesis may be grouped under the three headings

- a) Non linear material stress strain behaviour
- b) Non linear elastic member load deformation behaviour (member buckling)
- c) Change in structure geometry through large deformations.

The first two concern non linear behaviour of the member. Non linear material stress strain relationships may be due to the effects of material yielding or crushing. By designing the members so that the stress levels are not too high, such behaviour can generally be avoided. Thus it is considered that this will not usually be a problem for the types of structure considered here.

The second type of non linear behaviour, member buckling, is due to member deformations becoming large compared to the member size. Along with this the member material may also have a non linear stress strain relationship. It is usually possible to proportion the member so that the member actions are restricted to linear behaviour. If this is done, this type of non linear behaviour will not be a problem for the types of structure considered.

This leaves the last type, geometric non linear behaviour of the structure, to be considered. This is when the joint displacements are large and significant changes of geometry occur in the structure. The members may be behaving linearly or non linearly. From the results of chapter 8, it will be seen that the response of the structure under load depends on many parameters, and for some layouts the displacements can be large. This is so even when using member sections and materials which remain in the elastic range. It is to be noted that while the designer may choose the member sections and materials, he may not have such a choice about the structural layout. For those structures with large deformations, it is considered that geometric non linear behaviour can be relevant.

In the next section an outline is given of the procedures involved in an analysis where non linear behaviour is considered.

9.2 TREATMENT OF NON LINEAR BEHAVIOUR

In the general development in chapter 2 the joint equilibrium equation 2-13 is derived for a general structure and layout. In this equation, the matrix $[K(E_\alpha, E_\beta)]$ depends on the structure geometry, through the transformations $[T]$, and on the member properties, through the stiffness $[k]$. In the subsequent development in chapters 4, 5 and 6, the analysis was restricted to cases where the matrix $[K(E_\alpha, E_\beta)]$ did not depend on the joint coordinates α and β . It was noted that for such cases the equilibrium equation 2-13 is a system of linear partial difference equations with constant coefficients and for such equations it is relatively easy to obtain an analytic solution in terms of the eigenfunctions.

For the more general case where the geometry and/or properties vary with the coordinates, the equations are still linear but now have non constant coefficients. It may be possible to obtain the eigenfunction

series solution for this problem but this is generally difficult and purely numerical methods usually prove to be easier.

It is also possible that the member stiffnesses depend on the member actions (non linear member material properties) and/or the geometry depends on the joint deformations to an appreciable extent. For these cases the equilibrium equations are now non linear and have non constant coefficients. Paralleling the case of differential equations which are non linear and have variable coefficients, the solution of such equations is usually very difficult and is often considered intractable. There has been some effort devoted to non linear difference equations e.g. [74] but only very simple systems are considered. Because of the lack of available techniques for solving non linear difference equations, it is considered that the extension of the analysis to such cases is unwarranted at this stage.

9.3 NUMERICAL EXAMPLES

In order to gauge the influence of geometric non linear behaviour, it was desired to perform some numerical analyses incorporating this effect. The test structures used in chapter 7 were considered as suitable examples and an extension of the direct stiffness method was used to produce the analyses.

A computer program to perform a geometric non linear analysis was not available and thus some other procedure was required. A survey of the literature [28, 49, 66] indicated the types of methods available. It was decided to use an incremental loading technique which could be easily incorporated into the linear analysis program used to obtain the results presented in chapter 7.

The procedure followed is to perform a linear elastic analysis using a load increment on the original structure. Under this loading, the structure deforms and the joints are no longer at the original posi-

tions. The coordinates of the joints are changed to account for this, resulting in a new structure geometry, and another linear elastic analysis is performed for a further load increment. The joint coordinates are updated again and the procedure repeated for as many increments as required.

For each load increment a linear elastic analysis is made and this introduces some errors, as no account is taken of the load level in the members due to all the previous increments. The effect of allowing for these is to generally stiffen the members subjected to tension and soften those subjected to compression. It is felt that these effects are small for the structures and load intensities considered here.

Accuracy is improved by using small load increments, particularly where the structure is very flexible and the deformations are changing rapidly under load. However using many small increments results in consuming a large amount of computer time in the analysis and the procedure becomes expensive. Where the structure is stiff larger increments can be used. A trade-off is required between expense and acceptable accuracy.

Geometric non linear behaviour is more relevant when large deformations occur so particular attention was focussed on structures which have large elastic deformations. Of the test structures used in chapter 7, those of the single layer type generally had much larger displacements than the double layer type. For this reason it was considered unnecessary to perform a geometric non linear analysis on any double layer structures.

Descriptions of the single layer test structures numbered 1 to 5 are given in table 7.2 and in the text of section 7.5.1. Linear elastic analyses are presented in section 7.6.1. Non linear analyses were per-

formed on each of these structures and figures 9.1 to 9.5 show the loading path for the normal deflection of the centre joint as the load is incremented from zero to the service load. The procedure followed in each case was to first perform the analysis with five equal increments of load and then, depending on the results for each case, to adjust the increment sizes when necessary. The increment was reduced where the structure was flexible and increased in the regions where it stiffens. In this way a better indication of the response is obtained.

Structure 1 with $H_X = H_Y = 0.0$ is a flat grillage. The results are shown in figure 9.1 where the linear response is given along with results for five equal increments and a variable finer incremental loading. It can be seen that the linear response is large (~ 9.2) and as is to be expected the structure stiffens considerably under load so that the non linear deflection (~ 0.72) is only 8% of the linear elastic response. The curve shows that structure stiffening takes place at low load levels and the load deflection curve soon reaches a steady slope.

Figure 9.2 shows the response of the elliptic paraboloid test structure number 2 with $H_X = H_Y = +1.0$. The linear and non linear responses are very close and in practice could be considered the same. This is to be expected when the elastic deflection is small, as it is in this case, and no appreciable non linear behaviour takes place. It was unnecessary to refine the loading increments here.

For the cylindrical paraboloid with $H_X = 0.0$ and $H_Y = +1.0$ the results are shown in figure 9.3. As in the last case non linear behaviour is small with the non linear deflection under service load being 95% of the linear deflection. This structure, however, shows a different pattern of behaviour in that initially the structure stiffens and then at a load ratio $P/P_0 = 0.70$, the structure becomes more flexible. Under higher loads it would be expected to respond in a "snap through" type mode.

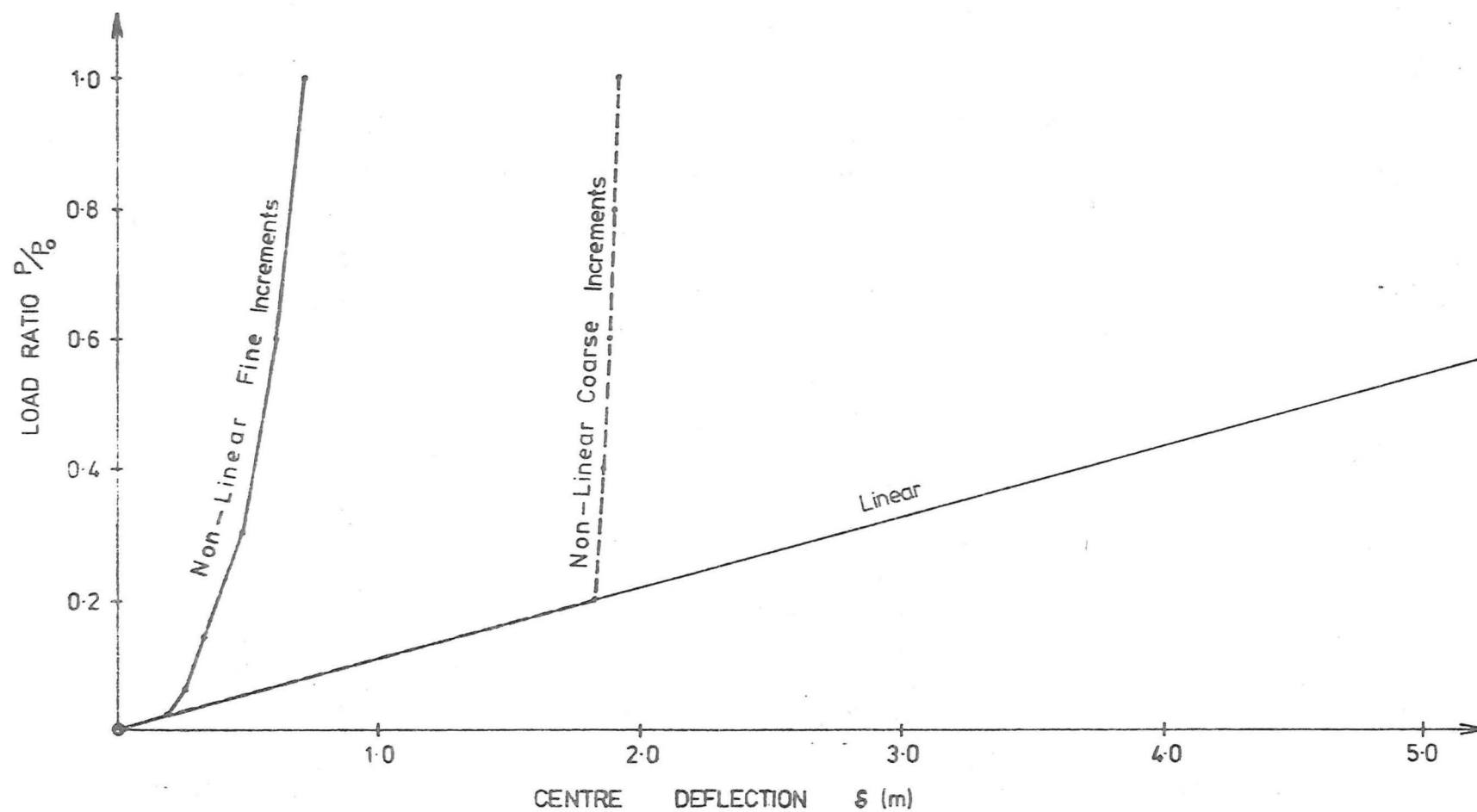


Fig. 9.1 CENTRE DEFLECTION/LOAD CHARACTERISTICS OF STRUCTURE №1 ($H_x=0.0, H_y=0.0$)

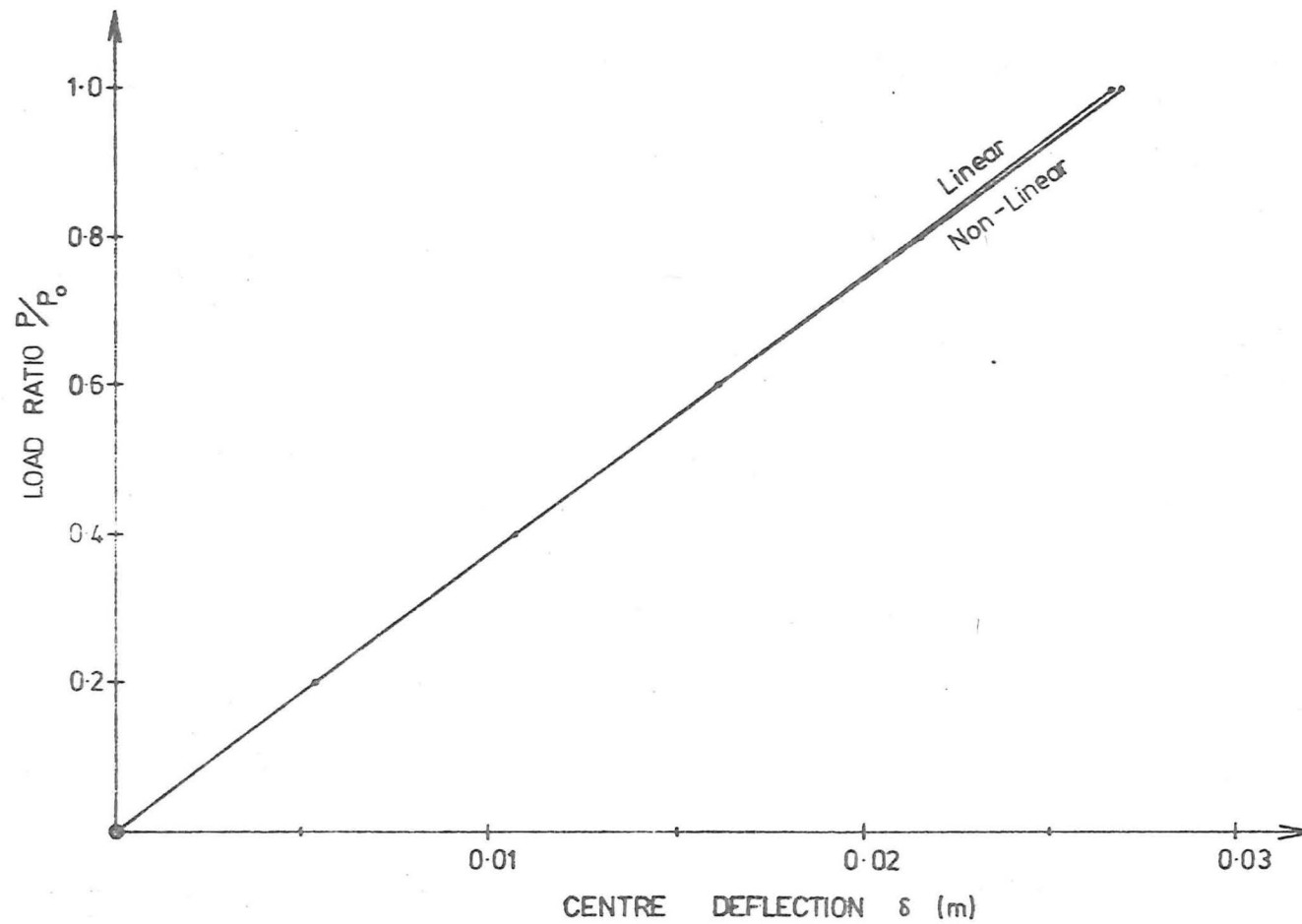


Fig. 9.2 CENTRE DEFLECTION/LOAD CHARACTERISTICS OF STRUCTURE N°2 ($H_x=+1.0, H_y=+1.0$)

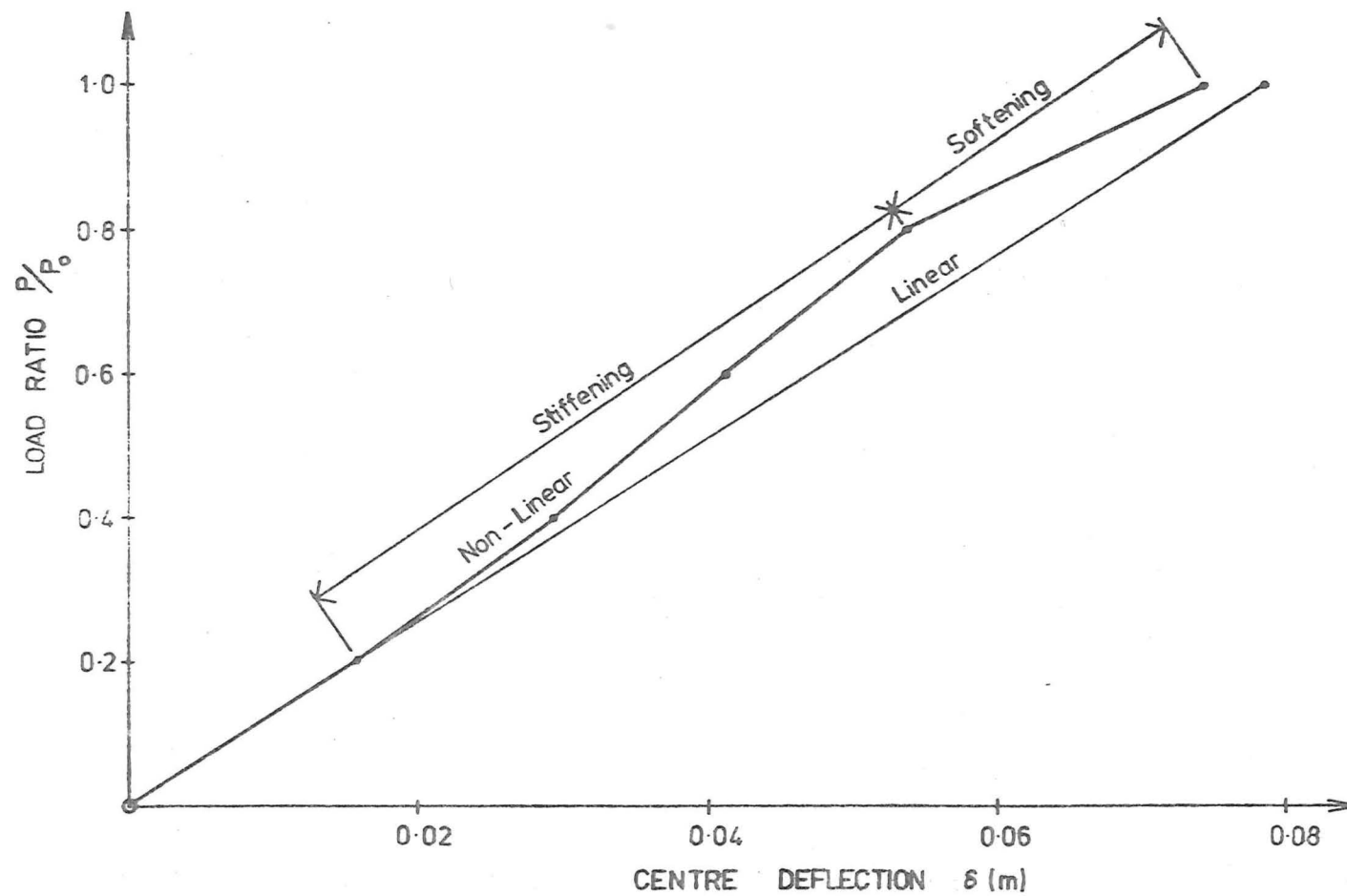


Fig.9.3 CENTRE DEFLECTION/LOAD CHARACTERISTICS OF STRUCTURE № 3 ($H_x=0.0, H_y=+1.0$)

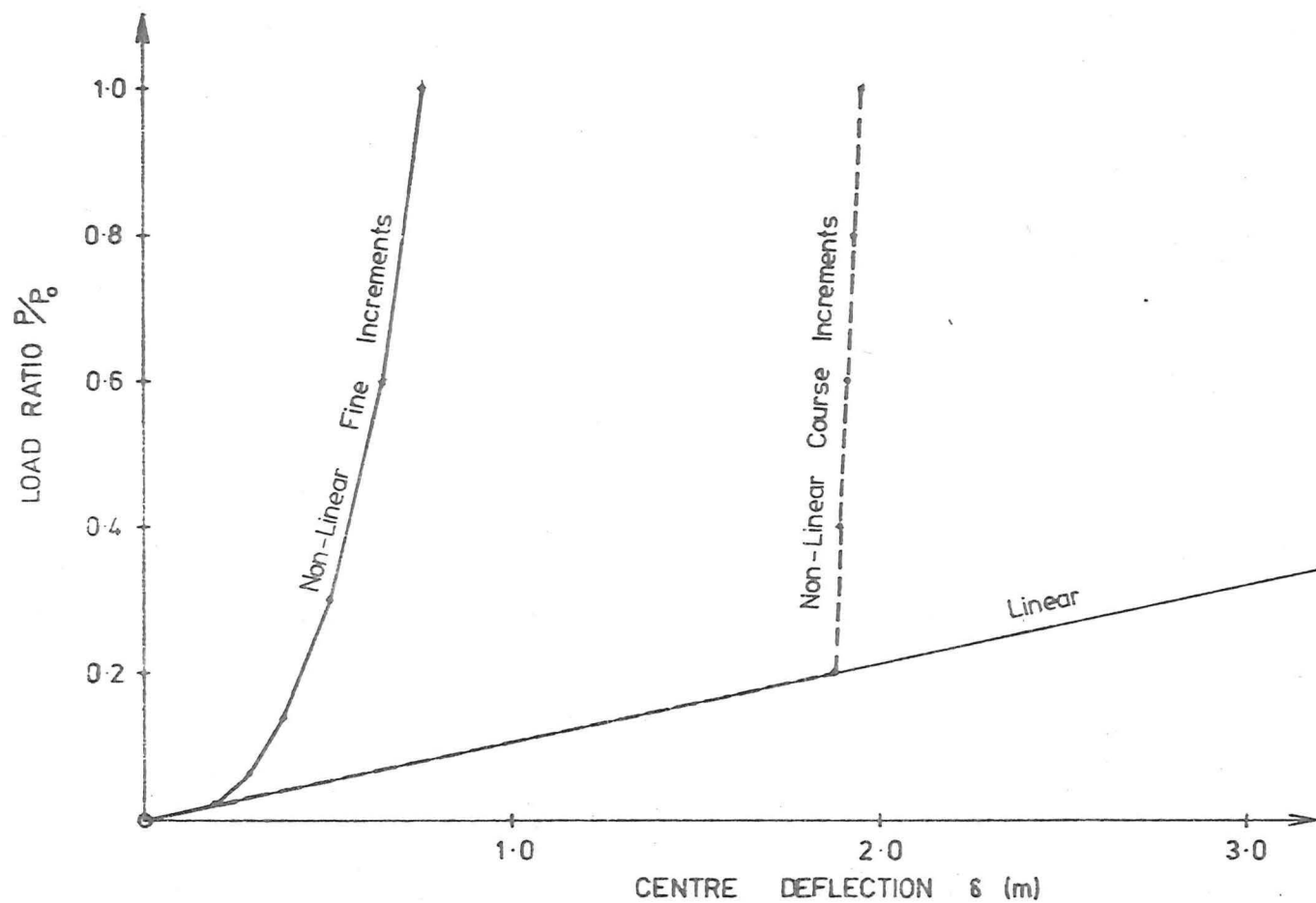


Fig.9.4 CENTRE DEFLECTION/LOAD CHARACTERISTICS OF STRUCTURE N° 4 ($H_x = -1.0, H_y = +1.0$)

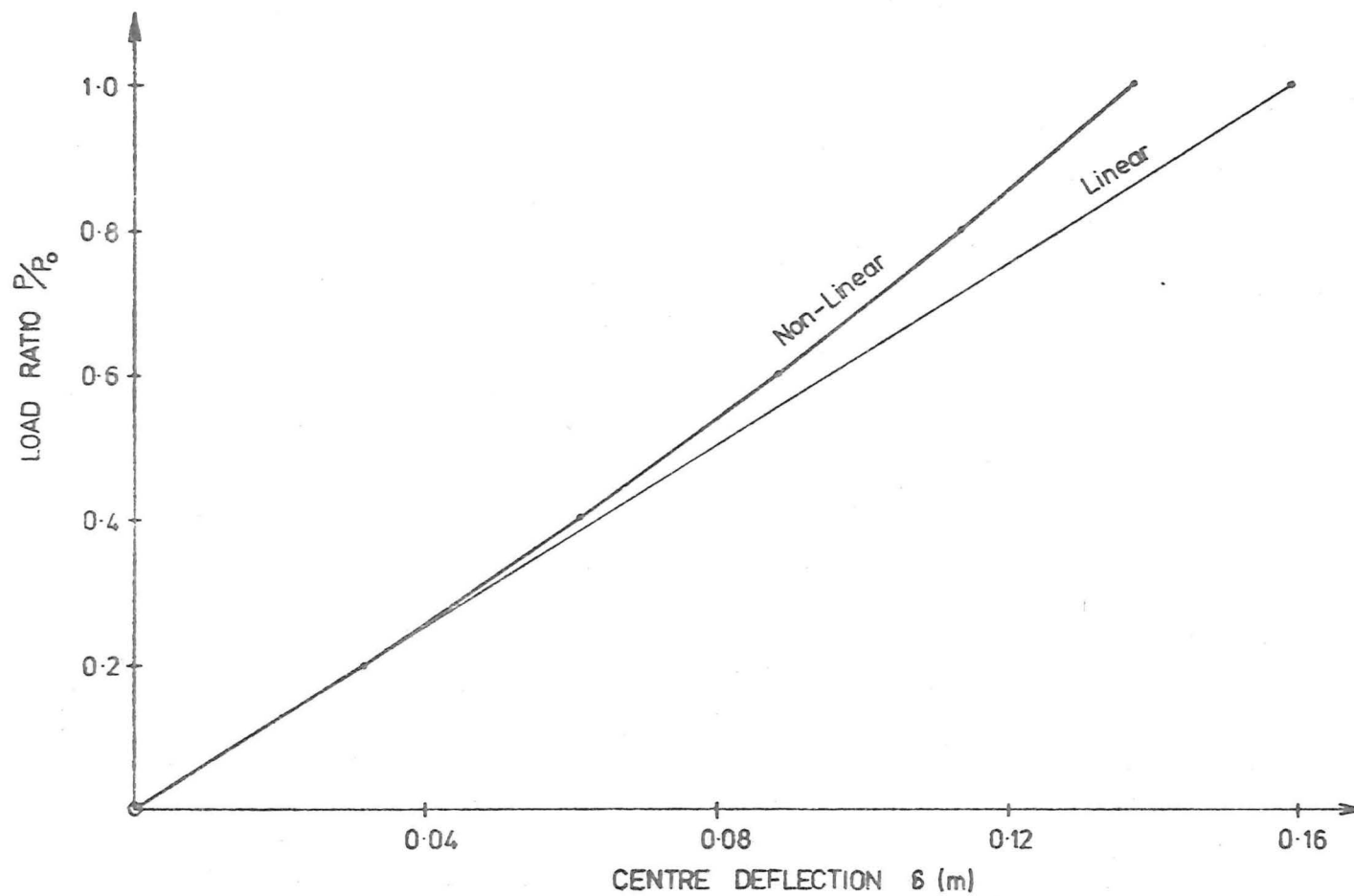


Fig.9.5 CENTRE DEFLECTION/LOAD CHARACTERISTICS OF STRUCTURE N° 5 ($H_x = -2.0, H_y = +1.0$)

Again because of only small changes in the stiffness, refinements of the load increments were not necessary.

Structure 4, as reported in chapter 7, is a very sensitive structure and it is to be expected that it will show highly non linear behaviour. This can be seen in figure 9.4 where the linear elastic response, the coarse increment response and the refined increment response are presented. The non linear behaviour here is similar to that of the flat grillage, structure number 1.

As the structure changes from the critical shape as represented by structure 4 to that of structure 5 with $H_X = -2.0$ and $H_Y = +1.0$, the response becomes more satisfactory with only a small amount of non linear behaviour. It would be expected that a linear analysis would be adequate for this case.

The trend shown here is the very obvious one that those structures which have "large" elastic displacements, also have significant geometric non linear behaviour. Those structures which have small elastic displacements i.e. stiff structures, have only a small amount of non linear behaviour and this can usually be neglected for practical purposes. What is "large" or "small" is hard to judge and depends mainly on what errors can be tolerated. From the results obtained here, a centre deflection in the order of $1/200$ of the span could be used as a guideline. It is not proposed that this figure is universal as very few cases have been considered. The values of parameters describing the structure, which lead to deflections of this order can be obtained from the results in chapter 8.

9.4 CONCLUSIONS REGARDING NON LINEAR BEHAVIOUR

Of the three types of non linear behaviour considered, that associated with the material and the member is generally insignificant as both the material and the member properties can be chosen so that the

relevant non linear behaviour is avoided. However the non linear behaviour associated with large displacements cannot always be avoided because structure shape is then an important factor and this is often dictated by other considerations e.g. architectural. Thus geometric non linear behaviour can be significant for some structures.

The extension of the finite difference method to cases involving non linear behaviour is possible, but the solution by analytic procedures is generally intractable. It is considered that the method used in this thesis is not practicable when non linear behaviour becomes significant. For such structures, an extension of the direct stiffness method is possible. Even this approach will generally prove to be expensive.

The structures for which geometric non linear behaviour is significant generally have large deformations when analysed by a linear elastic method. From the results of chapter 8 it is apparent that large deflections tend to be related to the structure geometry - particularly the rise or sag in each direction.

Figure 9.6 shows the range of the parameters H_x and H_y where large displacements are encountered and thus where non linear behaviour is to be expected. It is noted that for such structures with large displacements, the response, when non linear behaviour is considered, is to have a stiffening structure under load. This is a useful property as it means the inelastic displacements are less than the (large) elastic displacements.

In chapter 7 it was pointed out that those structures which have large deformations also tend to be very sensitive to the applied boundary conditions. Because of this sensitivity and the low stiffness, it is considered that if it is at all possible, such structures should be avoided in practice. Generally to obtain satisfactory performance from such structures would involve using more materials than for other more rigid structures.

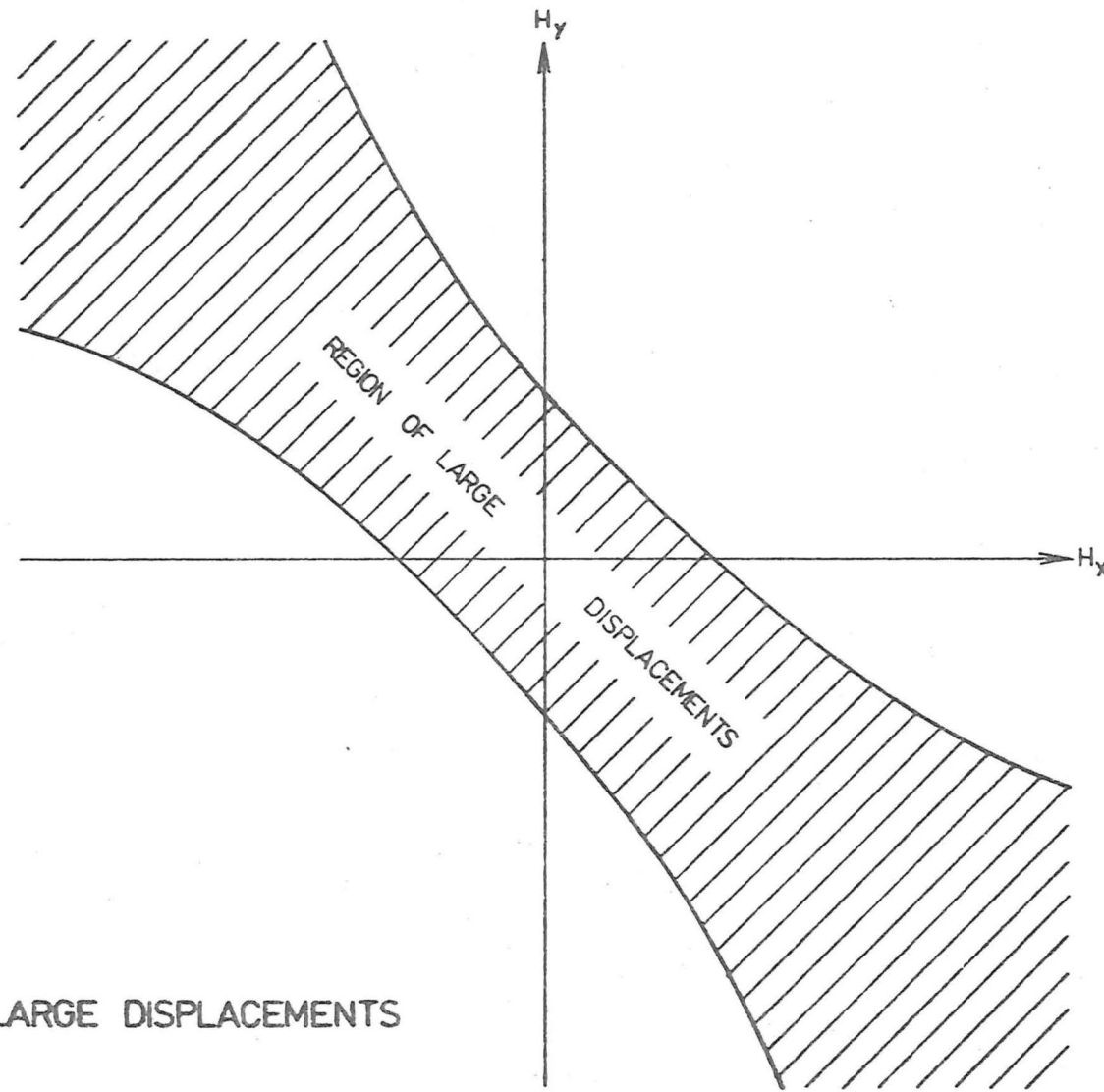


Fig. 9-6 REGION OF LARGE DISPLACEMENTS

CHAPTER TEN

SUMMARY AND CONCLUSIONS

The finite difference calculus method is an analytic technique that can be used to produce mathematical models for the response of a structure to load. The particular case of a linear elastic structure of regular lattice layout on a shallow curved surface is investigated in this thesis. The model produced is a set of partial difference equations for the unknowns, which in this case, are the joint displacements. These equations are solved analytically in much the same manner as partial differential equations, giving the joint displacements explicitly by formulae. The structural analyst then has the simple task of evaluating the formulae for the values of the parameters that describe the particular structure concerned. For other structures and shapes, even if an analytic solution and the resultant formulae cannot be found, then the equations can be solved numerically. Such a solution would usually involve a much larger amount of computer time and storage than the analytic method.

The method is described in general terms and is then used to produce analyses for three classes of structures. Two of these are single layer structures with one having pin joints and so being a special case of the other with rigid joints. The third structure is double layered with pin joints. All of these structures lie on a shallow second order surface which can take the form of an elliptic paraboloid, parabolic cylinder, flat surface or hyperbolic paraboloid by varying the parameters describing it. The structures have gable supports on the four sides of a rectangular boundary. While these are the specific structural layouts, shapes and boundary constraints that were considered here, it is possible that other shapes and boundary constraints could be

treated by the technique described. In particular structures with fully fixed supports were analysed although the results are not presented here.

The solutions produced for the joint deformations take the form of double trigonometric series with a finite number of terms. Thus there is no question of convergence as there is for an infinite series. Computer programs were used to perform all the required operations to produce numerical results for many structures. From these numerical experiments several conclusions were obtained.

The first conclusion is that the method as described and used is in fact a viable one. When compared with results from other methods and in particular the direct stiffness method, the results of the finite difference method are accurate and obtained at much less expense as measured by computer time and storage requirements. Typically the results quoted in chapter 7 indicate that the methods agree with the largest differences being of the order of 6%. However for the single layer rigid jointed structures, the direct stiffness method requires 19 times the computer time and 23 times the memory requirements of the finite difference method. For the double layer pin jointed structures these ratios are 10 and 20 respectively. It was also shown that as the structures become larger, these ratios remain advantageous to the finite difference method. It must be pointed out that these savings are very dependent on obtaining an analytic solution for the structure type. This in turn depends on several factors with perhaps the chief one being the regularity of the structure.

A study of the structure response as the parameters describing the structure geometry and member properties are varied, results in the conclusion that the geometry and member properties are very interdependent in determining the overall response of the structures studied. The effect of a single parameter cannot be isolated from the effect of all

others. Of particular interest is the interaction of the rise (or sag) of the surface in the two directions. When these two parameters are equal in magnitude but opposite in sign, the resulting structure shows a very marked tendency to carry load by bending action with low axial loads and large bending moments in the members. For this structure, the stiffness normal to the surface is very low and large deformations occur. While this happens for both the single and double layer structures, it is much more marked for the single layer type. To explain the behaviour of these structures a qualitative model based on the analogous continuum method was proposed. In this way the gross behaviour of the lattice is described by the behaviour of a shell with the same shape and supports. It is shown in chapter 8 that such a model is realistic and does indeed explain satisfactorily the observed behaviour.

A further conclusion is that non linear behaviour may be significant and especially so for those structures where the parameters describing the geometry and properties combine to produce large elastic deformations. The particular case of the hyperbolic paraboloid with the critical geometry $H_x = -H_y$ is one such structure. For such structures the geometry changes significantly as load is applied and it is expected that non linear behaviour would be exhibited.

From these last two conclusions, it is recommended that such combinations of parameters should be avoided if at all possible. The geometrical condition on the rise and sag of a hyperbolic paraboloid is the main criterion to avoid if a designer wishes to have an efficient structure. If it is not possible to avoid this particular geometry, say for architectural reasons, then a double layer structure is recommended as this is generally much stiffer than a single layer structure and would generally be a more serviceable structure.

REFERENCES

1. Ansah, A.M., "Elastic Analysis of Elliptic Paraboloids", Proc. Inst. Civil Engineers, Vol. 37, May 1967, pp 1-17.
2. Avent, R.R., "Nonlinear Field Analysis of Structural Nets", J. Struct. Div., ASCE, Vol. 95, No. ST5, May 1969, pp 889-907.
3. Avent, R.R., Dean, D.L., "Field Analysis for Prefabricated Ribbed Cylindrical Shells", IASS Int. Symp. on Prefabricated Shells, Haifa, Sept. 1973, pp 328-343.
4. Bayley, M.J., "An Experimental and Theoretical Investigation into the Behaviour of a Three Way Aluminium Grid Dome", Space Structures, R.M. Davis (Ed.), 1966, pp 703-717.
5. Bazant, Z.P., Christensen, M., "Analogy between Micropolar Continuum and Grid Frame Works under Initial Stress", Int. J. of Solids and Structures, Vol. 8, 1972, pp 327-346.
6. Bernoulli, D., "Observationes des seriebus recurrentibus", Comment acad. sc. Petrop. 3 (1728), 1732, pp 85-100.
7. Birkoff, G.D., "General Theory of Linear Difference Equations", Trans. Amer. Math. Soc., Vol. 12, April 1911, pp 243-284.
8. Bleich, F.R., Melan, E., "Die gewöhnlichen und partiellen Differenzengleichungen der Baustatic", Springer, Berlin, 1927.
9. Boole, G., "A Treatise on the Calculus of Finite Differences", 2nd Ed., McMillan, London, 1872. (1st Ed. 1860). Reprint by Dover, NY, 1960.
10. Brand, L., "Differential and Difference Equations", J. Wiley, NY, 1966.
11. Carpenter, J.E., et al, "Structural Model Testing-Techniques for Models of Plastic", J. PCA Research and Development Labs, Vol. 6, No. 2, May 1964, pp 26-47.
12. Carr, A.J., "2D Structure", University of Canterbury, Civil Engineering Department Computer Program Library, 1971.
13. Charlton, T.M., "Model Analysis of Structures", Spon, London, 1954.
14. Chitty, L., "On the Cantilever Composed of a Number of Parallel Beams Interconnected by Cross Bars", Phil. Mag., 38(285), 1947, pp 685-699.

15. Crooker, J.O., Buchert, K.P., *"Reticulated Space Structures"*, J. Struct. Div., ASCE, Vol. 96, No. ST3, March 1970, pp 687-700.
16. Davis, R.M., (Ed.), *"Space Structures"*, Proc. Int. Conference on Space Structures, Surrey, Sept. 1966.
17. Dean, D.L., Tauber, S., *"Solutions of One-Dimensional Structural Lattices"*, J. Eng. Mech. Div., ASCE, Vol. 85, No. EM4, Oct. 1959, pp 31-41.
18. Dean, D.L., *"Analysis of Curved Lattices with Generalised Joint Loadings"*, Publications, IABSE, Vol. 20, 1960, pp 43-73.
19. Dean, D.L., Ugarte, C.P., *"Analysis of Structural Nets"*, Publications, IABSE, Vol. 23, 1963, pp 71-89.
20. Dean, D.L., *"Lamella Beams and Grids"*, J. Eng. Mech. Div., ASCE, Vol. 90, No. EM2, April 1964, pp 107-129.
21. Dean, D.L., *"On the Statics of Latticed Shells"*, Publications, IABSE, Vol. 25, 1965, pp 65-81.
22. Dean, D.L., Ugarte, C.P., *"Field Solutions for Two-Dimensional Frameworks"*, Int. J. Mech. Sci., Vol. 10, 1968, pp 315-339.
23. Dean, D.L., Omid'varan, C., *"Analysis of Ribbed Plates"*, J. Struct. Div., ASCE, Vol. 95, No. ST3, March 1969, pp 411-440.
24. Dean, D.L., Ganga Rao, H.V.S., *"Macro Approach to Discrete Field Analysis"*, J. Eng. Mech. Div., ASCE, Vol. 96, No. EM4, Aug. 1970, pp 377-394.
25. Dean, D.L., *"Field Solutions for Shear Grids"*, J. Struct. Div., ASCE, Vol. 97, No. ST12, Dec. 1971, pp 2845-2860.
26. Dean, D.L., Ugarte, C.P., *"Design Formulas for Lattice Cylindrical Shells"*, Symp. on Industrialised Spacial and Shell Structures, Kielce, Poland, June 1973, pp 639-659.
27. Dean, D.L., Avent, R.R., *"State of the Art of Discrete Field Analysis of Space Structures"*, Proc. 2nd Int. Conference on Space Structures, Surrey, Sept. 1975.
28. Ebner, A.M., Ucciferro, J.J., *"A Theoretical and Numerical Comparison of Elastic Nonlinear Finite Element Methods"*, Computers and Structures, Vol. 2, 1972, pp 1043-1061.
29. Ellington, J.P., McCallion, H., *"Moments and Deflections of a Simply Supported Beam Grillage"*, Aero. Quarterly, Vol. VIII, Part 4, Nov. 1957, pp 360-368.

30. Ellington, J.P., McCallion, H., *"The Free Vibrations of Grillages"*, J. App. Mech., ASME, Vol. 26, Series E, No. 4, Dec. 1959, pp 603-607.
31. Euler, L., *"De serierum determinatione seu nova methodus inveniendi terminos generales serierum"*, Novi comment acad. sc. Petrop. 3 (1750/51), 1753, pp 36-85.
32. Fenves, S.J., et al, *"STRESS - A Users Manual"*, MIT Press, 1964.
33. Flower, W.R., Schmitt, L.C., *"Approximate Analysis of a Parallel-Chord Space Truss"*, Civil Eng. Trans. I.E. Aust., April 1971, pp 52-55.
34. Flügge, W., *"Stresses in Shells"*, 2nd Ed., Springer-Verlag, Berlin, 1973.
35. Fort, T., *"Finite Differences"*, Oxford University Press, 1948.
36. Ganga Rao, H.V.S., Smith, J.C., *"Dynamic Field Analysis of Torsionless Grids"*, J. Eng. Mech. Div., ASCE, Vol. 98, No. EM3, June 1973, pp 679-693.
37. Gol'denveizer, A.L., *"Theory of Elastic Thin Shells"*, Pergamon Press, Oxford, 1961.
38. Grigorian, M., *"Vibration of Multi-thread Networks with Quadrilateral Boundaries"*, Proc. 1971 IASS Pacific Symp. Part II on Tension Structures and Space Structures, Tokyo and Kyoto, pp 345-352.
39. Grigorian, M., *"On Diagrids of Vierendeel Frames"*, Proc. 1971 IASS Pacific Symp. Part II on Tension Structures and Space Structures, Tokyo and Kyoto, pp 617-625.
40. Gutkowski, W., *"Plane Polygonal Bars"*, Bull. Acad. Polon. Sci., Sér. sci. techn., Vol. XII, No. 9, 1964, p 437 (623).
41. Gutkowski, W., *"Cylindrical Grid Shells"*, Bull. Acad. Polon. Sci., Sér. sci. techn., Vol. XIII, No. 3, 1965, p 133(191).
42. Hendry, A.W., *"Elements of Experimental Stress Analysis"*, Pergamon Press, Oxford, 1964.
43. Holman, D.F., *"A Finite Series Solution for Grillages under Normal Loading"*, Aero. Quarterly, Vol. VIII, Part 1, Feb. 1957, pp 49-57.
44. Hussey, M.J.L., Tarzi, A.I., Theron, W.F.D., *"Simply Supported Rectangular Double-layered Grids"*, J. Struct. Div., ASCE, Vol. 97, No. ST3, Mar. 1971, pp 753-764.
45. IASS *"International Symposium on Prefabricated Shells"*, Haifa, Sept. 1973.

46. Jenkins, H.G., Park, G.A., *"Efficient Solutions for Linear Matrix Equations"*, J. Struct. Div., ASCE, Vol. 96, No. ST1, Jan. 1970, pp 49-64.
47. Jenkins, R.S., *"Theory and Design of Cylindrical Shell Structures"*, Ove Arup and Partners, London, 1947.
48. Jenkins, W.M., *"Matrix and Digital Computer Methods in Structural Analysis"*, McGraw Hill, London, 1969.
49. Jennings, A., *"Frame Analysis including Change of Geometry"*, J. Struct. Div., ASCE, Vol. 94, No. ST3, Mar. 1968, pp 627-644.
50. Jolley, L.B.W., *"Summation of Series"*, 2nd Ed., Dover Publications, NY, 1961.
51. Jordan, C., *"Calculus of Finite Differences"*, Chelsea, NY, 1950.
52. Kollar, L., *"Analysis of Double Layer Space Trusses by the Equivalent Continuum Method"*, 2nd Int. Conference on Space Structures, Surrey, Sept. 1975, pp 73-76.
53. Laplace, P.S., *"Memoire sur l'usage du calcul aux différences partielles dans la théorie des suites"*, Mém. (Historire) Acad. Sc. Paris, 1777 (1780), pp 99-122.
54. Levey, H., Lessman, F., *"Finite Difference Equations"*, Macmillan, NY, 1961.
55. Logcher, R.D., Sturman, G.M., *"STRUDL - A Computer System for Structural Design"*, J. Struct. Div., ASCE, Vol. 92, No. ST6, Dec. 1966, pp 191-211.
56. Loo Heino, *"The Design and Construction of Three Reticulated Steel Domes"*, Space Structures, R.M. Davis (Ed.), 1966, pp 527-541.
57. Mason, J., *"On the Problem of Edge Disturbances in Lattice Domes"*, Publications, IABSE, Vol. 30, 1970, pp 77-93.
58. Miller, K.S., *"Linear Difference Equations"*, Benjamin, NY, 1968.
59. Milne-Thompson, L.M., *"The Calculus of Finite Differences"*, Macmillan, London, 1933.
60. Mithaiwala, A.P., *"Micro and Macro Analysis of Cylindrical Ribbed and Latticed Shells"*, Thesis, PhD, University of Delaware, 1968, Xerox University Microfilms, 68-15 543.
61. Mondkar, D.P., Powell, G.H., *"Large Capacity Equation Solver for Structural Analysis"*, Computers and Structures, Vol. 4, 1974, pp 699-728.

62. Nörlund, N.E., "Vorlesungen über Differenzenrechnung", Springer, Berlin, 1924. Reprint by Chelsea, NY, 1954.
63. Pagaro, M., Catanzaro, C., Pedicini, G.C., "The Collapse Load of Braced Translation Vaults and Cylindrical Barrel Vaults", Space Structures, R.M. Davis (Ed.), 1966, pp 502-524.
64. Pipes, L.A., "Applied Mathematics for Engineers and Physicists", McGraw Hill, NY, 1946.
65. Poincaré, H., "Sur les équations linéaires aux différentielles ordinaires et aux différences finies", Am. J. Math., 7 (1885) pp 213-217, pp 237-258.
66. Rajasekaran, S., Murray, D.W., "Incremental Finite Element Matrices", J. Struct. Div., ASCE, Vol. 99, No. ST12, Dec. 1973, pp 2423-2438.
67. Renton, J.D., "A Finite Difference Analysis of the Flexural-Torsional Behaviour of Grillages", Int. J. Mech. Sci., Vol. 6, 1964, pp 209-224.
68. Renton, J.D., "On the Analysis of Triangular Mesh Grillages", Int. J. Solids and Structures, Vol. 2, No. 2, April 1966, pp 307-318.
69. Renton, J.D., "The Related Behaviour of Plane Grids, Space Grids and Plates", Space Structures, R.M. Davis (Ed.), 1966, pp 19-32.
70. Renton, J.D., "Behaviour of Howe, Pratt and Warren Trusses", J. Struct. Div., ASCE, Vol. 95, No ST2, Feb. 1969, pp 183-202.
71. Renton, J.D., "General Properties of Space Grids", Int. J. Mech. Sci., Vol. 12, 1970, pp 801-810.
72. Renton, J.D., "Buckling of Long Regular Trusses", Int. J. Solids and Structures, Vol. 9, No. 12, Dec. 1973, pp 1489-1500.
73. Rubinstein, M.F., "Matrix Computer Analysis of Structures", Prentice Hall, New Jersey, 1966.
74. Saaty, T.L., "Modern Nonlinear Equations", McGraw Hill, NY, 1967.
75. Sherman, D.R., et al, "Bibliography on Latticed Structures", J. Struct. Div., ASCE, Vol. 98, No. ST7, July 1972, pp 1545-1566.
76. Sherman, D.R., et al, "Latticed Structures: State-of-the-art Report", J. Struct. Div., ASCE, Vol. 102, No. ST11, Nov. 1976, pp 2197-2230.
77. Smith, J.C., Dean, D.L., "Field Analysis of Torsionless Bridge Grids", J. Struct. Div., ASCE, Vol. 99, No. ST9, Sept. 1973, pp 1837-1849.

78. Spillers, W.R., "Techniques for Analysis of Large Structures", J. Struct. Div., ASCE, Vol. 94, No. ST11, Nov. 1968, pp 2521-2534.
79. Steffensen, J.F., "Interpolation", 1st Ed., 1927, 2nd Ed., Chelsea, NY, 1950.
80. Stirling, J., "Methodus differentialis sive tractatus de summatione et interpolatione serierum infinitarum", London, 1730.
81. Supple, W.J., (Ed.), "2nd International Conference on Space Structures", University of Surrey, Sept. 1975.
82. Suzuki, E., Kitarmaru, H., Yamada, M., "The analysis of the Space Truss Plate by Difference Equations", Space Structures, R.M. Davis (Ed.), 1966, pp 136-144.
83. Tauber, S., Dean, D.L., "On Difference Equations Containing Step and Delta Functions", J. Soc. Indust. Appl. Math., Vol. 8, No. 1, Mar. 1960, pp 174-180.
84. Ugarte, C.P., "Closed Analysis of Lattice Structural Shells", Thesis, PhD, University of Delaware, 1965, Xerox University Microfilms, 66-5575.
85. Von Kármán, T., Biot, M.A., "Mathematical Methods in Engineering", McGraw Hill, NY, 1940.
86. Wah, T., "Natural Frequencies of Uniform Grillages", J. App. Mech., ASME, Vol. 30, Series E, No. 4, Dec. 1963, pp 571-578.
87. Wah, T., "Analysis of Laterally Loaded Gridworks", J. Eng. Mech. Div., ASCE, Vol. 90, No. EM2, April 1964, pp 83-106.
88. Wah, T., "Free Lateral Oscillations of a Supported Grillage", J. Franklin Inst., Vol. 277, No. 4, April 1964, pp 349-360.
89. Wah, T., "The Buckling of Gridworks", J. Mech. and Phys. Solids, Vol. 13, 1965, pp 1-16.
90. Wah, T., "Buckling of Longitudinally Stiffened Plates", Aero. Quarterly, Vol. XVIII, Part 1, Feb. 1967, pp 85-99.
91. Wah, T., Calcote, L.R., "Structural Analysis by Finite Differences", Van Nostrand, NY, 1970.
92. Wright, D.T., "Membrane Forces and Buckling in Reticulated Shells", J. Struct. Div., ASCE, Vol. 91, No. ST1, Feb. 1965, pp 173-201.
93. Wright, D.T., "A Continuum Analysis for Double Layer Space Frame Shells", Publications, IABSE, Vol. 26, 1966, pp 593-610.

94. Yoshitsura Yokoo, et al, (Editors), "*Tension Structures and Space Frames*", Proc. of the IASS Pacific Symp. Part II on Tension Structures and Space Frames, Tokyo and Kyoto, October 1971.

APPENDIX A

ACTION OF FINITE DIFFERENCE OPERATIONS ON TRIGONOMETRIC FUNCTIONS

The trigonometric functions used in chapters 4, 5 and 6 for the displacements are of the form

$$\sum_{i=0}^N \sum_{j=0}^M a_{ij} \left\{ \begin{matrix} \sin \\ \cos \end{matrix} \right\} \left(\frac{i\pi\alpha}{N} \right) \left\{ \begin{matrix} \sin \\ \cos \end{matrix} \right\} \left(\frac{j\pi\beta}{M} \right)$$

where there are the four possible combinations of the sine and cosine functions.

The finite difference operators used are of the form

$$(E_{\alpha}^{+g} \pm E_{\alpha}^{-g}) (E_{\beta}^{+h} \pm E_{\beta}^{-h})$$

where again there are four possible combinations.

In order to show the effect of all these it is only necessary to consider the two functions

$$\sin \frac{\ell\pi x}{L} \quad \text{and} \quad \cos \frac{\ell\pi x}{L}$$

and the two operations E_x^{+k} and E_x^{-k} in the combinations

$$(E_x^{+k} + E_x^{-k}) \text{ and } (E_x^{+k} - E_x^{-k})$$

From the four combinations of these functions and operators, it is possible to obtain the effect of all the operators on all the functions required.

Consider the function $\sin \frac{\ell\pi x}{L}$ and the operator E_x^{+k} . The combination of these gives [54]

$$\begin{aligned} E_x^{+k} \sin \frac{\ell\pi x}{L} &= \sin \frac{\ell\pi (x+k)}{L} \\ &= \sin \frac{\ell\pi x}{L} \cos \frac{\ell\pi k}{L} + \cos \frac{\ell\pi x}{L} \sin \frac{\ell\pi k}{L} \end{aligned}$$

In a similar manner the operator E_x^{-k} acts on $\sin \frac{\ell\pi x}{L}$ to give

$$E_x^{-k} \sin \frac{\ell\pi x}{L} = \sin \frac{\ell\pi x}{L} \cos \frac{\ell\pi k}{L} - \cos \frac{\ell\pi x}{L} \sin \frac{\ell\pi k}{L}$$

Combining these operators to give $(E_x^{+k} + E_x^{-k})$ acting on $\sin \frac{\ell\pi x}{L}$ as

$$\begin{aligned} (E_x^{+k} + E_x^{-k}) \sin \frac{\ell\pi x}{L} &= \sin \frac{\ell\pi x}{L} \cos \frac{\ell\pi k}{L} + \cos \frac{\ell\pi x}{L} \sin \frac{\ell\pi k}{L} \\ &\quad + \sin \frac{\ell\pi x}{L} \cos \frac{\ell\pi k}{L} - \cos \frac{\ell\pi x}{L} \sin \frac{\ell\pi k}{L} \\ &= (+2 \cos \frac{\ell\pi k}{L}) \sin \frac{\ell\pi x}{L} \end{aligned}$$

Similarly the combination $(E_x^{+k} - E_x^{-k})$ acting on $\sin \frac{\ell\pi x}{L}$ gives

$$(E_x^{+k} - E_x^{-k}) \sin \frac{\ell\pi x}{L} = (+2 \sin \frac{\ell\pi k}{L}) \cos \frac{\ell\pi x}{L}$$

In a similar manner the combined operators $(E_x^{+k} + E_x^{-k})$ and $(E_x^{+k} - E_x^{-k})$ acting on $\cos \frac{\ell\pi x}{L}$ give

$$\begin{aligned} (E_x^{+k} + E_x^{-k}) \cos \frac{\ell\pi x}{L} &= (+2 \cos \frac{\ell\pi k}{L}) \cos \frac{\ell\pi x}{L} \\ (E_x^{+k} - E_x^{-k}) \cos \frac{\ell\pi x}{L} &= (-2 \sin \frac{\ell\pi k}{L}) \sin \frac{\ell\pi x}{L} \end{aligned}$$

The results for all functions and operators used in chapters

4, 5 and 6 are summarised in table A.1.

TABLE A.1 Results of Operations on Trigonometric Functions

function operator	$\sin \frac{i\pi\alpha}{N}$ $\sin \frac{j\pi\beta}{M}$	$\cos \frac{i\pi\alpha}{N}$ $\sin \frac{j\pi\beta}{M}$	$\sin \frac{i\pi\alpha}{N}$ $\cos \frac{j\pi\beta}{M}$	$\cos \frac{i\pi\alpha}{N}$ $\cos \frac{j\pi\beta}{M}$
$(E_{\alpha}^{+g} + E_{\alpha}^{-g})(E_{\beta}^{+h} + E_{\beta}^{-h})$	+4 cg ch s α s β	+4 cg ch c α s β	+4 cg ch s α c β	+4 cg ch c α c β
$(E_{\alpha}^{+g} - E_{\alpha}^{-g})(E_{\beta}^{+h} + E_{\beta}^{-h})$	+4 sg ch c α s β	-4 sg ch s α s β	+4 sg ch c α c β	-4 sg ch s α c β
$(E_{\alpha}^{+g} + E_{\alpha}^{-g})(E_{\beta}^{+h} - E_{\beta}^{-h})$	+4 cg sh s α c β	+4 cg sh c α c β	-4 cg sh s α s β	-4 cg sh c α s β
$(E_{\alpha}^{+g} - E_{\alpha}^{-g})(E_{\beta}^{+h} - E_{\beta}^{-h})$	+4 sg sh c α c β	-4 sg sh s α c β	-4 sg sh c α s β	+4 sg sh s α s β

where

$$\begin{aligned} \text{sg} &= \sin \frac{i\pi g}{N} \\ \text{sh} &= \sin \frac{j\pi h}{M} \end{aligned}$$

$$\begin{aligned} \text{cg} &= \cos \frac{i\pi g}{N} \\ \text{ch} &= \cos \frac{j\pi h}{M} \end{aligned}$$

$$\begin{aligned} \text{s}\alpha &= \sin \frac{i\pi\alpha}{N} \\ \text{s}\beta &= \sin \frac{j\pi\beta}{M} \end{aligned}$$

$$\begin{aligned} \text{c}\alpha &= \cos \frac{i\pi\alpha}{N} \\ \text{c}\beta &= \cos \frac{j\pi\beta}{M} \end{aligned}$$

APPENDIX B

EXPANSION OF LOAD FUNCTIONS IN TRIGONOMETRIC SERIES

The load functions used in chapters 4, 5 and 6 must be expanded into finite trigonometric series of the form

$$\sum_{i=0}^N \sum_{j=0}^M a_{ij} \left\{ \begin{array}{c} \sin \\ \cos \end{array} \right\} \left(\frac{i\pi\alpha}{N} \right) \left\{ \begin{array}{c} \sin \\ \cos \end{array} \right\} \left(\frac{j\pi\beta}{M} \right)$$

where the fourier coefficients a_{ij} must be determined from the known loading function.

The determination of the a_{ij} 's depends on the orthogonality and normalization relations which are

$$\begin{aligned} \sum_{\ell=0}^L \sin \frac{\ell\pi i}{L} \sin \frac{\ell\pi j}{L} &= \frac{L}{2} & \text{if } i = j \neq 0 \text{ or } L \\ &= 0 & \text{if } i \neq j \text{ or } i = j = 0 \text{ or } L \end{aligned}$$

and

$$\begin{aligned} \sum_{\ell=0}^L r_{\ell} \cos \frac{\ell\pi i}{L} \cos \frac{\ell\pi j}{L} &= L & \text{if } i = j = 0 \text{ or } L \\ &= \frac{L}{2} & \text{if } i = j \neq 0 \text{ or } L \\ &= 0 & \text{if } i \neq j \end{aligned}$$

where r_{ℓ} , the weight function, is defined as

$$\begin{aligned} r_{\ell} &= \frac{1}{2} \text{ at end points } (\ell = 0 \text{ or } L \text{ here}) \\ &= 1 \text{ otherwise} \end{aligned}$$

B.1 GENERAL FUNCTIONS

As an example, consider the series expansion

$$f(\alpha, \beta) = \sum_{i=0}^N \sum_{j=0}^M a_{ij} \sin \frac{i\pi\alpha}{N} \cos \frac{j\pi\beta}{M}$$

Multiplying both sides by $r_{\beta} \sin \frac{k\pi\alpha}{N} \cos \frac{\ell\pi\beta}{M}$ and summing from $\alpha=0$ to N and from $\beta=0$ to M gives

$$\sum_{\alpha=0}^N \sum_{\beta=0}^M \left[f(\alpha, \beta) r_{\beta} \sin \frac{k\pi\alpha}{N} \cos \frac{l\pi\beta}{M} \right]$$

$$= \sum_{\alpha=0}^N \sum_{\beta=0}^M \sum_{i=0}^N \sum_{j=0}^M \left[a_{ij} r_{\beta} \sin \frac{i\pi\alpha}{N} \cos \frac{j\pi\beta}{M} \sin \frac{k\pi\alpha}{N} \cos \frac{l\pi\beta}{M} \right]$$

On the right hand side the order of summations can be changed to give

$$\text{RHS} = \sum_{i=0}^N \sum_{\alpha=0}^N \left[\sin \frac{i\pi\alpha}{N} \sin \frac{k\pi\alpha}{N} \left\{ \sum_{j=0}^M a_{ij} \left(\sum_{\beta=0}^M r_{\beta} \cos \frac{j\pi\beta}{M} \cos \frac{l\pi\beta}{M} \right) \right\} \right]$$

The innermost term can be evaluated from the orthogonality relations. The right hand side then becomes

$$\begin{aligned} \text{RHS} &= \sum_{i=0}^N \sum_{\alpha=0}^N \left[\sin \frac{i\pi\alpha}{N} \sin \frac{k\pi\alpha}{N} \{a_{i\ell} M\} \right] && \text{if } \ell = 0 \text{ or } M \\ &= \sum_{i=0}^N \sum_{\alpha=0}^N \left[\sin \frac{i\pi\alpha}{N} \sin \frac{k\pi\alpha}{N} \{a_{i\ell} \frac{M}{2}\} \right] && \text{if } \ell \neq 0 \text{ or } M \end{aligned}$$

These can be rearranged to become

$$\begin{aligned} \text{RHS} &= M \sum_{i=0}^N [a_{i\ell} \{ \sum_{\alpha=0}^N \sin \frac{i\pi\alpha}{N} \sin \frac{k\pi\alpha}{N} \}] && \text{if } \ell = 0 \text{ or } M \\ &= \frac{M}{2} \sum_{i=0}^N [a_{i\ell} \{ \sum_{\alpha=0}^N \sin \frac{i\pi\alpha}{N} \sin \frac{k\pi\alpha}{N} \}] && \text{if } \ell \neq 0 \text{ or } M \end{aligned}$$

and again using the orthogonality relations gives

$$\begin{aligned} \text{RHS} &= M \{a_{k\ell} \frac{N}{2}\} && \text{if } \ell = 0 \text{ or } M \\ &= \frac{M}{2} \{a_{k\ell} \frac{N}{2}\} && \text{if } \ell \neq 0 \text{ or } M \end{aligned}$$

Combining this with the left hand side gives for the fourier coefficients

$$\begin{aligned} a_{k\ell} &= \frac{2}{NM} \sum_{\alpha=0}^N \sum_{\beta=0}^M \left[f(\alpha, \beta) r_{\beta} \sin \frac{k\pi\alpha}{N} \cos \frac{l\pi\beta}{M} \right] && \text{if } \ell = 0 \text{ or } M \\ &= \frac{4}{NM} \sum_{\alpha=0}^N \sum_{\beta=0}^M \left[f(\alpha, \beta) r_{\beta} \sin \frac{k\pi\alpha}{N} \cos \frac{l\pi\beta}{M} \right] && \text{if } \ell \neq 0 \text{ or } M \end{aligned}$$

These coefficients could also be determined using the procedure

$$\begin{aligned}\bar{f}(\alpha, \beta) &= f(\alpha, \beta) & \beta \neq 0 \text{ or } M \\ &= \frac{f(\alpha, \beta)}{2} & \beta = 0 \text{ or } M\end{aligned}$$

$$\bar{a}_{k\ell} = \frac{4}{NM} \sum_{\alpha=0}^N \sum_{\beta=0}^M \left[\bar{f}(\alpha, \beta) \sin \frac{k\pi\alpha}{N} \cos \frac{\ell\pi\beta}{M} \right]$$

$$\begin{aligned}a_{k\ell} &= \bar{a}_{k\ell} & \ell \neq 0 \text{ or } M \\ &= \frac{\bar{a}_{k\ell}}{2} & \ell = 0 \text{ or } M\end{aligned}$$

This procedure takes account of the weight function for the orthogonality and normalization of the cosine series.

The expressions for the fourier coefficients of expansion in the other combinations of trigonometric functions are obtained in a similar manner. They are given in table B1.

B.2 SPECIAL FUNCTIONS

The special load cases considered are the unit point load and the unit uniformly distributed load.

B.2.1 Unit Point Load

This is defined as

$$\begin{aligned}f(\alpha, \beta) &= 1 & \text{at } \alpha = \zeta, \beta = \eta \\ &= 0 & \text{elsewhere}\end{aligned}$$

When this is substituted into the summation formulae of table B1 only one term is non zero and thus this case is particularly simple. Results for the expressions for the series coefficients of all combinations of trigonometric functions needed are given in table B2.

B.2.2. Unit Uniformly Distributed Load

This is defined as

$$f(\alpha, \beta) = 1 \quad \text{for all } \alpha = 0, 1, \dots, N$$

$$\text{and all } \beta = 0, 1, \dots, M$$

This is substituted into the formulae in table B1 and use is made of the summations

$$\sum_{\ell=0}^L \sin \frac{\ell \pi k}{L} = \cot \frac{k \pi}{2L} \quad k \neq 0 \text{ or } L \text{ and } k \text{ odd}$$

$$= 0 \quad k = 0 \text{ or } L \text{ or } k \text{ even}$$

$$\sum_{\ell=0}^L r_{\ell} \cos \frac{\ell \pi k}{L} = L \quad k = 0$$

$$= 0 \quad k \neq 0$$

The resulting expressions for the series coefficients are given in table B3 for all combinations of the trigonometric functions.

TABLE B.1 General Load Function Coefficients

$f(\alpha, \beta)$	a_{ij}
$\sum_{i=0}^N \sum_{j=0}^M [a_{ij} \sin \frac{i\pi\alpha}{N} \sin \frac{j\pi\beta}{M}]$	$\frac{4}{NM} \sum_{\alpha=0}^N \sum_{\beta=0}^M [f(\alpha, \beta) \sin \frac{i\pi\alpha}{N} \sin \frac{j\pi\beta}{M}]$ $i=0, 1, \dots, N$ $j=0, 1, \dots, M$
$\sum_{i=0}^N \sum_{j=0}^M [a_{ij} \cos \frac{i\pi\alpha}{N} \sin \frac{j\pi\beta}{M}]$	$\frac{4}{NM} \sum_{\alpha=0}^N \sum_{\beta=0}^M [f(\alpha, \beta) r_{\alpha} \cos \frac{i\pi\alpha}{N} \sin \frac{j\pi\beta}{M}]$ $i=1, 2, \dots, (N-1)$ $j=0, 1, \dots, M$ $\frac{2}{NM} \sum_{\alpha=0}^N \sum_{\beta=0}^M [f(\alpha, \beta) r_{\alpha} \cos \frac{i\pi\alpha}{N} \sin \frac{j\pi\beta}{M}]$ $i=0 \text{ or } N$ $j=0, 1, \dots, M$
$\sum_{i=0}^N \sum_{j=0}^M [a_{ij} \sin \frac{i\pi\alpha}{N} \cos \frac{j\pi\beta}{M}]$	$\frac{4}{NM} \sum_{\alpha=0}^N \sum_{\beta=0}^M [f(\alpha, \beta) r_{\beta} \sin \frac{i\pi\alpha}{N} \cos \frac{j\pi\beta}{M}]$ $i=0, 1, \dots, N$ $j=1, 2, \dots, (M-1)$ $\frac{2}{NM} \sum_{\alpha=0}^N \sum_{\beta=0}^M [f(\alpha, \beta) r_{\beta} \sin \frac{i\pi\alpha}{N} \cos \frac{j\pi\beta}{M}]$ $i=0, 1, \dots, N$ $j=0 \text{ or } M$
$\sum_{i=0}^N \sum_{j=0}^M [a_{ij} \cos \frac{i\pi\alpha}{N} \cos \frac{j\pi\beta}{M}]$	$\frac{4}{NM} \sum_{\alpha=0}^N \sum_{\beta=0}^M [f(\alpha, \beta) r_{\alpha} r_{\beta} \cos \frac{i\pi\alpha}{N} \cos \frac{j\pi\beta}{M}]$ $i=1, 2, \dots, (N-1)$ $j=1, 2, \dots, (M-1)$ $\frac{2}{NM} \sum_{\alpha=0}^N \sum_{\beta=0}^M [f(\alpha, \beta) r_{\alpha} r_{\beta} \cos \frac{i\pi\alpha}{N} \cos \frac{j\pi\beta}{M}]$ $i=0 \text{ or } N$ $j=1, 2, \dots, (M-1)$ or $i=1, 2, \dots, (N-1)$ $j=0 \text{ or } M$ $\frac{1}{NM} \sum_{\alpha=0}^N \sum_{\beta=0}^M [f(\alpha, \beta) r_{\alpha} r_{\beta} \cos \frac{i\pi\alpha}{N} \cos \frac{j\pi\beta}{M}]$ $i=0 \text{ or } N$ $j=0 \text{ or } M$

TABLE B.2 Unit Point Load Function Coefficients

$f(\alpha, \beta)$	a_{ij}
$\sum_{i=0}^N \sum_{j=0}^M [a_{ij} \sin \frac{i\pi\alpha}{N} \sin \frac{j\pi\beta}{M}]$	$\frac{4}{NM} \sin \frac{i\pi\zeta}{N} \sin \frac{j\pi\eta}{M}$ $i=0, 1, \dots, N$ $j=0, 1, \dots, M$
$\sum_{i=0}^N \sum_{j=0}^M [a_{ij} \cos \frac{i\pi\alpha}{N} \sin \frac{j\pi\beta}{M}]$	$\frac{4}{NM} r_{\zeta} \cos \frac{i\pi\zeta}{N} \sin \frac{j\pi\eta}{M}$ $i=1, 2, \dots, (N-1)$ $j=0, 1, \dots, M$ $\frac{2}{NM} r_{\zeta} \cos \frac{i\pi\zeta}{N} \sin \frac{j\pi\eta}{M}$ $i=0 \text{ or } N$ $j=0, 1, \dots, M$
$\sum_{i=0}^N \sum_{j=0}^M [a_{ij} \sin \frac{i\pi\alpha}{N} \cos \frac{j\pi\beta}{M}]$	$\frac{4}{NM} r_{\eta} \sin \frac{i\pi\zeta}{N} \cos \frac{j\pi\eta}{M}$ $i=0, 1, \dots, N$ $j=1, 2, \dots, (M-1)$ $\frac{2}{NM} r_{\eta} \sin \frac{i\pi\zeta}{N} \cos \frac{j\pi\eta}{M}$ $i=0, 1, \dots, N$ $j=0 \text{ or } M$
$\sum_{i=0}^N \sum_{j=0}^M [a_{ij} \cos \frac{i\pi\alpha}{N} \cos \frac{j\pi\beta}{M}]$	$\frac{4}{NM} r_{\zeta} r_{\eta} \cos \frac{i\pi\zeta}{N} \cos \frac{j\pi\eta}{M}$ $i=1, 2, \dots, (N-1)$ $j=1, 2, \dots, (M-1)$ $\frac{2}{NM} r_{\zeta} r_{\eta} \cos \frac{i\pi\zeta}{N} \cos \frac{j\pi\eta}{M}$ $i=0 \text{ or } N$ $j=1, 2, \dots, (M-1)$ $\text{or } i=1, 2, \dots, (N-1)$ $j=0 \text{ or } M$ $\frac{1}{NM} r_{\zeta} r_{\eta} \cos \frac{i\pi\zeta}{N} \cos \frac{j\pi\eta}{M}$ $i=0 \text{ or } N$ $j=0 \text{ or } M$

TABLE B.3 Unit Uniform Load Function Coefficients

B-7

$f(\alpha, \beta)$	a_{ij}
$\sum_{i=0}^N \sum_{j=0}^M [a_{ij} \sin \frac{i\pi\alpha}{N} \sin \frac{j\pi\beta}{M}]$	$\frac{4}{NM} \cot \frac{i\pi}{2N} \cot \frac{j\pi}{2M}$ $i \neq 0 \text{ or } N \text{ and } i \text{ odd}$ $j \neq 0 \text{ or } M \text{ and } j \text{ odd}$ 0 otherwise
$\sum_{i=0}^N \sum_{j=0}^M [a_{ij} \cos \frac{i\pi\alpha}{N} \sin \frac{j\pi\beta}{M}]$	$\frac{2}{M} \cot \frac{j\pi}{2M}$ $i = 0$ $j \neq 0 \text{ or } M \text{ and } j \text{ odd}$ 0 otherwise
$\sum_{i=0}^N \sum_{j=0}^M [a_{ij} \sin \frac{i\pi\alpha}{N} \cos \frac{j\pi\beta}{M}]$	$\frac{2}{N} \cot \frac{i\pi}{2N}$ $i \neq 0 \text{ or } N \text{ and } i \text{ odd}$ $j = 0$ 0 otherwise
$\sum_{i=0}^N \sum_{j=0}^M [a_{ij} \cos \frac{i\pi\alpha}{N} \cos \frac{j\pi\beta}{M}]$	1 $i = j = 0$ 0 otherwise

APPENDIX C

MATRICES K_{ij} FOR MEMBERS

The matrices K_{ij} for the members are defined by (see expression 4-11)

$$[K_{ij}] = [T_i][k_{ij}][T_j^T]$$

for $i = 1, 2$ and $j = 1, 2$

where the element stiffness matrices $[k_{ij}]$ are defined in expression 4-2 for a rod member and in expression 5-1 for a beam member. The transformation matrices $[T_1]$ and $[T_2]$ are defined in expressions 4-4 and 5-2 for rod and beam members respectively. The relevant matrix products that are needed are

- (a) $[k_{11}][T_1^T]$ and $[k_{12}][T_2^T]$ to give member actions
- (b) $[K_{11}]$ and $[K_{12}]$ to give stiffness relations.

C.1 ROD MEMBER

$$\text{Here } [k_{11}] = -[k_{12}] = \begin{bmatrix} S & \cdot & \cdot \\ \cdot & \cdot & \cdot \\ \cdot & \cdot & \cdot \end{bmatrix}$$

where $S = EA/L$

$$\text{and } [T_i] = \begin{bmatrix} +\cos\psi_i \cos\phi_i & +\sin\psi_i & -\cos\psi_i \sin\phi_i \\ -\sin\psi_i \cos\phi_i & +\cos\psi_i & +\sin\psi_i \sin\phi_i \\ +\sin\phi_i & 0 & +\cos\phi_i \end{bmatrix}$$

hence the required products are

$$[k_{11}][T_1^T] = \begin{bmatrix} +S\cos\psi_1 \cos\phi_1 & -S\sin\psi_1 \cos\phi_1 & +S\sin\phi_1 \\ \cdot & \cdot & \cdot \\ \cdot & \cdot & \cdot \end{bmatrix}$$

$$[k_{12}][T_2^T] = \begin{bmatrix} -S\cos\psi_2 \cos\phi_2 & +S\sin\psi_2 \cos\phi_2 & -S\sin\phi_2 \\ \cdot & \cdot & \cdot \\ \cdot & \cdot & \cdot \end{bmatrix}$$

$[K_{11}] = [T_1][k_{11}][T_1^T]$ is given by

$$\text{column 1} = \begin{Bmatrix} +S\cos^2\psi_1\cos^2\phi_1 \\ -S\cos\psi_1\sin\psi_1\cos^2\phi_1 \\ +S\cos\psi_1\cos\phi_1\sin\phi_1 \end{Bmatrix}$$

$$\text{column 2} = \begin{Bmatrix} -S\cos\psi_1\sin\psi_1\cos^2\phi_1 \\ +S\sin^2\psi_1\cos^2\phi_1 \\ -S\sin\psi_1\cos\phi_1\sin\phi_1 \end{Bmatrix}$$

$$\text{column 3} = \begin{Bmatrix} +S\cos\psi_1\cos\phi_1\sin\phi_1 \\ -S\sin\psi_1\cos\phi_1\sin\phi_1 \\ +S\sin^2\phi_1 \end{Bmatrix}$$

$[K_{12}] = [T_1][k_{12}][T_2^T]$ is given by

$$\text{column 1} = \begin{Bmatrix} -S\cos\psi_1\cos\psi_2\cos\phi_1\cos\phi_2 \\ +S\sin\psi_1\cos\psi_2\cos\phi_1\cos\phi_2 \\ -S\cos\psi_2\sin\phi_1\cos\phi_2 \end{Bmatrix}$$

$$\text{column 2} = \begin{Bmatrix} +S\cos\psi_1\sin\psi_2\cos\phi_1\cos\phi_2 \\ -S\sin\psi_1\sin\psi_2\cos\phi_1\cos\phi_2 \\ +S\sin\psi_1\sin\phi_1\cos\phi_2 \end{Bmatrix}$$

$$\text{column 3} = \begin{Bmatrix} -S\cos\psi_1\cos\phi_1\sin\phi_2 \\ +S\sin\psi_1\cos\phi_1\sin\phi_2 \\ -S\sin\phi_1\sin\phi_2 \end{Bmatrix}$$

C.2 BEAM MEMBER

For this type of member

$$[k_{11}] = \begin{bmatrix} \frac{EA}{L} & \cdot & \cdot & \cdot & \cdot & \cdot \\ \cdot & \frac{12EI}{L^3}z & \cdot & \cdot & \cdot & \frac{6EI}{L^2}z \\ \cdot & \cdot & \frac{12EI}{L^3}y & \cdot & \frac{-6EI}{L^2}y & \cdot \\ \cdot & \cdot & \cdot & \frac{GI}{L}x & \cdot & \cdot \\ \cdot & \cdot & \frac{-6EI}{L^2}y & \cdot & \frac{4EI}{L}y & \cdot \\ \cdot & \frac{6EI}{L^2}z & \cdot & \cdot & \cdot & \frac{4EI}{L}z \end{bmatrix}$$

$$[k_{12}] = \begin{bmatrix} \frac{-EA}{L} & . & . & . & . & . \\ . & \frac{-12EI}{L^3} z & . & . & . & \frac{6EI}{L^2} z \\ . & . & \frac{-12EI}{L^3} y & . & \frac{-6EI}{L^2} y & . \\ . & . & . & \frac{-GI}{L} x & . & . \\ . & . & \frac{6EI}{L^2} y & . & \frac{2EI}{L} y & . \\ . & \frac{-6EI}{L^2} z & . & . & . & \frac{2EI}{L} z \end{bmatrix}$$

and

$$[T_i] = \left[\begin{array}{ccc|c} +\cos\psi_i \cos\phi_i & +\sin\psi_i & -\cos\psi_i \sin\phi_i & 0 \\ -\sin\psi_i \cos\phi_i & +\cos\psi_i & +\sin\psi_i \sin\phi_i & 0 \\ +\sin\phi_i & 0 & +\cos\phi_i & 0 \\ \hline & & & \text{as in} \\ & & & \text{quadrant} \\ & & & \text{one} \end{array} \right]$$

The required products are

$$[k_{11}][T_1^T]$$

$$\text{column 1} = \left\{ \begin{array}{l} +\frac{EA}{L} \cos\psi_1 \cos\phi_1 \\ +\frac{12EI}{L^3} z \sin\psi_1 \\ -\frac{12EI}{L^3} y \cos\psi_1 \sin\phi_1 \\ 0 \\ +\frac{6EI}{L^2} y \cos\psi_1 \sin\phi_1 \\ +\frac{6EI}{L^2} z \sin\psi_1 \end{array} \right\}$$

$$\text{Column 2} = \left\{ \begin{array}{c} -\frac{EA}{L} \sin\psi_1 \cos\phi_1 \\ +\frac{12EI}{L^3} z \cos\psi_1 \\ +\frac{12EI}{L^3} y \sin\psi_1 \sin\phi_1 \\ 0 \\ -\frac{6EI}{L^2} y \sin\psi_1 \sin\phi_1 \\ +\frac{6EI}{L^2} z \cos\psi_1 \end{array} \right\}$$

$$\text{Column 3} = \left\{ \begin{array}{c} +\frac{EA}{L} \sin\phi_1 \\ 0 \\ +\frac{12EI}{L^3} y \cos\phi_1 \\ 0 \\ -\frac{6EI}{L^2} y \cos\phi_1 \\ 0 \end{array} \right\}$$

$$\text{Column 4} = \left\{ \begin{array}{c} 0 \\ -\frac{6EI}{L^2} z \cos\psi_1 \sin\phi_1 \\ -\frac{6EI}{L^2} y \sin\psi_1 \\ +\frac{GI}{L} x \cos\psi_1 \cos\phi_1 \\ +\frac{4EI}{L} y \sin\psi_1 \\ -\frac{4EI}{L} z \cos\psi_1 \sin\phi_1 \end{array} \right\}$$

$$\text{Column 5} = \left\{ \begin{array}{c} 0 \\ +\frac{6EI}{L^2} z \sin\psi_1 \sin\phi_1 \\ -\frac{6EI}{L^2} y \cos\psi_1 \\ -\frac{GI}{L} x \sin\psi_1 \cos\phi_1 \\ +\frac{4EI}{L} y \cos\psi_1 \\ +\frac{4EI}{L} z \sin\psi_1 \sin\phi_1 \end{array} \right\}$$

$$\text{Column 6} = \left\{ \begin{array}{c} 0 \\ +6EI \frac{z}{L^2} \cos\phi_1 \\ 0 \\ +GI \frac{x}{L} \sin\phi_1 \\ 0 \\ +4EI \frac{z}{L} \cos\phi_1 \end{array} \right\}$$

$$[k_{12}] [T_2^T]$$

$$\text{Column 1} = \left\{ \begin{array}{c} -\frac{EA}{L} \cos\psi_2 \cos\phi_2 \\ -\frac{12EI}{L^3} z \sin\psi_2 \\ +\frac{12EI}{L^3} y \cos\psi_2 \sin\phi_2 \\ 0 \\ -\frac{6EI}{L^2} y \cos\psi_2 \sin\phi_2 \\ -\frac{6EI}{L^2} z \sin\psi_2 \end{array} \right\}$$

$$\text{Column 2} = \left\{ \begin{array}{c} +\frac{EA}{L} \sin\psi_2 \cos\phi_2 \\ -\frac{12EI}{L^3} z \cos\psi_2 \\ +\frac{12EI}{L^3} y \sin\psi_2 \sin\phi_2 \\ 0 \\ +\frac{6EI}{L^2} y \sin\psi_2 \sin\phi_2 \\ -\frac{6EI}{L^2} z \cos\psi_2 \end{array} \right\}$$

$$\text{Column 3} = \left\{ \begin{array}{c} -\frac{EA}{L} \sin\phi_2 \\ 0 \\ -\frac{12EI}{L^3} y \cos\phi_2 \\ 0 \\ +\frac{6EI}{L^2} y \cos\phi_2 \\ 0 \end{array} \right\}$$

$$\text{Column 4} = \left\{ \begin{array}{c} 0 \\ -\frac{6EI}{L^2} z \cos\psi_2 \sin\phi_2 \\ -\frac{6EI}{L^2} y \sin\psi_2 \\ -\frac{GI}{L} x \cos\psi_2 \cos\phi_2 \\ +\frac{2EI}{L} y \sin\psi_2 \\ -\frac{2EI}{L} z \cos\psi_2 \sin\phi_2 \end{array} \right\}$$

$$\text{Column 5} = \left\{ \begin{array}{c} 0 \\ +\frac{6EI}{L^2} z \sin\psi_2 \sin\phi_2 \\ -\frac{6EI}{L^2} y \cos\psi_2 \\ +\frac{GI}{L} x \sin\psi_2 \cos\phi_2 \\ +\frac{2EI}{L} y \cos\psi_2 \\ +\frac{2EI}{L} z \sin\psi_2 \sin\phi_2 \end{array} \right\}$$

$$\text{Column 6} = \left\{ \begin{array}{c} 0 \\ +\frac{6EI}{L^2} z \cos\phi_2 \\ 0 \\ -\frac{GI}{L} x \sin\phi_2 \\ 0 \\ +\frac{2EI}{L} z \cos\phi_2 \end{array} \right\}$$

$$[k_{11}] = [T_1][k_{11}][T_1^T]$$

Column 1

$$\left\{ \begin{array}{l} \frac{+EA}{L} \cos^2 \psi_1 \cos^2 \phi_1 \\ \frac{-EA}{L} \cos \psi_1 \sin \psi_1 \cos^2 \phi_1 \\ \frac{+EA}{L} \cos \psi_1 \cos \phi_1 \sin \phi_1 \\ \\ \frac{+6EI}{L^2} Y \cos \psi_1 \sin \psi_1 \sin \phi_1 \\ \frac{+6EI}{L^2} Y \cos^2 \psi_1 \sin \phi_1 \end{array} \right\}$$

$$\left\{ \begin{array}{l} \frac{+12EI}{L^3} Y \cos^2 \psi_1 \sin^2 \phi_1 \\ \frac{-12EI}{L^3} Y \cos \psi_1 \sin \psi_1 \sin^2 \phi_1 \\ \frac{-12EI}{L^3} Y \cos \psi_1 \cos \phi_1 \sin \phi_1 \\ \\ \frac{+6EI}{L^2} Y \cos \psi_1 \sin \psi_1 \sin \phi_1 \\ \frac{+6EI}{L^2} Y \cos^2 \psi_1 \sin \phi_1 \end{array} \right\}$$

$$\left\{ \begin{array}{l} \frac{+12EI}{L^3} Z \sin^2 \psi_1 \\ \frac{+12EI}{L^3} Z \cos \psi_1 \sin \psi_1 \\ \\ \frac{-6EI}{L^2} Z \cos \psi_1 \sin \psi_1 \sin \phi_1 \\ \frac{+6EI}{L^2} Z \sin^2 \psi_1 \sin \phi_1 \\ \frac{+6EI}{L^2} Z \sin \psi_1 \cos \phi_1 \end{array} \right\}$$

Column 2

$$\left\{ \begin{array}{l} \frac{-EA}{L} \cos \psi_1 \sin \psi_1 \cos^2 \phi_1 \\ \frac{+EA}{L} \sin^2 \psi_1 \cos^2 \phi_1 \\ \frac{-EA}{L} \sin \psi_1 \cos \phi_1 \sin \phi_1 \\ \\ \\ \end{array} \right\}$$

$$\left\{ \begin{array}{l} \frac{-12EI}{L^3} Y \cos \psi_1 \sin \psi_1 \sin^2 \phi_1 \\ \frac{+12EI}{L^3} Y \sin^2 \psi_1 \sin^2 \phi_1 \\ \frac{+12EI}{L^3} Y \sin \psi_1 \cos \phi_1 \sin \phi_1 \\ \\ \frac{-6EI}{L^2} Y \sin^2 \psi_1 \sin \phi_1 \\ \frac{-6EI}{L^2} Y \cos \psi_1 \sin \psi_1 \sin \phi_1 \end{array} \right\}$$

$$\left\{ \begin{array}{l} \frac{+12EI}{L^3} Z \cos \psi_1 \sin \psi_1 \\ \frac{+12EI}{L^3} Z \cos^2 \psi_1 \\ \\ \frac{-6EI}{L^2} Z \cos^2 \psi_1 \sin \phi_1 \\ \frac{+6EI}{L^2} Z \cos \psi_1 \sin \psi_1 \sin \phi_1 \\ \frac{+6EI}{L^2} Z \cos \psi_1 \cos \phi_1 \end{array} \right\}$$

Column 3

$$\left\{ \begin{array}{l} \frac{+EA}{L} \cos \psi_1 \cos \phi_1 \sin \phi_1 \\ \frac{-EA}{L} \sin \psi_1 \cos \phi_1 \sin \phi_1 \\ \frac{+EA}{L} \sin^2 \phi_1 \\ \\ \\ \end{array} \right\}$$

$$\left\{ \begin{array}{l} \frac{-12EI}{L^3} Y \cos \psi_1 \cos \phi_1 \sin \phi_1 \\ \frac{+12EI}{L^3} Y \sin \psi_1 \cos \phi_1 \sin \phi_1 \\ \frac{+12EI}{L^3} Y \cos^2 \phi_1 \\ \\ \frac{-6EI}{L^2} Y \sin \psi_1 \cos \phi_1 \\ \frac{-6EI}{L^2} Y \cos \psi_1 \cos \phi_1 \end{array} \right\}$$

Column 4

$$\left\{ \begin{array}{ll}
 \frac{+6EI}{L^2} Y \cos \psi_1 \sin \psi_1 \sin \phi_1 & \frac{-6EI}{L^2} Z \cos \psi_1 \sin \psi_1 \sin \phi_1 \\
 \frac{-6EI}{L^2} Y \sin^2 \psi_1 \sin \phi_1 & \frac{-6EI}{L^2} Z \cos^2 \psi_1 \sin \phi_1 \\
 \frac{-6EI}{L^2} Y \sin \psi_1 \cos \phi_1 & \\
 \frac{+GI}{L} X \cos^2 \psi_1 \cos^2 \phi_1 & \frac{+4EI}{L} Y \sin^2 \psi_1 \\
 \frac{-GI}{L} X \cos \psi_1 \sin \psi_1 \cos^2 \phi_1 & \frac{+4EI}{L} Y \cos \psi_1 \sin \psi_1 \\
 \frac{+GI}{L} X \cos \psi_1 \cos \phi_1 \sin \phi_1 & \frac{+4EI}{L} Z \cos^2 \psi_1 \sin^2 \phi_1 \\
 & \frac{-4EI}{L} Z \cos \psi_1 \sin \psi_1 \sin^2 \phi_1 \\
 & \frac{-4EI}{L} Z \cos \psi_1 \cos \phi_1 \sin \phi_1
 \end{array} \right\}$$

Column 5

$$\left\{ \begin{array}{ll}
 \frac{+6EI}{L^2} Y \cos^2 \psi_1 \sin \phi_1 & \frac{+6EI}{L^2} Z \sin^2 \psi_1 \sin \phi_1 \\
 \frac{-6EI}{L^2} Y \cos \psi_1 \sin \psi_1 \sin \phi_1 & \frac{+6EI}{L^2} Z \cos \psi_1 \sin \psi_1 \sin \phi_1 \\
 \frac{-6EI}{L^2} Y \cos \psi_1 \cos \phi_1 & \\
 \frac{-GI}{L} X \cos \psi_1 \sin \psi_1 \cos^2 \phi_1 & \frac{+4EI}{L} Y \cos \psi_1 \sin \psi_1 \\
 \frac{+GI}{L} X \sin^2 \psi_1 \cos^2 \phi_1 & \frac{+4EI}{L} Y \cos^2 \psi_1 \\
 \frac{-GI}{L} X \sin \psi_1 \cos \phi_1 \sin \phi_1 & \frac{+4EI}{L} Z \cos^2 \psi_1 \sin^2 \phi_1 \\
 & \frac{+4EI}{L} Z \sin^2 \psi_1 \sin^2 \phi_1 \\
 & \frac{+4EI}{L} Z \sin \psi_1 \cos \phi_1 \sin \phi_1
 \end{array} \right\}$$

Column 6

$$\left\{ \begin{array}{ll}
 & \frac{+6EI}{L^2} Z \sin \psi_1 \cos \phi_1 \\
 & \frac{+6EI}{L^2} Z \cos \psi_1 \cos \phi_1 \\
 0 & \\
 \frac{+GI}{L} X \cos \psi_1 \cos \phi_1 \sin \phi_1 & \frac{-4EI}{L} Z \cos \psi_1 \cos \phi_1 \sin \phi_1 \\
 \frac{-GI}{L} X \sin \psi_1 \cos \phi_1 \sin \phi_1 & \frac{+4EI}{L} Z \sin \psi_1 \cos \phi_1 \sin \phi_1 \\
 \frac{+GI}{L} X \sin^2 \phi_1 & \frac{+4EI}{L} Z \cos^2 \phi_1
 \end{array} \right\}$$

$$[K_{12}] = [T_1][k_{12}][T_2^T]$$

Column 1

$$\left\{ \begin{array}{l} -\frac{EA}{L} \cos \psi_1 \cos \psi_2 \cos \phi_1 \cos \phi_2 \\ +\frac{EA}{L} \sin \psi_1 \cos \psi_2 \cos \phi_1 \cos \phi_2 \\ -\frac{EA}{L} \cos \psi_2 \sin \phi_1 \cos \phi_2 \\ \\ -\frac{6EI}{L^2} \sin \psi_1 \cos \psi_2 \sin \phi_2 \\ -\frac{6EI}{L^2} \cos \psi_1 \cos \psi_2 \sin \phi_2 \\ \\ \\ -\frac{6EI}{L^2} \sin \psi_1 \cos \psi_2 \sin \phi_2 \\ -\frac{6EI}{L^2} \cos \psi_1 \cos \psi_2 \sin \phi_2 \\ \\ \\ \end{array} \right\} \left\{ \begin{array}{l} -\frac{12EI}{L^3} y \cos \psi_1 \cos \psi_2 \sin \phi_1 \sin \phi_2 \\ +\frac{12EI}{L^3} y \sin \psi_1 \cos \psi_2 \sin \phi_1 \sin \phi_2 \\ +\frac{12EI}{L^3} y \cos \psi_2 \cos \phi_1 \sin \phi_2 \\ \\ -\frac{6EI}{L^2} y \sin \psi_1 \cos \psi_2 \sin \phi_2 \\ -\frac{6EI}{L^2} y \cos \psi_1 \cos \psi_2 \sin \phi_2 \\ \\ \\ -\frac{6EI}{L^2} y \sin \psi_1 \cos \psi_2 \sin \phi_2 \\ -\frac{6EI}{L^2} y \cos \psi_1 \cos \psi_2 \sin \phi_2 \\ \\ \\ \end{array} \right\} \left\{ \begin{array}{l} -\frac{12EI}{L^3} z \sin \psi_1 \sin \psi_2 \\ -\frac{12EI}{L^3} z \cos \psi_1 \sin \psi_2 \\ \\ +\frac{6EI}{L^2} z \cos \psi_1 \sin \psi_2 \sin \phi_1 \\ -\frac{6EI}{L^2} z \sin \psi_1 \sin \psi_2 \sin \phi_1 \\ \\ -\frac{6EI}{L^2} z \sin \psi_2 \cos \phi_1 \\ \\ \\ \end{array} \right\}$$

Column 2

$$\left\{ \begin{array}{l} +\frac{EA}{L} \cos \psi_1 \sin \psi_2 \cos \phi_1 \cos \phi_2 \\ -\frac{EA}{L} \sin \psi_1 \sin \psi_2 \cos \phi_1 \cos \phi_2 \\ +\frac{EA}{L} \sin \psi_2 \cos \phi_1 \cos \phi_2 \\ \\ +\frac{6EI}{L^2} \sin \psi_1 \sin \psi_2 \sin \phi_2 \\ +\frac{6EI}{L^2} \cos \psi_1 \sin \psi_2 \sin \phi_2 \\ \\ \\ +\frac{6EI}{L^2} \sin \psi_1 \sin \psi_2 \sin \phi_2 \\ +\frac{6EI}{L^2} \cos \psi_1 \sin \psi_2 \sin \phi_2 \\ \\ \\ \end{array} \right\} \left\{ \begin{array}{l} -\frac{12EI}{L^3} y \cos \psi_1 \sin \psi_2 \sin \phi_1 \sin \phi_2 \\ +\frac{12EI}{L^3} y \sin \psi_1 \sin \psi_2 \sin \phi_1 \sin \phi_2 \\ +\frac{12EI}{L^3} y \sin \psi_2 \cos \phi_1 \sin \phi_2 \\ \\ +\frac{6EI}{L^2} y \sin \psi_1 \sin \psi_2 \sin \phi_2 \\ +\frac{6EI}{L^2} y \cos \psi_1 \sin \psi_2 \sin \phi_2 \\ \\ \\ +\frac{6EI}{L^2} y \sin \psi_1 \sin \psi_2 \sin \phi_2 \\ +\frac{6EI}{L^2} y \cos \psi_1 \sin \psi_2 \sin \phi_2 \\ \\ \\ \end{array} \right\} \left\{ \begin{array}{l} -\frac{12EI}{L^3} z \sin \psi_1 \cos \psi_2 \\ -\frac{12EI}{L^3} z \cos \psi_1 \cos \psi_2 \\ \\ +\frac{6EI}{L^2} z \cos \psi_1 \cos \psi_2 \sin \phi_1 \\ -\frac{6EI}{L^2} z \sin \psi_1 \cos \psi_2 \sin \phi_1 \\ \\ -\frac{6EI}{L^2} z \cos \psi_2 \cos \phi_1 \\ \\ \\ \end{array} \right\}$$

Column 3

$$\left\{ \begin{array}{l} -\frac{EA}{L} \cos \psi_1 \cos \phi_1 \sin \phi_2 \\ +\frac{EA}{L} \sin \psi_1 \cos \phi_1 \sin \phi_2 \\ -\frac{EA}{L} \sin \phi_1 \sin \phi_2 \\ \\ \\ \\ \end{array} \right\} \left\{ \begin{array}{l} +\frac{12EI}{L^3} y \cos \psi_1 \sin \phi_1 \cos \phi_2 \\ -\frac{12EI}{L^3} y \sin \psi_1 \sin \phi_1 \cos \phi_2 \\ -\frac{12EI}{L^3} y \cos \phi_1 \cos \phi_2 \\ \\ +\frac{6EI}{L^2} y \sin \psi_1 \cos \phi_2 \\ +\frac{6EI}{L^2} y \cos \psi_1 \cos \phi_2 \\ \\ \\ \end{array} \right\} \left\{ \begin{array}{l} \\ \\ \\ \\ \\ \\ \end{array} \right\}$$

Column 4

$$\left\{ \begin{array}{ll}
 \frac{+6EI}{L^2} Y \cos \psi_1 \sin \psi_2 \sin \phi_1 & \frac{-6EI}{L^2} Z \sin \psi_1 \cos \psi_2 \sin \phi_2 \\
 \frac{-6EI}{L^2} Y \sin \psi_1 \sin \psi_2 \sin \phi_1 & \frac{-6EI}{L^2} Z \cos \psi_1 \cos \psi_2 \sin \phi_2 \\
 \frac{-6EI}{L^2} Y \sin \psi_2 \cos \phi_1 & \\
 \frac{-GI}{L} X \cos \psi_1 \cos \psi_2 \cos \phi_1 \cos \phi_2 & \frac{+2EI}{L} Y \sin \psi_1 \sin \psi_2 \\
 \frac{+GI}{L} X \sin \psi_1 \cos \psi_2 \cos \phi_1 \cos \phi_2 & \frac{+2EI}{L} Y \cos \psi_1 \sin \psi_2 \\
 \frac{-GI}{L} X \cos \psi_2 \sin \phi_1 \cos \phi_2 & \frac{+2EI}{L} Z \cos \psi_1 \cos \psi_2 \sin \phi_1 \sin \phi_2 \\
 & \frac{-2EI}{L} Z \sin \psi_1 \cos \psi_2 \sin \phi_1 \sin \phi_2 \\
 & \frac{-2EI}{L} Z \cos \psi_2 \cos \phi_1 \sin \phi_2
 \end{array} \right\}$$

Column 5

$$\left\{ \begin{array}{ll}
 \frac{+6EI}{L^2} Y \cos \psi_1 \cos \psi_2 \sin \phi_1 & \frac{+6EI}{L^2} Z \sin \psi_1 \sin \psi_2 \sin \phi_2 \\
 \frac{-6EI}{L^2} Y \sin \psi_1 \cos \psi_2 \sin \phi_1 & \frac{+6EI}{L^2} Z \cos \psi_1 \sin \psi_2 \sin \phi_2 \\
 \frac{-6EI}{L^2} Y \cos \psi_2 \cos \phi_1 & \\
 \frac{+GI}{L} X \cos \psi_1 \sin \psi_2 \cos \phi_1 \cos \phi_2 & \frac{+2EI}{L} Y \sin \psi_1 \cos \psi_2 \\
 \frac{-GI}{L} X \sin \psi_1 \sin \psi_2 \cos \phi_1 \cos \phi_2 & \frac{+2EI}{L} Y \cos \psi_1 \cos \psi_2 \\
 \frac{+GI}{L} X \sin \psi_2 \sin \phi_1 \cos \phi_2 & \frac{-2EI}{L} Z \cos \psi_1 \sin \psi_2 \sin \phi_1 \sin \phi_2 \\
 & \frac{+2EI}{L} Z \sin \psi_1 \sin \psi_2 \sin \phi_1 \sin \phi_2 \\
 & \frac{+2EI}{L} Z \sin \psi_2 \cos \phi_1 \sin \phi_2
 \end{array} \right\}$$

Column 6

$$\left\{ \begin{array}{ll}
 & \frac{+6EI}{L^2} Z \sin \psi_1 \cos \phi_2 \\
 & \frac{+6EI}{L^2} Z \cos \psi_1 \cos \phi_2 \\
 0 & \\
 \frac{-GI}{L} X \cos \psi_1 \cos \phi_1 \sin \phi_2 & \frac{-2EI}{L} Z \cos \psi_1 \sin \phi_1 \cos \phi_2 \\
 \frac{+GI}{L} X \sin \psi_1 \cos \phi_1 \sin \phi_2 & \frac{+2EI}{L} Z \sin \psi_1 \sin \phi_1 \cos \phi_2 \\
 \frac{-GI}{L} X \sin \phi_1 \sin \phi_2 & \frac{+2EI}{L} Z \cos \phi_1 \cos \phi_2
 \end{array} \right\}$$

APPENDIX D

GOVERNING PARTIAL DIFFERENCE EQUATIONSD.1 SINGLE LAYER PIN JOINTED LATTICE

For the layout and member properties given in figure 4.2 and table 4.1, the resulting equations are

$$\begin{Bmatrix} w_{\alpha} \\ w_{\beta} \\ w_{\gamma} \end{Bmatrix} = \begin{bmatrix} v_{11} & v_{12} & v_{13} \\ v_{21} & v_{22} & v_{23} \\ v_{31} & v_{32} & v_{33} \end{bmatrix} \begin{Bmatrix} \delta_{\alpha} \\ \delta_{\beta} \\ \delta_{\gamma} \end{Bmatrix}$$

where the elements are

$$\begin{aligned} v_{11} &= S_1 \cos^2 \sigma_1 \{ 2 - (E_{\alpha}^{+2} + E_{\alpha}^{-2}) \} + S_2 \cos^2 \theta \cos^2 \sigma_2 \{ 4 - (E_{\alpha}^{+1} + E_{\alpha}^{-1}) (E_{\beta}^{+1} + E_{\beta}^{-1}) \} \\ v_{12} &= v_{21} = S_2 \cos \theta \sin \theta \cos^2 \sigma_2 \{ - (E_{\alpha}^{+1} - E_{\alpha}^{-1}) (E_{\beta}^{+1} - E_{\beta}^{-1}) \} \\ v_{13} &= -v_{31} = S_1 \cos \sigma_1 \sin \sigma_1 \{ - (E_{\alpha}^{+2} - E_{\alpha}^{-2}) \} + S_2 \cos \theta \cos \sigma_2 \sin \sigma_2 \{ - (E_{\alpha}^{+1} - E_{\alpha}^{-1}) (E_{\beta}^{+1} + E_{\beta}^{-1}) \} \\ v_{22} &= S_2 \sin^2 \theta \cos^2 \sigma_2 \{ 4 - (E_{\alpha}^{+1} + E_{\alpha}^{-1}) (E_{\beta}^{+1} + E_{\beta}^{-1}) \} \\ v_{23} &= -v_{32} = S_2 \sin \theta \cos \sigma_2 \sin \sigma_2 \{ - (E_{\alpha}^{+1} + E_{\alpha}^{-1}) (E_{\beta}^{+1} - E_{\beta}^{-1}) \} \\ v_{33} &= S_1 \sin^2 \sigma_1 \{ 2 + (E_{\alpha}^{+2} + E_{\alpha}^{-2}) \} + S_2 \sin^2 \sigma_2 \{ 4 + (E_{\alpha}^{+1} + E_{\alpha}^{-1}) (E_{\beta}^{+1} + E_{\beta}^{-1}) \} \end{aligned}$$

where $S = (EA/L)$ with the subscript denoting the property type 1 or 2.

The other symbols are as defined in chapter 4.

D.2 SINGLE LAYER RIGID JOINTED LATTICE

The governing equation for this structure is defined by equation 5.3 and can be expressed as a 6 x 6 matrix equation which may be written

$$\begin{Bmatrix} w_{\alpha} \\ w_{\beta} \\ w_{\gamma} \\ m_{\alpha} \\ m_{\beta} \\ m_{\gamma} \end{Bmatrix} = \begin{bmatrix} v_{11} & v_{12} & v_{13} & \cdot & \cdot & v_{16} \\ v_{21} & v_{22} & & & & \\ v_{31} & & \cdot & & & \\ \cdot & & & \text{etc} & & \\ \cdot & & & & \cdot & \\ v_{61} & & & & & v_{66} \end{bmatrix} \begin{Bmatrix} \delta_{\alpha} \\ \delta_{\beta} \\ \delta_{\gamma} \\ \theta_{\alpha} \\ \theta_{\beta} \\ \theta_{\gamma} \end{Bmatrix}$$

where

$$\begin{aligned}
v_{11} = & \left(\frac{EA}{L}\right)_1 \cos^2 \sigma_1 \{2 - (E_\alpha^{+2} + E_\alpha^{-2})\} + \left(\frac{12EI}{L^3} Y\right)_1 \sin^2 \sigma_1 \{2 + (E_\alpha^{+2} + E_\alpha^{-2})\} \\
& + \left(\frac{EA}{L}\right)_2 \cos^2 \theta \cos^2 \sigma_2 \{4 - (E_\alpha^{+1} + E_\alpha^{-1})(E_\beta^{+1} + E_\beta^{-1})\} \\
& + \left(\frac{12EI}{L^3} Y\right)_2 \cos^2 \theta \sin^2 \sigma_2 \{4 + (E_\alpha^{+1} + E_\alpha^{-1})(E_\beta^{+1} + E_\beta^{-1})\} \\
& + \left(\frac{12EI}{L^3} Z\right)_2 \sin^2 \theta \{4 - (E_\alpha^{+1} + E_\alpha^{-1})(E_\beta^{+1} + E_\beta^{-1})\} \\
v_{12} = v_{21} = & \left(\frac{EA}{L}\right)_2 \cos \theta \sin \theta \cos^2 \sigma_2 \{-(E_\alpha^{+1} - E_\alpha^{-1})(E_\beta^{+1} - E_\beta^{-1})\} \\
& + \left(\frac{12EI}{L^3} Y\right)_2 \cos \theta \sin \theta \sin^2 \sigma_2 \{+(E_\alpha^{+1} - E_\alpha^{-1})(E_\beta^{+1} - E_\beta^{-1})\} \\
& + \left(\frac{12EI}{L^3} Z\right)_2 \cos \theta \sin \theta \{+(E_\alpha^{+1} - E_\alpha^{-1})(E_\beta^{+1} - E_\beta^{-1})\} \\
v_{13} = -v_{31} = & \left(\frac{EA}{L}\right)_1 \cos \sigma_1 \sin \sigma_1 \{-(E_\alpha^{+2} - E_\alpha^{-2})\} + \left(\frac{12EI}{L^3} Y\right)_1 \cos \sigma_1 \sin \sigma_1 \{-(E_\alpha^{+2} - E_\alpha^{-2})\} \\
& + \left(\frac{EA}{L}\right)_2 \cos \theta \cos \sigma_2 \sin \sigma_2 \{-(E_\alpha^{+1} - E_\alpha^{-1})(E_\beta^{+1} + E_\beta^{-1})\} \\
& + \left(\frac{12EI}{L^3} Y\right)_2 \cos \theta \cos \sigma_2 \sin \sigma_2 \{-(E_\alpha^{+1} - E_\alpha^{-1})(E_\beta^{+1} + E_\beta^{-1})\} \\
v_{14} = v_{41} = & \left(\frac{6EI}{L^2} Y\right)_2 \cos \theta \sin \theta \sin \sigma_2 \{+(E_\alpha^{+1} - E_\alpha^{-1})(E_\beta^{+1} - E_\beta^{-1})\} \\
& + \left(\frac{6EI}{L^2} Z\right)_2 \cos \theta \sin \theta \sin \sigma_2 \{+(E_\alpha^{+1} - E_\alpha^{-1})(E_\beta^{+1} - E_\beta^{-1})\} \\
v_{15} = v_{51} = & \left(\frac{6EI}{L^2} Y\right)_1 \sin \sigma_1 \{-2 - (E_\alpha^{+2} + E_\alpha^{-2})\} \\
& + \left(\frac{6EI}{L^2} Y\right)_2 \cos^2 \theta \sin \sigma_2 \{-4 - (E_\alpha^{+1} + E_\alpha^{-1})(E_\beta^{+1} + E_\beta^{-1})\} \\
& + \left(\frac{6EI}{L^2} Z\right)_2 \sin^2 \theta \sin \sigma_2 \{-4 + (E_\alpha^{+1} + E_\alpha^{-1})(E_\beta^{+1} + E_\beta^{-1})\} \\
v_{16} = -v_{61} = & \left(\frac{6EI}{L^2} Z\right)_2 \sin \theta \cos \sigma_2 \{-(E_\alpha^{+1} + E_\alpha^{-1})(E_\beta^{+1} - E_\beta^{-1})\} \\
v_{22} = & \left(\frac{12EI}{L^3} Z\right)_1 \{2 - (E_\alpha^{+2} + E_\alpha^{-2})\} \\
& + \left(\frac{EA}{L}\right)_2 \sin^2 \theta \cos^2 \sigma_2 \{4 - (E_\alpha^{+1} + E_\alpha^{-1})(E_\beta^{+1} + E_\beta^{-1})\} \\
& + \left(\frac{12EI}{L^3} Y\right)_2 \sin^2 \theta \sin^2 \sigma_2 \{4 + (E_\alpha^{+1} + E_\alpha^{-1})(E_\beta^{+1} + E_\beta^{-1})\} \\
& + \left(\frac{12EI}{L^3} Z\right)_2 \cos^2 \theta \{4 - (E_\alpha^{+1} + E_\alpha^{-1})(E_\beta^{+1} + E_\beta^{-1})\}
\end{aligned}$$

$$v_{23} = -v_{32} = \left(\frac{EA}{L}\right)_2 \sin\theta \cos\sigma_2 \sin\sigma_2 \{-(E_\alpha^{+1} - E_\alpha^{-1})(E_\beta^{+1} + E_\beta^{-1})\} \\ + \left(\frac{12EI}{L^3}Y\right)_2 \cos\theta \cos\sigma_2 \sin\sigma_2 \{-(E_\alpha^{+1} - E_\alpha^{-1})(E_\beta^{+1} + E_\beta^{-1})\}$$

$$v_{24} = v_{42} = \left(\frac{6EI}{L^2}Z\right)_1 \sin\sigma_1 \{2 - (E_\alpha^{+2} + E_\alpha^{-2})\} \\ + \left(\frac{6EI}{L^2}Y\right)_2 \sin^2\theta \sin\sigma_2 \{4 + (E_\alpha^{+1} + E_\alpha^{-1})(E_\beta^{+1} + E_\beta^{-1})\} \\ + \left(\frac{6EI}{L^2}Z\right)_2 \cos^2\theta \sin\sigma_2 \{4 - (E_\alpha^{+1} + E_\alpha^{-1})(E_\beta^{+1} + E_\beta^{-1})\}$$

$$v_{25} = v_{52} = \left(\frac{6EI}{L^2}Y\right)_2 \cos\theta \sin\theta \sin\sigma_2 \{-(E_\alpha^{+1} - E_\alpha^{-1})(E_\beta^{+1} - E_\beta^{-1})\} \\ + \left(\frac{6EI}{L^2}Z\right)_2 \cos\theta \sin\theta \sin\sigma_2 \{-(E_\alpha^{+1} - E_\alpha^{-1})(E_\beta^{+1} - E_\beta^{-1})\}$$

$$v_{26} = -v_{62} = \left(\frac{6EI}{L^2}Z\right)_1 \cos\sigma_1 \{+(E_\alpha^{+2} - E_\alpha^{-2})\} \\ + \left(\frac{6EI}{L^2}Z\right)_2 \cos\theta \cos\sigma_2 \{+(E_\alpha^{+1} - E_\alpha^{-1})(E_\beta^{+1} + E_\beta^{-1})\}$$

$$v_{33} = \left(\frac{EA}{L}\right)_1 \sin^2\sigma_1 \{2 + (E_\alpha^{+2} + E_\alpha^{-2})\} + \left(\frac{12EI}{L^3}Y\right)_1 \cos^2\sigma_1 \{2 - (E_\alpha^{+2} + E_\alpha^{-2})\} \\ + \left(\frac{EA}{L}\right)_2 \sin^2\sigma_2 \{4 + (E_\alpha^{+1} + E_\alpha^{-1})(E_\beta^{+1} + E_\beta^{-1})\} \\ + \left(\frac{12EI}{L^3}Y\right)_2 \cos^2\sigma_2 \{4 - (E_\alpha^{+1} + E_\alpha^{-1})(E_\beta^{+1} + E_\beta^{-1})\}$$

$$v_{34} = -v_{43} = \left(\frac{6EI}{L^2}Y\right)_2 \sin\theta \cos\sigma_2 \{+(E_\alpha^{+1} + E_\alpha^{-1})(E_\beta^{+1} - E_\beta^{-1})\}$$

$$v_{35} = -v_{53} = \left(\frac{6EI}{L^2}Y\right)_1 \cos\sigma_1 \sin\sigma_1 \{-(E_\alpha^{+2} - E_\alpha^{-2})\} \\ + \left(\frac{6EI}{L^2}Y\right)_2 \cos\theta \cos\sigma_2 \{-(E_\alpha^{+1} - E_\alpha^{-1})(E_\beta^{+1} + E_\beta^{-1})\}$$

$$v_{36} = v_{63} = 0$$

$$v_{44} = \left(\frac{GI}{L}X\right)_1 \cos^2\sigma_1 \{2 - (E_\alpha^{+2} + E_\alpha^{-2})\} + \left(\frac{2EI}{L}Z\right)_1 \sin^2\sigma_1 \{4 - (E_\alpha^{+2} + E_\alpha^{-2})\} \\ + \left(\frac{GI}{L}X\right)_2 \cos^2\theta \cos^2\sigma_2 \{4 - (E_\alpha^{+1} + E_\alpha^{-1})(E_\beta^{+1} + E_\beta^{-1})\} \\ + \left(\frac{2EI}{L}Y\right)_2 \sin^2\theta \{8 + (E_\alpha^{+1} + E_\alpha^{-1})(E_\beta^{+1} + E_\beta^{-1})\} \\ + \left(\frac{2EI}{L}Z\right)_2 \cos^2\theta \sin^2\sigma_2 \{8 - (E_\alpha^{+1} + E_\alpha^{-1})(E_\beta^{+1} + E_\beta^{-1})\}$$

$$\begin{aligned}
v_{45} = v_{54} = & \left(\frac{GI}{L}\right)_2 \cos\theta \sin\theta \cos^2\sigma_2 \{-(E_\alpha^{+1}-E_\alpha^{-1})(E_\beta^{+1}-E_\beta^{-1})\} \\
& + \left(\frac{2EI}{L}\right)_2 \cos\theta \sin\theta \{-(E_\alpha^{+1}-E_\alpha^{-1})(E_\beta^{+1}-E_\beta^{-1})\} \\
& + \left(\frac{2EI}{L}\right)_2 \cos\theta \sin\theta \sin^2\sigma_2 \{-(E_\alpha^{+1}-E_\alpha^{-1})(E_\beta^{+1}-E_\beta^{-1})\} \\
v_{46} = v_{64} = & \left(\frac{GI}{L}\right)_1 \cos\sigma_1 \sin\sigma_1 \{-(E_\alpha^{+2}-E_\alpha^{-2})\} \\
& + \left(\frac{2EI}{L}\right)_1 \cos\sigma_1 \sin\sigma_1 \{+(E_\alpha^{+2}-E_\alpha^{-2})\} \\
& + \left(\frac{GI}{L}\right)_2 \cos\theta \cos\sigma_2 \sin\sigma_2 \{-(E_\alpha^{+1}-E_\alpha^{-1})(E_\beta^{+1}+E_\beta^{-1})\} \\
& + \left(\frac{2EI}{L}\right)_2 \cos\theta \cos\sigma_2 \sin\sigma_2 \{+(E_\alpha^{+1}-E_\alpha^{-1})(E_\beta^{+1}+E_\beta^{-1})\} \\
v_{55} = & \left(\frac{2EI}{L}\right)_1 \{4+(E_\alpha^{+2}+E_\alpha^{-2})\} \\
& + \left(\frac{GI}{L}\right)_2 \sin^2\theta \cos^2\sigma_2 \{4-(E_\alpha^{+1}+E_\alpha^{-1})(E_\beta^{+1}+E_\beta^{-1})\} \\
& + \left(\frac{2EI}{L}\right)_2 \cos^2\theta \{8+(E_\alpha^{+1}+E_\alpha^{-1})(E_\beta^{+1}+E_\beta^{-1})\} \\
& + \left(\frac{2EI}{L}\right)_2 \sin^2\theta \sin^2\sigma_2 \{8+(E_\alpha^{+1}+E_\alpha^{-1})(E_\beta^{+1}+E_\beta^{-1})\} \\
v_{56} = -v_{65} = & \left(\frac{GI}{L}\right)_2 \sin\theta \cos\sigma_2 \sin\sigma_2 \{-(E_\alpha^{+1}+E_\alpha^{-1})(E_\beta^{+1}-E_\beta^{-1})\} \\
& + \left(\frac{2EI}{L}\right)_2 \sin\theta \cos\sigma_2 \sin\sigma_2 \{+(E_\alpha^{+1}+E_\alpha^{-1})(E_\beta^{+1}-E_\beta^{-1})\} \\
v_{66} = & \left(\frac{GI}{L}\right)_1 \sin^2\sigma_1 \{2+(E_\alpha^{+2}+E_\alpha^{-2})\} + \left(\frac{2EI}{L}\right)_1 \cos^2\sigma_1 \{4+(E_\alpha^{+2}+E_\alpha^{-2})\} \\
& + \left(\frac{GI}{L}\right)_2 \sin^2\sigma_2 \{4+(E_\alpha^{+1}+E_\alpha^{-1})(E_\beta^{+1}+E_\beta^{-1})\} \\
& + \left(\frac{2EI}{L}\right)_2 \cos^2\sigma_2 \{8+(E_\alpha^{+1}+E_\alpha^{-1})(E_\beta^{+1}+E_\beta^{-1})\}
\end{aligned}$$

where the symbols are as defined in chapter 5.

D.3 DOUBLE LAYER PIN JOINTED LATTICE

The governing partial difference equation for this structure can be written in the form

$$\begin{Bmatrix} w_\alpha \\ w_\beta \\ w_\gamma \\ -w_\alpha \\ -w_\beta \\ -w_\gamma \end{Bmatrix} = \begin{bmatrix} v_{11} & v_{12} & v_{13} & \cdot & \cdot & v_{16} \\ v_{21} & v_{22} & & & & \\ v_{31} & & \cdot & & & \\ \cdot & & & \text{etc} & & \\ \cdot & & & & \cdot & \\ v_{61} & & & & & v_{66} \end{bmatrix} \begin{Bmatrix} \delta_\alpha \\ \delta_\beta \\ \delta_\gamma \\ \bar{\delta}_\alpha \\ \bar{\delta}_\beta \\ \bar{\delta}_\gamma \end{Bmatrix}$$

where

$$v_{11} = S_\alpha \cos^2 \sigma_\alpha \{2 - (E_\alpha^{+2} + E_\alpha^{-2})\} + S_d \cos^2 \theta \cos^2 \phi \{4\}$$

$$v_{12} = v_{21} = 0$$

$$v_{13} = -v_{31} = S_\alpha \cos \sigma_\alpha \sin \sigma_\alpha \{-(E_\alpha^{+2} - E_\alpha^{-2})\}$$

$$v_{14} = v_{41} = S_d \cos^2 \theta \cos^2 \phi \{-(E_\alpha^{+1} + E_\alpha^{-1})(E_\beta^{+1} + E_\beta^{-1})\}$$

$$v_{15} = v_{51} = S_d \cos \theta \sin \theta \cos^2 \phi \{-(E_\alpha^{+1} - E_\alpha^{-1})(E_\beta^{+1} - E_\beta^{-1})\}$$

$$v_{16} = -v_{61} = S_d \sin \theta \cos \phi \sin \phi \{+(E_\alpha^{+1} + E_\alpha^{-1})(E_\beta^{+1} - E_\beta^{-1})\}$$

$$v_{22} = S_\beta \cos^2 \sigma_\beta \{2 - (E_\beta^{+2} + E_\beta^{-2})\} + S_d \sin^2 \theta \cos^2 \phi \{4\}$$

$$v_{23} = -v_{32} = S_\beta \cos \sigma_\beta \sin \sigma_\beta \{-(E_\beta^{+2} - E_\beta^{-2})\}$$

$$v_{24} = v_{42} = S_d \cos \theta \sin \theta \cos^2 \phi \{-(E_\alpha^{+1} - E_\alpha^{-1})(E_\beta^{+1} - E_\beta^{-1})\}$$

$$v_{25} = v_{52} = S_d \sin^2 \theta \cos^2 \phi \{-(E_\alpha^{+1} + E_\alpha^{-1})(E_\beta^{+1} + E_\beta^{-1})\}$$

$$v_{26} = -v_{62} = S_d \sin \theta \sin \phi \cos \phi \{+(E_\alpha^{+1} + E_\alpha^{-1})(E_\beta^{+1} - E_\beta^{-1})\}$$

$$v_{33} = S_\alpha \sin^2 \sigma_\alpha \{2 + (E_\alpha^{+2} + E_\alpha^{-2})\} + S_\beta \sin^2 \sigma_\beta \{2 + (E_\beta^{+2} + E_\beta^{-2})\} + S_d \sin^2 \phi \{4\}$$

$$v_{34} = -v_{43} = S_d \cos \theta \sin \phi \cos \phi \{+(E_\alpha^{+1} - E_\alpha^{-1})(E_\beta^{+1} + E_\beta^{-1})\}$$

$$v_{35} = -v_{53} = S_d \sin \theta \sin \phi \cos \phi \{+(E_\alpha^{+1} + E_\alpha^{-1})(E_\beta^{+1} - E_\beta^{-1})\}$$

$$v_{36} = v_{63} = S_d \sin^2 \phi \{-(E_\alpha^{+1} + E_\alpha^{-1})(E_\beta^{+1} + E_\beta^{-1})\}$$

$$v_{44} = \bar{S}_\alpha \cos^2 \sigma_\alpha \{2 - (E_\alpha^{+2} + E_\alpha^{-2})\} + S_d \cos^2 \theta \cos^2 \phi \{4\}$$

$$v_{45} = v_{54} = 0$$

$$v_{46} = -v_{64} = \bar{S}_\alpha \cos \sigma_\alpha \sin \sigma_\alpha \{-(E_\alpha^{+2} - E_\alpha^{-2})\}$$

$$v_{55} = \bar{S}_\beta \cos^2 \sigma_\beta \{2 - (E_\beta^{+2} + E_\beta^{-2})\} + S_d \sin^2 \theta \cos^2 \phi \{4\}$$

$$v_{56} = -v_{65} = \bar{S}_\beta \cos \sigma_\beta \sin \sigma_\beta \{-(E_\beta^{+2} - E_\beta^{-2})\}$$

$$v_{66} = \bar{S}_{\alpha} \sin^2 \sigma_{\alpha} \{2 + (E_{\alpha}^{+2} + E_{\alpha}^{-2})\} + \bar{S}_{\beta} \sin^2 \sigma_{\beta} \{2 + (E_{\beta}^{+2} + E_{\beta}^{-2})\} + S_d \sin^2 \phi \{4\}$$

where the symbols are defined in chapter 6.

APPENDIX E

FORCE BOUNDARY CONDITIONS

The boundary conditions on the structure can be classified as either direct conditions on the displacements or as conditions on the boundary forces. Because the solution process is carried out directly for the displacements and only involves the forces indirectly through the member force/displacement relations, it is necessary to express the force boundary conditions in terms of the displacements. This procedure was explained in section 4.3 and the detailed results are quoted here for the structure types treated in chapters 4, 5 and 6.

E.1 SINGLE LAYER PIN JOINTED LATTICE

The force boundary conditions for this structure are

- (a) Zero edge force in α direction at edges $\alpha = 0$ and $\alpha = N$
- (b) Zero edge force in β direction at edges $\beta = 0$ and $\beta = M$.

Following the procedure outlined in section 4.3 produces

$$\begin{aligned}
 (a) \quad & [S_1 \cos^2 \sigma_1 (E_{\alpha}^{+2} - E_{\alpha}^{-2}) + S_2 \cos^2 \theta \cos^2 \sigma_2 (E_{\alpha}^{+1} - E_{\alpha}^{-1}) (E_{\beta}^{+1} + E_{\beta}^{-1})] \delta_{\alpha}(\alpha, \beta) \\
 & + [S_2 \cos \theta \sin \theta \cos^2 \sigma_2 (E_{\alpha}^{+1} + E_{\alpha}^{-1}) (E_{\beta}^{+1} - E_{\beta}^{-1})] \delta_{\beta}(\alpha, \beta) \\
 & + [S_1 \cos \sigma_1 \sin \sigma_1 \{2 + (E_{\alpha}^{+2} + E_{\alpha}^{-2})\} \\
 & \quad + S_2 \cos \theta \cos \sigma_2 \sin \sigma_2 \{4 + (E_{\alpha}^{+1} + E_{\alpha}^{-1}) (E_{\beta}^{+1} + E_{\beta}^{-1})\}] \delta_{\gamma}(\alpha, \beta) = 0
 \end{aligned}$$

at $\alpha = 0$ and $\alpha = N$

and

$$\begin{aligned}
 (b) \quad & [S_2 \cos \theta \sin \theta \cos^2 \sigma_2 (E_{\alpha}^{+1} - E_{\alpha}^{-1}) (E_{\beta}^{+1} + E_{\beta}^{-1})] \delta_{\alpha}(\alpha, \beta) \\
 & + [S_2 \sin^2 \theta \cos^2 \sigma_2 (E_{\alpha}^{+1} + E_{\alpha}^{-1}) (E_{\beta}^{+1} - E_{\beta}^{-1})] \delta_{\beta}(\alpha, \beta) \\
 & + [S_2 \sin \theta \cos \sigma_2 \sin \sigma_2 \{4 + (E_{\alpha}^{+1} + E_{\alpha}^{-1}) (E_{\beta}^{+1} + E_{\beta}^{-1})\}] \delta_{\gamma}(\alpha, \beta) = 0
 \end{aligned}$$

at $\beta = 0$ and $\beta = M$

E.2 SINGLE LAYER RIGID JOINTED LATTICE

The conditions on the boundary of this structure involve forces and moments. The requirements are

- (a) Zero edge force in α direction at edges $\alpha = 0$ and $\alpha = N$
- (b) Zero edge force in β direction at edges $\beta = 0$ and $\beta = M$
- (c) Zero edge moment about β axis at edges $\alpha = 0$ and $\alpha = N$
- (d) Zero edge moment about α axis at edges $\beta = 0$ and $\beta = M$
- (e) Zero edge moment about γ axis at edges $\alpha = 0$ and $\alpha = N$
- (f) Zero edge moment about γ axis at edges $\beta = 0$ and $\beta = M$

These are expressed in terms of the displacements to give the conditions

$$\begin{aligned}
 (a) \quad & \left[\left\{ \left(\frac{EA}{L} \right)_1 \cos^2 \sigma_1 - \left(\frac{12EI}{L^3} \right)_1 \sin^2 \sigma_1 \right\} (E_\alpha^{+2} - E_\alpha^{-2}) \right. \\
 & + \left\{ \left(\frac{EA}{L} \right)_2 \cos^2 \theta \cos^2 \sigma_2 - \left(\frac{12EI}{L^3} \right)_2 \cos^2 \theta \sin^2 \sigma_2 + \left(\frac{12EI}{L^3} \right)_2 \sin^2 \theta \right\} \\
 & \quad \left. (E_\alpha^{+1} - E_\alpha^{-1}) (E_\beta^{+1} + E_\beta^{-1}) \right] \delta_\alpha \\
 & + \left[\left\{ \left(\frac{EA}{L} \right)_2 \cos \theta \sin \theta \cos^2 \sigma_2 - \left(\frac{12EI}{L^3} \right)_2 \cos \theta \sin \theta \sin^2 \sigma_2 - \left(\frac{12EI}{L^3} \right)_2 \cos \theta \sin \theta \right\} \right. \\
 & \quad \left. (E_\alpha^{+1} + E_\alpha^{-1}) (E_\beta^{+1} - E_\beta^{-1}) \right] \delta_\beta \\
 & + \left[\left\{ \left(\frac{EA}{L} \right)_1 \cos \sigma_1 \sin \sigma_1 - \left(\frac{12EI}{L^3} \right)_1 \cos \sigma_1 \sin \sigma_1 \right\} \{2\} \right. \\
 & \quad + \left\{ \left(\frac{EA}{L} \right)_1 \cos \sigma_1 \sin \sigma_1 + \left(\frac{12EI}{L^3} \right)_1 \cos \sigma_1 \sin \sigma_1 \right\} (E_\alpha^{+2} + E_\alpha^{-2}) \\
 & \quad + \left\{ \left(\frac{EA}{L} \right)_2 \cos \theta \cos \sigma_2 \sin \sigma_2 - \left(\frac{12EI}{L^3} \right)_2 \cos \theta \cos \sigma_2 \sin \sigma_2 \right\} \{4\} \\
 & \quad + \left\{ \left(\frac{EA}{L} \right)_2 \cos \theta \cos \sigma_2 \sin \sigma_2 + \left(\frac{12EI}{L^3} \right)_2 \cos \theta \cos \sigma_2 \sin \sigma_2 \right\} \\
 & \quad \left. (E_\alpha^{+1} + E_\alpha^{-1}) (E_\beta^{+1} + E_\beta^{-1}) \right] \delta_\gamma \\
 & + \left[\left\{ \left(\frac{6EI}{L^2} \right)_2 \cos \theta \sin \theta \sin \sigma_2 + \left(\frac{6EI}{L^2} \right)_2 \cos \theta \sin \theta \sin \sigma_2 \right\} \right. \\
 & \quad \left. \{ - (E_\alpha^{+1} + E_\alpha^{-1}) (E_\beta^{+1} - E_\beta^{-1}) \} \right] \theta_\alpha \\
 & + \left[\left\{ \left(\frac{6EI}{L^2} \right)_1 \sin \sigma_1 (E_\alpha^{+2} - E_\alpha^{-2}) \right. \right. \\
 & \quad + \left\{ \left(\frac{6EI}{L^2} \right)_2 \cos^2 \theta \sin \sigma_2 - \left(\frac{6EI}{L^2} \right)_2 \sin^2 \theta \sin \sigma_2 \right\} (E_\alpha^{+1} - E_\alpha^{-1}) (E_\beta^{+1} + E_\beta^{-1}) \left. \right] \theta_\beta \\
 & + \left[\left\{ \left(\frac{6EI}{L^2} \right)_2 \sin \theta \cos \sigma_2 (E_\alpha^{+1} - E_\alpha^{-1}) (E_\beta^{+1} - E_\beta^{-1}) \right\} \right] \theta_\gamma \\
 & = 0 \quad \text{at } \alpha = 0 \text{ and } \alpha = N
 \end{aligned}$$

$$\begin{aligned}
(b) \quad & \left[\left(\frac{EA}{L} \right)_2 \cos\theta \sin\theta \cos^2\sigma_2 - \left(\frac{12EI}{L^3} Y \right)_2 \cos\theta \sin\theta \sin^2\sigma_2 - \left(\frac{12EI}{L^3} Z \right)_2 \cos\theta \sin\theta \right] \\
& \quad (E_\alpha^{+1} - E_\alpha^{-1}) (E_\beta^{+1} + E_\beta^{-1}) \delta_\alpha \\
& + \left[\left\{ \left(\frac{EA}{L} \right)_2 \sin^2\theta \cos^2\sigma_2 - \left(\frac{12EI}{L^3} Y \right)_2 \sin^2\theta \sin^2\sigma_2 + \left(\frac{12EI}{L^3} Z \right)_2 \cos^2\theta \right\} \right. \\
& \quad \left. (E_\alpha^{+1} + E_\alpha^{-1}) (E_\beta^{+1} - E_\beta^{-1}) \right] \delta_\beta \\
& + \left[\left\{ \left(\frac{EA}{L} \right)_2 \sin\theta \cos\sigma_2 \sin\sigma_2 - \left(\frac{12EI}{L^3} Y \right)_2 \sin\theta \cos\sigma_2 \sin\sigma_2 \right\} \{4\} \right. \\
& \quad \left. + \left\{ \left(\frac{EA}{L} \right)_2 \sin\theta \cos\sigma_2 \sin\sigma_2 + \left(\frac{12EI}{L^3} Y \right)_2 \sin\theta \cos\sigma_2 \sin\sigma_2 \right\} \right. \\
& \quad \left. (E_\alpha^{+1} + E_\alpha^{-1}) (E_\beta^{+1} + E_\beta^{-1}) \right] \delta_\gamma \\
& + \left[\left\{ \left(\frac{6EI}{L^2} Y \right)_2 \sin^2\theta \sin\sigma_2 - \left(\frac{6EI}{L^2} Z \right)_2 \cos^2\theta \sin\sigma_2 \right\} \right. \\
& \quad \left. \{ -(E_\alpha^{+1} + E_\alpha^{-1}) (E_\beta^{+1} - E_\beta^{-1}) \} \right] \theta_\alpha \\
& + \left[\left\{ \left(\frac{6EI}{L^2} Y \right)_2 \cos\theta \sin\theta \sin\sigma_2 + \left(\frac{6EI}{L^2} Z \right)_2 \cos\theta \sin\theta \sin\sigma_2 \right\} \right. \\
& \quad \left. (E_\alpha^{+1} - E_\alpha^{-1}) (E_\beta^{+1} + E_\beta^{-1}) \right] \theta_\beta \\
& + \left[\left(\frac{6EI}{L^2} Z \right)_2 \cos\theta \cos\sigma_2 \{ -(E_\alpha^{+1} - E_\alpha^{-1}) (E_\beta^{+1} - E_\beta^{-1}) \} \right] \theta_\gamma \\
& = 0 \quad \text{at } \beta = 0 \text{ and } \beta = M
\end{aligned}$$

$$\begin{aligned}
(c) \quad & \left[\left(\frac{6EI}{L^2} Y \right)_1 \sin\sigma_1 (E_\alpha^{+2} - E_\alpha^{-2}) \right. \\
& \quad \left. + \left\{ \left(\frac{6EI}{L^2} Y \right)_2 \cos^2\theta \sin\sigma_2 - \left(\frac{6EI}{L^2} Z \right)_2 \sin^2\theta \sin\sigma_2 \right\} \right. \\
& \quad \left. (E_\alpha^{+1} - E_\alpha^{-1}) (E_\beta^{+1} + E_\beta^{-1}) \right] \delta_\alpha \\
& + \left[\left\{ \left(\frac{6EI}{L^2} Y \right)_2 \cos\theta \sin\theta \sin\sigma_2 + \left(\frac{6EI}{L^2} Z \right)_2 \cos\theta \sin\theta \sin\sigma_2 \right\} \right. \\
& \quad \left. (E_\alpha^{+1} + E_\alpha^{-1}) (E_\beta^{+1} - E_\beta^{-1}) \right] \delta_\beta \\
& + \left[\left(\frac{6EI}{L^2} Y \right)_1 \cos\sigma_1 \{2\} + \left(\frac{6EI}{L^2} Y \right)_1 \cos\sigma_1 \{ -(E_\alpha^{+2} + E_\alpha^{-2}) \} \right. \\
& \quad + \left(\frac{6EI}{L^2} Y \right)_2 \cos\theta \cos\sigma_2 \{4\} + \left(\frac{6EI}{L^2} Y \right)_2 \cos\theta \cos\sigma_2 \{ -(E_\alpha^{+1} + E_\alpha^{-1}) (E_\beta^{+1} + E_\beta^{-1}) \} \right] \delta_\gamma \\
& + \left[\left\{ \left(\frac{GI}{L} \right)_2 \cos\theta \sin\theta \cos^2\sigma_2 + \left(\frac{2EI}{L} Y \right)_2 \cos\theta \sin\theta - \left(\frac{2EI}{L} Z \right)_2 \cos\theta \sin\theta \sin^2\sigma_2 \right\} \right. \\
& \quad \left. (E_\alpha^{+1} + E_\alpha^{-1}) (E_\beta^{+1} - E_\beta^{-1}) \right] \theta_\alpha
\end{aligned}$$

$$\begin{aligned}
& + \left[\left(\frac{2EI}{L} \right)_1 \{ -(E_\alpha^{+2} - E_\alpha^{-2}) \} \right. \\
& + \left\{ \left(\frac{GI}{L} \right)_2 \sin^2 \theta \cos^2 \sigma_2 - \left(\frac{2EI}{L} \right)_2 \cos^2 \theta + \left(\frac{2EI}{L} \right)_2 \sin^2 \theta \sin^2 \sigma_2 \right\} \\
& \quad \left. (E_\alpha^{+1} - E_\alpha^{-1}) (E_\beta^{+1} + E_\beta^{-1}) \right] \theta_\beta \\
& + \left[\left\{ \left(\frac{GI}{L} \right)_2 \sin \theta \cos \sigma_2 \sin \sigma_2 - \left(\frac{2EI}{L} \right)_2 \sin \theta \cos \sigma_2 \sin \sigma_2 \right\} \right. \\
& \quad \left. (E_\alpha^{+1} - E_\alpha^{-1}) (E_\beta^{+1} - E_\beta^{-1}) \right] \theta_\gamma \\
& = 0 \quad \text{at } \alpha = 0 \text{ and } \alpha = N
\end{aligned}$$

$$\begin{aligned}
(d) \quad & \left[\left\{ \left(\frac{6EI}{L^2} \right)_2 \cos \theta \sin \theta \sin \sigma_2 + \left(\frac{6EI}{L^2} \right)_2 \cos \theta \sin \theta \sin \sigma_2 \right\} \right. \\
& \quad \left. \{ -(E_\alpha^{+1} - E_\alpha^{-1}) (E_\beta^{+1} + E_\beta^{-1}) \} \right] \delta_\alpha \\
& + \left[\left\{ \left(\frac{6EI}{L^2} \right)_2 \sin^2 \theta \sin \sigma_2 - \left(\frac{6EI}{L^2} \right)_2 \cos^2 \theta \sin \sigma_2 \right\} \right. \\
& \quad \left. \{ -(E_\alpha^{+1} + E_\alpha^{-1}) (E_\beta^{+1} - E_\beta^{-1}) \} \right] \delta_\beta \\
& + \left[\left(\frac{6EI}{L^2} \right)_2 \sin \theta \cos \sigma_2 \{ -4 \} + \left(\frac{6EI}{L^2} \right)_2 \sin \theta \cos \sigma_2 (E_\alpha^{+1} + E_\alpha^{-1}) (E_\beta^{+1} + E_\beta^{-1}) \right] \delta_\gamma \\
& + \left[\left\{ \left(\frac{GI}{L} \right)_2 \cos^2 \theta \cos^2 \sigma_2 - \left(\frac{2EI}{L} \right)_2 \sin^2 \theta + \left(\frac{2EI}{L} \right)_2 \cos^2 \theta \sin^2 \sigma_2 \right\} \right. \\
& \quad \left. (E_\alpha^{+1} + E_\alpha^{-1}) (E_\beta^{+1} - E_\beta^{-1}) \right] \theta_\alpha \\
& + \left[\left\{ \left(\frac{GI}{L} \right)_2 \cos \theta \sin \theta \cos^2 \sigma_2 + \left(\frac{2EI}{L} \right)_2 \cos \theta \sin \theta + \left(\frac{2EI}{L} \right)_2 \cos \theta \sin \theta \sin^2 \sigma_2 \right\} \right. \\
& \quad \left. (E_\alpha^{+1} - E_\alpha^{-1}) (E_\beta^{+1} + E_\beta^{-1}) \right] \theta_\beta \\
& + \left[\left\{ \left(\frac{GI}{L} \right)_2 \cos \theta \cos \sigma_2 \sin \sigma_2 - \left(\frac{2EI}{L} \right)_2 \cos \theta \cos \sigma_2 \sin \sigma_2 \right\} \right. \\
& \quad \left. (E_\alpha^{+1} - E_\alpha^{-1}) (E_\beta^{+1} - E_\beta^{-1}) \right] \theta_\gamma \\
& = 0 \quad \text{at } \beta = 0 \text{ and } \beta = M
\end{aligned}$$

$$\begin{aligned}
(e) \quad & \left[\left(\frac{6EI}{L^2} \right)_2 \sin \theta \cos \sigma_2 (E_\alpha^{+1} - E_\alpha^{-1}) (E_\beta^{+1} - E_\beta^{-1}) \right] \delta_\alpha \\
& + \left[\left(\frac{6EI}{L^2} \right)_1 \cos \sigma_1 \{ 2 \} + \left(\frac{6EI}{L^2} \right)_1 \cos \sigma_1 \{ -(E_\alpha^{+2} + E_\alpha^{-2}) \} \right. \\
& + \left(\frac{6EI}{L^2} \right)_2 \cos \theta \cos \sigma_2 \{ 4 \} + \left(\frac{6EI}{L^2} \right)_2 \cos \theta \cos \sigma_2 \{ -(E_\alpha^{+1} + E_\alpha^{-1}) (E_\beta^{+1} + E_\beta^{-1}) \} \left. \right] \delta_\beta \\
& + \left[0 \right] \delta_\gamma
\end{aligned}$$

$$\begin{aligned}
& + \left[\left\{ \left(\frac{GI}{L} \right)_1 \cos \sigma_1 \sin \sigma_1 - \left(\frac{4EI}{L} \right)_1 \cos \sigma_1 \sin \sigma_1 \right\} \{-2\} \right. \\
& + \left\{ \left(\frac{GI}{L} \right)_1 \cos \sigma_1 \sin \sigma_1 - \left(\frac{2EI}{L} \right)_1 \cos \sigma_1 \sin \sigma_1 \right\} (E_\alpha^{+2} + E_\alpha^{-2}) \\
& + \left\{ \left(\frac{GI}{L} \right)_2 \cos \theta \cos \sigma_2 \sin \sigma_2 - \left(\frac{4EI}{L} \right)_2 \cos \theta \cos \sigma_2 \sin \sigma_2 \right\} \{-4\} \\
& + \left\{ \left(\frac{GI}{L} \right)_2 \cos \theta \cos \sigma_2 \sin \sigma_2 - \left(\frac{2EI}{L} \right)_2 \cos \theta \cos \sigma_2 \sin \sigma_2 \right\} \\
& \quad \left. (E_\alpha^{+1} + E_\alpha^{-1}) (E_\beta^{+1} + E_\beta^{-1}) \right] \theta_\alpha \\
& + \left[\left\{ \left(\frac{GI}{L} \right)_2 \sin \theta \cos \sigma_2 \sin \sigma_2 - \left(\frac{2EI}{L} \right)_2 \sin \theta \cos \sigma_2 \sin \sigma_2 \right\} \right. \\
& \quad \left. (E_\alpha^{+1} - E_\alpha^{-1}) (E_\beta^{+1} - E_\beta^{-1}) \right] \theta_\beta \\
& + \left[\left\{ \left(\frac{GI}{L} \right)_1 \sin^2 \sigma_1 + \left(\frac{2EI}{L} \right)_1 \cos^2 \sigma_1 \right\} (E_\alpha^{+2} - E_\alpha^{-2}) \right. \\
& + \left\{ \left(\frac{GI}{L} \right)_2 \sin^2 \sigma_2 + \left(\frac{2EI}{L} \right)_2 \cos^2 \sigma_2 \right\} (E_\alpha^{+1} - E_\alpha^{-1}) (E_\beta^{+1} + E_\beta^{-1}) \left. \right] \theta_\gamma \\
& = 0 \quad \text{at } \alpha = 0 \text{ and } \alpha = N
\end{aligned}$$

$$\begin{aligned}
(f) \quad & \left[\left(\frac{6EI}{L^2} \right)_2 \sin \theta \cos \sigma_2 \{-4\} + \left(\frac{6EI}{L^2} \right)_2 \sin \theta \cos \sigma_2 (E_\alpha^{+1} + E_\alpha^{-1}) (E_\beta^{+1} + E_\beta^{-1}) \right] \delta_\alpha \\
& + \left[\left(\frac{6EI}{L^2} \right)_2 \cos \theta \cos \sigma_2 \{- (E_\alpha^{+1} - E_\alpha^{-1}) (E_\beta^{+1} - E_\beta^{-1}) \} \right] \delta_\beta \\
& + [0] \delta_\gamma \\
& + \left[\left\{ \left(\frac{GI}{L} \right)_2 \cos \theta \cos \sigma_2 \sin \sigma_2 - \left(\frac{2EI}{L} \right)_2 \cos \theta \cos \sigma_2 \sin \sigma_2 \right\} \right. \\
& \quad \left. (E_\alpha^{+1} - E_\alpha^{-1}) (E_\beta^{+1} - E_\beta^{-1}) \right] \theta_\alpha \\
& + \left[\left\{ \left(\frac{GI}{L} \right)_2 \sin \theta \cos \sigma_2 \sin \sigma_2 - \left(\frac{4EI}{L} \right)_2 \sin \theta \cos \sigma_2 \sin \sigma_2 \right\} \{-4\} \right. \\
& + \left\{ \left(\frac{GI}{L} \right)_2 \sin \theta \cos \sigma_2 \sin \sigma_2 - \left(\frac{2EI}{L} \right)_2 \sin \theta \cos \sigma_2 \sin \sigma_2 \right\} \\
& \quad \left. (E_\alpha^{+1} + E_\alpha^{-1}) (E_\beta^{+1} + E_\beta^{-1}) \right] \theta_\beta \\
& + \left[\left\{ \left(\frac{GI}{L} \right)_2 \sin^2 \sigma_2 + \left(\frac{2EI}{L} \right)_2 \cos^2 \sigma_2 \right\} \right. \\
& \quad \left. (E_\alpha^{+1} + E_\alpha^{-1}) (E_\beta^{+1} - E_\beta^{-1}) \right] \theta_\gamma \\
& = 0 \quad \text{at } \beta = 0 \text{ and } \beta = M
\end{aligned}$$

E.3 DOUBLE LAYER PIN JOINTED LATTICE

The force boundary conditions involve forces in the members of both layers and in the diagonal web members. The force boundary conditions are

- (a) Zero edge force in α direction at edges $\alpha = 0$ and $\alpha = N$ for top layer.
- (b) Zero edge force in α direction at edges $\alpha = 0$ and $\alpha = N$ for bottom layer.
- (c) Zero edge force in β direction at edges $\beta = 0$ and $\beta = M$ for top layer.
- (d) Zero edge force in β direction at edges $\beta = 0$ and $\beta = M$ for bottom layer.

The resulting conditions on the displacements are

$$\begin{aligned}
 \text{(a)} \quad & \left[S_{\alpha} \cos^2 \sigma_{\alpha} (E_{\alpha}^{+2} - E_{\alpha}^{-2}) \right] \delta_{\alpha} \\
 & + \left[0 \right] \delta_{\beta} \\
 & + \left[S_{\alpha} \cos \sigma_{\alpha} \sin \sigma_{\alpha} \{ 2 + (E_{\alpha}^{+2} + E_{\alpha}^{-2}) \} + S_d \cos \theta \cos \phi \sin \phi \{ 4 \} \right] \delta_{\gamma} \\
 & + \left[S_d \cos^2 \theta \cos^2 \phi (E_{\alpha}^{+1} - E_{\alpha}^{-1}) (E_{\beta}^{+1} + E_{\beta}^{-1}) \right] \bar{\delta}_{\alpha} \\
 & + \left[S_d \cos \theta \sin \theta \cos^2 \phi (E_{\alpha}^{+1} + E_{\alpha}^{-1}) (E_{\beta}^{+1} - E_{\beta}^{-1}) \right] \bar{\delta}_{\beta} \\
 & + \left[S_d \cos \theta \cos \phi \sin \phi \{ - (E_{\alpha}^{+1} + E_{\alpha}^{-1}) (E_{\beta}^{+1} + E_{\beta}^{-1}) \} \right] \bar{\delta}_{\gamma} = 0
 \end{aligned}$$

at $\alpha = 0$ and $\alpha = N$

$$\begin{aligned}
 \text{(b)} \quad & \left[S_d \cos^2 \theta \cos^2 \phi (E_{\alpha}^{+1} - E_{\alpha}^{-1}) (E_{\beta}^{+1} + E_{\beta}^{-1}) \right] \delta_{\alpha} \\
 & + \left[S_d \cos \theta \sin \theta \cos^2 \phi (E_{\alpha}^{+1} + E_{\alpha}^{-1}) (E_{\beta}^{+1} - E_{\beta}^{-1}) \right] \delta_{\beta} \\
 & + \left[S_d \cos \theta \cos \phi \sin \phi (E_{\alpha}^{+1} + E_{\alpha}^{-1}) (E_{\beta}^{+1} + E_{\beta}^{-1}) \right] \delta_{\gamma} \\
 & + \left[\bar{S}_{\alpha} \cos^2 \sigma_{\alpha} (E_{\alpha}^{+2} - E_{\alpha}^{-2}) \right] \bar{\delta}_{\alpha} \\
 & + \left[0 \right] \bar{\delta}_{\beta} \\
 & + \left[\bar{S}_{\alpha} \cos \sigma_{\alpha} \sin \sigma_{\alpha} \{ 2 + (E_{\alpha}^{+2} + E_{\alpha}^{-2}) \} + S_d \cos \theta \cos \phi \sin \phi \{ -4 \} \right] \bar{\delta}_{\gamma} = 0
 \end{aligned}$$

at $\alpha = 0$ and $\alpha = N$

$$\begin{aligned}
(c) \quad & \left[0 \right] \delta_\alpha \\
& + [S_\beta \cos^2 \sigma_\beta (E_\beta^{+2} - E_\beta^{-2})] \delta_\beta \\
& + [S_\beta \cos \sigma_\beta \sin \sigma_\beta \{2 + (E_\beta^{+2} + E_\beta^{-2})\} + S_d \sin \theta \cos \phi \sin \phi \{4\}] \delta_\gamma \\
& + [S_d \cos \theta \sin \theta \cos^2 \phi (E_\alpha^{+1} - E_\alpha^{-1}) (E_\beta^{+1} + E_\beta^{-1})] \bar{\delta}_\alpha \\
& + [S_d \sin^2 \theta \cos^2 \phi (E_\alpha^{+1} + E_\alpha^{-1}) (E_\beta^{+1} - E_\beta^{-1})] \bar{\delta}_\beta \\
& + [S_d \sin \theta \cos \phi \sin \phi \{-(E_\alpha^{+1} + E_\alpha^{-1}) (E_\beta^{+1} + E_\beta^{-1})\}] \bar{\delta}_\gamma = 0
\end{aligned}$$

at $\beta = 0$ and $\beta = M$

$$\begin{aligned}
(d) \quad & [S_d \cos \theta \sin \theta \cos^2 \phi (E_\alpha^{+1} - E_\alpha^{-1}) (E_\beta^{+1} + E_\beta^{-1})] \delta_\alpha \\
& + [S_d \sin^2 \theta \cos^2 \phi (E_\alpha^{+1} + E_\alpha^{-1}) (E_\beta^{+1} - E_\beta^{-1})] \delta_\beta \\
& + [S_d \sin \theta \cos \phi \sin \phi (E_\alpha^{+1} + E_\alpha^{-1}) (E_\beta^{+1} + E_\beta^{-1})] \delta_\gamma \\
& + [0] \bar{\delta}_\alpha \\
& + [\bar{S}_\beta \cos^2 \sigma_\beta (E_\beta^{+2} - E_\beta^{-2})] \bar{\delta}_\beta \\
& + [\bar{S}_\beta \cos \sigma_\beta \sin \sigma_\beta \{2 + (E_\beta^{+2} + E_\beta^{-2})\} + S_d \sin \theta \cos \phi \sin \phi \{-4\}] \bar{\delta}_\gamma = 0
\end{aligned}$$

at $\beta = 0$ and $\beta = M$

APPENDIX F

MATRIX EQUATIONS FOR DISPLACEMENT COEFFICIENTS

In the solution method used, the displacement series coefficients must be determined by solving a set of simultaneous linear equations for each fourier term in the series. A convenient form to present these equations is as a matrix equation with the general form

$$\begin{bmatrix} v_{11} & v_{12} & \cdot & \cdot \\ v_{21} & v_{22} & \cdot & \cdot \\ \cdot & \cdot & \cdot & \cdot \\ \cdot & \cdot & \cdot & \cdot \end{bmatrix}_{ij} \begin{Bmatrix} a_{ij} \\ b_{ij} \\ \cdot \\ \cdot \end{Bmatrix} = \begin{Bmatrix} p_{ij} \\ q_{ij} \\ \cdot \\ \cdot \end{Bmatrix} \quad \dots (F-1)$$

where the terms of the matrix $[v]_{ij}$ are dependent on the values of indices i and j . The load series coefficients p_{ij} , q_{ij} , \dots are found from the known load pattern and then the displacement series coefficients a_{ij} , b_{ij} , \dots are found by solving the set of equations F-1.

The matrix $[v]_{ij}$ is square and symmetric with its size being the number of unknown coefficients in each set. This is 3 for the single layer pin jointed lattice of chapter 4, and 6 for the single layer rigid jointed structure of chapter 5 and for the double layer pin jointed structure of chapter 6.

F.1 SINGLE LAYER PIN JOINTED LATTICE

For this structure the elements of matrix $[v]_{ij}$ in the equation are

$$v_{11} = +2S_1 \cos^2 \sigma_1 \{1 - \cos \frac{i\pi}{N}\} + 4S_2 \cos^2 \theta \cos^2 \sigma_2 \{1 - \cos \frac{i\pi}{N} \cos \frac{j\pi}{M}\}$$

$$v_{12} = v_{21} = +4S_2 \cos \theta \sin \theta \cos^2 \sigma_2 \{ \sin \frac{i\pi}{N} \sin \frac{j\pi}{M} \}$$

$$v_{13} = v_{31} = -2S_1 \cos \sigma_1 \sin \sigma_1 \{ \sin \frac{i\pi}{N} \} - 4S_2 \cos \theta \cos \sigma_2 \sin \sigma_2 \{ \sin \frac{i\pi}{N} \cos \frac{j\pi}{M} \}$$

$$v_{22} = +4S_2 \sin^2 \theta \cos^2 \sigma_2 \{1 - \cos \frac{i\pi}{N} \cos \frac{j\pi}{M}\}$$

$$v_{23} = v_{32} = -4S_2 \sin \theta \cos \sigma_2 \sin \sigma_2 \{ \cos \frac{i\pi}{N} \sin \frac{j\pi}{M} \}$$

$$v_{33} = +2S_1 \sin^2 \sigma_1 \{1 + \cos \frac{i\pi}{N}\} + 4S_2 \sin^2 \sigma_2 \{1 + \cos \frac{i\pi}{N} \cos \frac{j\pi}{M}\}$$

F.2

SINGLE LAYER RIGID JOINTED LATTICE

The elements of the six by six matrix $[v]_{ij}$ for this structure are

$$v_{11} = +2\left(\frac{EA}{L}\right)_1 \cos^2 \sigma_1 \left\{1 - \cos \frac{i\pi 2}{N}\right\} + 4\left(\frac{EA}{L}\right)_2 \cos^2 \theta \cos^2 \sigma_2 \left\{1 - \cos \frac{i\pi}{N} \cos \frac{j\pi}{M}\right\} \\ + 24\left(\frac{EI}{L^3}\right)_1 \sin^2 \sigma_1 \left\{1 + \cos \frac{i\pi 2}{N}\right\} + 48\left(\frac{EI}{L^3}\right)_2 \cos^2 \theta \sin^2 \sigma_2 \left\{1 + \cos \frac{i\pi}{N} \cos \frac{j\pi}{M}\right\} \\ + 48\left(\frac{EI}{L^3}\right)_2 \sin^2 \theta \left\{1 - \cos \frac{i\pi}{N} \cos \frac{j\pi}{M}\right\}$$

$$v_{12} = v_{21} = +4\left(\frac{EA}{L}\right)_2 \cos \theta \sin \theta \cos^2 \sigma_2 \left\{\sin \frac{i\pi}{N} \sin \frac{j\pi}{M}\right\} \\ - 48\left(\frac{EI}{L^3}\right)_2 \cos \theta \sin \theta \sin^2 \sigma_2 \left\{\sin \frac{i\pi}{N} \sin \frac{j\pi}{M}\right\} \\ - 48\left(\frac{EI}{L^3}\right)_2 \cos \theta \sin \theta \left\{\sin \frac{i\pi}{N} \sin \frac{j\pi}{M}\right\}$$

$$v_{13} = v_{31} = -4\left(\frac{EA}{L}\right)_1 \cos \sigma_1 \sin \sigma_1 \left\{\sin \frac{i\pi 2}{N}\right\} - 4\left(\frac{EA}{L}\right)_2 \cos \theta \cos \sigma_2 \sin \sigma_2 \left\{\sin \frac{i\pi}{N} \cos \frac{j\pi}{M}\right\} \\ - 48\left(\frac{EI}{L^3}\right)_1 \cos \sigma_1 \sin \sigma_1 \left\{\sin \frac{i\pi 2}{N}\right\} - 48\left(\frac{EI}{L^3}\right)_2 \cos \theta \cos \sigma_2 \sin \sigma_2 \left\{\sin \frac{i\pi}{N} \cos \frac{j\pi}{M}\right\}$$

$$v_{14} = v_{41} = -24\left(\frac{EI}{L^3}\right)_2 \cos \theta \sin \theta \sin \sigma_2 \left\{\sin \frac{i\pi}{N} \sin \frac{j\pi}{M}\right\} \\ - 24\left(\frac{EI}{L^3}\right)_2 \cos \theta \sin \theta \sin \sigma_2 \left\{\sin \frac{i\pi}{N} \sin \frac{j\pi}{M}\right\}$$

$$v_{15} = v_{51} = -12\left(\frac{EI}{L^2}\right)_1 \sin \sigma_1 \left\{1 + \cos \frac{i\pi 2}{N}\right\} - 24\left(\frac{EI}{L^2}\right)_2 \cos^2 \theta \sin \sigma_2 \left\{1 + \cos \frac{i\pi}{N} \cos \frac{j\pi}{M}\right\} \\ - 24\left(\frac{EI}{L^2}\right)_2 \sin^2 \theta \sin \sigma_2 \left\{1 - \cos \frac{i\pi}{N} \cos \frac{j\pi}{M}\right\}$$

$$v_{16} = v_{61} = +24\left(\frac{EI}{L^2}\right)_2 \sin \theta \cos \sigma_2 \left\{\cos \frac{i\pi}{N} \sin \frac{j\pi}{M}\right\}$$

$$v_{22} = +4\left(\frac{EA}{L}\right)_2 \sin^2 \theta \cos^2 \sigma_2 \left\{1 - \cos \frac{i\pi}{N} \cos \frac{j\pi}{M}\right\} \\ + 48\left(\frac{EI}{L^3}\right)_2 \sin^2 \theta \sin^2 \sigma_2 \left\{1 + \cos \frac{i\pi}{N} \cos \frac{j\pi}{M}\right\} \\ + 24\left(\frac{EI}{L^3}\right)_1 \left\{1 - \cos \frac{i\pi 2}{N}\right\} + 48\left(\frac{EI}{L^3}\right)_2 \cos^2 \theta \left\{1 - \cos \frac{i\pi}{N} \cos \frac{j\pi}{M}\right\}$$

$$v_{23} = v_{32} = -4\left(\frac{EA}{L}\right)_2 \sin \theta \cos \sigma_2 \sin \sigma_2 \left\{\cos \frac{i\pi}{N} \sin \frac{j\pi}{M}\right\} \\ - 48\left(\frac{EI}{L^3}\right)_2 \sin \theta \cos \sigma_2 \sin \sigma_2 \left\{\cos \frac{i\pi}{N} \sin \frac{j\pi}{M}\right\}$$

$$v_{24} = v_{42} = +24 \left(\frac{EI}{L^2} \right)_2 \sin^2 \theta \sin \sigma_2 \left\{ 1 + \cos \frac{i\pi}{N} \cos \frac{j\pi}{M} \right\}$$

$$+ 12 \left(\frac{EI}{L^2} \right)_1 \sin \sigma_1 \left\{ 1 - \cos \frac{i\pi}{N} \right\} + 24 \left(\frac{EI}{L^2} \right)_2 \cos^2 \theta \sin \sigma_2 \left\{ 1 - \cos \frac{i\pi}{N} \cos \frac{j\pi}{M} \right\}$$

$$v_{25} = v_{52} = +24 \left(\frac{EI}{L^2} \right)_2 \cos \theta \sin \theta \sin \sigma_2 \left\{ \sin \frac{i\pi}{N} \sin \frac{j\pi}{M} \right\}$$

$$+ 24 \left(\frac{EI}{L^2} \right)_2 \cos \theta \sin \theta \sin \sigma_2 \left\{ \sin \frac{i\pi}{N} \sin \frac{j\pi}{M} \right\}$$

$$v_{26} = v_{62} = -12 \left(\frac{EI}{L^2} \right)_1 \cos \sigma_1 \left\{ \sin \frac{i\pi}{N} \right\} - 24 \left(\frac{EI}{L^2} \right)_2 \cos \theta \cos \sigma_2 \left\{ \sin \frac{i\pi}{N} \cos \frac{j\pi}{M} \right\}$$

$$v_{33} = +2 \left(\frac{EA}{L} \right)_1 \sin^2 \sigma_1 \left\{ 1 + \cos \frac{i\pi}{N} \right\} + 4 \left(\frac{EA}{L} \right)_2 \sin^2 \sigma_2 \left\{ 1 + \cos \frac{i\pi}{N} \cos \frac{j\pi}{M} \right\}$$

$$+ 24 \left(\frac{EI}{L^3} \right)_1 \cos^2 \sigma_1 \left\{ 1 - \cos \frac{i\pi}{N} \right\} + 48 \left(\frac{EI}{L^3} \right)_2 \cos^2 \sigma_2 \left\{ 1 - \cos \frac{i\pi}{N} \cos \frac{j\pi}{M} \right\}$$

$$v_{34} = v_{43} = -24 \left(\frac{EI}{L^2} \right)_2 \sin \theta \cos \sigma_2 \left\{ \cos \frac{i\pi}{N} \sin \frac{j\pi}{M} \right\}$$

$$v_{35} = v_{53} = +12 \left(\frac{EI}{L^2} \right)_1 \cos \sigma_1 \left\{ \sin \frac{i\pi}{N} \right\} + 24 \left(\frac{EI}{L^2} \right)_2 \cos \theta \cos \sigma_2 \left\{ \sin \frac{i\pi}{N} \cos \frac{j\pi}{M} \right\}$$

$$v_{36} = v_{63} = 0$$

$$v_{44} = +2 \left(\frac{GI}{L} \right)_1 \cos^2 \sigma_1 \left\{ 1 - \cos \frac{i\pi}{N} \right\} + 4 \left(\frac{GI}{L} \right)_2 \cos^2 \theta \cos^2 \sigma_2 \left\{ 1 - \cos \frac{i\pi}{N} \cos \frac{j\pi}{M} \right\}$$

$$+ 8 \left(\frac{EI}{L} \right)_2 \sin^2 \theta \left\{ 2 + \cos \frac{i\pi}{N} \cos \frac{j\pi}{M} \right\}$$

$$+ 4 \left(\frac{EI}{L} \right)_1 \sin^2 \sigma_1 \left\{ 2 - \cos \frac{i\pi}{N} \right\} + 8 \left(\frac{EI}{L} \right)_2 \cos^2 \theta \sin^2 \sigma_2 \left\{ 2 - \cos \frac{i\pi}{N} \cos \frac{j\pi}{M} \right\}$$

$$v_{45} = v_{54} = +4 \left(\frac{GI}{L} \right)_2 \cos \theta \sin \theta \cos^2 \sigma_2 \left\{ \sin \frac{i\pi}{N} \sin \frac{j\pi}{M} \right\}$$

$$+ 8 \left(\frac{EI}{L} \right)_2 \cos \theta \sin \theta \left\{ \sin \frac{i\pi}{N} \sin \frac{j\pi}{M} \right\}$$

$$+ 8 \left(\frac{EI}{L} \right)_2 \cos \theta \sin \theta \sin^2 \sigma_2 \left\{ \sin \frac{i\pi}{N} \sin \frac{j\pi}{M} \right\}$$

$$v_{46} = v_{64} = +2 \left(\frac{GI}{L} \right)_1 \cos \sigma_1 \sin \sigma_1 \left\{ \sin \frac{i\pi}{N} \right\} + 4 \left(\frac{GI}{L} \right)_2 \cos \theta \cos \sigma_2 \sin \sigma_2 \left\{ \sin \frac{i\pi}{N} \cos \frac{j\pi}{M} \right\}$$

$$- 4 \left(\frac{EI}{L} \right)_1 \cos \sigma_1 \sin \sigma_1 \left\{ \sin \frac{i\pi}{N} \right\} - 8 \left(\frac{EI}{L} \right)_2 \cos \theta \cos \sigma_2 \sin \sigma_2 \left\{ \sin \frac{i\pi}{N} \cos \frac{j\pi}{M} \right\}$$

$$v_{55} = +4 \left(\frac{GI}{L} \right)_2 \sin^2 \theta \cos^2 \sigma_2 \left\{ 1 - \cos \frac{i\pi}{N} \cos \frac{j\pi}{M} \right\}$$

$$+ 4 \left(\frac{EI}{L} \right)_1 \left\{ 2 + \cos \frac{i\pi}{N} \right\} + 8 \left(\frac{EI}{L} \right)_2 \cos^2 \theta \left\{ 2 + \cos \frac{i\pi}{N} \cos \frac{j\pi}{M} \right\}$$

$$+ 8 \left(\frac{EI}{L} \right)_2 \sin^2 \theta \sin^2 \sigma_2 \left\{ 2 - \cos \frac{i\pi}{N} \cos \frac{j\pi}{M} \right\}$$

$$\begin{aligned}
v_{56} = v_{65} &= +4\left(\frac{GI}{L}\right)_2 \sin\theta \cos\sigma_2 \sin\sigma_2 \left\{ \cos\frac{i\pi}{N} \sin\frac{j\pi}{M} \right\} \\
&\quad - 8\left(\frac{EI}{L}\right)_2 \sin\theta \cos\sigma_2 \sin\sigma_2 \left\{ \cos\frac{i\pi}{N} \sin\frac{j\pi}{M} \right\} \\
v_{66} &= +2\left(\frac{GI}{L}\right)_1 \sin^2\sigma_1 \left\{ 1 + \cos\frac{i\pi 2}{N} \right\} + 4\left(\frac{GI}{L}\right)_2 \sin^2\sigma_2 \left\{ 1 + \cos\frac{i\pi}{N} \cos\frac{j\pi}{M} \right\} \\
&\quad + 4\left(\frac{EI}{L}\right)_1 \cos^2\sigma_1 \left\{ 2 + \cos\frac{i\pi 2}{N} \right\} + 8\left(\frac{EI}{L}\right)_2 \cos^2\sigma_2 \left\{ 2 + \cos\frac{i\pi}{N} \cos\frac{j\pi}{M} \right\}
\end{aligned}$$

where the symbols are defined in chapter 5.

F.3 DOUBLE LAYER PIN JOINTED LATTICE

The matrix elements for this structure are

$$\begin{aligned}
v_{11} &= +2S_\alpha \cos^2\sigma_\alpha \left\{ 1 - \cos\frac{i\pi 2}{N} \right\} + 4S_d \cos^2\theta \cos^2\phi \\
v_{12} = v_{21} &= 0 \\
v_{13} = v_{31} &= -2S_\alpha \cos\sigma_\alpha \sin\sigma_\alpha \left\{ \sin\frac{i\pi 2}{N} \right\} \\
v_{14} = v_{41} &= -4S_d \cos^2\theta \cos^2\phi \left\{ \cos\frac{i\pi}{N} \cos\frac{j\pi}{M} \right\} \\
v_{15} = v_{51} &= +4S_d \cos\theta \sin\theta \cos^2\phi \left\{ \sin\frac{i\pi}{N} \sin\frac{j\pi}{M} \right\} \\
v_{16} = v_{61} &= +4S_d \cos\theta \cos\phi \sin\phi \left\{ \sin\frac{i\pi}{N} \cos\frac{j\pi}{M} \right\} \\
v_{22} &= +2S_\beta \cos^2\sigma_\beta \left\{ 1 - \cos\frac{j\pi 2}{M} \right\} + 4S_d \sin^2\theta \cos^2\phi \\
v_{23} = v_{32} &= -2S_\beta \cos\sigma_\beta \sin\sigma_\beta \left\{ \sin\frac{j\pi 2}{M} \right\} \\
v_{24} = v_{42} &= +4S_d \cos\theta \sin\theta \cos^2\phi \left\{ \sin\frac{i\pi}{N} \sin\frac{j\pi}{M} \right\} \\
v_{25} = v_{52} &= -4S_d \sin^2\theta \cos^2\phi \left\{ \cos\frac{i\pi}{N} \cos\frac{j\pi}{M} \right\} \\
v_{26} = v_{62} &= +4S_d \sin\theta \cos\phi \sin\phi \left\{ \cos\frac{i\pi}{N} \sin\frac{j\pi}{M} \right\} \\
v_{33} &= +2S_\alpha \sin^2\sigma_\alpha \left\{ 1 + \cos\frac{i\pi 2}{N} \right\} + 2S_\beta \sin^2\sigma_\beta \left\{ 1 + \cos\frac{j\pi 2}{M} \right\} + 4S_d \sin^2\phi \\
v_{34} = v_{43} &= -4S_d \cos\theta \cos\phi \sin\phi \left\{ \sin\frac{i\pi}{N} \cos\frac{j\pi}{M} \right\} \\
v_{35} = v_{53} &= -4S_d \sin\theta \cos\phi \sin\phi \left\{ \cos\frac{i\pi}{N} \sin\frac{j\pi}{M} \right\}
\end{aligned}$$

$$v_{36} = v_{63} = -4S_d \sin^2 \phi \left\{ \cos \frac{i\pi}{N} \cos \frac{j\pi}{M} \right\}$$

$$v_{44} = +2\bar{S}_\alpha \cos^2 \sigma_\alpha \left\{ 1 - \cos \frac{i\pi 2}{N} \right\} + 4S_d \cos^2 \theta \cos^2 \phi$$

$$v_{45} = v_{54} = 0$$

$$v_{46} = v_{64} = -2\bar{S}_\alpha \cos \sigma_\alpha \sin \sigma_\alpha \left\{ \sin \frac{i\pi 2}{N} \right\}$$

$$v_{55} = +2\bar{S}_\beta \cos^2 \sigma_\beta \left\{ 1 - \cos \frac{j\pi 2}{M} \right\} + 4S_d \sin^2 \theta \cos^2 \phi$$

$$v_{56} = v_{65} = -2\bar{S}_\beta \cos \sigma_\beta \sin \sigma_\beta \left\{ \sin \frac{j\pi 2}{M} \right\}$$

$$v_{66} = +2\bar{S}_\alpha \sin^2 \sigma_\alpha \left\{ 1 + \cos \frac{i\pi 2}{N} \right\} + 2\bar{S}_\beta \sin^2 \sigma_\beta \left\{ 1 + \cos \frac{j\pi 2}{M} \right\} + 4S_d \sin^2 \phi$$

where the symbols are as defined in chapter 6.

APPENDIX G

DETAILS AND LISTING OF COMPUTER PROGRAM

The program to analyse a single layer rigid jointed lattice structure is presented here. The relevant theory is contained in chapter 5.

INPUT DATA

Input is in the form of a card deck consisting of

- i) Heading (80H1), one card containing a short description of the structure. This heading is printed on the output.
- ii) Structure Geometry Data (2I10, 4F10.0), one card containing the geometry parameters N , M , L_X , H_X , L_Y and H_Y of the structure.
- iii) Member Property Data (6F10.0), two cards, containing the member properties E , G , A , I_X , I_Y and I_Z for the two types of members.
- iv) Loading Data There are three types, viz. the general, uniform or point loading cases. In each case the data consists of two or more cards, the first specifying the type of load and a heading. The second and subsequent cards specify the joint loads. The first card contains in columns 1 to 6 the characters

GENERA for a general load case

UNIFOR for a uniform load case

POINT b for a point load case

Columns 7 to 80 of this card can contain a heading which is printed on the output.

The second and subsequent cards depend on the type of load.

- a) General Load (2I10, 6F10.0), one card for each loaded joint, containing the joint coordinates (integers) and the loads and moments on the joint. Terminate with a card containing a 9 in column 1.
- b) Uniform Load (20X, 6F10.0), one card specifying the loads and moments on all joints.
- c) Point Load (2I10, 6F10.0), one card specifying the coordinates of the loaded joint and the loads and moments thereon.

The total data deck can be repeated as many times as required for one run of the program. It is only necessary to place them together in sequence.

OUTPUT DATA

The output data consists of

- i) Echo of all input data
- ii) Displacements and rotations at all joints
- iii) Member actions for all members
- iv) Joint residuals at all joints. At boundary joints these are the reactions.

The program could be modified to reduce the quantity of results obtained.

C THIS IS THE PROGRAM FOR A SINGLE LAYER RIGID JOINTED STRUCTURE

C
C
C
C
C
C
C

P N DAVENPORT -UNIVERSITY OF CANTERBURY- 1975

MAIN LINE PROGRAM - CALLS SUBROUTINES

```
COMMON /ARRAY/P(2000),D(2000)
DIMENSION INPUT(14)
REAL GENERA/6HGENERA/,UNIFOR/6HUNIFOR/,POINT/6HPOINT /
10 CONTINUE
  READ(5,2000,END=999) (INPUT(I),I=1,14)
2000 FORMAT(13A6,A2)
  WRITE(6,1000) (INPUT(I),I=1,14)
1000 FORMAT(1H1,56HANALYSIS OF SINGLE LAYER RIGID JOINTED LATTICE STRUC
  TURE //1X,13A6,A2//)
  CALL DATA16(NP1,MP1)
  READ(5,2000) (INPUT(I),I=1,14)
  WRITE(6,1010) (INPUT(I),I=1,14)
1010 FORMAT(1H1,13A6,A2)
  IF (INPUT(1).EQ.GENERA) GO TO 42
  IF (INPUT(1).GT.EQ.UNIFOR) GO TO 44
  IF (INPUT(1).EQ.POINT ) GO TO 46
  GO TO 999
42 CONTINUE
  CALL LOADG6(NP1,MP1,P,D)
  GO TO 40
44 CONTINUE
  CALL LOADU6(NP1,MP1,P,D)
  GO TO 40
46 CONTINUE
  CALL LOADP6(NP1,MP1,P,D)
  GO TO 40
40 CONTINUE
  CALL SOLVE6(NP1,MP1,D,P)
  CALL DISPT6(NP1,MP1,P,D)
  CALL MEMB6(NP1,MP1,D)
  CALL BDRY6(NP1,MP1,D)
  GO TO 10
999 CONTINUE
STOP
END
```

SUBROUTINE DATA16(NP1,MP1)

C
C
C
C

THIS ROUTINE INPUTS DATA ABOUT THE STRUCTURE AND DOES THE PRELIMINARY CALCULATIONS FROM IT

```
COMMON /DATA1/CN,SN,CM,SM
COMMON/DATA2/SC(36),SV1(36),SV2(36)
COMMON/DATA3/SR(12,12,3)
COMMON/DATA4/SS(12,12,3)
DIMENSION NN(2),S(6)
DIMENSION PROP1(6),PROP2(6)
DATA PI/3.1415926535897932/
```

C
C
C
C

INPUT STRUCTURE DATA AND DETERMINE GEOMETRY

```
READ(5,2000) NN(1),NN(2),(S(I),I=1,4)
2000 FORMAT(2I10,4F10.0)
  WRITE(6,1020) NN(1),NN(2),(S(I),I=1,4)
  N=NN(1)
  M=NN(2)
  READ(5,2010) (PROP1(I),I=1,6)
  READ(5,2010) (PROP2(I),I=1,6)
2010 FORMAT(6E10.0)
  WRITE(6,1030) (PROP1(I),PROP2(I),I=1,6)
  NP1=N+1
  MP1=M+1
  CN=FLOAT(NP1-1)
  CM=PI/CN
  SN=SIN(CN)
  CS=COS(CN)
  CM=FLOAT(MP1-1)
  CM=PI/CM
  SM=SIN(CM)
  CS=COS(CM)
  AL1=S(1)/FLOAT(N/2)
  AL2=S(3)/FLOAT(M)
  THETA=ATAN2((AL2+AL2),AL1)
  CT=COS(THETA)
  ST=SIN(THETA)
  AL2=AL1/(CT+CT)
  PHI1=4.0*S(2)/(S(1)*FLOAT(N/2))
  CI=COS(PHI1)
  SI=SIN(PHI1)
  PHI2=PHI1*CT/2.0+4.0*S(4)*ST/(S(3)*FLOAT(M))
  CJ=COS(PHI2)
  SJ=SIN(PHI2)
  EAL1=PROP1(1)*PROP1(3)/AL1
  EAL2=PROP2(1)*PROP2(3)/AL2
  GJL1=PROP1(2)*PROP1(4)/AL1
  GJL2=PROP2(2)*PROP2(4)/AL2
  EYL1=PROP1(1)*PROP1(5)/AL1
```

```

EYL2=PROP2(1)*PROP2(5)/AL2
EYLL1=EYL1/AL1
EYLL2=EYL2/AL2
EYLLL1=EYLL1/AL1
EYLLL2=EYLL2/AL2
EZL1=PROP1(1)*PROP1(6)/AL1
EZL2=PROP2(1)*PROP2(6)/AL2
EZLL1=EZL1/AL1
EZLL2=EZL2/AL2
EZLLL1=EZLL1/AL1
EZLLL2=EZLL2/AL2

```

FORM MATRIX "V" OF THEORY HERE

```

DO 10 I=1,36
SC(I)=0.0
SV1(I)=0.0
SV2(I)=0.0
10 CONTINUE
SC(1)=2.0*GJL1*CI*CI+4.0*GJL2*CT*CT*CJ*CJ
1+16.0*EYL2*ST*ST+8.0*EZL1*SI*SI+16.0*EZL2*CT*CT*SJ*SJ
SV1(1)=-GJL1*CI*CI-2.0*EZL1*SI*SI
SV2(1)=-GJL2*CT*CT*CJ*CJ+2.0*EYL2*ST*ST-2.0*EZL2*CT*CT*SJ*SJ
SC(2)=4.0*GJL2*ST*ST*CJ*CJ+8.0*EYL1+16.0*EYL2*CT*CT
1+16.0*EZL2*ST*ST*SJ*SJ
SV1(2)=2.0*EYL1
SV2(2)=-GJL2*ST*ST*CJ*CJ+2.0*EYL2*CT*CT-2.0*EZL2*ST*ST*SJ*SJ
SC(3)=2.0*GJL1*SI*SI+4.0*GJL2*SJ*SJ+8.0*EZL1*CI*CI+16.0*EZL2*CJ*CJ
SV1(3)=GJL1*SI*SI+2.0*EZL1*CI*CI
SV2(3)=GJL2*SJ*SJ+2.0*EZL2*CJ*CJ
SC(4)=2.0*EAL1*CI*CI+4.0*EAL2*CT*CT*CJ*CJ
1+24.0*EYLLL1*SI*SI+48.0*EYLLL2*CT*CT*SJ*SJ+48.0*EZLLL2*ST*ST
SV1(4)=-EAL1*CI*CI+12.0*EYLLL1*SI*SI
SV2(4)=-EAL2*CT*CT*CJ*CJ+12.0*EYLLL2*CT*CT*SJ*SJ-12.0*EZLLL2*ST*ST
SC(5)=4.0*EAL2*ST*ST*CJ*CJ+48.0*EYLLL2*ST*ST*SJ*SJ
1+24.0*EZLLL1+48.0*EZLLL2*CT*CT
SV1(5)=-12.0*EZLLL1
SV2(5)=-EAL2*ST*ST*CJ*CJ+12.0*EYLLL2*ST*ST*SJ*SJ-12.0*EZLLL2*CT*CT
SC(6)=2.0*EAL1*SI*SI+4.0*EAL2*SJ*SJ
1+24.0*EYLLL1*CI*CI+48.0*EYLLL2*CJ*CJ
SV1(6)=EAL1*SI*SI-12.0*EYLLL1*CI*CI
SV2(6)=EAL2*SJ*SJ-12.0*EYLLL2*CJ*CJ
SV2(7)=GJL2*CT*CT*CJ*CJ+2.0*EYL2*CT*ST+2.0*EZL2*CT*ST*SJ*SJ
SV2(8)=+GJL2*ST*CT*SJ-2.0*EZL2*ST*CT*SJ
SV2(9)=6.0*EZLL2*ST*CT
SV2(10)=EAL2*CT*ST*CT*CJ-12.0*EYLLL2*CT*ST*SJ*SJ-12.0*EZLLL2*CT*ST
SV2(11)=-EAL2*ST*CT*SJ-12.0*EYLLL2*ST*CT*SJ
SV1(13)=+GJL1*CI*SI-2.0*EZL1*CI*SI
SV2(13)=+GJL2*CT*CT*SJ-2.0*EZL2*CT*CT*SJ
SC(14)=-12.0*EYLL1*SI-24.0*EYLL2*CT*CT*SJ-24.0*EZLL2*ST*ST*SJ
SV1(14)=-6.0*EYLL1*SI
SV2(14)=-6.0*EYLL2*CT*CT*SJ+6.0*EZLL2*ST*ST*SJ

```

```

SV1(15)=-6.0*EZLL1*CI
SV2(15)=-6.0*EZLL2*CT*CT
SV1(16)=-EAL1*CI*SI+12.0*EYLLL1*CI*SI
SV2(16)=-EAL2*CT*CT*SJ-12.0*EYLLL2*CT*CT*SJ
SV2(19)=-6.0*EYLL2*CT*ST*SJ-6.0*EZLL2*CT*ST*SJ
SV2(20)=+6.0*EYLL2*CT*ST*SJ+6.0*EZLL2*CT*ST*SJ
SC(25)=+24.0*EYLL2*ST*ST*SJ+12.0*EZLL1*SI+24.0*EZLL2*CT*CT*SJ
SV1(25)=-6.0*EZLL1*SI
SV2(25)=+6.0*EYLL2*CT*ST*SJ-6.0*EZLL2*CT*CT*SJ
SV1(26)=+6.0*EYLL1*CI
SV2(26)=+6.0*EYLL2*CT*CT
SV2(31)=-6.0*EYLL2*ST*CT
DO 15 I=1,36
SV1(I)=2.0*SV1(I)
SV2(I)=4.0*SV2(I)

```

15 CONTINUE

FORM MEMBER ACTION MATRICIES HERE

```

CALL STIFM6(SR,SS,1,1.0,0.0,CI,SI,EAL1,GJL1,EYL1,EYLL1,EYLLL1,
1EZL1,EZLL1,EZLLL1)
CALL STIFM6(SR,SS,2,CT,ST,CJ,SJ,EAL2,GJL2,EYL2,EYLL2,EYLLL2,EZL2,
1EZLL2,EZLLL2)
CALL STIFM6(SR,SS,3,-CT,ST,CJ,SJ,EAL2,GJL2,EYL2,EYLL2,EYLLL2,EZL2,
1EZLL2,EZLLL2)
RETURN
999 CONTINUE
RETURN
1020 FORMAT(7H N ,114,5X,7H M ,114/7H A ,1PE14.5,5X,
*7H HX ,1PE14.5/7H B ,1PE14.5,5X,7H HY ,1PE14.5)
1030 FORMAT(/8X,17HMEMBER PROPERTIES//6X,8HMEMBER 1,7X,8HMEMBER 2,
*/5H E ,1PE10.3,5X,1PE10.3,
*/5H G ,1PE10.3,5X,1PE10.3,
*/5H AR ,1PE10.3,5X,1PE10.3,
*/5H IX ,1PE10.3,5X,1PE10.3,
*/5H IY ,1PE10.3,5X,1PE10.3,
*/5H IZ ,1PE10.3,5X,1PE10.3)
END

```

SUBROUTINE STIFM6(SR,SS,N,CT,ST,CP,SP,EA,GJ,EY1,EY2,EY3,EZ1,EZ2,
EZ3)

C
C
C

THIS ROUTINE FORMS MEMBER ACTION MATRICIES

DIMENSION SR(12,12,3),SS(12,12,3),T(12,12)

DO 10 I=1,12

DO 10 J=1,12

T(I,J)=0.0

SS(I,J,N)=0.0

SR(I,J,N)=0.0

10 CONTINUE

SS(1,1,N)=GJ

SS(1,7,N)=-GJ

SS(2,2,N)=4.0*EY1

SS(2,6,N)=-6.0*EY2

SS(2,8,N)=2.0*EY1

SS(2,12,N)=6.0*EY2

SS(3,3,N)=4.0*EZ1

SS(3,5,N)=6.0*EZ2

SS(3,9,N)=2.0*EZ1

SS(3,11,N)=-6.0*EZ2

SS(4,4,N)=EA

SS(4,10,N)=-EA

SS(5,3,N)=6.0*EZ2

SS(5,5,N)=12.0*EZ3

SS(5,9,N)=6.0*EZ2

SS(5,11,N)=-12.0*EZ3

SS(6,2,N)=-6.0*EY2

SS(6,6,N)=12.0*EY3

SS(6,8,N)=-6.0*EY2

SS(6,12,N)=-12.0*EY3

SS(7,1,N)=-GJ

SS(7,7,N)=GJ

SS(8,2,N)=2.0*EY1

SS(8,6,N)=-6.0*EY2

SS(8,8,N)=4.0*EY1

SS(8,12,N)=6.0*EY2

SS(9,3,N)=2.0*EZ1

SS(9,5,N)=6.0*EZ2

SS(9,9,N)=4.0*EZ1

SS(9,11,N)=-6.0*EZ2

SS(10,4,N)=-EA

SS(10,10,N)=EA

SS(11,3,N)=-6.0*EZ2

SS(11,5,N)=-12.0*EZ3

SS(11,9,N)=6.0*EZ2

SS(11,11,N)=12.0*EZ3

SS(12,2,N)=6.0*EY2

SS(12,6,N)=-12.0*EY3

SS(12,8,N)=6.0*EY2

SS(12,12,N)=12.0*EY3

T(1,1)=CT*CP

T(2,1)=-ST

T(3,1)=CT*SP

T(1,2)=ST*CP

T(2,2)=CT

T(3,2)=ST*SP

T(1,3)=-SP

T(3,3)=CP

T(7,7)=CT*CP

T(8,7)=-ST

T(9,7)=-CT*SP

T(7,8)=ST*CP

T(8,8)=CT

T(9,8)=-ST*SP

T(7,9)=SP

T(9,9)=CP

DO 20 I=1,3

DO 20 J=1,3

T(I+3,J+3)=T(I,J)

T(I+9,J+9)=T(I+6,J+6)

20 CONTINUE

DO 30 I=1,12

DO 30 J=1,12

TEMP=0.0

DO 40 K=1,12

TEMP=TEMP+SS(I,K,N)*T(K,J)

40 CONTINUE

SR(I,J,N)=TEMP

30 CONTINUE

DO 50 I=1,12

DO 50 J=1,12

TEMP=0.0

DO 60 K=1,12

TEMP=TEMP+T(K,I)*SR(K,J,N)

60 CONTINUE

SS(I,J,N)=TEMP

50 CONTINUE

RETURN

END


```

C
C
C
SUBROUTINE LOADG6(NP1,MP1,P,PB)

THIS ROUTINE INPUTS A GENERAL LOAD CASE AND
DECOMPOSES IT INTO ITS FOURIER COMPONENTS

COMMON/DATA1/CH,SN,CM,SM
DIMENSION P(6,MP1,NP1)
DIMENSION PB(6,MP1,NP1)
DIMENSION S(6),NN(2),PN(6),PH(6)
ANM=(NP1-1)*(MP1-1)
ANM=4.0/ANM
DO 10 I=1,NP1
DO 20 J=1,MP1
DO 5 K=1,6
P(K,J,I)=0.0
25 CONTINUE
20 CONTINUE
10 CONTINUE
30 CONTINUE
READ(5,2000) I,J,(S(K),K=1,6)
2000 FORMAT(2I10,6F10.0)
IF((I.GT.NP1).OR.(J.GT.MP1))GO TO 40
IF((I.LT.0).OR.(J.LT.0))GO TO 30
IP=I+1
JP=J+1
DO 35 K=1,6
P(K,JP,IP)=S(K)
35 CONTINUE
WRITE(6,1010)I,J,(S(K),K=1,6)
GO TO 30
40 CONTINUE
DO 50 J=1,MP1
P(2,J,1)=P(2,J,1)/2.0
P(3,J,1)=P(3,J,1)/2.0
P(4,J,1)=P(4,J,1)/2.0
P(2,J,NP1)=P(2,J,NP1)/2.0
P(3,J,NP1)=P(3,J,NP1)/2.0
P(4,J,NP1)=P(4,J,NP1)/2.0
50 CONTINUE
DO 60 I=1,NP1
P(1,1,I)=P(1,1,I)/2.0
P(3,1,I)=P(3,1,I)/2.0
P(5,1,I)=P(5,1,I)/2.0
P(1,MP1,I)=P(1,MP1,I)/2.0
P(3,MP1,I)=P(3,MP1,I)/2.0
P(5,MP1,I)=P(5,MP1,I)/2.0
60 CONTINUE
CII=1.0
SII=0.0
DO 70 I=1,NP1
C1J=1.0
S1J=0.0

```

```

DO 80 J=1,MP1
C1IN=1.0
S1IN=0.0
DO 65 K=1,6
PN(K)=0.0
65 CONTINUE
DO 90 N=1,NP1
C1JM=1.0
S1JM=0.0
DO 75 K=1,6
PM(K)=0.0
75 CONTINUE
DO 100 M=1,MP1
PH(1)=PM(1)+P(1,M,N)*C1JM
PH(2)=PM(2)+P(2,M,N)*S1JM
PH(3)=PM(3)+P(3,M,N)*C1JM
PH(4)=PM(4)+P(4,M,N)*S1JM
PH(5)=PM(5)+P(5,M,N)*C1JM
PH(6)=PM(6)+P(6,M,N)*S1JM
TEMP=C1JM*C1J-S1JM*S1J
S1JM=S1JM*C1J+C1JM*S1J
C1JM=TEMP
100 CONTINUE
PN(1)=PN(1)+PM(1)*S1IN
PN(2)=PN(2)+PM(2)*C1IN
PN(3)=PN(3)+PM(3)*C1IN
PN(4)=PN(4)+PM(4)*C1IN
PN(5)=PN(5)+PM(5)*S1IN
PN(6)=PN(6)+PM(6)*S1IN
TEMP=C1IN*C1I-S1IN*S1I
S1IN=S1IN*C1I+C1IN*S1I
C1IN=TEMP
90 CONTINUE
DO 95 K=1,6
PB(K,J,I)=PN(K)*ANM
95 CONTINUE
TEMP=C1J*CM-S1J*SM
S1J=S1J*CM+C1J*SM
C1J=TEMP
80 CONTINUE
TEMP=C1I*CN-S1I*SN
S1I=S1I*CN+C1I*SN
C1I=TEMP
70 CONTINUE
DO 110 J=1,MP1
PB(2,J,1)=PB(2,J,1)/2.0
PB(3,J,1)=PB(3,J,1)/2.0
PB(4,J,1)=PB(4,J,1)/2.0
PB(2,J,NP1)=PB(2,J,NP1)/2.0
PB(3,J,NP1)=PB(3,J,NP1)/2.0
PB(4,J,NP1)=PB(4,J,NP1)/2.0
P(2,J,1)=P(2,J,1)*2.0

```

```

P(3,J,1)=P(3,J,1)*2.0
P(4,J,1)=P(4,J,1)*2.0
P(2,J,NP1)=P(2,J,NP1)*2.0
P(3,J,NP1)=P(3,J,NP1)*2.0
P(4,J,NP1)=P(4,J,NP1)*2.0
110 CONTINUE
DO 120 I=1,NP1
  PS(1,1,I)=PB(1,1,I)/2.0
  PE(3,1,I)=PE(3,1,I)/2.0
  PS(5,1,I)=PB(5,1,I)/2.0
  PB(1,MP1,I)=PB(1,MP1,I)/2.0
  PB(3,MP1,I)=PB(3,MP1,I)/2.0
  PB(5,MP1,I)=PB(5,MP1,I)/2.0
  P(1,1,I)=P(1,1,I)*2.0
  P(3,1,I)=P(3,1,I)*2.0
  P(5,1,I)=P(5,1,I)*2.0
  P(1,MP1,I)=P(1,MP1,I)*2.0
  P(3,MP1,I)=P(3,MP1,I)*2.0
  P(5,MP1,I)=P(5,MP1,I)*2.0
120 CONTINUE
RETURN
999 CONTINUE
RETURN
1000 FORMAT(21H1LOAD CASE -GENERAL-,10X,13A6,A2)
1010 FORMAT(218,1P6E15.5)
END

```

```

C SUBROUTINE LOADP6(NP1,MP1,P,PB)
C THIS ROUTINE INPUTS A POINT LOAD CASE AND
C DECOMPOSES IT INTO ITS FOURIER COMPONENTS
C
COMMON/DATA1/CN,SN,CM,SM
DIMENSION P(6,MP1,NP1)
DIMENSION PB(6,MP1,NP1)
DIMENSION S(6),NN(2),PN(6),PM(6)
ANN=(NP1-1)*(NP1-1)
ANN=4.0/ANN
DO 10 I=1,NP1
DO 20 J=1,MP1
DO 25 K=1,6
  P(K,J,I)=0.0
25 CONTINUE
20 CONTINUE
10 CONTINUE
READ(5,2000) NN(1),NN(2),(S(K),K=1,6)
2000 FORMAT(2I10,6F10.0)
WRITE(6,1010) NN(1),NN(2),(S(K),K=1,6)
I=NN(1)+1
J=NN(2)+1
DO 35 K=1,6
  P(K,J,I)=S(K)
35 CONTINUE
C11N=1.0
S11N=0.0
N=1
30 CONTINUE
IF (N.GE.1) GO TO 40
TEMP=C11N*CN-S11N*SN
S11N=S11N*CN+C11N*SN
C11N=TEMP
N=N+1
GO TO 30
40 CONTINUE
C1JM=1.0
S1JM=0.0
M=1
50 CONTINUE
IF (M.GE.J) GO TO 60
TEMP=C1JM*CM-S1JM*SM
S1JM=S1JM*CM+C1JM*SM
C1JM=TEMP
M=M+1
GO TO 50
60 CONTINUE
DO 65 K=1,6
  PN(K)=S(K)*ANN
65 CONTINUE
IF ((I.NE.1).AND.(I.NE.NP1)) GO TO 67

```

```

PN(2)=PN(2)/2.0
PN(3)=PN(3)/2.0
PN(4)=PN(4)/2.0
67 CONTINUE
IF((J.NE.1).AND.(J.NE.MP1)) GO TO 69
PN(1)=PN(1)/2.0
PN(3)=PN(3)/2.0
PN(5)=PN(5)/2.0
69 CONTINUE
CII=1.0
SII=0.0
DO 70 I=1,MP1
PN(1)=PN(1)*SII
PN(2)=PN(2)*CII
PN(3)=PN(3)*CII
PN(4)=PN(4)*CII
PN(5)=PN(5)*SII
PN(6)=PN(6)*SII
CIJ=1.0
SIJ=0.0
DO 80 J=1,MP1
PB(1,J,I)=PN(1)*CIJ
PB(2,J,I)=PN(2)*SIJ
PB(3,J,I)=PN(3)*CIJ
PB(4,J,I)=PN(4)*SIJ
PB(5,J,I)=PN(5)*CIJ
PB(6,J,I)=PN(6)*SIJ
TEMP=CIJ*CIJ+SIJ*SIJ
SIJ=SIJ*CIJ+CIJ*SIJ
CIJ=TEMP
80 CONTINUE
TEMP=CII*CII+SII*SII
SII=SII*CII+CII*SII
CII=TEMP
70 CONTINUE
DO 110 J=1,MP1
PB(2,J,I)=PB(2,J,I)/2.0
PB(3,J,I)=PB(3,J,I)/2.0
PB(4,J,I)=PB(4,J,I)/2.0
PB(2,J,MP1)=PB(2,J,MP1)/2.0
PB(3,J,MP1)=PB(3,J,MP1)/2.0
PB(4,J,MP1)=PB(4,J,MP1)/2.0
110 CONTINUE
DO 120 I=1,MP1
PB(1,I,I)=PB(1,I,I)/2.0
PB(3,I,I)=PB(3,I,I)/2.0
PB(5,I,I)=PB(5,I,I)/2.0
PB(1,MP1,I)=PB(1,MP1,I)/2.0
PB(3,MP1,I)=PB(3,MP1,I)/2.0
PB(5,MP1,I)=PB(5,MP1,I)/2.0
120 CONTINUE
RETURN

```

```

999 CONTINUE
RETURN
1000 FORMAT(21H1LOAD CASE -POINT- ,10X,13A6,A2)
1010 FORMAT(16HOPPOINT LOAD AT (,I4,1H,,I4,5H) OF ,1P6E15.5)
END

```

```

C      SUBROUTINE LOADU6(NP1,MP1,P,PB)
C
C      THIS ROUTINE INPUTS A UNIFORM LOAD CASE AND
C      DECOMPOSES IT INTO ITS FOURIER COMPONENTS
C
COMMON/DATA1/CN,SN,CN,SM
DIMENSION P(6,MP1,NP1)
DIMENSION PB(6,MP1,NP1)
DIMENSION S(6),NN(2)
AN=1.0/FLOAT(NP1-1)
AM=1.0/FLOAT(MP1-1)
2000 READ(5,2000) (S(K),K=1,6)
      FORMAT(20X,6F10.0)
      WRITE(6,1010) (S(K),K=1,6)
      DO 10 I=1,NP1
      DO 20 J=1,MP1
      DO 25 K=1,6
      P(K,J,I)=0.0
      PB(K,J,I)=0.0
25  CONTINUE
      L=I+J
      IF ((L/2)*2.NE.L) GO TO 40
      DO 35 K=1,6
      P(K,J,I)=S(K)
35  CONTINUE
40  CONTINUE
20  CONTINUE
10  CONTINUE
      C1I=1.0
      S1I=0.0
      DO 50 I=1,NP1
      IF ((I/2)*2.NE.I) GO TO 60
      CT=(1.0+C1I)/S1I
      TC=1.0/CT
      PB(1,1,I)=AN*CT
      PB(1,MP1,I)=-AN*TC
60  CONTINUE
      TEMP=C1I*CN-S1I*SN
      S1I=S1I*CN+C1I*SN
      C1I=TEMP
50  CONTINUE
      C1J=1.0
      S1J=0.0
      DO 70 J=1,MP1
      IF ((J/2)*2.NE.J) GO TO 80
      CT=(1.0+C1J)/S1J
      TC=1.0/CT
      PB(2,J,1)=AM*CT
      PB(2,J,MP1)=-AM*TC
80  CONTINUE
      TEMP=C1J*CM-S1J*SM
      S1J=S1J*CM+C1J*SM

```

```

      C1J=TEMP
70  CONTINUE
      DO 90 I=1,NP1
      IF ((I/2)*2.NE.I) GO TO 90
      DO 100 J=1,MP1
      IF ((J/2)*2.NE.J) GO TO 100
      PB(6,J,I)=PB(1,1,I)*PB(2,J,1)+PB(1,MP1,I)*PB(2,J,MP1)*2.0*S(6)
100 CONTINUE
90  CONTINUE
      PB(3,1,1)=S(3)/2.0
      PB(3,MP1,NP1)=S(3)/2.0
      DO 110 I=1,NP1
      PB(5,1,I)=PB(1,1,I)*S(5)
      PB(1,1,I)=PB(1,1,I)*S(1)
      PB(5,MP1,I)=PB(1,MP1,I)*S(5)
      PB(1,MP1,I)=PB(1,MP1,I)*S(1)
110 CONTINUE
      DO 120 J=1,MP1
      PB(4,J,1)=PB(2,J,1)*S(4)
      PB(2,J,1)=PB(2,J,1)*S(2)
      PB(4,J,NP1)=PB(2,J,NP1)*S(4)
      PB(2,J,NP1)=PB(2,J,NP1)*S(2)
120 CONTINUE
      RETURN
999 CONTINUE
      RETURN
1000 FORMAT(21HLOAD CASE -UNIFORM-,10X,13A6,A2)
1010 FORMAT(17HUNIFORM LOAD OF ,1P6E15.5)
      END

```

SUBROUTINE SOLVE6(NP1,MP1,PB,DB)

THIS ROUTINE TRANSFORMS THE LOAD FOURIER COEFFICIENTS INTO
DISPLACEMENT FOURIER COEFFICIENTS USING MATRIX "C"

COMMON/DATA1/CN,SN,CN,SN

COMMON/DATA2/SC(36),SV1(36),SV2(36)

DIMENSION PB(6,MP1,NP1)

DIMENSION DB(6,MP1,NP1)

DIMENSION S(36),T(6)

C11=1.0

S11=0.0

DO 10 I=1,NP1

C1J=1.0

S1J=0.0

DO 20 J=1,MP1

DO 50 K=1,6

DB(K,J,I)=0.0

T(K)=PB(K,J,I)

50 CONTINUE

IF(((I.EQ.1).OR.(I.EQ.NP1)).AND.((J.EQ.1).OR.(J.EQ.MP1))) GO TO 25

DO 55 K=1,36

S(K)=0.0

55 CONTINUE

C12=2.0*C11*C11-1.0

S12=2.0*S11*C11

C1CJ=C11*C1J

C1SJ=C11*S1J

S1CJ=S11*C1J

S1SJ=S11*S1J

S(1)=SC(1)+SV1(1)*C12+SV2(1)*C1CJ

S(2)=SC(2)+SV1(2)*C12+SV2(2)*C1CJ

S(3)=SC(3)+SV1(3)*C12+SV2(3)*C1CJ

S(4)=SC(4)+SV1(4)*C12+SV2(4)*C1CJ

S(5)=SC(5)+SV1(5)*C12+SV2(5)*C1CJ

S(6)=SC(6)+SV1(6)*C12+SV2(6)*C1CJ

S(7)=SV2(7)*S1SJ

S(8)=SV2(8)*C1SJ

S(9)=SV2(9)*C1SJ

S(10)=SV2(10)*S1SJ

S(11)=SV2(11)*C1SJ

S(12)=SV1(12)*S12+SV2(12)*S1CJ

S(13)=SV1(13)*S12+SV2(13)*S1CJ

S(14)=SC(14)+SV1(14)*C12+SV2(14)*C1CJ

S(15)=SV1(15)*S12+SV2(15)*S1CJ

S(16)=SV1(16)*S12+SV2(16)*S1CJ

S(17)=SV2(17)*S1SJ

S(18)=SV2(18)*C1SJ

S(19)=SV2(19)*C1SJ

S(20)=SV2(20)*S1SJ

S(21)=SC(21)+SV1(21)*C12+SV2(21)*C1CJ

S(22)=SV1(22)*S12+SV2(22)*S1CJ

S(23)=SV1(23)*S12+SV2(23)*S1CJ

S(24)=SV2(24)*S1SJ

S(25)=SV2(25)*C1SJ

S(26)=SV2(26)*C1SJ

S(27)=SV2(27)*S1SJ

S(28)=SV2(28)*C1SJ

S(29)=SV2(29)*C1SJ

S(30)=SV2(30)*S1SJ

S(31)=SV2(31)*C1SJ

S(32)=SV2(32)*C1SJ

S(33)=SV2(33)*S1SJ

S(34)=SV2(34)*C1SJ

S(35)=SV2(35)*C1SJ

S(36)=SV2(36)*S1SJ

S(37)=SV2(37)*C1SJ

S(38)=SV2(38)*C1SJ

S(39)=SV2(39)*S1SJ

S(40)=SV2(40)*C1SJ

S(41)=SV2(41)*C1SJ

S(42)=SV2(42)*S1SJ

S(43)=SV2(43)*C1SJ

S(44)=SV2(44)*C1SJ

S(45)=SV2(45)*S1SJ

S(46)=SV2(46)*C1SJ

S(47)=SV2(47)*C1SJ

S(48)=SV2(48)*S1SJ

S(49)=SV2(49)*C1SJ

S(50)=SV2(50)*C1SJ

S(51)=SV2(51)*S1SJ

S(52)=SV2(52)*C1SJ

S(53)=SV2(53)*C1SJ

S(54)=SV2(54)*S1SJ

S(55)=SV2(55)*C1SJ

S(56)=SV2(56)*C1SJ

S(57)=SV2(57)*S1SJ

S(58)=SV2(58)*C1SJ

S(59)=SV2(59)*C1SJ

S(60)=SV2(60)*S1SJ

S(61)=SV2(61)*C1SJ

S(62)=SV2(62)*C1SJ

S(63)=SV2(63)*S1SJ

S(64)=SV2(64)*C1SJ

S(65)=SV2(65)*C1SJ

S(66)=SV2(66)*S1SJ

S(67)=SV2(67)*C1SJ

S(68)=SV2(68)*C1SJ

S(69)=SV2(69)*S1SJ

S(70)=SV2(70)*C1SJ

S(71)=SV2(71)*C1SJ

S(72)=SV2(72)*S1SJ

S(73)=SV2(73)*C1SJ

S(74)=SV2(74)*C1SJ

S(75)=SV2(75)*S1SJ

S(76)=SV2(76)*C1SJ

S(77)=SV2(77)*C1SJ

S(78)=SV2(78)*S1SJ

S(79)=SV2(79)*C1SJ

S(80)=SV2(80)*C1SJ

S(81)=SV2(81)*S1SJ

S(82)=SV2(82)*C1SJ

S(83)=SV2(83)*C1SJ

S(84)=SV2(84)*S1SJ

S(85)=SV2(85)*C1SJ

S(86)=SV2(86)*C1SJ

S(87)=SV2(87)*S1SJ

S(88)=SV2(88)*C1SJ

S(89)=SV2(89)*C1SJ

S(90)=SV2(90)*S1SJ

S(91)=SV2(91)*C1SJ

S(92)=SV2(92)*C1SJ

S(93)=SV2(93)*S1SJ

S(94)=SV2(94)*C1SJ

S(95)=SV2(95)*C1SJ

S(96)=SV2(96)*S1SJ

S(97)=SV2(97)*C1SJ

S(98)=SV2(98)*C1SJ

S(99)=SV2(99)*S1SJ

S(100)=SV2(100)*C1SJ

S(101)=SV2(101)*C1SJ

S(102)=SV2(102)*S1SJ

S(103)=SV2(103)*C1SJ

S(104)=SV2(104)*C1SJ

S(105)=SV2(105)*S1SJ

S(106)=SV2(106)*C1SJ

S(107)=SV2(107)*C1SJ

S(108)=SV2(108)*S1SJ

S(109)=SV2(109)*C1SJ

S(110)=SV2(110)*C1SJ

S(111)=SV2(111)*S1SJ

S(112)=SV2(112)*C1SJ

S(113)=SV2(113)*C1SJ

S(114)=SV2(114)*S1SJ

S(115)=SV2(115)*C1SJ

S(116)=SV2(116)*C1SJ

S(117)=SV2(117)*S1SJ

S(118)=SV2(118)*C1SJ

S(119)=SV2(119)*C1SJ

S(120)=SV2(120)*S1SJ

S(121)=SV2(121)*C1SJ

S(122)=SV2(122)*C1SJ

S(123)=SV2(123)*S1SJ

S(124)=SV2(124)*C1SJ

S(125)=SV2(125)*C1SJ

S(126)=SV2(126)*S1SJ

S(127)=SV2(127)*C1SJ

S(128)=SV2(128)*C1SJ

S(129)=SV2(129)*S1SJ

S(130)=SV2(130)*C1SJ

S(131)=SV2(131)*C1SJ

S(132)=SV2(132)*S1SJ

S(133)=SV2(133)*C1SJ

S(134)=SV2(134)*C1SJ

S(135)=SV2(135)*S1SJ

S(136)=SV2(136)*C1SJ

S(137)=SV2(137)*C1SJ

S(138)=SV2(138)*S1SJ

S(139)=SV2(139)*C1SJ

S(140)=SV2(140)*C1SJ

S(141)=SV2(141)*S1SJ

S(142)=SV2(142)*C1SJ

S(143)=SV2(143)*C1SJ

S(144)=SV2(144)*S1SJ

S(145)=SV2(145)*C1SJ

S(146)=SV2(146)*C1SJ

S(147)=SV2(147)*S1SJ

S(148)=SV2(148)*C1SJ

S(149)=SV2(149)*C1SJ

S(150)=SV2(150)*S1SJ

S(151)=SV2(151)*C1SJ

S(152)=SV2(152)*C1SJ

S(153)=SV2(153)*S1SJ

S(154)=SV2(154)*C1SJ

S(155)=SV2(155)*C1SJ

S(156)=SV2(156)*S1SJ

S(157)=SV2(157)*C1SJ

S(158)=SV2(158)*C1SJ

S(159)=SV2(159)*S1SJ

S(160)=SV2(160)*C1SJ

S(161)=SV2(161)*C1SJ

S(162)=SV2(162)*S1SJ

S(163)=SV2(163)*C1SJ

S(164)=SV2(164)*C1SJ

S(165)=SV2(165)*S1SJ

S(166)=SV2(166)*C1SJ

S(167)=SV2(167)*C1SJ

S(168)=SV2(168)*S1SJ

S(169)=SV2(169)*C1SJ

S(170)=SV2(170)*C1SJ

S(171)=SV2(171)*S1SJ

S(172)=SV2(172)*C1SJ

S(173)=SV2(173)*C1SJ

S(174)=SV2(174)*S1SJ

S(175)=SV2(175)*C1SJ

S(176)=SV2(176)*C1SJ

S(177)=SV2(177)*S1SJ

S(178)=SV2(178)*C1SJ

S(179)=SV2(179)*C1SJ

S(180)=SV2(180)*S1SJ

S(181)=SV2(181)*C1SJ

S(182)=SV2(182)*C1SJ

S(183)=SV2(183)*S1SJ

S(184)=SV2(184)*C1SJ

S(185)=SV2(185)*C1SJ

S(186)=SV2(186)*S1SJ

S(187)=SV2(187)*C1SJ

S(188)=SV2(188)*C1SJ

S(189)=SV2(189)*S1SJ

S(190)=SV2(190)*C1SJ

S(191)=SV2(191)*C1SJ

S(192)=SV2(192)*S1SJ

S(193)=SV2(193)*C1SJ

S(194)=SV2(194)*C1SJ

S(195)=SV2(195)*S1SJ

S(196)=SV2(196)*C1SJ

S(197)=SV2(197)*C1SJ

S(198)=SV2(198)*S1SJ

S(199)=SV2(199)*C1SJ

S(200)=SV2(200)*C1SJ

S(201)=SV2(201)*S1SJ

S(202)=SV2(202)*C1SJ

S(203)=SV2(203)*C1SJ

S(204)=SV2(204)*S1SJ

S(205)=SV2(205)*C1SJ

S(206)=SV2(206)*C1SJ

S(207)=SV2(207)*S1SJ

```

C      SUBROUTINE SYMSOL(NN,MM,KKK,A,B)
C      *****
C      BANDED SYMMETRIC MATRIX EQUATION SOLVER CROUT METHOD
C      *****
C      DIMENSION A(100),B(100)
C      LOC(I,J)=I+(J-1)*NN
C      GO TO (1000,2000),KKK
C
C      REDUCE MATRIX
1000 DO 260 N= 1,NN
      NI = LOC(N,1)
      DO 260 L = 2,MM
        NL = LOC(N,L)
        C=A(NL)/A(NI)
        I=N+L-1
        IF(MM.LT.I)GO TO 260
        J=0
        DO 250 K=L,MM
          J=J+1
          IJ=LOC(I,J)
          NK=LOC(N,K)
250   A(IJ)=A(IJ)-C*A(NK)
260   A(NL)=C
260   CONTINUE
      GO TO 500
C
C      REDUCE VECTOR
2000 DO 290 N=1,NN
      NI=LOC(N,1)
      DO 285 L=2,MM
        NL=LOC(N,L)
        I=N+L-1
        IF(MM.LT.I)GO TO 290
285   B(I)=B(I)-A(NL)*B(N)
290   B(N)=B(N)/A(NI)
C
C      BACK SUBSTITUTION
C      N=NN
300 N=N-1
      IF(N.EQ.0)GO TO 500
      DO 400 K=2,MM
        NK=LOC(N,K)
        L=N+K-1
        IF(MM.LT.L)GO TO 400
        B(N)=B(N)-A(NK)*B(L)
400   CONTINUE
      GO TO 300
C
500 RETURN
      END

```

```

C
C
C
SUBROUTINE DISPT6(NP1,MP1,DB,D)
THIS ROUTINE EVALUATES THE DISPLACEMENT FOURIER SERIES
AND OUTPUTS THE DISPLACEMENTS
COMMON/DATA1/CH,SN,CM,SM
DIMENSION D(6,MP1,NP1)
DIMENSION DB(6,MP1,NP1)
DIMENSION DN(6),DM(6)
WRITE(6,1000)
C1I=1.0
S1I=0.0
DO 10 I=1,NP1
  C1J=1.0
  S1J=0.0
  DO 20 J=1,MP1
    DO 5 K=1,6
      DN(K)=0.0
5 CONTINUE
  K=I+J
  IF ((K/2)*2.NE.K) GO TO 25
  C1IN=1.0
  S1IN=0.0
  DO 30 N=1,NP1
    DO 15 K=1,6
      DM(K)=0.0
15 CONTINUE
    C1JM=1.0
    S1JM=0.0
    DO 40 M=1,MP1
      DM(1)=DM(1)+DB(1,M,N)*C1JM
      DM(2)=DM(2)+DB(2,M,N)*S1JM
      DM(3)=DM(3)+DB(3,M,N)*C1JM
      DM(4)=DM(4)+DB(4,M,N)*S1JM
      DM(5)=DM(5)+DB(5,M,N)*C1JM
      DM(6)=DM(6)+DB(6,M,N)*S1JM
      C2JM=C1JM*C1J-S1JM*S1J
      S2JM=S1JM*C1J+C1JM*S1J
      C1JM=C2JM
      S1JM=S2JM
40 CONTINUE
    DM(1)=DM(1)+DM(1)*S1IN
    DM(2)=DM(2)+DM(2)*C1IN
    DM(3)=DM(3)+DM(3)*C1IN
    DM(4)=DM(4)+DM(4)*C1IN
    DM(5)=DM(5)+DM(5)*S1IN
    DM(6)=DM(6)+DM(6)*S1IN
    C2IN=C1IN*C1I-S1IN*S1I
    S2IN=S1IN*C1I+C1IN*S1I
    C1IN=C2IN
    S1IN=S2IN
30 CONTINUE

```

```

IM1=I-1
JM1=J-1
WRITE(6,1010) IM1,JM1,(DN(K),K=1,6)
25 CONTINUE
DO 35 K=1,6
  D(K,J,I)=DN(K)
35 CONTINUE
  C2J=C1J*CM-S1J*SM
  S2J=S1J*CM+C1J*SM
  C1J=C2J
  S1J=S2J
20 CONTINUE
  C2I=C1I*CN-S1I*SN
  S2I=S1I*CN+C1I*SN
  C1I=C2I
  S1I=S2I
10 CONTINUE
  RETURN
1000 FORMAT(1H1,13HDISPLACEMENTS//5X,1H1,4X,1HJ,4X,1OHX ROTATION,5X,
* 1OHY ROTATION,5X,1OHZ ROTATION,6X,8HX DISPLT,7X,8HY DISPLT,7X,
* 8HZ DISPLT)
1010 FORMAT(1X,2I5,1P6E15.5)
END

```

C
C
C

```

SUBROUTINE MEMB6(NP1,MP1,D)
THIS ROUTINE CALCULATES THE MEMBER ACTIONS FROM THE JOINT
DISPLACEMENTS AND OUTPUTS THEM

COMMON/DATA3/SR(12,12,3)
DIMENSION D(6,MP1,NP1)
DIMENSION T(12,3),S(8,3)
WRITE(6,1000)
DO 10 I=1,NP1
DO 20 J=1,MP1
DO 5 K=1,3
DO 5 M=1,12
T(M,K)=0.0
5 CONTINUE
L=I+J
IF((L/2)*2.NE.L)GO TO 30
IF (I.EQ.NP1) GO TO 40
IF ((J.EQ.1).OR.(J.EQ.MP1)) GO TO 43
IF (I.EQ.(NP1-1)) GO TO 46
DO 41 N=1,12
DO 42 M=1,6
T(N,1)=T(N,1)-(SR(N,M,1)*D(M,J,I)+SR(N,M+6,1)*D(M,J,I+2))
42 CONTINUE
41 CONTINUE
GO TO 40
43 CONTINUE
DO 44 N=1,12
DO 45 M=1,6
T(N,1)=T(N,1)-(SR(N,M,1)*D(M,J,I)+SR(N,M+6,1)*D(M,J,I+2))/2.0
45 CONTINUE
44 CONTINUE
GO TO 40
46 CONTINUE
DO 47 M=1,12
T(N,1)=T(N,1)-{SR(N,1,1)-SR(N,7,1)}*D(1,J,I)
* -{SR(N,2,1)+SR(N,8,1)}*D(2,J,I)
* -{SR(N,3,1)+SR(N,9,1)}*D(3,J,I)
* -{SR(N,4,1)+SR(N,10,1)}*D(4,J,I)
* -{SR(N,5,1)-SR(N,11,1)}*D(5,J,I)
* -{SR(N,6,1)-SR(N,12,1)}*D(6,J,I)
47 CONTINUE
GO TO 40
40 CONTINUE
IF(J.EQ.MP1.OR.I.EQ.NP1)GO TO 50
DO 51 N=1,12
DO 52 M=1,6
T(N,2)=T(N,2)-(SR(N,M,2)*D(M,J,I)+SR(N,M+6,2)*D(M,J,I+1))
52 CONTINUE
51 CONTINUE
50 CONTINUE
IF(J.EQ.MP1.OR.I.EQ.1)GO TO 60

```

```

DO 61 N=1,12
DO 62 M=1,6
T(N,3)=T(N,3)-(SR(N,M,3)*D(M,J,I)+SR(N,M+6,3)*D(M,J,I+1))
62 CONTINUE
61 CONTINUE
60 CONTINUE
DO 70 K=1,3
S(1,K)=T(4,K)
S(2,K)=T(2,K)
S(3,K)=T(3,K)
S(4,K)=T(1,K)
S(5,K)=T(8,K)
S(6,K)=T(9,K)
S(7,K)=T(5,K)
S(8,K)=T(6,K)
70 CONTINUE
IM1=I-1
JM1=J-1
WRITE(6,1010) IM1,JM1,((S(M,K),M=1,8),K=1,3)
30 CONTINUE
20 CONTINUE
10 CONTINUE
RETURN
1000 FORMAT(1H1,14HMEMBER ACTIONS//5X,1HI,4X,1HJ,4X,10HAXIAL LOAD,7X,
* 6HY BM 1,9X,6HZ BM 1,8X,7HTORSION,9X,6HY BM 2,9X,6HZ BM 2,8X,
* 7HY SHEAR,8X,7HZ SHEAR)
1010 FORMAT(/1X,2I5,1P8E15.5,2(/11X,1P8E15.5))
END

```



```

C
C
C
SUBROUTINE BDRY6(NP1,MP1,D)
THIS ROUTINE CALCULATES THE JOINT RESIDUALS FROM THE JOINT
DISPLACEMENTS AND OUTPUTS THEM

COMMON/DATA4/SS(12,12,3)
DIMENSION D(6,MP1,NP1)
DIMENSION S(6)
WRITE(6,1000)
DO 10 I=1,NP1
DO 20 J=1,MP1
DO 30 K=1,6
S(K)=0.0
30 CONTINUE
L=I+1
IF((L/2)*2.NE.L) GO TO 40
IF (I.EQ.NP1) GO TO 50
IF ((J.EQ.1).OR.(J.EQ.MP1)) GO TO 55
IF (I.EQ.(NP1-1)) GO TO 54
DO 51 K=1,6
DO 52 L=1,6
S(K)=S(K)-(SS(K,L,1)*D(L,J,I)+SS(K,L+6,1)*D(L,J,I+2))
52 CONTINUE
51 CONTINUE
GO TO 50
54 CONTINUE
DO 53 K=1,6
S(K)=S(K)-((SS(K,1,1)-SS(K,7,1))*D(1,J,I)
+((SS(K,2,1)+SS(K,8,1))*D(2,J,I)
* -((SS(K,3,1)+SS(K,9,1))*D(3,J,I)
* -((SS(K,4,1)+SS(K,10,1))*D(4,J,I)
* -((SS(K,5,1)-SS(K,11,1))*D(5,J,I)
* -((SS(K,6,1)-SS(K,12,1))*D(6,J,I)
53 CONTINUE
GO TO 50
55 CONTINUE
DO 56 K=1,6
DO 57 L=1,6
S(K)=S(K)-(SS(K,L,1)*D(L,J,I)+SS(K,L+6,1)*D(L,J,I+2))/2.0
57 CONTINUE
56 CONTINUE
GO TO 50
50 CONTINUE
IF ((I.EQ.NP1).OR.(J.EQ.MP1)) GO TO 60
DO 61 K=1,6
DO 62 L=1,6
S(K)=S(K)-(SS(K,L,2)*D(L,J,I)+SS(K,L+6,2)*D(L,J,I+1))
62 CONTINUE
61 CONTINUE
60 CONTINUE
IF ((I.EQ.1).OR.(J.EQ.MP1)) GO TO 70
DO 71 K=1,6

```

```

DO 72 L=1,6
S(K)=S(K)-(SS(K,L,3)*D(L,J,I)+SS(K,L+6,3)*D(L,J,I+1))
72 CONTINUE
71 CONTINUE
70 CONTINUE
IF (I.EQ.1) GO TO 80
IF ((J.EQ.1).OR.(J.EQ.MP1)) GO TO 85
IF (I.EQ.2) GO TO 84
DO 81 K=1,6
DO 82 L=1,6
S(K)=S(K)-(SS(K+6,L,1)*D(L,J,I-2)+SS(K+6,L+6,1)*D(L,J,I))
82 CONTINUE
81 CONTINUE
GO TO 80
84 CONTINUE
DO 83 K=1,6
S(K)=S(K)-((-SS(K+6,1,1)+SS(K+6,7,1))*D(1,J,I)
* -((SS(K+6,2,1)+SS(K+6,8,1))*D(2,J,I)
* -((SS(K+6,3,1)+SS(K+6,9,1))*D(3,J,I)
* -((SS(K+6,4,1)+SS(K+6,10,1))*D(4,J,I)
* -((SS(K+6,5,1)+SS(K+6,11,1))*D(5,J,I)
* -((SS(K+6,6,1)+SS(K+6,12,1))*D(6,J,I)
83 CONTINUE
GO TO 80
85 CONTINUE
DO 86 K=1,6
DO 87 L=1,6
S(K)=S(K)-(SS(K+6,L,1)*D(L,J,I-2)+SS(K+6,L+6,1)*D(L,J,I))/2.0
87 CONTINUE
86 CONTINUE
GO TO 80
80 CONTINUE
IF ((I.EQ.1).OR.(J.EQ.1)) GO TO 90
DO 91 K=1,6
DO 92 L=1,6
S(K)=S(K)-(SS(K+6,L,2)*D(L,J-1,I-1)+SS(K+6,L+6,2)*D(L,J,I))
92 CONTINUE
91 CONTINUE
90 CONTINUE
IF ((I.EQ.NP1).OR.(J.EQ.1)) GO TO 100
DO 101 K=1,6
DO 102 L=1,6
S(K)=S(K)-(SS(K+6,L,3)*D(L,J-1,I+1)+SS(K+6,L+6,3)*D(L,J,I))
102 CONTINUE
101 CONTINUE
100 CONTINUE
IM1=I-1
JM1=J-1
WRITE(6,1010)IM1,JM1,(S(K),K=1,6)
40 CONTINUE
20 CONTINUE
10 CONTINUE

```

```
RETURN  
1000 FORMAT(1H1,15HJOINT RESIDUALS//5X,1H1,4X,1HJ,6X,2HMX,13X,2HMY,  
213X,2HYZ,13X,2HPX,13X,2HPY,13X,2HPZ)  
1010 FORMAT(1X,2I5,1P6E15.5)  
END
```

APPENDIX H

ANALOGOUS CONTINUUM METHOD

The analogous continuum method as outlined in chapter 3 and used in chapter 7 to obtain numerical results is presented in more detail here. The assumptions made are that both the lattice and continuum are linear elastic, the stress resultants in the shell continuum are statically equivalent to the member actions in the lattice and that specific deformations of the continuum and the lattice are the same. By this latter requirement on the deformations, it is intended that the displacements of the joints in the lattice are the same as the displacements at the corresponding position in the continuum.

These assumptions lead to the continuum stress/member action and continuum strain/member deformation relationships which can be combined with the member deformation/member action relationship to yield the continuum stress/strain relationship. This stress/strain relationship is the constitutive relationship for the analogous continuum and can be used in a shell theory to obtain a solution.

The derivation of the analogous continuum properties for the single layer rigid jointed lattice and the double layer pin jointed lattice will be described and they will be used in a shell theory to illustrate the numerical procedures.

H.1 CONTINUUM ANALOGY FOR A SINGLE LAYER LATTICE

Although the method can be applied to more general cases, the special case of a lattice layout consisting of equilateral triangles of identical members will be considered to demonstrate the method. Such a layout is shown in figure H.1. In order to derive the constitutive relationship, a small flat portion of the structure is considered and curvature effects are introduced in the analysis of the continuum.

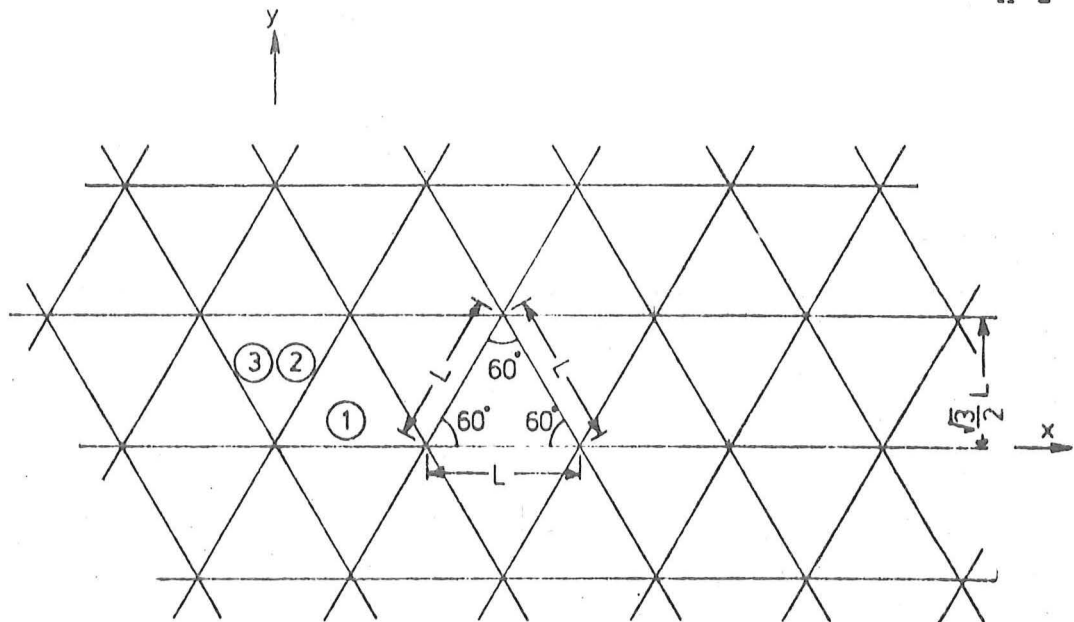


Fig. H.1 LATTICE LAYOUT

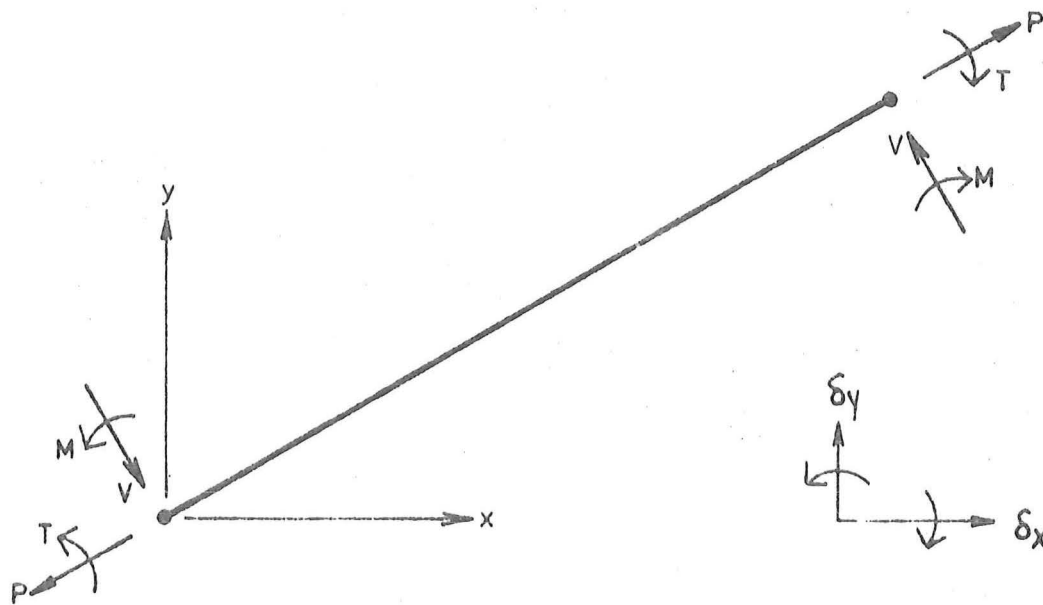


Fig. H.2 LATTICE MEMBER ACTIONS AND DISPLACEMENTS

For the lattice member, the actions and deformations shown in figure H.2 are considered while for the continuum, the stress resultants and displacements shown in figure H.3 are considered. The shears and bending moments neglected in the lattice member correspond to the transverse shears and the moment about the normal axis which are usually neglected in the theory of thin shells.

The analogy requires that the lattice member actions are statically equivalent to the continuum stresses. In order to derive the form of this relation, it is convenient to first consider a single member that is arbitrarily orientated, and cut by faces parallel to the x and y axes as shown in figures H.4a and H.4b. Consider the x face where, for equilibrium, the requirements are

$$\begin{aligned}
 N_{x y} \ell_y &= +P \cos\theta - V \sin\theta \\
 N_{y x} \ell_y &= +P \sin\theta + V \cos\theta \\
 M_{x y} \ell_y &= +M \cos\theta + T \sin\theta \\
 M_{y x} \ell_y &= +M \sin\theta - T \cos\theta
 \end{aligned}
 \tag{H-1}$$

Here ℓ_y is the repeating length measured in the y direction and is the distance between members, with similar properties and orientation, crossing the x face.

In a similar manner, for the y face and repeating length ℓ_x measured along the x axis, the equilibrium requirements are

$$\begin{aligned}
 N_{y x} \ell_x &= +P \sin\theta + V \cos\theta \\
 N_{x y} \ell_x &= +P \cos\theta - V \sin\theta \\
 M_{y x} \ell_x &= +M \sin\theta - T \cos\theta \\
 M_{x y} \ell_x &= +M \cos\theta + T \sin\theta
 \end{aligned}
 \tag{H-2}$$

When the complete lattice is considered, all members crossing each face must be accounted for, and from the lattice shown in figure

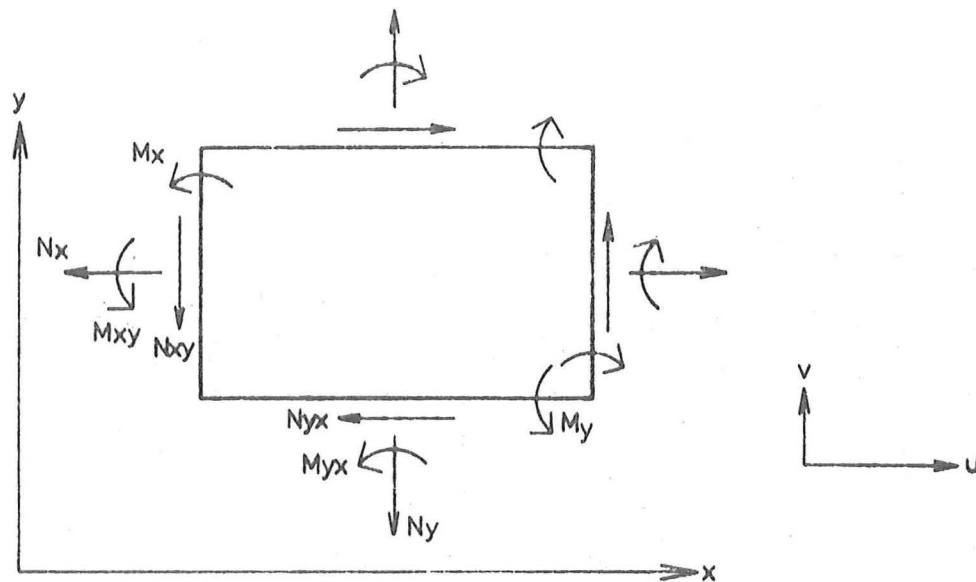


Fig. H.3 CONTINUUM ACTIONS AND DISPLACEMENTS

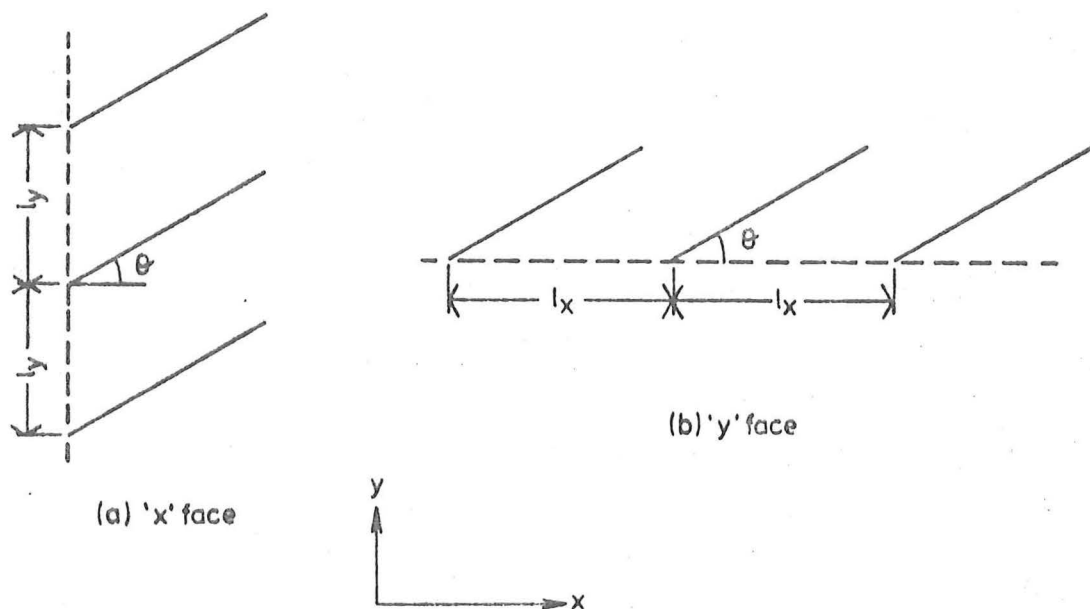


Fig. H. 4 MEMBER CROSSING - (a)'x' FACE, (b)'y' FACE

TABLE H.1 Members Crossing x and y Faces

x faceRepeating length: $\ell_y = \sqrt{3} L$

Member No.	Number of Members Crossing Face	Angle θ
1	2	0°
2	1	60°
3	1	-60°

y faceRepeating length: $\ell_x = L$

Member No.	Number of Members Crossing Face	Angle θ
1	0	-
2	1	60°
3	1	-60°

H-1, a small portion that represents the repeating module is selected and shown in figure H-5. From this, the members which cross each face and the orientation of the members is given in table H.1. This allows the relations for static equivalence of the continuum stresses and the lattice actions to be determined for this geometry. For the x face these are

$$\begin{aligned}
 N_x &= \frac{1}{L} \left[\frac{2}{\sqrt{3}} P_1 + \frac{1}{2\sqrt{3}} P_2 + \frac{1}{2\sqrt{3}} P_3 + OV_1 - \frac{1}{2} V_2 + \frac{1}{2} V_3 \right] \\
 N_{xy} &= \frac{1}{L} \left[OP_1 + \frac{1}{2} P_2 - \frac{1}{2} P_3 + \frac{2}{\sqrt{3}} V_1 + \frac{1}{2\sqrt{3}} V_2 + \frac{1}{2\sqrt{3}} V_3 \right] \\
 M_x &= \frac{1}{L} \left[\frac{2}{\sqrt{3}} M_1 + \frac{1}{2\sqrt{3}} M_2 + \frac{1}{2\sqrt{3}} M_3 + OT_1 + \frac{1}{2} T_2 - \frac{1}{2} T_3 \right] \\
 M_{xy} &= \frac{1}{L} \left[OM_1 + \frac{1}{2} M_2 - \frac{1}{2} M_3 - \frac{2}{\sqrt{3}} T_1 - \frac{1}{2\sqrt{3}} T_2 - \frac{1}{2\sqrt{3}} T_3 \right]
 \end{aligned}
 \tag{H-3}$$

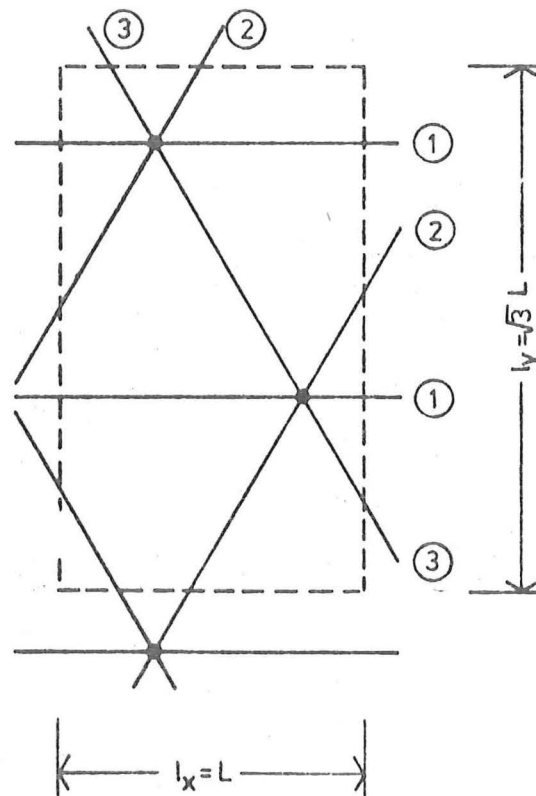
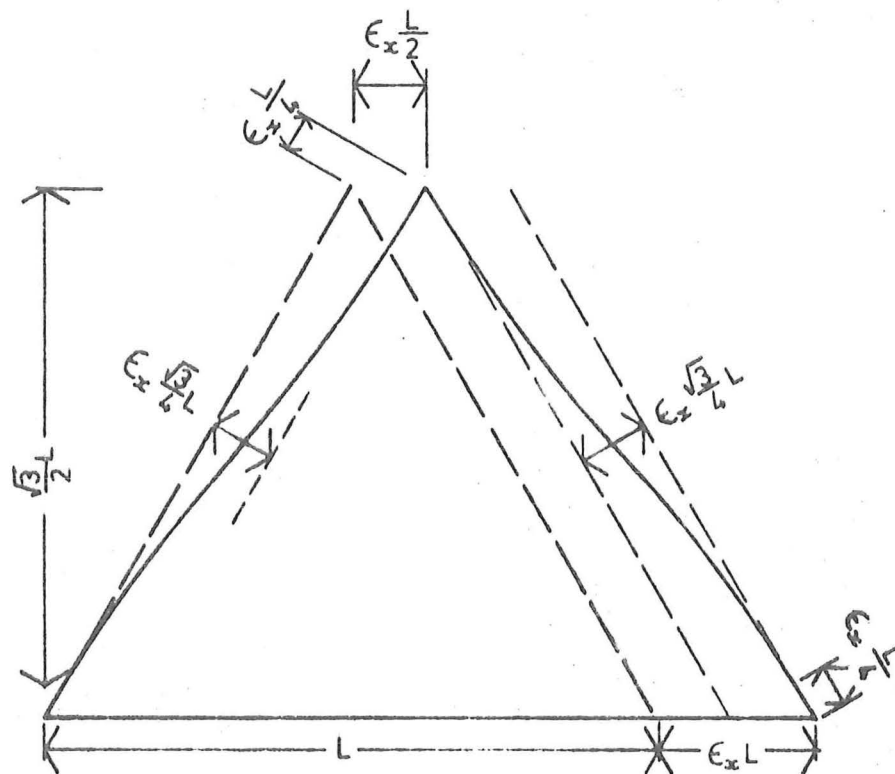


Fig.H.5 REPEATING LATTICE MODULE

Fig. H.6 DEFORMATION UNDER STRAIN ϵ_x

On a y face they are

$$\begin{aligned}
 N_y &= \frac{1}{L} \left[OP_1 + \frac{\sqrt{3}}{2} P_2 + \frac{\sqrt{3}}{2} P_3 + OV_1 + \frac{1}{2} V_2 - \frac{1}{2} V_3 \right] \\
 N_{yx} &= \frac{1}{L} \left[OP_1 + \frac{1}{2} P_2 - \frac{1}{2} P_3 + OV_1 - \frac{\sqrt{3}}{2} V_2 - \frac{\sqrt{3}}{2} V_3 \right] \\
 M_y &= \frac{1}{L} \left[OM_1 + \frac{\sqrt{3}}{2} M_2 - \frac{\sqrt{3}}{2} M_3 + OT_1 - \frac{1}{2} T_2 + \frac{1}{2} T_3 \right] \\
 M_{yx} &= \frac{1}{L} \left[OM_1 + \frac{1}{2} M_2 - \frac{1}{2} M_3 + OT_1 + \frac{\sqrt{3}}{2} T_2 + \frac{\sqrt{3}}{2} T_3 \right]
 \end{aligned}
 \tag{H-4}$$

In relations H-3 and H-4, the subscripts 1, 2 and 3 refer to the orientation of the member in the lattice, as shown in figures H.1 and H.5.

The analogy requires that the gross deformations of the lattice and the continuum are the same. This can be achieved if the three linear deformations of the lattice joints are identical to the continuum displacements at the same points.

To use this, the continuum strains ϵ_x , ϵ_y and γ_{xy} and the curvatures χ_x , χ_y and χ_{xy} are applied one at a time and the continuum deformations are determined. Because the lattice deformations at the joints are assumed to be identical to the continuum deformations at these points, the resulting lattice actions can be determined from the member deformation/action relationship. For convenience these two steps are combined into a single operation and the member actions are obtained directly from the strain pattern.

As an example consider the in-plane strain ϵ_x . When this is applied, the member deformations are those shown in figure H.6 and the member actions are then determined as

$$\begin{aligned}
 P_1 &= + EA \epsilon_x & V_1 &= 0 \\
 P_2 &= + \frac{1}{4} EA \epsilon_x & V_2 &= - 3\sqrt{3} \frac{EI}{L^2} \epsilon_x \\
 P_3 &= + \frac{1}{4} EA \epsilon_x & V_3 &= + 3\sqrt{3} \frac{EI}{L^2} \epsilon_x
 \end{aligned}
 \tag{H-5}$$

where E , A , I_z and L are the member elastic modulus, cross sectional area, second moment of area about an axis normal to the surface and length respectively. For later reference it is noted that G , I_y and I_x are the shear modulus, second moment of area about an axis in the surface and the polar moment of inertia of the member.

The expressions H-5 are substituted into the relations H-3 and H-4 to give the continuum actions due to this one continuum strain component

$$\begin{aligned} N_x &= \left[\frac{3}{4} \sqrt{3} \frac{EA}{L} + 3\sqrt{3} \frac{EI_z}{L^3} \right] \epsilon_x \\ N_y &= \left[\frac{\sqrt{3}}{4} \frac{EA}{L} - 3\sqrt{3} \frac{EI_z}{L^3} \right] \epsilon_x \end{aligned} \quad \dots (H-6)$$

$$N_{xy} = N_{yx} = M_x = M_y = M_{xy} = M_{yx} = 0$$

Similarly applying the other strains and the curvatures one at a time results in expressions for the actions in terms of each strain. These can be expressed in a matrix notation, and for the case considered, this takes the form

$$\begin{Bmatrix} N_x \\ N_y \\ N_{xy} \\ M_x \\ M_y \\ M_{xy} \end{Bmatrix} = \begin{bmatrix} v_{11} & v_{12} & 0 & & & \\ v_{21} & v_{22} & 0 & & 0 & \\ 0 & 0 & v_{33} & & & \\ & & & v_{44} & v_{45} & 0 \\ & 0 & & v_{54} & v_{55} & 0 \\ & & & 0 & 0 & v_{66} \end{bmatrix} \begin{Bmatrix} \epsilon_x \\ \epsilon_y \\ \gamma_{xy} \\ \chi_x \\ \chi_y \\ \chi_{xy} \end{Bmatrix} \quad \dots (H-7)$$

where

$$\begin{aligned} v_{11} &= v_{22} = 3 \frac{\sqrt{3}}{4} \frac{EA}{L} + 3\sqrt{3} \frac{EI_z}{L^3} \\ v_{12} &= v_{21} = \frac{\sqrt{3}}{4} \frac{EA}{L} - 3\sqrt{3} \frac{EI_z}{L^3} \\ v_{33} &= \frac{\sqrt{3}}{4} \frac{EA}{L} + 3\sqrt{3} \frac{EI_z}{L^3} \\ v_{44} &= v_{55} = -3 \frac{\sqrt{3}}{4} \frac{EI_y}{L} - \frac{\sqrt{3}}{4} \frac{GI_x}{L} \end{aligned}$$

$$v_{45} = v_{54} = -\frac{\sqrt{3}}{4} \frac{EI_y}{L} + \frac{\sqrt{3}}{4} \frac{GI_x}{L}$$

$$v_{66} = -\frac{\sqrt{3}}{4} \frac{EI_y}{L} - \frac{\sqrt{3}}{2} \frac{GI_x}{L}$$

where the symbols are the same as defined previously. It should be noted that the shears N_{xy} and N_{yx} are equal as are the twisting moments M_{xy} and M_{yx} .

The appropriate relationship for a conventional isotropic shell material takes a similar matrix form but with the terms given by

$$v_{11} = v_{22} = \frac{E^*h^*}{1-\nu^2}$$

$$v_{12} = v_{21} = \frac{E^*h^*\nu}{1-\nu^2}$$

$$v_{33} = \frac{E^*h^*}{2(1+\nu)}$$

$$v_{44} = v_{55} = \frac{-E^*h^{*3}}{12(1-\nu^2)}$$

$$v_{45} = v_{54} = \frac{-E^*h^{*3}\nu}{12(1-\nu^2)}$$

$$v_{66} = \frac{-E^*h^{*3}}{12(1+\nu)}$$

... (H-8)

where E^* , ν and h^* are the shell material elastic modulus, Poissons ratio and thickness respectively.

The form of the matrices in equations H-7 and H-8 are similar. However if they are equated term by term it is not generally possible to determine uniquely the three continuum variables E^* , ν and h^* from the four independent lattice variables EA/L , EI_z/L^3 , EI_y/L and GI_x/L . Hence in general the lattice does not have a conventional isotropic shell material as an analogous continuum. This does not mean that the lattice does not have an analogous continuum, but only that it does not take the form of the conventional isotropic shell for which there are some analysis solutions available. The analysis of a shell with the more complex constitutive relationship in equation H-7 is considered in section H.3 of this appendix.

As an example, the properties of the analogous continuum that correspond to the single layer lattice layout used in chapter 7 are determined. The properties are the same for all the structures as they depend only on the layout in the surface and not on the geometry of the surface. Using the details given in chapter 7, the constitutive relations H-7 can be evaluated to produce

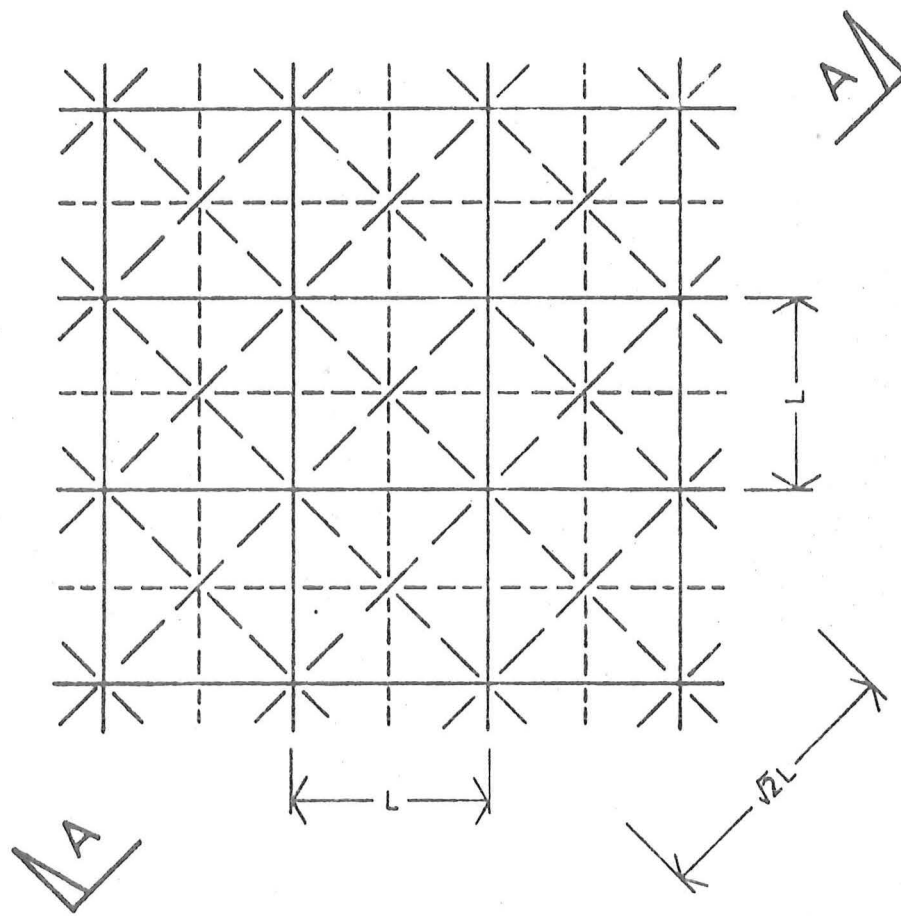
$$\begin{Bmatrix} N_x \\ N_y \\ N_{xy} \\ M_x \\ M_y \\ M_{xy} \end{Bmatrix} = \begin{bmatrix} 16.45 \times 10^6 & 5.47 \times 10^6 & 0 & 0 & 0 & 0 \\ 5.47 \times 10^6 & 16.45 \times 10^6 & 0 & 0 & 0 & 0 \\ 0 & 0 & 5.49 \times 10^6 & -10280. & -683. & 0 \\ 0 & 0 & -10280. & -683. & -10280. & 0 \\ 0 & 0 & -683. & -10280. & 0 & -9600. \\ 0 & 0 & 0 & 0 & -9600. & 0 \end{bmatrix} \begin{Bmatrix} \epsilon_x \\ \epsilon_y \\ \gamma_{xy} \\ \chi_x \\ \chi_y \\ \chi_{xy} \end{Bmatrix} \dots (H-9)$$

For this simple layout with realistic members, it is seen that the relationship does not correspond to that for a conventional isotropic shell material. In particular the apparent Poissons ratio for the in-plane components of 0.332 (ratio of 5.47×10^6 to 16.45×10^6) differs from that for the bending components of 0.066 (ratio of -683. to -10280.). It will also be noted that the magnitude of the bending components (e.g. -10280.) are very much smaller than those of the in-plane components (e.g. 16.45×10^6). This would indicate that the corresponding shell was "thin".

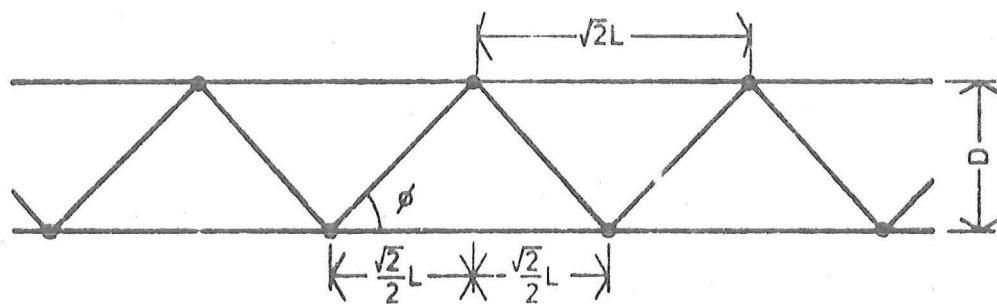
H.2 CONTINUUM ANALOGY FOR DOUBLE LAYER LATTICE

The layout of the members in the two layers and of the inter-connecting members is identical to that used in chapter 6 and is shown in figure H.7.

For this lattice type, the procedure used to derive the continuum properties is similar to that described in section H.1 for the single layer structure. The actions and deformations of the continuum are identical to those considered in section H.1 (see figure H.3). The



(a) Plan



(b) Section A-A parallel to diagonals

Fig H-7 DOUBLE LAYER STRUCTURE LAYOUT

members of the double layer lattice, however, are considered to be pin jointed and thus they only sustain axial loads.

Following the detailed procedure described previously results in the constitutive relation for the double layer lattice being

$$\begin{Bmatrix} N_x \\ N_y \\ N_{xy} \\ M_x \\ M_y \\ M_{xy} \end{Bmatrix} = \begin{bmatrix} 2 \frac{EA}{L} & 0 & 0 & | & 0 \\ 0 & \frac{2EA}{L} & 0 & | & 0 \\ 0 & 0 & \frac{\sqrt{2}}{2} \cos^3 \phi \frac{EA}{L} & | & 0 \\ \hline 0 & 0 & 0 & | & -\frac{D}{2} \frac{EA}{L} \\ 0 & 0 & 0 & | & 0 \\ 0 & 0 & 0 & | & 0 \end{bmatrix} \begin{Bmatrix} \epsilon_x \\ \epsilon_y \\ \gamma_{xy} \\ \chi_x \\ \chi_y \\ \chi_{xy} \end{Bmatrix} \quad \dots (H-10)$$

where E , A are the member elastic modulus and cross sectional area and L , D and ϕ are defined in the figure H.7. The angle ϕ is obtained from

$$\tan \phi = \frac{\sqrt{2}D}{L}$$

As discussed in section H.1, the form of this constitutive relation differs from that for a conventional isotropic shell material and thus will lead to the same problems.

As an example, the double layer lattice used in chapter 7 has an analogous continuum with the constitutive relations

$$\begin{Bmatrix} N_x \\ N_y \\ N_{xy} \\ M_x \\ M_y \\ M_{xy} \end{Bmatrix} = \begin{bmatrix} 25.32 \times 10^6 & 0 & 0 & | & 0 \\ 0 & 25.32 \times 10^6 & 0 & | & 0 \\ 0 & 0 & 3.97 \times 10^6 & | & 0 \\ \hline 0 & 0 & 6.33 \times 10^6 & | & 0 \\ 0 & 0 & 0 & | & 6.33 \times 10^6 \\ 0 & 0 & 0 & | & 0 \end{bmatrix} \begin{Bmatrix} \epsilon_x \\ \epsilon_y \\ \gamma_{xy} \\ \chi_x \\ \chi_y \\ \chi_{xy} \end{Bmatrix} \quad \dots (H-11)$$

For this double layer structure, the magnitude of the bending components (e.g. 6.33×10^6) is similar to the magnitude of the in-plane components (e.g. 25.32×10^3). This would indicate that in the analogous shell,

bending will be a significant mode of resistance and thus the shell would be considered "thick".

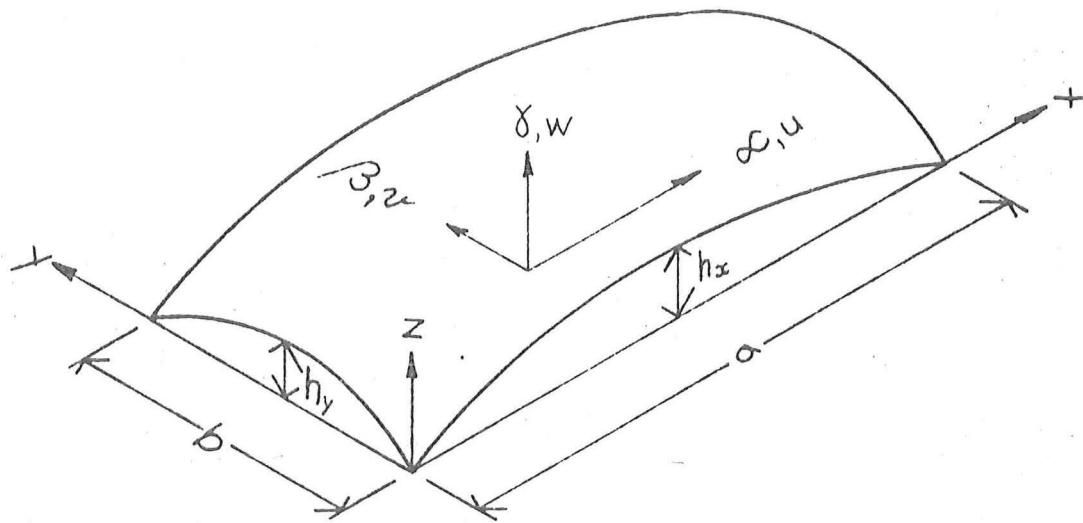
H.3 ANALYSIS OF THE CONTINUUM SHELL

An analysis of a continuum shell with constitutive relations similar to that given in equations H-9 and H-11 could not be located in the literature. For the specific case of a thin shell on a shallow second order surface, and with the constitutive relations needed, the analysis was formulated and a solution obtained. This is presented in this section.

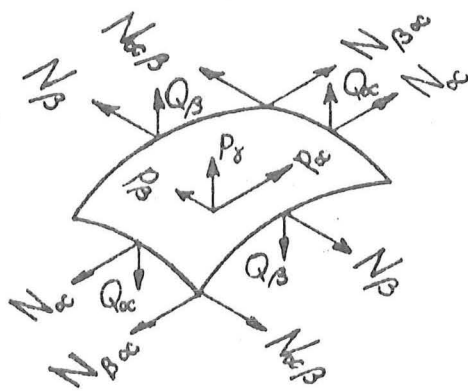
For the shell element shown in figure H.8 the equilibrium equations are [1]

$$\begin{aligned}
 \frac{\partial N_{\alpha}}{\partial \alpha} + \frac{\partial N_{\beta\alpha}}{\partial \beta} - \left(\frac{Q_{\alpha}}{R_{\alpha}} \right) + p_{\alpha} &= 0 \\
 \frac{\partial N_{\beta}}{\partial \beta} + \frac{\partial N_{\alpha\beta}}{\partial \alpha} - \left(\frac{Q_{\beta}}{R_{\beta}} \right) + p_{\beta} &= 0 \\
 \frac{\partial Q_{\alpha}}{\partial \alpha} + \frac{\partial Q_{\beta}}{\partial \beta} + \frac{N_{\alpha}}{R_{\alpha}} + \frac{N_{\beta}}{R_{\beta}} + p_{\gamma} &= 0 \\
 \frac{\partial M_{\alpha}}{\partial \alpha} + \frac{\partial M_{\beta\alpha}}{\partial \beta} - Q_{\alpha} &= 0 \\
 \frac{\partial M_{\beta}}{\partial \beta} + \frac{\partial M_{\alpha\beta}}{\partial \alpha} - Q_{\beta} &= 0 \\
 N_{\beta\alpha} - N_{\alpha\beta} + \left(\frac{M_{\alpha\beta}}{R_{\alpha}} - \frac{M_{\beta\alpha}}{R_{\beta}} \right) &= 0
 \end{aligned}
 \tag{H-12}$$

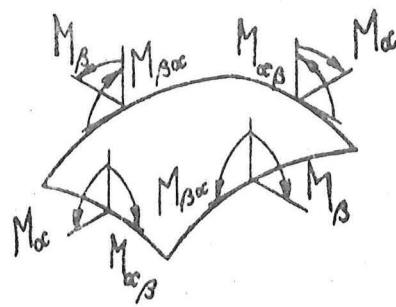
where α, β are the curvilinear coordinates on the middle surface and γ is the direction orthogonal to α, β . (N_{α}, N_{β}) , $(N_{\alpha\beta}, N_{\beta\alpha})$, (M_{α}, M_{β}) , $(M_{\alpha\beta}, M_{\beta\alpha})$ and (Q_{α}, Q_{β}) are respectively the normal forces, the normal shears, the bending moments, the twisting moments and the transverse shears per unit length. $(p_{\alpha}, p_{\beta}, p_{\gamma})$ are the load components per unit area parallel to the (α, β, γ) axes and (R_{α}, R_{β}) are the radii of curvature of the surface in the



(a) Geometry, Co-ordinates and Displacements



(b) Force System



(c) Moments

Fig. H.8 CONTINUUM SHELL

(α, β) directions. The surface twist $1/R_{\alpha\beta}$ is zero for this choice of surface and axes.

Experience has shown that the terms in brackets in equation H-12 are insignificant and for convenience they are neglected.

To use the analysis for the continuum considered in sections H.1 and H.2, the constitutive relations for the shell are chosen in the general form

$$\begin{Bmatrix} N_{\alpha} \\ N_{\beta} \\ N_{\alpha\beta} \\ M_{\alpha} \\ M_{\beta} \\ M_{\alpha\beta} \end{Bmatrix} = \begin{bmatrix} a_{11} & a_{12} & 0 & & & \\ a_{21} & a_{22} & 0 & & 0 & \\ 0 & 0 & a_{33} & & & \\ & & & b_{11} & b_{12} & 0 \\ & 0 & & b_{21} & b_{22} & 0 \\ & & & 0 & 0 & b_{33} \end{bmatrix} \begin{Bmatrix} \epsilon_{\alpha} \\ \epsilon_{\beta} \\ \gamma_{\alpha\beta} \\ \chi_{\alpha} \\ \chi_{\beta} \\ \chi_{\alpha\beta} \end{Bmatrix} \quad \dots (H-13)$$

The strain/displacement or compatibility relations for this shallow surface and axes are

$$\begin{Bmatrix} \epsilon_{\alpha} \\ \epsilon_{\beta} \\ \gamma_{\alpha\beta} \\ \chi_{\alpha} \\ \chi_{\beta} \\ \chi_{\alpha\beta} \end{Bmatrix} = \begin{Bmatrix} \frac{\partial u}{\partial \alpha} - w/R_{\alpha} \\ \frac{\partial v}{\partial \beta} - w/R_{\beta} \\ \frac{\partial v}{\partial \alpha} + \frac{\partial u}{\partial \beta} \\ \frac{\partial^2 w}{\partial \alpha^2} \\ \frac{\partial^2 w}{\partial \beta^2} \\ \frac{\partial^2 w}{\partial \alpha \partial \beta} \end{Bmatrix} \quad \dots (H-14)$$

where (u, v, w) are the displacements of the middle surface in the (α, β, γ) directions.

The constitutive relations, H-13, and the compatibility relations, H-14, are substituted into the equilibrium equations H-12 to produce

$$a_{11} \frac{\partial^2 u}{\partial \alpha^2} + a_{33} \frac{\partial^2 u}{\partial \beta^2} + (a_{12} + a_{33}) \frac{\partial^2 v}{\partial \alpha \partial \beta} - \left(\frac{a_{11}}{R_{\alpha}} + \frac{a_{12}}{R_{\beta}} \right) \frac{\partial w}{\partial \alpha} + p_{\alpha} = 0$$

$$(a_{21}+a_{33})\frac{\partial^2 u}{\partial \alpha \partial \beta} + a_{22}\frac{\partial^2 v}{\partial \beta^2} + a_{33}\frac{\partial^2 v}{\partial \alpha^2} - \left(\frac{a_{21}}{R_\alpha} + \frac{a_{22}}{R_\beta}\right)\frac{\partial w}{\partial \beta} + p_\beta = 0 \quad \dots (H-15)$$

$$\left(\frac{a_{11}}{R_\alpha} + \frac{a_{21}}{R_\beta}\right)\frac{\partial u}{\partial \alpha} + \left(\frac{a_{12}}{R_\alpha} + \frac{a_{22}}{R_\beta}\right)\frac{\partial v}{\partial \beta} - \left(\frac{a_{11}}{R_\alpha^2} + \frac{a_{12}+a_{21}}{R_\alpha R_\beta} + \frac{a_{22}}{R_\beta^2}\right)w$$

$$+ b_{11}\frac{\partial^4 w}{\partial \alpha^4} + (b_{12}+b_{21}+2b_{33})\frac{\partial^4 w}{\partial \alpha^2 \partial \beta^2} + b_{22}\frac{\partial^4 w}{\partial \beta^4} + p_\gamma = 0$$

as the governing partial differential equations for the deformations u , v and w of the shell.

When the shell is bounded by gable supports on a rectangle, a suitable form for the displacements u , v and w is the double trigonometric series

$$\begin{Bmatrix} u \\ v \\ w \end{Bmatrix} = \sum_{i=0}^{\infty} \sum_{j=0}^{\infty} \begin{Bmatrix} a_{ij} \cos \frac{i\pi\alpha}{a} \sin \frac{j\pi\beta}{b} \\ b_{ij} \sin \frac{i\pi\alpha}{a} \cos \frac{j\pi\beta}{b} \\ c_{ij} \sin \frac{i\pi\alpha}{a} \sin \frac{j\pi\beta}{b} \end{Bmatrix}$$

The loads p_α , p_β and p_γ are also expanded into a similar double series viz.

$$\begin{Bmatrix} p_\alpha \\ p_\beta \\ p_\gamma \end{Bmatrix} = \sum_{i=0}^{\infty} \sum_{j=0}^{\infty} \begin{Bmatrix} r_{ij} \cos \frac{i\pi\alpha}{a} \sin \frac{j\pi\beta}{b} \\ s_{ij} \sin \frac{i\pi\alpha}{a} \cos \frac{j\pi\beta}{b} \\ t_{ij} \sin \frac{i\pi\alpha}{a} \sin \frac{j\pi\beta}{b} \end{Bmatrix}$$

where the series coefficients r_{ij} , s_{ij} and t_{ij} are obtained by the usual procedures. In passing it is noted that for the special case of a uniform normal load $p_\alpha = p_\beta = 0$ and $p_\gamma = p$, a constant, the coefficients become $r_{ij} = s_{ij} = 0$ and $t_{ij} = 16p/ij\pi^2$.

The expansions given above for the displacements and for the loads are substituted into the governing partial differential equation H-15 to produce the equations

$$\begin{bmatrix} v_{11} & v_{12} & v_{13} \\ v_{21} & v_{22} & v_{23} \\ v_{31} & v_{32} & v_{33} \end{bmatrix} \begin{Bmatrix} a_{ij} \\ b_{ij} \\ c_{ij} \end{Bmatrix} + \begin{Bmatrix} r_{ij} \\ s_{ij} \\ t_{ij} \end{Bmatrix} = 0 \quad \dots (H-16)$$

for $i = 0, 1, 2, \dots$ and $j = 0, 1, 2, \dots$

where

$$\begin{aligned} v_{11} &= -a_{11} \left(\frac{i\pi}{a} \right)^2 - a_{33} \left(\frac{j\pi}{b} \right)^2 \\ v_{12} &= v_{21} = - (a_{12} + a_{33}) \left(\frac{i\pi}{a} \right) \left(\frac{j\pi}{b} \right) \\ v_{13} &= v_{31} = + \frac{a_{11}}{R_\alpha} + \frac{a_{12}}{R_\beta} \left(\frac{i\pi}{a} \right) \\ v_{22} &= -a_{22} \left(\frac{j\pi}{b} \right)^2 - a_{33} \left(\frac{i\pi}{a} \right)^2 \\ v_{23} &= v_{32} = + \left(\frac{a_{12}}{R_\alpha} + \frac{a_{22}}{R_\beta} \right) \left(\frac{j\pi}{b} \right) \\ v_{33} &= b_{11} \left(\frac{i\pi}{a} \right)^4 + 2(b_{12} + b_{33}) \left(\frac{i\pi}{a} \right)^2 \left(\frac{j\pi}{b} \right)^2 + b_{22} \left(\frac{j\pi}{b} \right)^4 \\ &\quad - \left(\frac{a_{11}}{R_\alpha^2} + \frac{2a_{12}}{R_\alpha R_\beta} + \frac{a_{22}}{R_\beta^2} \right) \end{aligned}$$

These equations (H-16) can be solved for the displacement series coefficients and hence the displacements can be determined. Once the displacement functions are known, the strains, curvatures and actions can be determined to complete the solution.

Numerical solutions using this method were obtained and are presented as part of the results in chapter 7 on figures 7.4 to 7.13.